



# **Modifiers of Renal Response to Injury**

(With a Focus on CTGF)



**Lucas L. Falke**





© Lucas L. Falke, 2016

The copyright of articles that have been published or have been accepted for publication has been transferred to the respective journals.

ISBN/EAN: 978-94-623-3364-2

Cover & Lay-out: Lucas Falke

Printed by: Gildeprint, Enschede

Cover: Adaptation of a sixteenth century drawing of the adrenal glands originally published in the *Tabulae Anatomicae* by Bartholomaei Eustachii

Financial support for the publication and defence of this thesis is gratefully acknowledged and was provided by: ChipSoft, the Dutch Kidney Foundation, Servier Nederland Farma B.V. and the department of Pathology (UMC Utrecht).

# **Modifiers of Renal Response to Injury**

(with a Focus on CTGF)

## **Factoren die de renale respons op schade beïnvloeden**

(met een focus op CTGF)

(met een samenvatting in het Nederlands)

### **Proefschrift**

ter verkrijging van de graad van doctor aan de Universiteit Utrecht  
op gezag van de rector magnificus, prof. dr. G.J. van der Zwaan,  
ingevolge het besluit van het college voor promoties  
in het openbaar te verdedigen  
op dinsdag 4 oktober 2016 des middags te 2.30 uur

door

**Lucas Lodewijk Falke**

geboren op 28 oktober 1985 te Nashville, Verenigde Staten van Amerika

Promotor: Prof. dr. R. Goldschmeding

Copromotor: Dr. T.Q. Nguyen

**Voor mijn familie**  
(met een focus op THMF)

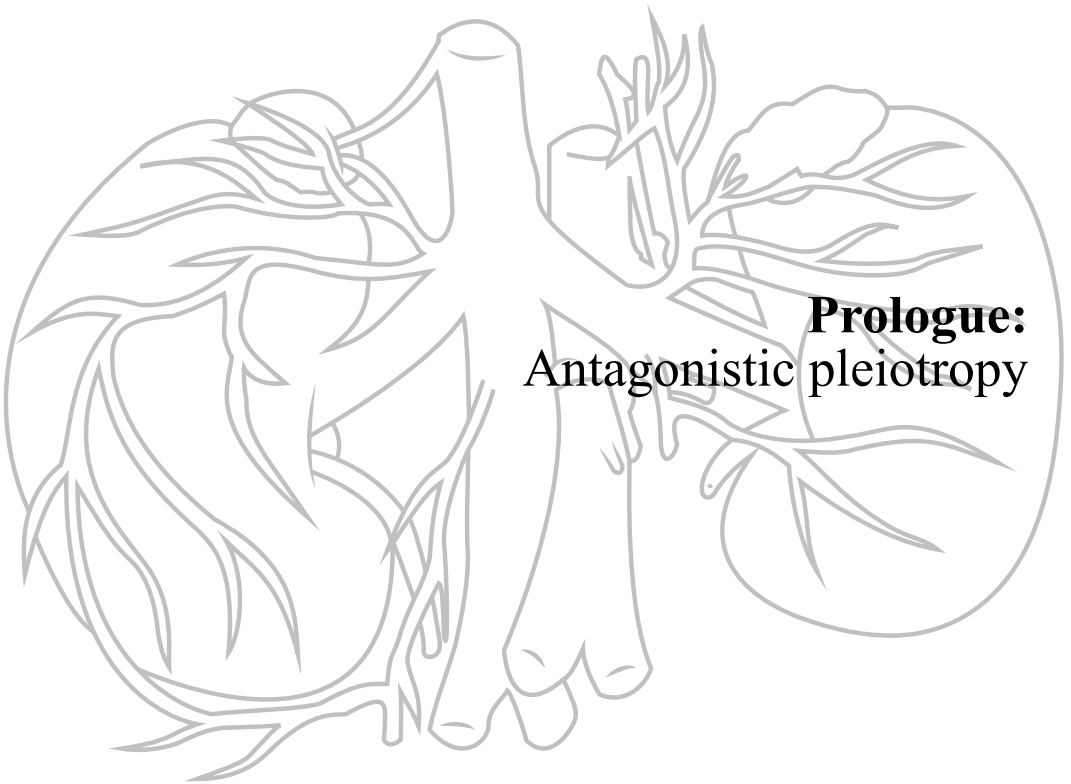
# Contents

Prologue	Antagonistic pleiotropy	9
Chapter 1	General introduction	13
<b>Part 1</b>		
Chapter 2	A Novel Histological Damage Score predicts outcome of delayed graft function after renal transplantation	21
Chapter 3	Plasma CTGF is independently related with an increased risk of cardiovascular events and mortality in patients with atherosclerotic disease: The SMART study	37
Chapter 4	Diverse origins of the myofibroblast - implications for kidney fibrosis	53
Chapter 5	Local therapeutic efficacy with reduced systemic side effects by rapamycin-loaded subcapsular microspheres	73
Chapter 6	Tamoxifen induced Cre-recombination confounds fibrosis outcome in experimental kidney disease	89
Chapter 7	CCN2 reduction mediates protective effects of BMP7 treatment in obstructive nephropathy	99
<b>Part 2</b>		
Chapter 8	Targeting CTGF, EGF and PDGF pathways to prevent progression of kidney disease	111
Chapter 9	Hemizygous deletion of CTGF/CCN2 does not suffice to prevent fibrosis of the severely injured kidney	131
Chapter 10	CTGF regulates lymphangiogenesis in severe obstructive nephropathy by regulating VEGF-C expression and activity	149
Chapter 11	Age dependent shifts in renal response to injury relate to altered BMP6/CTGF expression and signaling	165
Chapter 12	Summarizing discussion	183
	Samenvatting	189
	Dankwoord	1
	List of publications	199
	Curriculum vitae	199









**Prologue:**

**Antagonistic pleiotropy**



### Antagonistic pleiotropy

Fibrosis is the endpoint of renal disease and targeting thereof is the central subject of this thesis. Fibrosis is not unique to the kidney, but occurs in virtually every organ in an approximately similar fashion (1). When maladaptive, fibrosis causes loss of organ function. Extrapolating from the wound healing response, the acute phase of renal injury can be regarded as the infiltrative phase that is followed by a regenerative phase and thirdly a remodelling phase that normally diminishes over time, but in the case of chronic kidney disease (CKD) ensues. A notion that is backed by the fact that CKD is linked to a continuous systemic inflammatory state in patients (2). An interesting almost philosophical question is why fibrosis occurs in the first place. The answer seems to lie in antagonistic pleiotropy, a concept first described in 1957 that encompasses the idea that every advantage holds certain disadvantages in the context of evolution (3). One of the oldest and most famous examples of antagonistic pleiotropy is the disease condition called sickle cell anemia (4). This disease is characterized by misshapen erythrocytes, a feature that, although severely disabling, offers protection from malarial infection. Fibrosis is also regarded as a result of antagonistic pleiotropy (5, 6).

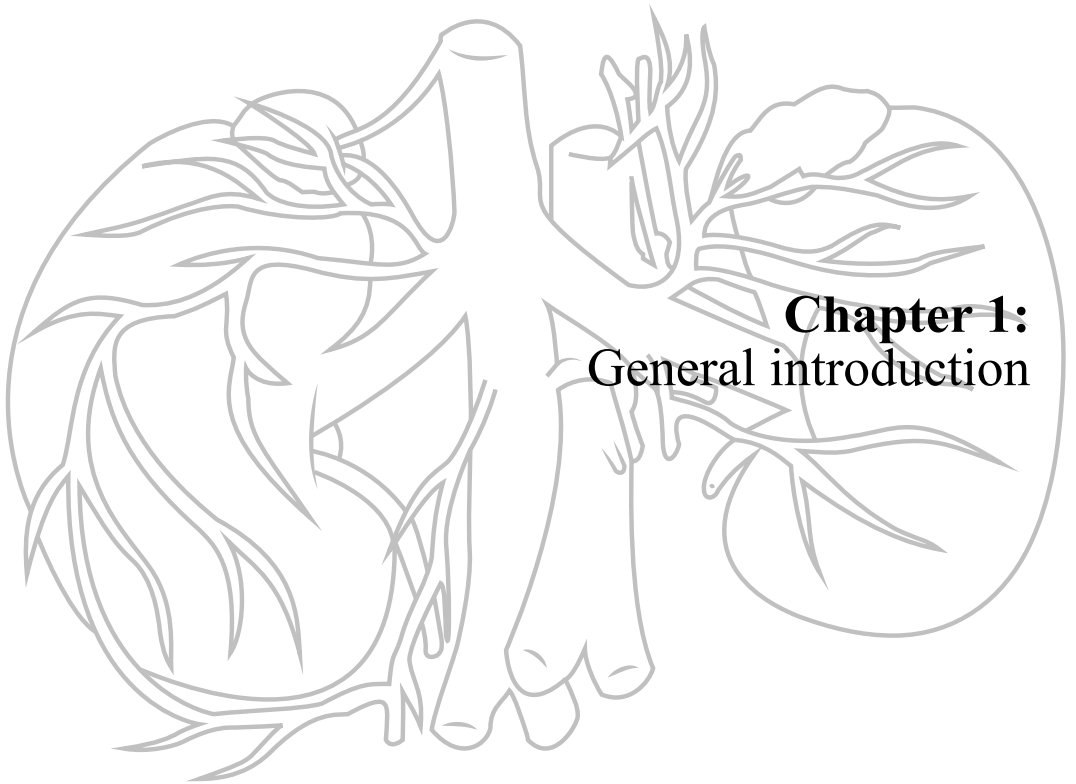
Early vertebrates such as salamanders have a less well developed immune system which is associated with better regenerative capabilities (7). Furthermore, skin wounds heal residue-free at early stages of gestation in mammals, a feature lost later in life in parallel with immune system maturation (8). In higher vertebrates such as humans, it is now becoming widely recognized that early inflammation and immune cell infiltration is causative of acute kidney injury (AKI) (9), with the macrophage being most notorious with regards to AKI to CKD progression (10). Indeed macrophage depletion reduces ischemia reperfusion induced AKI development and subsequent CKD development in experimental models (11, 12). Translated to CKD it can be argued that, from an evolutionary perspective, the detrimental loss of organ function due to overenthusiastic wound healing response is the unavoidable trade-off of an advanced immune system mediating quick fibrotic organ repair during early reproductive life. In other words, longevity in function is sacrificed for a greater chance of survival/recovery in earlier, reproductive stages of life. However, rapid environmental changes, in particular improved health care, have reduced the need for maximal wound healing response, that the benefits thereof are now outweighed by its threats in the context of increasing risk factors for CKD and cardiovascular disease. As such, the evolutionary early benefit no longer outweighs the late cost.

However, it is apparently possible in mammals with highly developed immune systems to fully regenerate without fibrosis. The search for reversibility of fibrosis started with two hallmark papers which show that, in type I diabetic patients with manifest diabetic nephropathy and accompanying glomerulosclerosis and tubulointerstitial fibrosis, fibrosis regressed after pancreas transplantation (13, 14). This shows that renal fibrosis is reversible under the right circumstances.

**References:**

1. Ben Amar M, Bianca C. Towards a unified approach in the modeling of fibrosis: A review with research perspectives. *Phys Life Rev.* 2016.
2. Machowska A, Carrero JJ, Lindholm B, Stenvinkel P. Therapeutics targeting persistent inflammation in chronic kidney disease. *Transl Res.* 2016;167(1):204-13.
3. Williams GC. Pleiotropy, Natural Selection, and the Evolution of Senescence. *Evolution.* 1957;11(4):398-411.
4. Allison AC. Protection afforded by sickle-cell trait against subtertian malarial infection. *Br Med J.* 1954;1(4857):290-4.
5. Elena SF, Sanjuan R. Evolution. Climb every mountain? *Science.* 2003;302(5653):2074-5.
6. Harty M, Neff AW, King MW, Mescher AL. Regeneration or scarring: an immunologic perspective. *Dev Dyn.* 2003;226(2):268-79.
7. Torres VE, Leof EB. Fibrosis, regeneration, and aging: playing chess with evolution. *J Am Soc Nephrol.* 2011;22(8):1393-6.
8. Ferguson MW, O'Kane S. Scar-free healing: from embryonic mechanisms to adult therapeutic intervention. *Philos Trans R Soc Lond B Biol Sci.* 2004;359(1445):839-50.
9. Rabb H. The promise of immune cell therapy for acute kidney injury. *J Clin Invest.* 2012;122(11):3852-4.
10. Noronha IL, Fujihara CK, Zatz R. The inflammatory component in progressive renal disease--are interventions possible? *Nephrol Dial Transplant.* 2002;17(3):363-8.
11. Lu L, Faubel S, He Z, Andres Hernando A, Jani A, Kedl R, et al. Depletion of macrophages and dendritic cells in ischemic acute kidney injury. *Am J Nephrol.* 2012;35(2):181-90.
12. Ko GJ, Boo CS, Jo SK, Cho WY, Kim HK. Macrophages contribute to the development of renal fibrosis following ischaemia/reperfusion-induced acute kidney injury. *Nephrol Dial Transplant.* 2008;23(3):842-52.
13. Fioretto P, Steffes MW, Sutherland DE, Goetz FC, Mauer M. Reversal of lesions of diabetic nephropathy after pancreas transplantation. *N Engl J Med.* 1998;339(2):69-75.
14. Fioretto P, Sutherland DE, Najafian B, Mauer M. Remodeling of renal interstitial and tubular lesions in pancreas transplant recipients. *Kidney Int.* 2006;69(5):907-12.

1



### Chronic kidney disease is a major health burden

Ever since Richard Bright and F. Theodor von Frerichs published their detailed description of kidney diseases in the 19th century, the diseased kidney and potential therapy thereof have been subjects of extensive investigation (1, 2). This investment of time and effort in kidney research has led to better overall survival from historically fatal renal illness, but an unequivocal worldwide rise in both prevalence and incidence of chronic kidney disease (CKD) is also evident (3, 4). The United States renal data System annual report of 2013 reports a CKD incidence of approximately 14% in the adult general population with CKD stage 3 having risen from 4.5% in 1988 to a current prevalence of 6% (5). In the Netherlands, prevalence of CKD is estimated to be around 7% (6). Furthermore, in both countries, the prevalence of CKD was highest in patients aged 60 and higher (26% and 30% respectively). This increased prevalence of CKD is multifactorial, but transgression from acute (no longer lethal) kidney disease to CKD, an increasing elderly population, and a detrimental lifestyle are major contributors. CKD is accompanied by a high burden of co-morbidity and loss of quality of life, eventually resulting in end stage renal disease and ultimately in death (7, 8). To increase treatment efficacy of CKD, a profound understanding of CKD pathophysiology is needed to find appropriate leads for interventional strategies.

### Pathophysiology of CKD as foundation for interventional strategies

Chronic kidney disease is defined as a chronic state of reduced renal function and/or structural renal damage. Parenchymal scarring with tubulointerstitial fibrosis or glomerulosclerosis, is pathognomonic for CKD, and fibrogenesis is often considered the main driving force of CKD progression (9). To what extent fibrosis is actually the culprit or a secondary response to a severe incapability of kidney cells to proliferate and reconstitute lost kidney tissue however is debatable (10, 11). During transition from acute kidney injury to CKD, the fibrosis is in itself not intrinsically progressive and needs continuous stimulation to progress (12). Initial observations showed that glomerulosclerosis in diabetic nephropathy could be reversed (13), and reversibility of kidney fibrosis in general is now slowly becoming accepted (14). This suggests that halting fibrogenesis might not be the most effective approach. Even more so given the self-limiting nature of fibrosis when the underlying stimulus is targeted as seen during diabetic nephropathy. Furthermore, a factor potentially complicating interventional strategies in fibrogenesis is the altered matrix metabolism associated with ageing (15).

Other pathophysiological stimuli that underlie CKD development and progression to which fibrogenesis is secondary involve capillary rarefaction, hypoxia, cell-cycle arrest and DNA damage, autophagy, tubular atrophy and impaired regeneration (16-21). As such, these processes might qualify as alternative starting points for therapeutic intervention ultimately yielding better outcome.

A multitude of other potential interventions to improve CKD outcome have been proposed, of which safety and efficacy is being tested (14, 22, 23). For instance Bone Morphogenetic Protein (BMP)/TGF $\beta$  interaction have been subject of study (24), and exogenous administration of recombinant BMP7 has been shown to counteract TGF $\beta$  mediated kidney fibrosis (25). Alternatively, during AKI, mTOR inhibition with Rapamycin delays recovery (26), but inhibition of mTOR once AKI has subsided might actually prevent development of CKD (27). Therapeutic use of Rapamycin is frequently accompanied by side effects (28). Therefore, alternative administrative strategies reducing systemic exposure might prove clinically useful. Tamoxifen is a widely used selective estrogen receptor modulator (SERM), and scarce evidence exists that Tamoxifen protects against chronic renal damage (29). Furthermore, Tamoxifen is a widely used experimental tool to accomplish genetic recombination in genetically modified mice. Given the potential anti-fibrotic properties of Tamoxifen, the use of this biochemical during animal experiments aimed at studying fibrotic disease is debatable.

In the first part of this thesis, several pathophysiological mechanisms underlying chronic kidney disease are analyzed. Alterations in renal pathophysiology in the context of intervention by means of BMP7 administration, targeted Rapamycin delivery or Tamoxifen pre-treatment are then described.

**Connective Tissue Growth Factor in CKD**

Connective Tissue Growth Factor, (CTGF) is a protein that holds a central role in the regulome during fibrotic development in many organs as is depicted in Figure 1. Initially, CTGF was identified via differential display as a gene overexpressed in atherosclerotic plaques and in high glucose treated glomerular mesangial cells plaque hybridization. It was characterized as an immediately early gene in mouse fibroblasts exposed to fetal calf serum and appropriately dubbed fibroblast serum protein 12 (fsp-12; sample A12 in the phage assay) (30, 31). Few months later, the human variant CTGF was identified independently, and functionally characterized as a factor harboring potent mitogenic and chemotactic properties (32). Since then, it has rapidly become evident that CTGF is both a rapid responder during tissue damage and a major determinant of the balance between the ensuing regenerative and fibrotic responses. CTGF has been shown to be a mediator of angiogenesis (33), hypoxia (34), and a regulator of proliferation (35, 36), inflammation (36), and autophagy (37), phenomena which all occur simultaneously during development of CKD. In light of this, CTGF inhibition might not only prove to potentially reduce fibrosis, but also lead to better renal outcome with regards to GFR, endocrine function, blood pressure regulation and electrolyte/phosphate homeostasis by targeting these pathophysiological phenomena all at once. The second part of this thesis involves in depth analysis of CTGF involvement in kidney disease and the alteration of pathophysiology upon CTGF intervention.

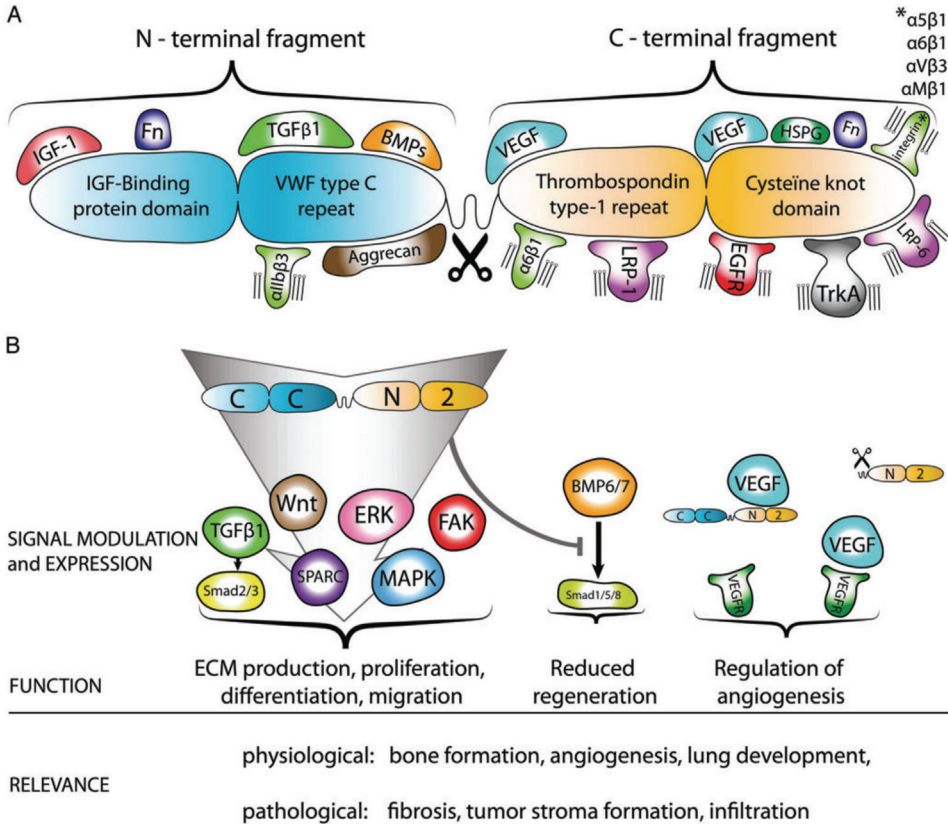


**Figure 1.** (A) Factors interacting with CTGF and (B) downstream regulatory effects (figure as published in *Nephrology Dialysis and Transplantation*, 2014 (38)).

**Outline of thesis***Part 1:*

The first part of the thesis focuses on the identification of patients at risk, pathological mechanisms and associated therapeutic targets. **Chapter 2** describes a histological scoring method capable of predicting development of CKD after renal transplantation. **Chapter 3** addresses the predictive value of increased plasma CTGF levels and the occurrence of cardiovascular events (morbidity and mortality). In **Chapter 4**, the origin of the myofibroblast, the cell type considered largely responsible for renal fibrogenesis, is discussed followed by a section providing therapeutic targeting strategies based upon these origins. **Chapters 5** and **6** describe interventional studies aimed at combating CKD by targeted Rapamycin delivery, or Tamoxifen treatment respectively in animal models of renal injury. In **Chapter 7**, evidence is provided that suggests BMP7 exerts anti-fibrotic effects in a CTGF dependent fashion.

*Part 2:*

The second part describes research performed in order to 1) unravel the functionality of CTGF during the chronic response to renal injury, and 2) determine the feasibility of targeting CTGF as an interventional strategy. This is ultimately combined with a general discussion linking both the former and the latter parts of this thesis. **Chapter 8** provides a general introduction further outlining the functions of CTGF, and reviews experimental work performed regarding CTGF intervention. A section addressing Platelet Derived Growth Factor (PDGF) and Epidermal Growth Factor (EGF), two alternative driving forces in CKD progression, complements the former. **Chapter 9** describes how 50% CTGF reduction is insufficient to reduce disease progression in severe models of CKD. **Chapter 10** shows that CTGF reduction below baseline levels is renoprotective with regards to fibrogenesis even in a severe model of CKD and that CTGF silencing is associated with reduced lymphangiogenesis. Additionally, it is shown that CTGF actively increases expression but halts biological functionality of VEGF-C, a major driving force of lymphangiogenesis. In **Chapter 11**, we identify a shift in CTGF/BMP6 ratio as a potential driving force underlying an age related differential response to kidney injury. Finally, **Chapter 12** is an overarching discussion of the novel insights gained in this thesis including opportunities for implementation and follow-up.



**References:**

1. Bright R. Reports of Medical Cases, Selected with a View of Illustrating the Symptoms and Cure of Diseases by a Reference to Morbid Anatomy. London: Longmans. 1827.
2. Wolf G, Friedrich Theodor von Frerichs (1819-1885) and Bright's disease. *Am J Nephrol.* 2002;22(5-6):596-602.
3. Bertram JF, Goldstein SL, Pape L, Schaefer F, Shroff RC, Warady BA. Kidney disease in children: latest advances and remaining challenges. *Nat Rev Nephrol.* 2016;12(3):182-91.
4. Goldberg R, Dennen P. Long-term outcomes of acute kidney injury. *Adv Chronic Kidney Dis.* 2008;15(3):297-307.
5. Collins AJ, Foley RN, Chavers B, Gilbertson D, Herzog C, Johansen K, et al. 'United States Renal Data System 2011 Annual Data Report: Atlas of chronic kidney disease & end-stage renal disease in the United States. *Am J Kidney Dis.* 2012;59(1 Suppl 1):A7, e1-420.
6. van Blijderveen JC, Straus SM, Zietse R, Stricker BH, Sturkenboom MC, Verhamme KM. A population-based study on the prevalence and incidence of chronic kidney disease in the Netherlands. *Int Urol Nephrol.* 2014;46(3):583-92.
7. Wetmore JB, Peng Y, Jackson S, Matlon TJ, Collins AJ, Gilbertson DT. Patient characteristics, disease burden, and medication use in stage 4 - 5 chronic kidney disease patients. *Clin Nephrol.* 2016;85(2):101-11.
8. Tonelli M, Wiebe N, Cullerton B, House A, Rabbat C, Fok M, et al. Chronic kidney disease and mortality risk: a systematic review. *J Am Soc Nephrol.* 2006;17(7):2034-47.
9. Bohle A, Kressel G, Muller CA, Muller GA. The pathogenesis of chronic renal failure. *Pathol Res Pract.* 1989;185(4):421-40.
10. Ferenbach DA, Bonventre JV. Mechanisms of maladaptive repair after AKI leading to accelerated kidney ageing and CKD. *Nat Rev Nephrol.* 2015;11(5):264-76.
11. Forbes MS, Thornhill BA, Minor JJ, Gordon KA, Galarreta CI, Chevalier RL. Fight-or-flight: murine unilateral ureteral obstruction causes extensive proximal tubular degeneration, collecting duct dilatation, and minimal fibrosis. *Am J Physiol Renal Physiol.* 2012;303(1):F120-9.
12. Venkatachalam MA, Weinberg JM, Kriz W, Bidani AK. Failed Tubule Recovery, AKI-CKD Transition, and Kidney Disease Progression. *J Am Soc Nephrol.* 2015;26(8):1765-76.
13. Fioretto P, Steffes MW, Sutherland DE, Goetz FC, Mauer M. Reversal of lesions of diabetic nephropathy after pancreas transplantation. *N Engl J Med.* 1998;339(2):69-75.
14. Tampe D, Zeisberg M. Potential approaches to reverse or repair renal fibrosis. *Nat Rev Nephrol.* 2014;10(4):226-37.
15. Sangaralingham SJ, Wang BH, Huang L, Kumfu S, Ichiki T, Krum H, et al. Cardiorenal fibrosis and dysfunction in aging: Imbalance in mediators and regulators of collagen. *Peptides.* 2016;76:108-14.
16. Kida Y, Tchao BN, Yamaguchi I. Peritubular capillary rarefaction: a new therapeutic target in chronic kidney disease. *Pediatr Nephrol.* 2014;29(3):333-42.
17. Tanaka S, Tanaka T, Nangaku M. Hypoxia as a key player in the AKI-to-CKD transition. *Am J Physiol Renal Physiol.* 2014;307(11):F1187-95.
18. Schelling JR. Tubular atrophy in the pathogenesis of chronic kidney disease progression. *Pediatr Nephrol.* 2015.
19. Kawakami T, Gomez IG, Ren S, Hudkins K, Roach A, Alpers CE, et al. Deficient Autophagy Results in Mitochondrial Dysfunction and FSGS. *J Am Soc Nephrol.* 2015;26(5):1040-52.
20. Bonventre JV. Maladaptive proximal tubule repair: cell cycle arrest. *Nephron Clin Pract.* 2014;127(1-4):61-4.
21. Yang L, Besschetnova TY, Brooks CR, Shah JV, Bonventre JV. Epithelial cell cycle arrest in G2/M mediates kidney fibrosis after injury. *Nat Med.* 2010;16(5):535-43, 1p following 143.
22. Ramos AM, Gonzalez-Guerrero C, Sanz A, Sanchez-Nino MD, Rodriguez-Osorio L, Martin-Cleary C, et al. Designing drugs that combat kidney damage. *Expert Opin Drug Discov.* 2015;10(5):541-56.
23. Nanthakumar CB, Hatley RJ, Lemma S, Gaudie J, Marshall RP, Macdonald SJ. Dissecting fibrosis: therapeutic insights from the small-molecule toolbox. *Nat Rev Drug Discov.* 2015;14(10):693-720.
24. Munoz-Felix JM, Gonzalez-Nunez M, Martinez-Salgado C, Lopez-Novoa JM. TGF-beta/BMP proteins as therapeutic targets in renal fibrosis. Where have we arrived after 25years of trials and tribulations? *Pharmacol Ther.* 2015;156:44-58.
25. Zeisberg M, Hanai J, Sugimoto H, Mammoto T, Charytan D, Strutz F, et al. BMP-7 counteracts TGF-beta1-induced epithelial-to-mesenchymal transition and reverses chronic renal injury. *Nat Med.* 2003;9(7):964-8.
26. Lieberthal W, Fuhro R, Andry CC, Renne H, Abernathy VE, Koh JS, et al. Rapamycin impairs recovery from acute renal failure: role of cell-cycle arrest and apoptosis of tubular cells. *Am J Physiol Renal Physiol.* 2001;281(4):F693-706.
27. Lieberthal W, Levine JS. The role of the mammalian target of rapamycin (mTOR) in renal disease. *J Am Soc Nephrol.* 2009;20(12):2493-502.
28. Rostaing L, Kamar N. mTOR inhibitor/proliferation signal inhibitors: entering or leaving the field? *J Nephrol.* 2010;23(2):133-42.
29. Kim D, Lee AS, Jung YJ, Yang KH, Lee S, Park SK, et al. Tamoxifen ameliorates renal tubulointerstitial fibrosis by modulation of estrogen receptor alpha-mediated transforming growth factor-beta1/Smad signaling pathway. *Nephrol Dial Transplant.* 2014;29(11):2043-53.
30. Almdendal JM, Sommer D, Macdonald-Bravo H, Burckhardt J, Perera J, Bravo R. Complexity of the early genetic response to growth factors in mouse fibroblasts. *Mol Cell Biol.* 1988;8(5):2140-8.

31. Ryseck RP, Macdonald-Bravo H, Mattei MG, Bravo R. Structure, mapping, and expression of fisp-12, a growth factor-inducible gene encoding a secreted cysteine-rich protein. *Cell Growth Differ.* 1991;2(5):225-33.
32. Bradham DM, Igarashi A, Potter RL, Grotendorst GR. Connective tissue growth factor: a cysteine-rich mitogen secreted by human vascular endothelial cells is related to the SRC-induced immediate early gene product CEF-10. *J Cell Biol.* 1991;114(6):1285-94.
33. Inoki I, Shiomi T, Hashimoto G, Enomoto H, Nakamura H, Makino K, et al. Connective tissue growth factor binds vascular endothelial growth factor (VEGF) and inhibits VEGF-induced angiogenesis. *FASEB J.* 2002;16(2):219-21.
34. Higgins DF, Biju MP, Akai Y, Wutz A, Johnson RS, Haase VH. Hypoxic induction of Ctgf is directly mediated by Hif-1. *Am J Physiol Renal Physiol.* 2004;287(6):F1223-32.
35. Kothapalli D, Hayashi N, Grotendorst GR. Inhibition of TGF-beta-stimulated CTGF gene expression and anchorage-independent growth by cAMP identifies a CTGF-dependent restriction point in the cell cycle. *FASEB J.* 1998;12(12):1151-61.
36. Chien W, Yin D, Gui D, Mori A, Frank JM, Said J, et al. Suppression of cell proliferation and signaling transduction by connective tissue growth factor in non-small cell lung cancer cells. *Mol Cancer Res.* 2006;4(8):591-8.
37. Capparelli C, Whitaker-Menezes D, Guido C, Balliet R, Pestell TG, Howell A, et al. CTGF drives autophagy, glycolysis and senescence in cancer-associated fibroblasts via HIF1 activation, metabolically promoting tumor growth. *Cell Cycle.* 2012;11(12):2272-84.
38. Falke LL, Goldschmeding R, Nguyen TQ. A perspective on anti-CCN2 therapy for chronic kidney disease. *Nephrol Dial Transplant.* 2014;29 Suppl 1:i30-i7.



2



## **Chapter 2:** A novel histological damage score predicts outcome of delayed graft function after renal transplantation

L.L. Falke\*<sup>1</sup>, T.T. Pieters\*<sup>2</sup>, T.Q. Nguyen<sup>1</sup>, M.C. Verhaar<sup>2</sup>  
S. Florquin<sup>3</sup>, R. Goldschmeding<sup>1</sup>, M.B. Rookmaaker<sup>2</sup>

1. Dept. of Pathology, University Medical Center Utrecht, The Netherlands
2. Dept. of Nephrology, University Medical Center Utrecht, The Netherlands
3. Dept. of Pathology, Academic Medical Center, Amsterdam, The Netherlands

\* Contributed equally

Submitted

**Abstract:**

**Introduction:** Acute Tubular Injury (ATI) is a common cause of Delayed Graft Function (DGF) after renal transplantation (RTX). Currently no histological model is available to predict renal outcome. Recovery of ATI is the result of the balance between damage and repair. In this study we evaluated the prognostic value of morphological and immunohistochemical parameters of renal damage and regeneration.

**Methods:** 25 RTX patients with DGF caused by ATI only were evaluated retrospectively. Biopsies were evaluated for histological tubular damage by our newly developed histological damage score (atrophy, edema, casts, vacuolization and dilatation) by three independent blinded observers thus allowing for determination of reproducibility by inter-observer variation. By staining for stem cell marker CD133 and proliferation marker Ki67, regenerative potential was assessed. The correlation between these parameters and renal outcome was assessed individually as well as a combined, because damage may be a confounder for regeneration. The correlation of the histological score and renal outcome was compared to that of clinical parameters as previously described in the Deceased Donor Score (DDS).

**Results:** Our newly developed histological damage score was highly reproducible, and significantly correlated to renal outcome ( $R = -0.55$ ,  $P < 0.01$ ). The magnitude of correlation was similar to the correlation between the DDS and renal outcome ( $R = -0.52$ ,  $P < 0.01$ ). Of individual parameters of the DDS however, only donor age correlated significantly ( $R = -0.60$ ,  $P < 0.01$ ). The investigated parameters for regeneration (CD133 and Ki67) did not correlate to renal outcome ( $R = -0.25$ ,  $P = 0.23$  and  $R = -0.10$ ,  $P = 0.63$  respectively), even after correction for histological renal damage.

**Conclusion:** We have developed a reproducible histological score that significantly and superiorly predicts renal outcome after post transplantation ATI as compared to clinical parameters. Despite the crucial role of regeneration in recovery after ATI, we did not find a correlation between stem cell marker CD133, proliferation marker Ki67 and renal outcome.

## Introduction

Acute Kidney Injury is a major clinical problem, afflicting as much as 20% of hospitalized patients with acute illness and more than 50% of patients in the ICU worldwide, with up to 20-40% of these patients requiring dialysis (1, 2). In addition, the amount of patients with acute kidney injury requiring renal replacement therapy continues to rise (3-5). Acute Tubular Injury (ATI) is the most prevalent cause of acute kidney injury. Although reversible in many cases, ATI is associated with an increased risk of progression to Chronic Kidney Disease (CKD). The balance between inflicted damage and ensuing regeneration determines renal function after ATI. Unraveling the cells and mechanisms involved in this balance helps understanding the pathophysiology of reversible ATI which can facilitate the development of new diagnostic and even therapeutic strategies in this prevalent condition (6-8).

In renal biopsies ATI is characterized by specific immunohistochemical changes of the tubuli (9). After loss of brush border and non-isometric cytoplasmic vacuolization, cells either lose fragments of their cytoplasm or detach entirely into the lumen producing the characteristic casts causing obstruction, which is thought to contribute to the tubule dilation (10-12). As a result of the obstruction and parallel development of inflammation, fluid oozes through tubule epithelium and the basal membrane causing interstitial edema. Finally, tubular atrophy and interstitial fibrosis arise, leading to a chronic phase of renal functional impairment (13). This chronic phase is characterized by a vicious circle, during which continuous tubule atrophy, fibrosis and glomerulosclerosis ultimately cause end stage renal disease (14). Simultaneously, the regenerative response starts almost instantly after the damage has been inflicted and involves the proliferation and differentiation of surviving renal tubular cells that express immature markers like CD133 and markers of proliferation like Ki67 (15-17). As such, the number of CD133+ cells has been shown to be increased after post-transplant ATI (17). Although it is still disputed whether cells expressing these markers are consistently present renal progenitor cells or dedifferentiated mature tubular cells, it is generally accepted that (dedifferentiated) proliferating cells with an immature phenotype play an important role in recovery after injury (18, 19).

Despite substantial knowledge about morphological changes and regenerative mechanisms following renal injury in animal models, no histological model is currently available that predicts renal outcome after ATI in humans. We hypothesize that histological and immunohistochemical parameters for ATI and regeneration correlate to renal outcome. For this purpose we evaluated biopsies of patients who suffered from ATI 1 week after renal transplantation (RTX) (20). ATI after RTX is an excellent human model for ischemic ATI as it is very similar to non-transplant ATI with rather standardized ischemic damage in a homogenous clinical situation, given that other causes of DGF are excluded (21). Histological and immunohistochemical parameters of damage and regeneration were correlated to renal outcome, defined as speed of recovery as well as eGFR at 6 months, prognosticators of long-term renal transplant function (22, 23). The strength of the correlation of parameters to renal outcome was evaluated by comparing it to the well-established clinical prognostic parameters described by Nyberg et al. (24, 25). A model that correlates histological and immunohistochemical characteristics to renal outcome will not only provide a powerful tool for prognostication but will also provide insight into the cells and mechanisms involved in renal damage and regeneration as an important step towards the development of new therapeutic strategies to limit renal damage and enhance renal regeneration.

## Materials and methods

### *Renal transplant patients*

We retrospectively evaluated all patients aged over 18 who received a Non-Heart Beating type III donor kidney in our institution since 2005 (26), and were biopsied 5-9 days after RTX because of DGF back to 2005. DGF was defined as the need for dialysis in the first week post-transplantation. All patients with DGF due to ATI only were included. Biopsies showing concurrent kidney pathology, e.g. acute rejection and tubulointerstitial nephritis, in renal biopsy at 7 days after RTX or during the 6 months follow up were excluded, because of the interference between parameters of ATI damage and regeneration 7 days after RTX and renal function 6 months after RTX. In order to compose a deceased donor score (DDS) similar to the score described by Nyberg et al. (25, 27), the following parameters were collected: donor age, gender, cause of death, end point creatinine, CMV status, cold ischemia time, side of kidney (left vs right), as well as recipient: age, gender and number of HLA mismatches. Donor history of hypertension yielded too many missing data points to compose the full Nyberg DDS score for the entire group.

According to protocol renal biopsies were taken approximately 7 days after RTX when the transplanted kidney had not regained function at that time, after informed consent of the patient. 54 Patients were selected. Of these, we excluded 29 patients: 20 patients because of other kidney pathology in the biopsy, 1 was excluded because of loss to follow-up, 1 because no material was available and 7 were excluded because they developed kidney pathology not related to the ATI injury within 6 months after transplantation therefore obscuring the relation between the findings in the renal biopsy at one week and renal function at 6 months (Supplemental Figure 1). All patients received a combination of prednisolone, tacrolimus and mycophenolate mofetil as standard immunosuppressive therapy in our institution. This study was performed according to the ethical guidelines of the UMC Utrecht. In the Netherlands, the use of left over material for scientific purposes is included in standard treatment contract and no additional informed consent is required (28).

Renal outcome was defined as estimated Glomerular Filtration (eGFR) at 6 months after RTX, as recovery DGF due to ATI is thought to be resolved at this time and stable situation is reached. eGFR was calculated using the Chronic Kidney Disease Epidemiology Collaboration (CKD-EPI) formula (29). Serum creatinine levels were assessed by colorimetric enzymatic assay (Beckman Coulter, Brea, CA). During clinical recovery creatinine levels were measured daily and upon discharge every other week.

### *Histochemistry*

An ultrasound-guided 22 mm biopsy was taken from the renal cortex using a 16 Gauge needle. Renal biopsies were formalin fixed and paraffin-embedded (FFPE) using standard procedures. For all staining procedures 3µm sections were cut, deparaffinised with xylene and rehydrated with a 100%, 96% and 70% ethanol sequence. Once rehydrated, sections were stained with periodic acid-Schiff (PAS) or haematoxylin and eosin (H&E) using standard procedures. Assessing the amount of chronic damage in renal biopsies is standard practice in our institute. From the diagnostic pathology reports, we extracted data describing the amount of glomerular sclerosis, tubular atrophy, interstitial fibrosis and arterial/arteriolar narrowing and created a composite score as described by Remuzzi et al. (27).

For the histological damage score (HDS), PAS stained slides were scored for ATI by three blinded and independent observers, two in the UMCU and one in the AMC. Damage in cortical tissue was assessed by scoring (A) tubular dilation, (B) tubular atrophy, (C) tubular edema, (D) tubular cell vacuolization and (E) casts as a percentage of the total biopsy. A score between 0 and 5 was given to each of these parameters (0= 0-1%, 1= 1-10%, 2= 10-25%, 3= 25-50%, 4= 50-75% and 5= 75-100%) with the percentage describing affected cortical area per biopsy for A, B, C, D or E respectively. Aggregation of individual parameters was performed to generate the HDS.



*CD133 and Ki67 Immunohistochemistry*

Endogenous peroxidase was blocked by H<sub>2</sub>O<sub>2</sub> incubation followed by antigen retrieval by boiling in EDTA pH 9 or Citrate pH 6 followed by overnight incubation at 4°C with mouse anti-CD133 (1:10; AC133, Miltenyi, Bergisch-Gladbach, Germany), 1h at room temperature with rabbit anti-Ki67 (1:200; SP6, Thermo-Fisher, Waltham, USA). After thorough rinsing with PBS, sections were incubated with Brightvision Alkaline-Phosphatase linked secondary antibodies (Immunologic, Duiven, the Netherlands) according to initial primary antibody species. For CD133 and Ki67 quantification, biopsies were blinded and 10 high power fields (HPF) per biopsy (200x magnification) were studied by two independent observers. The number of immunopositive tubular cells or nuclei respectively were counted and averaged per biopsy and expressed as average +/- standard deviation.

*Statistics*

Intergroup difference was compared with the Student's t-test or the Wilcoxon rank-sum test where appropriate. Correlations between continuous and/or ordinal variables were tested using linear regression or Spearman's Rho where appropriate. Continuous variables were assessed for normality using P-plots, histograms and the Shapiro-Wilk test. Highly skewed variables were analyzed via non-parametric tests or bootstrapping. Statistical correction for possible confounders was performed via hierarchical multiple regression. Using multiple linear regression in multivariate analysis, continuous outcomes were predicted. Logistic regression was used in multivariate analysis for predicting dichotomous outcome. Ordinal variables were coded using polynomial contrast coding when added in a multiple or hierarchical regression model. Kaplan Meier analysis was performed by dividing HDS group in two split along the average of 7. Statistical significance in days regaining an eGFR above 30 or 45 between HDS, Ki67 or CD133 groups respectively was tested using Log rank analysis. P-values below 0.05 were considered statistically significant. For multivariate analysis Cox logistic regression analysis was performed using donor age, and Remuzzi score as co-variables. Missing values were analyzed via pairwise exclusion. Statistical analysis was performed with SPSS for Windows version 20.0.0. Interobserver variation was statistically tested with Kendall's coefficient of concordance by using statistical program R.

## Results

### *Clinical characteristics and renal outcome after DGF due to ATI*

Baseline characteristics of the 25 RTX patients that met our inclusion criteria are shown in Table 1. In addition, the eGFR at 6 months after renal transplantation is shown as well as the correlation between clinical donor characteristics (Deceased Donor Score, DDS) and histological parameters for chronic damage (Remuzzi score) are shown. In our population the DDS score correlated significantly to renal outcome ( $R=-0.52$ ,  $P=0.01$ ). Of the individual parameters of the DDS score, donor age, recipient age and the number of HLA mismatches correlated to renal outcome (Table 1) (25). Using multivariate analysis however, donor age was the only correlate when corrected for either recipient age ( $p=0.025$ ), or number of HLA mismatches ( $p=0.016$ ). Finally, the Remuzzi score did not relate to renal outcome ( $R=0.04$ ,  $p=0.86$ ; Table 1).

### *HDS scoring has a low interobserver variability*

Histological evaluation of histological damage parameters by 3 independent observers demonstrated a low interobserver variability. Tubular dilatation, epithelial vacuolization, intraluminal cast formation, interstitial edema and tubular atrophy are hallmark morphological phenomena occurring during ATI which were quantified by 3 blinded observers using periodic acid stained sections (Figure 1A). We determined interobserver variation for both the individual parameters as well as a combined histological damage score (HDS) using Kendall's coefficient of concordance (Table 2). All parameters showed a significant interobserver agreement. From the scored parameters, best agreement was seen for vacuolization score ( $W=0.85$ ,  $p<0.001$ ), and dilatation score showed the worst agreement ( $W=0.62$ ,  $p<0.001$ ). The combination of all parameters into an aggregated Histological Damage Score (HDS) showed a Kendall coefficient of 0.74 ( $p<0.001$ ). *Aggregated Histological Damage Parameters correlate with eGFR at 6 month* Next, the HDS was correlated to the estimated GFR 6 months after renal transplantation. An

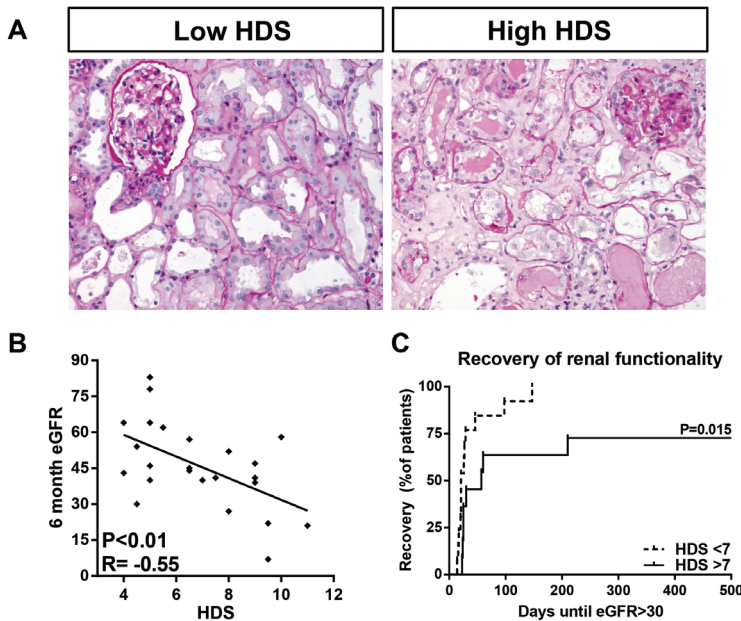


**Figure 1:** Histological damage score predicts level and rate of renal recovery after DGF. **A.** Representative PAS stained micrographs of renal cortex with low and high HDS respectively (200x magnified). **B.** Pearson correlation between HDS and eGFR 6 months after DGF. **C.** Kaplan-Meier one minus survival plot showing days until eGFR>30ml/min/1.73m<sup>2</sup> is reached; stratified in HDS above group average >7 or below average <7; log rank statistic is shown.

inverse correlation between the HDS and 6-month eGFR was observed ( $R=-0.55$ ,  $p<0.01$ ; Figure 1B; Table 3). Of the individual parameters of the HDS, edema and atrophy correlated significantly to renal outcome defined as eGFR 6 months after RTX ( $R=-0.44$ ,  $p<0.05$  and  $R=-0.41$ ,  $p<0.01$  respectively; Table 3). Furthermore, the correlation to 6-month eGFR was strongest when all individual morphological damage parameters were aggregated and thus all were included in the HDS.

<b>Table 1: Baseline characteristics</b>		correlation with eGFR after 6 months	
Characteristic		R	p-values†, (‡)
Patients (N)	25	-	-
eGFR after 6 months (ml/min/1.73 m2)	45.2±17.8	-	-
Deceased donor score (Nyberg)	2.3±0.7	-0.52	0.01(-)
Donor age (yrs) *	51.9±14.2	-0.60	<0.01(0.025/0.016)
Weight donor	82.9±16.1	-0.41	0.10 (0.18)
Cause of death (CVA/other/unknown)	7/17/1	-0.11	0.33 (0.38)
CMV mismatch D+/R-	6/19	-0.08	0.75 (0.36)
Donor serum creatinine (µg/L)	78.3±22.7	-0.23	0.34 (0.89)
Side kidney (left/right)	10/8	0.09	0.71 (0.90)
Cold Ischemia Time (hours/minutes)	18h12m ± 4h18m	-0.11	0.61 (0.28)
Recipient age (yrs)	56.6±12.8	-0.54	0.02 (0.38)
Recipient sex (m/f)	10/15	-0.25	0.23 (0.15)
HLA mismatches (N)	3.0 ± 1.4	-0.42	0.04 (0.47)
Remuzzi score	2.2±1.35	0.04	0.86 (0.38)
Glomerular global sclerosis&	0.71±0.15	0.149	0.48 (-)
Tubular atrophy&	0.65±0.1	-0.145	0.51 (-)
Interstitial fibrosis&	0.65±0.1	-0.145	0.51 (-)
Arterial and arteriolar narrowing&	0.28±0.09	-0.148	0.48 (-)

Values are shown as means ± SD. † P-values were obtained by linear regression; Significant values are highlighted. ‡ P-value corrected for donor-age with hierarchial multiple regression between parentheses. \* Donor age was corrected for recipient age or the number of HLA mismatchwches; corresponding p-values are shown. & Tested with Spearman non-parametric univariate correlation

<b>Table 2: Interobserver agreement*</b>		
Characteristic	W	p-value†
<b>HDS**</b>	<b>0.74</b>	<b>&lt;0.001</b>
Dilatation	0.62	<0.001
Vacuolization	0.85	<0.001
Casts	0.61	<0.001
Edema	0.65	<0.001
Atrophy	0.57	<0.001

\* inter-observer agreement between 3 independent observers and 2 institutions was calculated using Kendall’s coefficient of concordance; 0 represents no agreement and 1 perfect agreement. † p-values were obtained by Kendall’s coefficient of concordance. Significant values are highlighted. P-values of <0.05 were considered significant. \*\*Histological Damage Score (HDS) = Dilatation + Vacuolization + Casts + Edema + Atrophy

As chronic damage and donor age might confound the correlation between histological parameters for acute damage as well as renal outcome, we performed multivariate analysis, with HDS and chronic pre-existing damage (Remuzzi) and donor age. The correlation with eGFR at 6 months however, remained significant after correction for donor age (Beta= -0.48,  $p=0.005$ ) and chronic damage (as described by the Remuzzi score; Beta= -0.56,  $p=0.006$ ) or both (Beta= -0.47,  $p=0.008$ ) (Table 3).

#### *High HDS correlates to delayed recovery*

The HDS correlated to time to recovery of renal function (eGFR  $\geq 30$ ml/min/1.73m<sup>2</sup>). Both a retarded recovery and an eGFR below 30ml/min/1.73m<sup>2</sup> at 3 and 12 months are negative prognosticators for graft survival (23). To analyze whether a high HDS in patients with DGF due to ATI correlate to delayed recovery of renal function we dichotomized the cohort in a low and high HDS group. Biopsies were dichotomized into a group with HDS above average (7, see Table 3;  $n=12$ ) and a group with HDS below average ( $n=13$ ). Survival analysis, stratified in the number of days until an eGFR above 30/min/1.73m<sup>2</sup> was reached by Kaplan-Meier analysis, revealed a faster recovery when the HDS score was below 7 (Log rank;  $p=0.015$ ; Figure 1C). Additionally, multivariate cox regression with Remuzzi and donor age as co-variables showed that only the HDS was an independent predictor of recovery time to an eGFR above 30 ml/min/1.73m<sup>2</sup> (HDS: B -0.295 (CI 0.58 – 0.961), Remuzzi: B -0.05 (CI 0.64 – 1.4), donor age: B -0.007 (CI 0.95 – 1.04).

#### *Immunohistochemical markers of regeneration do not correlate to eGFR at 6 months*

The Ki67 antigen is expressed in non-quiescent cells during all phases of the cell cycle, and as such has been used as a marker of proliferating cells (30). To assess the proliferative response in ATI mediated DGF, we quantified the number of positive tubular nuclei in our post RTX renal biopsy cohort (Figure 2A). Despite the crucial role of tubular cell proliferation in regeneration and therefore the recovery of renal function, we did not find a correlation between Ki67 staining and functional renal outcome defined as eGFR at 6 months ( $R=-0.10$ ,  $p=0.63$ ; Figure 2B; Table 4).

Cluster of Differentiation 133 (CD133) is an epitope found on the glycoprotein

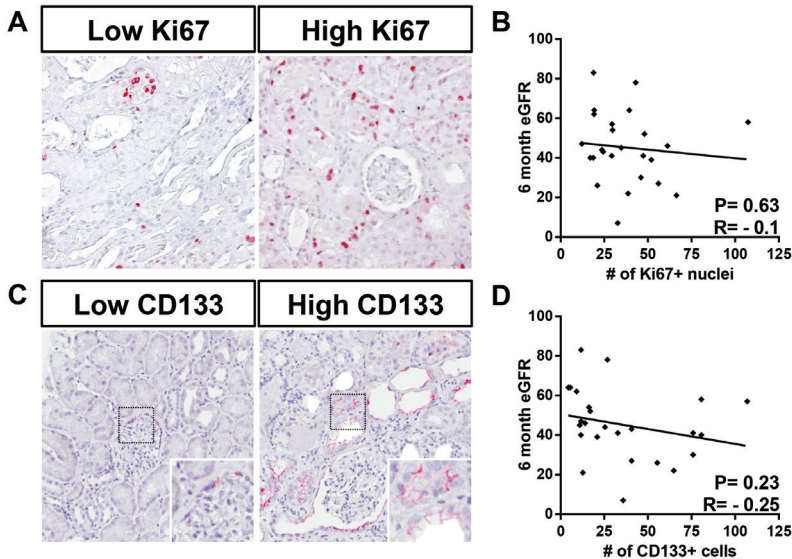


**Figure 2:** Ki67 and CD133 do not predict renal recovery after DGF. **A.** Micrographs of biopsies with low and respectively high numbers of Ki67+ tubular cells (200x magnification). **B.** Pearson correlation between 6-month eGFR and the number of Ki67+ tubular cells. **C.** Low and respectively high numbers of CD133+ tubular cells (200x magnification). **D.** Correlation between 6-month eGFR and the number of CD133+ tubular cells.

**Table 3:** Correlations between renal outcome and morphological damage characteristics\*

Characteristic	Mean ± SD	Median (range)	eGFR at 6 months			
			R	p-value†	corrected p-value‡	corrected p-value††
<b>HDS**</b>	<b>6.85±2.13</b>	<b>6.5 (4-11)</b>	<b>-0.55</b>	<b>&lt;0.01</b>	<b>&lt;0.01</b>	<b>&lt;0.01</b>
Dilatation	1.85±0.79	2 (1-3.5)	0.02	0.99	0.67	0.99
Vacuolization	1.69±0.79	1.75 (0.5-3.0)	-0.20	0.36	0.53	0.25
Casts	1.63±1.1	1 (0-4)	-0.34	0.10	0.18	0.13
Edema	0.75±0.68	0.5 (0-2)	-0.44	0.03	<0.01	<0.01
<b>Atrophy</b>	<b>0.94±0.63</b>	<b>1 (0-2.5)</b>	<b>-0.41</b>	<b>0.05</b>	<b>0.64</b>	<b>0.05</b>

\* Values shown were averaged from observations of two independent observers. \*\*Histological Damage Score (HDS) = Dilatation + Vacuolization + Casts + Edema + Atrophy. † p-values were obtained by linear regression or spearman’s rho where appropriate. Significant values are highlighted. p-values of <0.05 were considered significant. ‡ corrected for donor-age with hierarchical multiple regression. †† corrected for Remuzzi score with hierarchical multiple regression

**Table 4:** Association between eGFR at 6 months and regenerative characteristics\*

Characteristic	mean ± SD	R	p-value†
Tubular CD133 (cells)	35.5 ± 29.4	-0.25	0.23
Tubular Ki67 (cells)	37.4 ± 20.8	-0.10	0.63

\* Values are shown as mean ± SD. Values are average number of cells per high powered field averaged from observations of two independent observers. † p-values were obtained by linear regression. Significant values are highlighted. P-values of <0.05 were considered significant.

Prominin-1 and is expressed in a wide variety of stem cells (31). CD133 is present on the apical side of tubules and at the parietal epithelial cell’s (PEC’s) of glomeruli (Figure 2C) (32, 33). In the kidney, mainly CD133+ tubule cells have been shown to contribute to renal regeneration following ischemic injury (33, 34). In our cohort however, the number of CD133+ tubule cells did not correlate to 6-month eGFR (R=-0.25, p=0.23; Figure 2D; Table 4).

*Immunohistochemical markers of regeneration do not correlate to renal recovery rate*

For survival analysis of days until renal eGFR recovery above 30ml/min/1.73m2, dichotomous groups with either low or high Ki67 and low or high CD133 were created. Next Kaplan-Meier with log rank test was performed. This revealed no significant difference in days when looking at high or

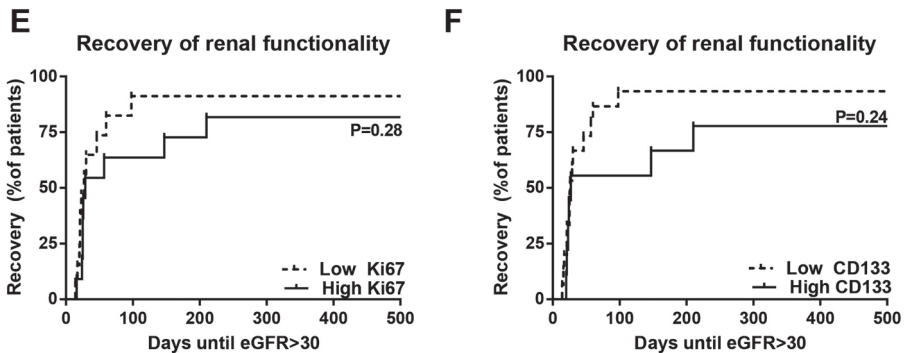


**Figure 2 (continued):** E. Kaplan-Meier one minus survival plot showing days until eGFR>30ml/min/1.73m2 is reached; stratified in # of Ki67+ cells above (high) or below average (low); log rank statistic is shown. F. Kaplan-Meier one minus survival plot showing days until eGFR>30ml/min/1.73m2 is reached; stratified in # CD133+ tubules above (high) or below average (low); log rank statistic is shown.

low Ki67 expression for obtaining an eGFR equal to or above 30 ml/min/1.73m<sup>2</sup> (P=0.28, Figure 2E). When looking at CD133 there was no significant correlation between recovery time (defined as time to eGFR above 30 ml/min/1.73m<sup>2</sup>) and CD133 positive tubular cells (P=0.24, Figure 2F). *Immunohistochemical parameters of regeneration do not correlate to renal outcome in the context of histological damage*

The amount of damage might confound the correlation between parameters of regeneration and renal eGFR at 6 month, concealing a correlation between the latter two. Insufficient regeneration as response to a certain amount of damage might cause a worse outcome. To evaluate the latter hypothesis, we compared the relation between parameters of renal damage (HDS) and regeneration (CD133 and Ki67) in the patients with the best (eGFR>45ml/min/1.73m<sup>2</sup> at 6 months, n=13) and worst functional renal outcome (eGFR<45ml/min/1.73m<sup>2</sup> at 6 months, n=12). In graphs plotting Ki67 or CD133 against HDS, renal outcome was annotated per patient in a dichotomized fashion (Figure 3A and 3B). Regression analysis of Ki67 and HDS shows that directionality was similar in both outcome groups (>45: R=-0.16 and p=0.63, <45: R=0.26 and P value=0.34, Figure 3A). Similarly, the number of CD133+ tubule cells and HDS do not correlate in the outcome groups (>45: R=0.45 and p=0.14, <45: R=0.01 and p=0.98, Figure 3B). Likewise, Ki67/HDS or CD133/HDS ratios did not correlate to renal outcome (Ki67/HDS p=0.24, R=-0.27; CD133/HDS p=0.28; R=-0.25). Thus, neither proliferation markers Ki67 nor stem cell marker CD133 correlate to renal functional outcome even when assessed in the context of histological damage.

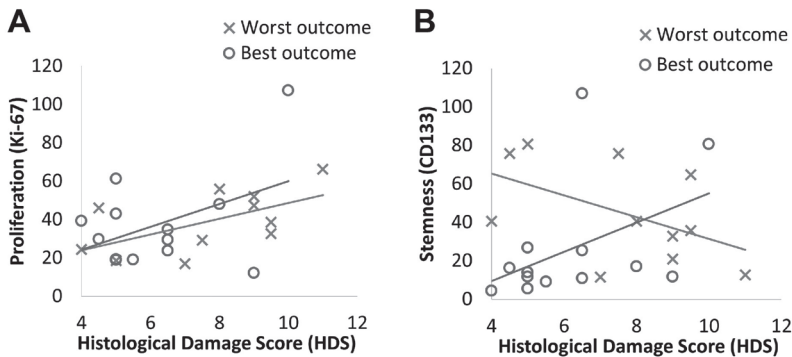


**Figure 3:** Markers of proliferation and regeneration do not show distinct clusters of favorable outcome in context of histological renal damage. A. Scatter plot of # of Ki67+ nuclei and HDS with distinct regression lines for best (eGFR>45ml/min) and worst (eGFR<45ml/min) renal outcomes. B. Scatter plot of # of CD133+ cells and HDS with distinct regression lines for best (eGFR>45ml/min) and worst (eGFR<45ml/min) renal outcomes.

## Discussion

We present a new histological scoring system for ATI that independently predicts renal outcome and recovery time in patients with delayed graft function due to ATI after RTX. Evaluation of the histological parameters dilatation, atrophy, vacuolization, luminal casts and interstitial edema were highly reproducible. This reproducibility is in line with other validated highly reproducible scoring methods such as The Oxford classification of IgA nephropathy (35). When aggregated into a single histological damage score, our parameters correlate to renal outcome defined as eGFR 6 months after transplantation. Although most parameters correlated to renal outcome individually, the correlation was strongest when all five parameters were included in the HDS. In addition, patients with a low HDS had a shorter recovery time after ATI than those with a high HDS. Moreover the correlation of the HDS to renal outcome and renal recovery time appeared to be independent of currently used clinical and histological parameters.

Our data is in line with scarce publications that previously have shown a correlation between histological damage and long term prognosis after ATI in humans. Cosio et al. show in RTX biopsies taken 1-year after transplantation that reduced damage correlates to better long term graft survival (36). A second study shows in protocol biopsies taken 6 weeks post-transplantation that ATI inversely associates with renal recovery and was associated with DGF (37). Moreover, Abdulkader et al. showed in biopsies from native kidneys taken during ATI of heterogeneous origin, that histological damage parameters correlate to functional renal outcome (38). We extend these finding in a population of ATI of homogeneous origin and even show a correlation between our HDS and renal recovery rate.

It is of note that the number of Ki67+ tubular cells correlated significantly with the HDS ( $R=0.54$ ,  $P=0.006$ ). This is in line with the previous observations during ATI in renal transplants (39). However, the lack of correlation between repair and renal outcome, even in the context of damage, suggests that this marker might in part reflect dysfunctional regeneration. Under physiological conditions, renal tubular cells are mainly in G0 phase of the cell cycle. Upon injury, tubular cells enter G1 of the cell cycle, however, this is not necessarily followed by completion of the entire cell cycle (40). Cell cycle arrest at the G2/M transition can occur, for instance due to DNA damage, hampering the completion of the cell cycle (41). G2/M arrested cells acquire a pro-fibrotic and pro-inflammatory phenotype, negatively affecting renal outcome for instance by expressing CTGF (42). Tubular CD133 and/or ki67 consequently not exclusively mark regenerating cells, but also pro-fibrotic, pro-inflammatory G2/M arrested tubular cells. Finally, we cannot exclude that other factors like rejection, drug toxicity, cellular senescence or vascular rarefaction have obscured the correlation of our regenerative parameters and functional renal outcome (14, 41, 43).

Although the clinical Nyberg score correlated to renal outcome in our cohort, the histological score for chronic renal damage did not. The highly validated Nyberg deceased donor score composed of clinical parameters is widely used to predict outcome after renal transplantation (24, 25), and indeed the Nyberg score correlated with renal outcome in our cohort supporting clinical validity of selected DGF patients. The histological damage scoring system composed by Remuzzi et al. is a valuable tool in determining pre-existent baseline chronic damage in donor kidneys (44). The lack of correlation seen in our study might be caused by the low level of variance in baseline chronic histological damage in our cohort and/or the fact that the acute renal damage more pronouncedly affected renal outcome than the underlying chronic renal damage. This suggests that the Remuzzi score is best applied on pre-implantation donor biopsies whereas our HDS is best applied in the acute phase of ATI following RTX.

The findings of this study have several interesting implications for both research and the clinic. This human cohort of ATI induced DGF provides insight in the human pathobiology ATI in RTX patients. Furthermore, our HDS might be used to prognosticate functional renal outcome in patients suffering DGF due to ATI after RTX. Although our study is limited to RTX patients with DGF due to ATI, the parameters used in the HDS are universal tubular damage markers and might also be applied in non-RTX associated ATI. The latter is supported by previous findings of Abdulkader et al. (38). A model to assess tubular damage might also be used to evaluate the effect of interventions aimed at reducing post

RTX ATI such as machine perfusion of donor organs or specific medical treatment (45-47). Although we did not find a correlation between parameters of regeneration and renal outcome, our findings form a promising starting point to evaluate the concept of dysfunctional regeneration in the human situation.

In conclusion, we have developed a reproducible histological damage scoring system that predicts renal function after six months as well as speed of recovery of renal function in RTX patients with DGF due to ATI. However, despite the crucial role of regeneration in renal outcome after ATI in experimental models, the regeneration markers used in our study did not correlate to renal outcome 6 months after RTX, which might be explained by the concept of dysfunctional regeneration.

**Acknowledgements**

We would kindly like to thank Roel Broekhuizen for his excellent technical assistance. Lucas L. Falke was sponsored by the Netherlands Institute for Regenerative Medicine (Grant. No. FES0908).



**References**

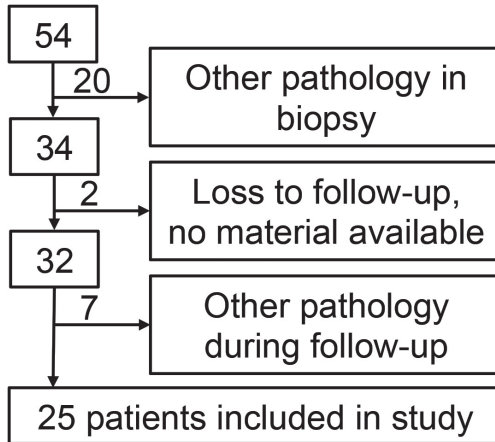
1. Hoste EA, Clermont G, Kersten A, Venkataraman R, Angus DC, De Bacquer D, et al. RIFLE criteria for acute kidney injury are associated with hospital mortality in critically ill patients: a cohort analysis. *Crit Care*. 2006;10(3):R73.
2. Susantitaphong P, Cruz DN, Cerda J, Abulfaraj M, Alqahtani F, Koulouridis I, et al. World incidence of AKI: a meta-analysis. *Clin J Am Soc Nephrol*. 2013;8(9):1482-93.
3. Challiner R, Ritchie JP, Fullwood C, Loughnan P, Hutchison AJ. Incidence and consequence of acute kidney injury in unselected emergency admissions to a large acute UK hospital trust. *BMC Nephrol*. 2014;15:84.
4. Wald R, McArthur E, Adhikari NK, Bagshaw SM, Burns KE, Garg AX, et al. Changing incidence and outcomes following dialysis-requiring acute kidney injury among critically ill adults: a population-based cohort study. *Am J Kidney Dis*. 2015;65(6):870-7.
5. Waikar SS, Curhan GC, Wald R, McCarthy EP, Chertow GM. Declining mortality in patients with acute renal failure, 1988 to 2002. *J Am Soc Nephrol*. 2006;17(4):1143-50.
6. Hsu Y-HR, Sis B. Molecular transplantation pathology: the interface between molecules and histopathology. *Current opinion in organ transplantation*. 2013;18:354-62.
7. Coca SG, Yusuf B, Shlipak MG, Garg AX, Parikh CR. Long-term risk of mortality and other adverse outcomes after acute kidney injury: a systematic review and meta-analysis. *Am J Kidney Dis*. 2009;53(6):961-73.
8. Chawla LS, Kimmel PL. Acute kidney injury and chronic kidney disease: an integrated clinical syndrome. *Kidney Int*. 2012;82(5):516-24.
9. Famulski KS, de Freitas DG, Kreepala C, Chang J, Sellares J, Sis B, et al. Molecular Phenotypes of Acute Kidney Injury in Kidney Transplants. *Journal of the American Society of Nephrology*. 2012;23:948-58.
10. Solez K, Racusen LC, Marcussen N, Slatnik I, Keown P, Burdick JF, et al. Morphology of ischemic acute renal failure, normal function, and cyclosporine toxicity in cyclosporine-treated renal allograft recipients. *Kidney Int*. 1993;43(5):1058-67.
11. Nonclercq D, Toubeau G, Laurent G, Tulkens PM, Heuson-Stiennon JA. Tissue injury and repair in the rat kidney after exposure to cisplatin or carboplatin. *Exp Mol Pathol*. 1989;51(2):123-40.
12. Shimizu A, Masuda Y, Ishizaki M, Sugisaki Y, Yamanaka N. Tubular dilatation in the repair process of ischaemic tubular necrosis. *Virchows Arch*. 1994;425(3):281-90.
13. Adachi T, Sugiyama N, Yagita H, Yokoyama T. Renal atrophy after ischemia-reperfusion injury depends on massive tubular apoptosis induced by TNFalpha in the later phase. *Med Mol Morphol*. 2014;47(4):213-23.
14. Ferenbach DA, Bonventre JV. Mechanisms of maladaptive repair after AKI leading to accelerated kidney ageing and CKD. *Nat Rev Nephrol*. 2015;11(5):264-76.
15. Bussolati B, Bruno S, Grange C, Buttiglieri S, Deregius MC, Cantino D, et al. Isolation of renal progenitor cells from adult human kidney. *The American journal of pathology*. 2005;166:545-55.
16. Kusaba T, Lalli M, Kramann R, Kobayashi A, Humphreys BD. Differentiated kidney epithelial cells repair injured proximal tubule. *Proceedings of the National Academy of Sciences of the United States of America*. 2014;111:1527-32.
17. Loverre A, Capobianco C, Ditonno P, Battaglia M, Grandaliano G, Schena FP. Increase of proliferating renal progenitor cells in acute tubular necrosis underlying delayed graft function. *Transplantation*. 2008;85:1112-9.
18. Kusaba T, Humphreys BD. Controversies on the origin of proliferating epithelial cells after kidney injury. *Pediatric Nephrology*. 2014;29:673-9.
19. Lombardi D, Becherucci F, Romagnani P. How much can the tubule regenerate and who does it? An open question. *Nephrol Dial Transplant*. 2015.
20. Liano F, Pascual J. Epidemiology of acute renal failure: a prospective, multicenter, community-based study. *Madrid Acute Renal Failure Study Group*. *Kidney Int*. 1996;50(3):811-8.
21. Rosen S, Heyman SN. Difficulties in understanding human "acute tubular necrosis": Limited data and flawed animal models. *Kidney International*. 2001;60:1220-4.
22. Shin JH, Koo EH, Ha SH, Park JH, Jang HR, Lee JE, et al. The impact of slow graft function on graft outcome is comparable to delayed graft function in deceased donor kidney transplantation. *Int Urol Nephrol*. 2016;48(3):431-9.
23. Resende L, Guerra J, Santana A, Mil-Homens C, Abreu F, da Costa AG. First year renal function as a predictor of kidney allograft outcome. *Transplant Proc*. 2009;41(3):846-8.
24. Nyberg SL, Matas AJ, Kremers WK, Thostenson JD, Larson TS, Prieto M, et al. Improved scoring system to assess adult donors for cadaver renal transplantation. *American journal of transplantation : official journal of the American Society of Transplantation and the American Society of Transplant Surgeons*. 2003;3:715-21.
25. Nyberg SL, Matas AJ, Rogers M, Harmsen WS, Velosa JA, Larson TS, et al. Donor scoring system for cadaveric renal transplantation. *Am J Transplant*. 2001;1(2):162-70.
26. Kootstra G, Daemen J, Oomen A. Categories of non-heart-beating donors. *Transplantation Proceedings*. 1995;5:2893-4.
27. Remuzzi G, Grinyo J, Ruggenti P, Beatini M, Cole EH, Milford EL, et al. Early experience with dual kidney transplantation in adults using expanded donor criteria. *Double Kidney Transplant Group (DKG)*. *J Am Soc Nephrol*. 1999;10(12):2591-8.
28. van Diest PJ. No consent should be needed for using leftover body material for scientific purposes. *For. BMJ*. 2002;325(7365):648-51.
29. Levey AS, Stevens LA, Schmid CH, Zhang YL, Castro AF, 3rd, Feldman HI, et al. A new equation to estimate glomerular filtration rate. *Ann Intern Med*. 2009;150(9):604-12.
30. Jurikova M, Danihel L, Polak S, Varga I. Ki67, PCNA, and MCM proteins: Markers of proliferation in

the diagnosis of breast cancer. *Acta Histochem.* 2016.

31. Shmelkov SV, St Clair R, Lyden D, Rafii S. AC133/CD133/Prominin-1. *Int J Biochem Cell Biol.* 2005;37(4):715-9.
32. Angelotti ML, Ronconi E, Ballerini L, Peired A, Mazzinghi B, Sagrinati C, et al. Characterization of renal progenitors committed toward tubular lineage and their regenerative potential in renal tubular injury. *Stem Cells.* 2012;30:1714-25.
33. Smeets B, Boor P, Dijkman H, Sharma SV, Jirak P, Mooren F, et al. Proximal tubular cells contain a phenotypically distinct, scattered cell population involved in tubular regeneration. *Journal of Pathology.* 2013;229:645-59.
34. Romagnani P, Remuzzi G. CD133+ renal stem cells always co-express CD24 in adult human kidney tissue. *Stem Cell Research.* 2014;12:828-9.
35. Working Group of the International Ig ANN, the Renal Pathology S, Roberts IS, Cook HT, Troyanov S, Alpers CE, et al. The Oxford classification of IgA nephropathy: pathology definitions, correlations, and reproducibility. *Kidney Int.* 2009;76(5):546-56.
36. Cosio FG, El Ters M, Cornell LD, Schinstock CA, Stegall MD. Changing Kidney Allograft Histology Early Posttransplant: Prognostic Implications of 1-Year Protocol Biopsies. *Am J Transplant.* 2016;16(1):194-203.
37. Gwinner W, Hinzmann K, Erdbruegger U, Scheffner I, Broecker V, Vaske B, et al. Acute tubular injury in protocol biopsies of renal grafts: prevalence, associated factors and effect on long-term function. *Am J Transplant.* 2008;8(8):1684-93.
38. Abdulkader RCRM, Libório AB, Malheiros DMaC. Histological features of acute tubular necrosis in native kidneys and long-term renal function. *Renal failure.* 2008;30:667-73.
39. Pizov G, Friedlaender MM. Immunohistochemical staining for proliferation antigen as a predictor of chronic graft dysfunction and renal graft loss. *Nephron.* 2002;92(3):738-42.
40. Thomasova D, Anders HJ. Cell cycle control in the kidney. *Nephrol Dial Transplant.* 2014.
41. Yang L, Besschetnova TY, Brooks CR, Shah JV, Bonventre JV. Epithelial cell cycle arrest in G2/M mediates kidney fibrosis after injury. *Nat Med.* 2010;16(5):535-43, 1p following 143.
42. Falke LL, Goldschmeding R, Nguyen TQ. A perspective on anti-CCN2 therapy for chronic kidney disease. *Nephrol Dial Transplant.* 2014;29 Suppl 1:i30-i7.
43. Rosen S, Stillman IE. Acute tubular necrosis is a syndrome of physiologic and pathologic dissociation. *J Am Soc Nephrol.* 2008;19(5):871-5.
44. De Vusser K, Lerut E, Kuypers D, Vanrenterghem Y, Jochmans I, Monbaliu D, et al. The Predictive Value of Kidney Allograft Baseline Biopsies for Long-Term Graft Survival. *Journal of the American Society of Nephrology.* 2013;24:1913-23.
45. Hosgood SA, Saeb-Parsy K, Hamed MO, Nicholson ML. Successful transplantation of human kidneys deemed untransplantable but resuscitated by ex-vivo normothermic machine perfusion. *Am J Transplant.* 2016.
46. Jochmans I, Akhtar MZ, Nasralla D, Kocabayoglu P, Boffa C, Kaiser M, et al. Past, present and future of dynamic kidney and liver preservation and resuscitation. *Am J Transplant.* 2016.
47. Aufhauser DD, Jr., Wang Z, Murken DR, Bhatti TR, Wang Y, Ge G, et al. Improved renal ischemia tolerance in females influences kidney transplantation outcomes. *J Clin Invest.* 2016;126(5):1968-77.

Supplementary material

**A**



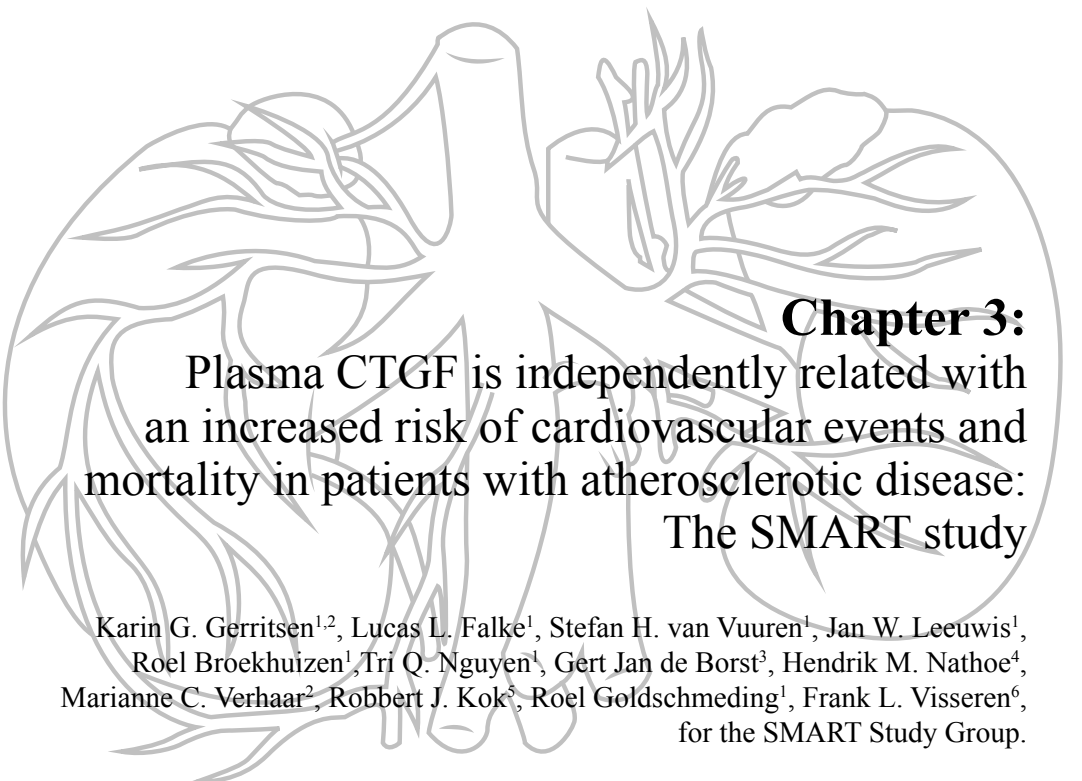

**B**

<b>Appendix to supplemental figure 1</b>	
<b>Reason for exclusion</b>	<b>N</b>
<b>Other pathology in biopsy</b>	
Rejection	12
CNI-toxicity	4
Venous thrombosis, explantation within a month	1
Oxalosis	1
Hilar bleed, venous thrombosis	1
Thrombotic Microangiopathy	1
<b>Other pathology within 6 months after transplantation</b>	
Rejection	4
BK-nephropathy	1
Tubulointerstitial infiltrate and transplantate vasculopathy	1
Chronic ureteric obstruction	1

**Supplemental Figure 1:**

**A:** Flow diagram describing cohort selection process. **B:** Table showing diagnoses in excluded patients who were excluded for cohort because they had pathology other than DGF.

3



## **Chapter 3:** Plasma CTGF is independently related with an increased risk of cardiovascular events and mortality in patients with atherosclerotic disease: The SMART study

Karin G. Gerritsen<sup>1,2</sup>, Lucas L. Falke<sup>1</sup>, Stefan H. van Vuuren<sup>1</sup>, Jan W. Leeuwis<sup>1</sup>,  
Roel Broekhuizen<sup>1</sup>, Tri Q. Nguyen<sup>1</sup>, Gert Jan de Borst<sup>3</sup>, Hendrik M. Nathoe<sup>4</sup>,  
Marianne C. Verhaar<sup>2</sup>, Robbert J. Kok<sup>5</sup>, Roel Goldschmeding<sup>1</sup>, Frank L. Visseren<sup>6</sup>,  
for the SMART Study Group.

1. Dept. of Pathology, University Medical Center Utrecht, The Netherlands
2. Dept. of Nephrology and Hypertension, University Medical Center Utrecht, The Netherlands
3. Dept. of Vascular Surgery, University Medical Center Utrecht, The Netherlands
4. Dept. of Cardiology, University Medical Center Utrecht, The Netherlands
5. Dept. of Pharmaceutics, Utrecht Institute for Pharmaceutical Sciences, Utrecht University,
6. Dept. of Vascular Medicine, University Medical Center Utrecht, The Netherlands

**Abstract**

**Aims:** CTGF plays a key role in tissue fibrogenesis and growing evidence indicates a pathogenic role in cardiovascular disease. Aim of this study is to investigate the association of connective tissue growth factor (CTGF/CCN2) with cardiovascular risk and mortality in patients with manifest vascular disease. **Methods&Results:** Plasma CTGF was measured by ELISA in a prospective cohort study of 1227 patients with manifest vascular disease (mean age 59.0±9.9 years). Linear regression analysis was performed to quantify the association between CTGF and cardiovascular risk factors. Results are expressed as beta ( $\beta$ ) regression coefficients with 95% confidence intervals (CI). The relation between CTGF and the occurrence of new cardiovascular events and mortality was assessed with Cox proportional hazard analysis. Adjustments were made for potential confounding factors. Plasma CTGF was positively related to total cholesterol ( $\beta$  0.040;95%CI 0.013-0.067) and LDL cholesterol ( $\beta$  0.031;95%CI 0.000-0.062) and inversely to glomerular filtration rate ( $\beta$  -0.004;95%CI -0.005 to -0.002). CTGF was significantly lower in patients with cerebrovascular disease. During a median follow-up of 6.5 years (IQR 5.3-7.4) 131 subjects died, 92 experienced an ischemic cardiac complication and 45 an ischemic stroke. CTGF was associated with an increased risk of new vascular events (HR 1.21;95%CI 1.04-1.42), ischemic cardiac events (HR 1.41;95%CI 1.18-1.67) and all-cause mortality (HR 1.18;95%CI 1.00-1.38) for every 1 nmol/L increase in CTGF. No relation was observed between CTGF and the occurrence of ischemic stroke. **Conclusions:** In patients with manifest vascular disease, elevated plasma CTGF confers an increased risk of new cardiovascular events and all-cause mortality.

**Abbreviations and Acronyms**

ACR	-	albumin-to-creatinine ratio
CI	-	confidence interval
cIMT	-	carotid intima media thickness
CTGF	-	connective tissue growth factor
eGFR	-	estimated glomerular filtration rate
DM	-	diabetes mellitus
ELISA	-	enzyme-linked immunosorbent assay
HDL	-	high density lipoprotein
HR	-	hazard ratio
hsCRP	-	high-sensitivity C-reactive protein
IQR	-	interquartile range
LDL	-	low density lipoprotein
LVH	-	left ventricular hypertrophy
NYHA	-	New York Heart Association
RAAS	-	renin-angiotensin-aldosterone system
SMART	-	Secondary Manifestations of ARTERial disease

## Introduction

Cardiovascular risk is a growing concern and major health burden. Several management strategies exist, but healthcare could benefit from additional interventional strategies. Connective tissue growth factor (CTGF/CCN2) is a key mediator of tissue fibrogenesis in various chronic diseases (1). Many cell types express CTGF, including endothelial cells, vascular smooth muscle cells, fibroblasts and cardiac myocytes (2-4). CTGF is upregulated by stimuli involved in cardiovascular damage, including angiotensin II, oxidative stress, endothelin-1, hyperglycaemia, advanced glycation end products, transforming growth factor  $\beta$  and mechanical stretch (5-8). Depending on cell type and pathological context, CTGF is involved in various biological processes, including extracellular matrix production, proliferation, apoptosis, chemotaxis and angiogenesis. Plasma CTGF is elevated in patients with type 1 diabetes mellitus (DM), chronic kidney disease and chronic heart failure (9-14). In patients with type 1 diabetes, plasma CTGF is associated with increased urinary albumin excretion, hypertension and increased carotid intima media thickness (cIMT) and in macroalbuminuric patients also with progression to end stage renal disease and increased mortality (9, 10, 15). Reduction of vascular stiffness in hypertensive patients is associated with a reduction in CTGF expression levels (16). In patients with both acute and chronic heart failure plasma CTGF is related to brain natriuretic peptide, NYHA class and echocardiographic parameters of diastolic dysfunction (14, 17). Emerging evidence also indicates a role of CTGF in the pathogenesis of cardiovascular disease. While being minimally expressed in healthy tissue, CTGF is strongly upregulated in atherosclerotic plaques, in cardiac tissue after myocardial infarction, in cardiac fibrosis and in vascular and cardiac tissues in experimental hypertension (6, 14, 18-20). Thus far however, plasma CTGF has not been studied in patients with clinically manifest vascular disease. Considering the role of CTGF in the pathogenesis of cardiovascular fibrosis, we hypothesized that baseline plasma CTGF may reflect cardiovascular disease burden and may identify vascular patients at the highest risk of recurrent cardiovascular events. Therefore, in the present study we aimed to investigate the association of baseline plasma CTGF with future cardiovascular risk and mortality in a high-risk population of patients with manifest atherosclerotic vascular disease.

## Methods

### *Study design and patients*

We used data from patients enrolled in the Second Manifestations of ARterial disease (SMART) study, an ongoing prospective single-center cohort study in patients with manifest atherosclerotic disease or cardiovascular risk factors that started in September 1996 (21). Patients aged 18-80 years, newly referred to the University Medical Center (UMC) Utrecht with manifest atherosclerotic disease or a cardiovascular risk factor, underwent a vascular screening program including a questionnaire, laboratory assessments and non-invasive screening for manifestations of atherosclerotic disease and cardiovascular risk factors other than the qualifying diagnosis. Patients with terminal malignant disease, those not independent in daily activities (Rankin scale >3) or not sufficiently fluent in Dutch were excluded. The rationale and design of the study, including the criteria for the various manifestations of atherosclerotic disease, have been described in detail (21). The Medical Ethics Committee approved the study, and all participants gave their written informed consent.

For the current study, data of 1227 participants with clinically manifest atherosclerotic disease (coronary heart disease, cerebrovascular disease, peripheral arterial disease or abdominal aortic aneurysm), included between June 2001 and January 2006, was analysed.

### *Data acquisition*

Baseline measurements were performed on a single day at the UMC Utrecht. Medical history, use of current medication and current and past cigarette smoking behaviour were derived from a standardized questionnaire described previously (21). Height, weight and blood pressure were measured. Glomerular filtration rate (GFR) was estimated by the abbreviated Modification of Diet in Renal Disease equation (22). The Framingham 10 year cardiovascular risk score (%) was calculated using gender, age, smoking behaviour, blood levels of HDL and total cholesterol, and systolic blood pressure as parameters as described (23). Ultrasound measurements of cIMT and abdominal adipose tissue were performed as described (21, 24).

Electrocardiographic left ventricular hypertrophy (LVH) was assessed by the Sokolow-Lyon voltage criterion ( $SV1 + RV5/6 > 3.5$  mV)(25) and the Cornell voltage criterion ( $RaVL + SV3 > 2.0$  mV in women and  $>2.8$  mV in men) (26). Patients meeting either criterion were considered to have LVH. For 46 patients no valid electrocardiogram was available.

Blood samples were collected after an overnight fast. Plasma total cholesterol, low density lipoprotein (LDL)-cholesterol, high density lipoprotein (HDL)-cholesterol, triglycerides, homocysteine and creatinine were determined as described (21). High sensitivity C-reactive protein (hsCRP) was measured by immunonephelometry (Nephelometer Analyzer BN II, Dade-Behring, Marburg, Germany). HsCRP measurements below the lower limit of detection of 0.2 mg/l were set at 0.2 mg/l.

Plasma CTGF levels were determined by sandwich ELISA, using two humanized monoclonal antibodies, one for capture and one for detection (FibroGen Inc., San Francisco, CA, USA) against two distinct epitopes on the aminoterminal part of CTGF, detecting both full length CTGF and the N-fragment, as described (9). The detection limit of the assay was 0.02 nmol/L and intra- and interassay variations were <1 and 10%, respectively.

Urine albumin and creatinine were determined as described (21). The albumin-to-creatinine ratio (ACR) was used to estimate albuminuria. Microalbuminuria was defined as  $ACR \geq 3.5$  and  $<25$  mg/mmol (female) or  $\geq 2.5$  and  $<25$  mg/mmol (male) and macroalbuminuria as  $ACR \geq 25$  mg/mmol (27).

### *Follow up*

Patients received a questionnaire every 6 months to provide information on hospitalization and outpatient clinic visits. Outcomes of interest for this study were a composite endpoint of vascular death, ischemic stroke and ischemic cardiac complications (Table 1). All-cause mortality was recorded as well. If a possible event was reported, original source documents were retrieved and reviewed. All possible events were audited by 3 independent physicians of the End Point Committee.



If a patient had multiple events, the first event was used for analysis. Follow-up duration (years) was defined as the period between study inclusion and date of first cardiovascular event, date of death, date of loss to follow-up or the preselected date of 1 March 2010. From 1996 until 1 March 2010, 52 (4%) patients were lost to follow-up due to migration or discontinuation of the study.

**Table 1:** Definition of study outcome events

Ischemic cardiac complication	Myocardial infarction, sudden death or fatal congestive heart failure
Ischemic stroke	Relevant clinical features that caused an increase in impairment of at least one grade on the modified Rankin scale, with or without a new relevant ischemic lesion at brain imaging
Vascular death	Death caused by myocardial infarction, stroke, sudden death (unexpected cardiac death occurring within 1 hour after onset of symptoms, or within 24 hours given convincing circumstantial evidence), congestive heart failure, rupture of abdominal aortic aneurysm or death from another vascular cause
Composite vascular outcome event/ Vascular event	A composite of stroke, ischemic cardiac complication, vascular mortality, retinal infarction or bleeding or fatal rupture of abdominal aortic aneurysm
Other vascular event	A composite of hemorrhagic stroke, retinal infarction or bleeding, sudden death, fatal rupture of abdominal aortic aneurysm and other vascular complications or death.
Nonvascular death	Death caused by infection, cancer, unnatural death, or death from another nonvascular cause.
All-cause mortality	Death of a vascular or non-vascular cause

### Data analysis

Continuous variables are expressed as mean  $\pm$  standard deviation (SD) when normal distributed or as median (interquartile range (IQR)) in case of skewed distribution. Categorical variables are expressed as numbers (percentage). The relation between various patient characteristics and plasma CTGF was quantified with linear regression analysis with CTGF as the dependent variable, and adjustments were made for age, gender and estimated GFR (eGFR). The natural logarithm of CTGF was used to get a normal distribution that allowed parametric analysis. Results are expressed as beta ( $\beta$ ) regression coefficients with 95% confidence intervals (95%CI) denoting the change in plasma CTGF for every change in each individual patient characteristic. Cox proportional hazards analysis was performed to estimate hazard ratios (HRs) with 95% confidence intervals for the occurrence of a new vascular event and all-cause mortality associated with every 1 nmol/L increase in plasma CTGF. Three models were used. In model 1 the unadjusted association between plasma CTGF, cardiovascular events and mortality was examined. In model 2 adjustments were made for age, gender and eGFR, since eGFR was independently associated with plasma CTGF and is also related to cardiovascular outcome. In model 3 additional adjustments were made for the Framingham risk score (%), diabetes mellitus, systolic and diastolic blood pressure, total cholesterol, LDL cholesterol, use of renin angiotensin aldosterone system (RAAS) blockers and use of statins, which are all considered as potentially confounding factors in the relation between CTGF and vascular events. To investigate whether the relation between CTGF and new vascular events and between CTGF and all-cause mortality was modified by gender, we included these interaction terms in the Cox model. If the p-value of the interaction term was  $<0.05$  effect-modification was considered to be present. Next, the study population was divided into tertiles of plasma CTGF and HRs for the occurrence of cardiovascular events and mortality were estimated for each tertile using the lowest plasma CTGF tertile as reference. In addition, one minus survival plots based on Cox regression analysis were made for each CTGF tertile with adjustment for the same confounding variables as included in model 3 (gender, age, eGFR, DM, blood pressure, total cholesterol, use of RAAS blockers and use of statins).

Single imputation methods were used to reduce missing covariate data for smoking (n=8 (<1%)), use of statins (n=48 (4%)), systolic blood pressure (n=1 (<1%)), diastolic blood pressure (n=1 (<1%)), body mass index (n=1 (<1%)), abdominal adipose tissue (n=8 (<1%)), intima media thickness (n=25 (2%)), eGFR (n=14 (1%)), total cholesterol (n=16 (1%)), LDL-cholesterol (n=21 (2%)), HDL-cholesterol (n=21 (2%)), triglycerides (n=19 (2%)), homocysteine (n=18 (1%)) and albuminuria (n=107 (9%)),

since incomplete case analysis leads to loss of statistical power and possibly bias.  $P < 0.05$  was considered significant (two-tailed). All analyses were performed with SPSS software (version 16.0; SPSS Inc., Chicago, Illinois, USA).

## Results

### Relationship between plasma CTGF and patient baseline characteristics

In Table 2 the baseline characteristics of the study population are presented. Mean age was  $59.0 \pm 9.9$  years and 80% was male. The majority of the patients had an eGFR  $>60$  ml/min/1.73m<sup>2</sup> ( $n=1074$  (88%)). Median plasma CTGF was 1.18 nmol/L with a range of 0.18-6.47 nmol/L.

Compared to patients with other vascular disease localizations, plasma CTGF was lowest in patients with cerebrovascular disease. Plasma CTGF was inversely related to eGFR, adjusted for age and gender ( $\beta$  -0.004 using the natural logarithm of CTGF; 95%CI -0.005 to -0.002), which implies that for every 1 mL/min/1.73m<sup>2</sup> increase in eGFR plasma CTGF decreased with 0.4% (95%CI 0.2 to 0.5) (Table 3). Univariate analysis revealed that plasma CTGF relates to total cholesterol and LDL cholesterol ( $R^2 = 0.0061$ ,  $p < 0.01$  and  $R^2 = 0.0031$ ,  $p < 0.01$  respectively; Suppl. Fig. 1). After adjustment for age, gender and eGFR, plasma CTGF remained positively associated with total cholesterol ( $\beta$  0.040; 95%CI 0.013 to 0.067) and LDL cholesterol ( $\beta$  0.031; 95%CI 0.000 to 0.062) concentrations, after adjustment for age, gender and eGFR. Plasma CTGF was not related to DM, blood pressure or pulse pressure, BMI or abdominal adipose tissue, left ventricular hypertrophy, cIMT, smoking, use of RAAS blockers, hsCRP or albuminuria. There were no indications for presence of a J-shaped relationship between these variables and plasma CTGF.

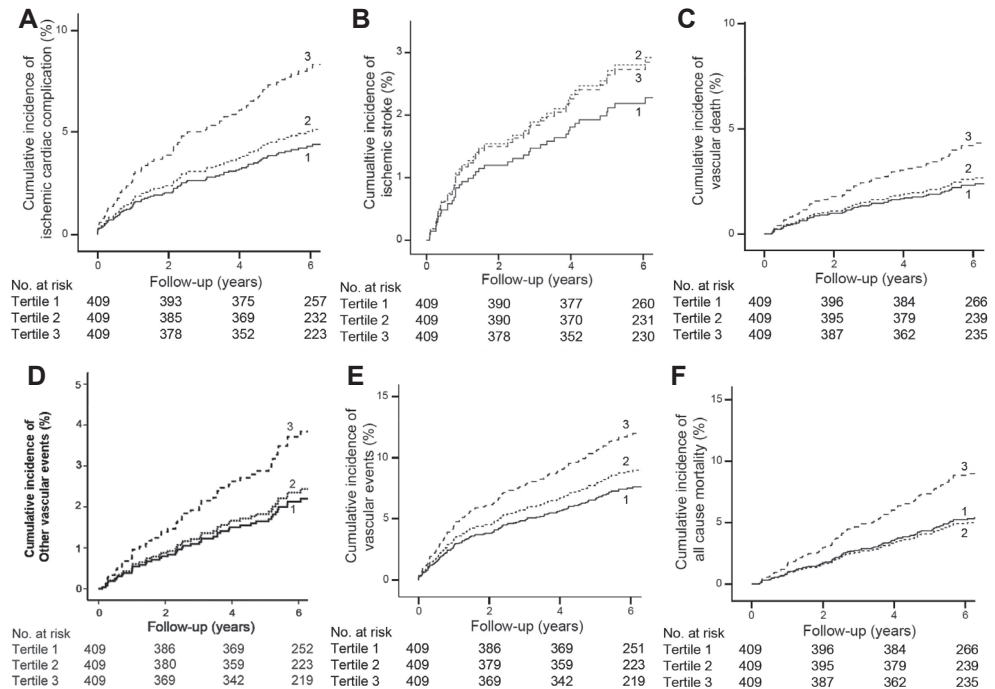


**Figure 1:** Cumulative percentage of study population with a new cardiovascular event or death according to tertiles of plasma CTGF. One minus survival plots based on Cox regressions using multivariate model III (age, gender, estimated glomerular filtration rate, diabetes mellitus, blood pressure, use of RAAS blockers, total cholesterol and use of statins). (A) Ischemic cardiac complication. (B) Ischemic stroke. (C) Vascular death. (D) Other vascular events. (E) All vascular events. (F) All-cause mortality.

**Table 2:** Baseline characteristics of the study population (n=1227).

Characteristic	
Age (years)	59.0 ± 9.9
Male gender, n (%)	986 (80)
Hypertension (ever or current), n (%)	638 (52)
Diabetes mellitus, n (%)	199 (16)
Type 1, n (%)	6 (1)
Type 2, n (%)	193 (16)
Smoking	
Former, n (%); current, n (%)	578 (47); 438 (36)
Pack years	20.2 (6.1-34.2)
Framingham risk score (average 10year risk in %)	13.4 ± 9.27
Medication	
Blood pressure lowering agents, n (%)	914 (75)
RAAS blocker, n (%)	409 (33)
Statin, n (%)	786 (64)
Anti-platelet agents, n (%)	933 (76)
Measurements	
Systolic blood pressure (mmHg)	142 ± 22
Diastolic blood pressure (mmHg)	82 ± 12
Pulse pressure (mmHg)	58 (50-69)
Body mass index (kg/m <sup>2</sup> )	26.9 ± 3.8
Abdominal adipose tissue (cm)	9.5 ± 2.6
Intima media thickness (mm)	0.90 (0.75-1.07)
eGFR (mL/min/1.73m <sup>2</sup> )	78.1 (67.3-88.8)
Left ventricular hypertrophy*, n (%)	294 (25)
Laboratory measurements	
Total cholesterol (mmol/L)	4.9 ± 1.0
LDL cholesterol (mmol/L)	2.9 ± 0.9
HDL cholesterol (mmol/L)	1.3 ± 0.4
Triglycerides (mmol/L)	1.50 (1.10-2.11)
HsCRP (mg/L)	2.0 (0.9-4.1)
Homocysteine (μmol/l.)	12.8 (10.5-15.5)
Microalbuminuria, n (%)	233 (19)
Macroalbuminuria, n (%)	39 (3)
Plasma CTGF (nmol/L)	1.18 (0.89-1.64)
Localization of vascular disease†	
Cerebrovascular disease, n (%)	293 (24)
Coronary artery disease, n (%)	755 (62)
Aneurysm abdominal aorta, n (%)	112 (9)
Peripheral arterial disease, n (%)	279 (23)

Data are expressed as mean ± SD, median (interquartile range) or absolute number (percentage).

\*A valid ECG was available in 1181 patients. †Patients could be classified into one or more categories.

#### CTGF and risk of cardiovascular events and mortality

During a median follow-up of 6.5 years (IQR 5.3-7.4) (total number of follow-up years 7637), 131 subjects died (of whom 73 due to a cardiovascular cause), 92 experienced an ischemic cardiac complication and 45 an ischemic stroke. After adjustment for age, gender and eGFR, every 1 nmol/L increase in plasma CTGF was associated with an increased risk of all vascular events (HR 1.21; 95%CI 1.04-1.41), ischemic cardiac events (HR 1.39; 95%CI 1.17-1.65) and all-cause mortality (HR 1.19; 95%CI 1.02-1.39) (Table 4). RAAS activation, diabetes mellitus and changes in cholesterol metabolism are phenomena known to influence plasma CTGF levels (28-30). Therefore, additional adjustment for DM, blood pressure, total cholesterol, LDL cholesterol, use of RAAS blockers and use of statins

were made. However, none substantially changed the relation between CTGF and cardiovascular events (model 3). Additional analyses adjusting for factors that were possibly in the causal pathway (Framingham risk score, cIMT, pulse pressure, hsCRP, left ventricular hypertrophy, LDL and albuminuria) also did not markedly alter the HRs (data not shown). The risk of ischemic stroke associated with plasma CTGF was not significantly increased (HR 0.88; 95%CI 0.61-1.27). The relation between CTGF and subsequent vascular events and between CTGF and all-cause mortality was not modified by gender (p-values for interaction 0.335 for all vascular events and 0.223 for all-cause mortality). We further assessed the relationship between plasma CTGF and cardiovascular events and mortality by dividing the study population into tertiles of plasma CTGF (Figure 1, Table 5). Compared to patients in the lowest tertile of plasma CTGF, patients in the highest tertile had a 61% higher risk of developing a new cardiovascular event and a 75% higher risk of dying from any cause, after adjustment for age, gender and eGFR (Table 5). HR for nonvascular death in the highest tertile did not reach significance when the lowest tertile was used as reference, but was significantly higher when the lowest and middle tertile were combined into a single reference group (HR 1.79; 95%CI 1.06-3.03).

**Table 3:** Relation between various patient characteristics and plasma CTGF (n=1227).

Characteristic	$\beta$ (95% CI)*	CTGF change (%) (95% CI)†
Age (years)	0.003 (0.000 to 0.006)*	0.3 (0.0-0.6)
Gender (male=1)	-0.053 (-0.125 to 0.018)	-5.2 (-11.8 to 1.8)
Hypertension (ever or current) (yes=1)	0.009 (-0.049 to 0.066)	0.9 (-4.8 to 6.8)
Diabetes mellitus (yes=1)	0.039 (-0.116 to 0.037)	4.0 (-11.0 to 3.8)
Type 1 (yes=1)	0.019 (-0.386 to 0.423)	1.9 (-32.0 to 52.7)
Type 2 (yes=1)	-0.041 (-0.118 to 0.037)	-4.0 (-11.1 to 3.7)
Smoking		
Smoking status‡	0.019 (-0.006 to 0.044)	1.9 (-0.6 to 4.5)
Pack years	0.001 (-0.001 to 0.002)	0.1 (0.0 to 0.2)
Framingham Risk score (%)	0.002 (-0.001 to 0.006)	1.0 (0.99 to 1.01)
Medication		
RAAS blocker (yes=1)	-0.004 (-0.067 to 0.059)	-0.4 (-6.5 to 6.1)
Statin (yes=1)	-0.031 (-0.091 to 0.029)	-3.1 (-8.7 to 2.9)
Measurements		
Systolic blood pressure (per 10 mmHg)	-0.001 (-0.015 to 0.012)	-0.1 (-1.5 to 1.2)
Diastolic blood pressure (per 10 mmHg)	-0.010 (-0.034 to 0.014)	-1.0 (-3.3 to 1.4)
Pulse pressure (per 10 mmHg)	0.009 (-0.011 to 0.030)	0.9 (-1.1 to 3.0)
Body mass index (kg/m <sup>2</sup> )	-0.003 (-0.011 to 0.004)	-0.3 (-1.1 to 0.4)
Abdominal adipose tissue (cm)	0.000 (-0.011 to 0.012)	0.0 (-1.1 to 1.2)
Intima media thickness (mm)	-0.004 (-0.097 to 0.090)	-0.4 (-9.2 to 9.4)
eGFR (mL/min/1.73m <sup>2</sup> )	-0.004 (-0.005 to -0.002)*	-0.4 (-0.5 to -0.2)
Left ventricular hypertrophy§ (yes=1)	-0.027 (-0.095 to 0.041)	-2.7 (-9.1 to 4.2)
Laboratory measurements		
Lipids		
Total cholesterol (mmol/L)	0.040 (0.013 to 0.067)*	4.1 (1.3 to 6.9)
LDL cholesterol (mmol/L)	0.031 (0.000 to 0.062)*	3.1 (0.0 to 6.4)
HDL cholesterol (mmol/L)	0.051 (-0.029 to 0.130)	5.2 (-2.9 to 13.9)
Triglycerides (mmol/L)	0.023 (-0.002 to 0.048)	2.3 (-0.2 to 4.9)
HsCRP (mg/L)	0.002 (-0.002 to 0.005)	0.2 (-0.2 to 0.5)
Homocysteine (μmol/L)	0.003 (-0.002 to 0.008)	0.3 (-0.2 to 0.8)
Albuminuria	0.020 (-0.036 to 0.077)	2.0 (-3.5 to 8.0)

Adjustment for age, gender and eGFR. \*Data are expressed as beta regression coefficient ( $\beta$ ) with 95% CI calculated with multiple linear regression. The natural logarithm of CTGF will increase with  $\beta$  and CTGF will be multiplied by  $e\beta$  if the variable increases by 1 unit or changes from 0 to 1 for a dichotomous variable.

†Relative change in CTGF (with CI) if the patient variable increases by 1 unit or changes from 0 to 1 for a dichotomous variable. ‡Never=0, former=1, current=3. §N=1181. ¶Normoalbuminuria=0, microalbuminuria=1, macroalbuminuria=2. \*significant correlation (p<0.05)

**Table 4:** HR for vascular events and mortality for each 1nmol/L increase of plasma CTGF

	# Events	Hazard ratio (95% CI)		
		Model I	Model II	Model III
Ischemic cardiac complication	92	1.44 (1.22-1.71)	1.39 (1.17-1.65)	1.41 (1.18-1.67)
Ischemic stroke	45	1.01 (0.72-1.42)	0.88 (0.61-1.27)	0.88 (0.61-1.28)
Vascular death	73*	1.31 (1.07-1.60)	1.13 (0.91-1.40)	1.11 (0.89-1.38)
All vascular events	153	1.30 (1.12-1.50)	1.21 (1.04-1.41)	1.21 (1.04-1.42)
Other vascular events	61	1.38 (1.12-1.72)	1.24 (0.99-1.55)	1.21 (0.96-1.54)
Nonvascular death	57*	1.31 (1.04-1.64)	1.25 (0.99-1.57)	1.26 (1.00-1.60)
All cause mortality	131	1.31 (1.13-1.52)	1.19 (1.02-1.39)	1.18 (1.00-1.38)

Uni/Multivariate Cox proportional hazards regression analysis Model I = univariate; model II = adjustment for age, gender and estimated glomerular filtration rate; model III = model II with additional adjustment for type I and type II diabetes mellitus, systolic and diastolic blood pressure, total cholesterol, use of RAAS blockers and use of statins.

\*One deceased patient was not classified as vascular or nonvascular death.

**Table 5:** Hazard ratios of plasma CTGF tertiles for new vascular events and all-cause mortality.

Plasma CTGF	Tertile 1		Tertile 2		Tertile 3	
Median (range)	0.78 (0.18-0.98)		1.18 (0.98-1.48)		1.85 (1.48-6.47)	
(nmol/L)						
Tertile size	n=409		n=409		n=409	
	Model	Events ref.†	Events	HR (95% CI)	Events	HR (95% CI)
Ischemic cardiac complication	I	23 1.00	27	1.22 (0.70-2.13)	42	2.02 (1.22-3.37)
	II	1.00		1.19 (0.68-2.08)		1.89 (1.13-3.17)
	III	1.00		1.17 (0.67-2.05)		1.93 (1.15-3.23)
Ischemic stroke	I	11 1.00	17	1.57 (0.74-3.36)	17	1.63 (0.77-3.49)
	II	1.00		1.37 (0.64-2.95)		1.28 (0.59-2.77)
	III	1.00		1.29 (0.60-2.78)		1.25 (0.57-2.73)
Vascular death	I	17 1.00	21	1.30 (0.68-2.46)	35*	2.32 (1.30-4.15)
	II	1.00		1.15 (0.60-2.18)		1.81 (1.00-3.27)
	III	1.00		1.12 (0.59-2.13)		1.83 (1.00-3.34)
All vascular events	I	39 1.00	49	1.31 (0.86-2.00)	65	1.83 (1.23-2.73)
	II	1.00		1.22 (0.80-1.87)		1.61 (1.08-2.41)
	III	1.00		1.19 (0.78-1.82)		1.61 (1.08-2.42)
Other vascular events	I	15 1.00	18	1.28 (0.64-2.53)	28	2.13 (1.13-3.99)
	II	1.00		1.14 (0.57-2.28)		1.79 (0.94-3.39)
	III	1.00		1.11 (0.56-2.22)		1.76 (0.92-3.37)
Nonvascular death	I	17 1.00	14	0.86 (0.42-1.74)	26*	1.73 (0.94-3.19)
	II	1.00		0.81 (0.40-1.65)		1.62 (0.87-3.00)
	III	1.00		0.79 (0.39-1.61)		1.58 (0.85-2.95)
All cause mortality	I	34 1.00	35	1.08 (0.67-1.72)	62*	2.06 (1.35-3.13)
	II	1.00		0.98 (0.61-1.58)		1.75 (1.15-2.69)
	III	1.00		0.94 (0.58-1.51)		1.72 (1.21-2.65)

Uni/Multivariate Cox proportional hazards regression analysis. Model I = univariate; model II = adjustment for age, gender and estimated glomerular filtration rate; model III = model II with additional adjustment for type I and type II diabetes mellitus, systolic and diastolic blood pressure, total cholesterol, use of RAAS blockers and use of statins. \*One deceased patient was not classified as vascular or nonvascular death. † Reference HR for tertile 2 and 3.

## Discussion

The main finding of the present study is that baseline plasma CTGF is associated with an increased risk of new cardiovascular events and mortality in patients with clinically manifest atherosclerotic vascular disease in a large population of patients with manifest vascular disease. This was independent of established cardiovascular risk factors

Plasma CTGF has been studied in patients with type I DM and was found to be an independent predictor of all-cause mortality in patients with diabetic nephropathy (10). We recently found a positive association between plasma CTGF and risk of all-cause mortality in end stage renal disease patients on hemodialysis (31). In line with these findings, we observed a robust relationship between plasma CTGF and risk of death in the current study population of patients with manifest vascular disease. CTGF was associated with both vascular and nonvascular death. This might be explained by CTGF as a key determinant of activity of tissue fibrogenesis, and fibrosis as the common final pathway of chronic diseases of diverse etiology. Besides fibrosis, CTGF has been implicated in various other pathological processes, such as ischemia, inflammation and metabolic derangements (4, 32, 33).

In addition to the association with mortality, we found a clear association between CTGF and risk of new cardiovascular events and, in particular, of ischemic cardiac complications. This finding raises the question whether CTGF has a causal role in atherosclerosis and ischemic heart disease or merely reflects a large cardiovascular disease burden. In atherosclerotic plaques and fibrotic myocardium CTGF expression is strongly upregulated (6) and high plasma CTGF levels may result from high CTGF release into the circulation. In the current study, however, plasma CTGF was not associated with surrogate markers of atherosclerotic burden such as cIMT (34) and pulse pressure (35), nor with left ventricular hypertrophy which is linked to cardiac fibrosis (36). Pre-clinical studies suggest a role for CTGF in atherogenesis. *In vitro*, CTGF increases vascular smooth muscle cell (VSMC) proliferation, migration and extracellular matrix production, which may contribute to neointima formation (37). Mesenchymal Stem Cells (MSCs) are circulating cells involved in arterial repair by mesenchymal to endothelial transdifferentiation (38). Stimulation of mesenchymal stem with CTGF leads to fibroblastic differentiation and increased extracellular matrix production (39, 40). Pericytes are the major vascular supportive cell type involved in maintenance of vascular homeostasis and integrity. Under pathological conditions pericytes transdifferentiate to myofibroblasts, thus compromising their role in vascular support (41, 42). Culturing pericytes with CTGF under pathological conditions increased expression of extracellular matrix genes Col1 $\alpha$ 2 and Fibronectin as well as myofibroblast associated gene  $\alpha$ Smooth Muscle Actin (Supp. Fig. 2), which are all markers associated with neointima hyperplasia and myofibroblast accumulation. Furthermore, CTGF promoted adherence and migration of monocytes and activated platelets to VSMCs (43-45). *In vitro* it has been shown that CTGF stimulates osteogenic differentiation of VSMC (46). For instance, CTGF is associated with angiogenesis (47), and CTGF mediated modulation results in reduced VEGF-A signaling (48). Taken together, this suggests a major role for CTGF in vascular disease by switching angiogenesis and vascular repair towards neointima formation and atherogenesis.

In a murine model, CTGF injection leads to increased oxidative stress and a vascular inflammatory response associated with endothelial dysfunction (49). CTGF has been implicated in hypertension induced organ damage via mechanical stress induced CTGF gene expression in endothelial cells, vascular smooth muscle cells and cardiomyocytes (50-52). The role of CTGF in the aetiology of cardiomyopathy is controversial. Cardiac CTGF expression is increased after ischemic-reperfusion injury and is associated with replacement and reactive fibrosis following myocardial infarction (6). Myocardial overexpression of CTGF in transgenic mice promoted age-dependent development of cardiac hypertrophy (53) and enhanced pressure-overload induced cardiac fibrosis (54). In line with this, dilating cardiomyopathy appears to be CTGF regulated (55), and CTGF reduction attenuates left ventricular remodeling and dysfunction in models of pressure overload (56). However, in other animal models of chronic pressure overload it has been reported that alteration of CTGF levels are of little consequence to the phenotype (57, 58). In stark contrast, it has also been reported that CTGF

exerts protective effects during experimental cardiac pressure overload (59). Additional evidence for a pathogenic role of CTGF in cardiovascular disease comes from a study in experimental diabetes, which showed that neutralizing anti-CTGF antibody therapy prevented and reversed arterial stiffening, cardiac dysfunction and hypertension (60). Future studies should clarify the role of CTGF in the pathogenesis of cardiovascular disease and should evaluate whether anti-CTGF therapies are beneficial.

An interesting question is what the source is of the increased plasma CTGF in patients with manifest cardiovascular disease. The N-terminal CTGF cleavage fragment is the predominant form of CTGF in plasma and is largely cleared by the kidney (61). Indeed in our study, plasma CTGF was negatively related to eGFR. However, multivariate survival analysis adjusting for eGFR showed CTGF to be independent of renal clearance, indicating an additional contribution of locoregional de novo production. Under physiological circumstances CTGF is produced at low levels. As discussed in cardiovascular pathology increased CTGF expression has been shown in many tissues and cells, including atherosclerotic plaques and fibrotic myocardium (6, 20), cardiomyocytes and fibroblasts upon myocardial infarction (6) and endothelial cells, vascular smooth muscle cells and cardiomyocytes exposed to mechanical stress as in hypertension (50-52). However, given the wide variety of tissues that overexpress CTGF during disease that are also involved in cardiovascular disease, the source of the excessive plasma CTGF is probably even more diverse.

Our finding that CTGF is associated with total and LDL cholesterol may suggest that CTGF is involved in the pathway through which lipoproteins promote the development of atherosclerotic vascular disease. This is supported by previous observations that treatment of human aortic endothelial cells with LDL induced CTGF gene expression (62) and that HMG-CoA reductase inhibitors inhibited CTGF induction in human umbilical cord endothelial cells exposed to non-uniform shear stress (63).

Remarkably, while the association with the composite endpoint of vascular events was evident, we did not observe an increased risk of ischemic stroke in patients with higher baseline plasma CTGF. Plasma CTGF was lower in patients with previous cerebrovascular disease, but stratification for prior cerebrovascular disease did not substantially change the results. Although our study provides no proper explanation for the discrepancy between cerebrovascular and other vascular events, it is interesting to note that in a previous study we observed an association between CTGF levels in carotid plaques from patients undergoing carotid endarterectomy and stable plaque characteristics (19).

### Study limitations

We acknowledge several limitations of this study. First, we measured CTGF only once at baseline. However, it is not known to what extent CTGF levels vary over time in the individual patient. Second, recruitment was conducted at a single center and the study population included mainly Caucasian patients. Both facts limit the generalization of our results to a wider-ranging population with manifest vascular disease. Strengths of the present study are the large number of well-described patients with various manifestations of atherosclerotic vascular disease and the virtually complete follow-up.

### Conclusions

Elevated plasma CTGF increases the risk of cardiovascular events and all-cause mortality in patients with manifest vascular disease. CTGF may therefore be regarded as a novel marker to identify vascular patients at the highest risk of recurrent cardiovascular events and mortality.

## References

1. Dendooven A, Gerritsen KG, Nguyen TQ, Kok RJ, Goldschmeding R. Connective tissue growth factor (CTGF/CCN2) ELISA: a novel tool for monitoring fibrosis. *Biomarkers : biochemical indicators of exposure, response, and susceptibility to chemicals.* 2011;16(4):289-301.
2. Yan LF, Wei YN, Nan HY, Yin Q, Qin Y, Zhao X, et al. Proliferative phenotype of pulmonary microvascular endothelial cells plays a critical role in the overexpression of CTGF in the bleomycin-injured rat. *Experimental and toxicologic pathology : official journal of the Gesellschaft für Toxikologische Pathologie.* 2014;66(1):61-71.
3. Van Geest RJ, Leeuwis JW, Dendooven A, Pfister F, Bosch K, Hoeben KA, et al. Connective tissue growth factor is involved in structural retinal vascular changes in long-term experimental diabetes. *The journal of histochemistry and cytochemistry : official journal of the Histochemistry Society.* 2014;62(2):109-18.
4. Ohnishi H, Oka T, Kusachi S, Nakanishi T, Takeda K, Nakahama M, et al. Increased expression of connective tissue growth factor in the infarct zone of experimentally induced myocardial infarction in rats. *Journal of molecular and cellular cardiology.* 1998;30(11):2411-22.
5. Ruiz-Ortega M, Rodriguez-Vita J, Sanchez-Lopez E, Carvajal G, Egido J. TGF-beta signaling in vascular fibrosis. *Cardiovascular research.* 2007;74(2):196-206.
6. Daniels A, van Bilzen M, Goldschmeding R, van der Vusse GJ, van Nieuwenhoven FA. Connective tissue growth factor and cardiac fibrosis. *Acta Physiol (Oxf).* 2009;195(3):321-38.
7. Cicha I, Goppelt-Strube M. Connective tissue growth factor: context-dependent functions and mechanisms of regulation. *Biofactors.* 2009;35(2):200-8.
8. Lan TH, Huang XQ, Tan HM. Vascular fibrosis in atherosclerosis. *Cardiovascular pathology : the official journal of the Society for Cardiovascular Pathology.* 2013;22(5):401-7.
9. Roestenberg P, van Nieuwenhoven FA, Wieten L, Boer P, Diekman T, Tiller AM, et al. Connective tissue growth factor is increased in plasma of type 1 diabetic patients with nephropathy. *Diabetes care.* 2004;27(5):1164-70.
10. Nguyen TQ, Tarnow L, Jorsal A, Oliver N, Roestenberg P, Ito Y, et al. Plasma connective tissue growth factor is an independent predictor of end-stage renal disease and mortality in type 1 diabetic nephropathy. *Diabetes care.* 2008;31(6):1177-82.
11. Cheng O, Thuillier R, Sampson E, Schultz G, Ruiz P, Zhang X, et al. Connective tissue growth factor is a biomarker and mediator of kidney allograft fibrosis. *American journal of transplantation : official journal of the American Society of Transplantation and the American Society of Transplant Surgeons.* 2006;6(10):2292-306.
12. Slagman MC, Nguyen TQ, Waanders F, Vogt L, Hemmelder MH, Laverman GD, et al. Effects of antiproteinuric intervention on elevated connective tissue growth factor (CTGF/CCN-2) plasma and urine levels in nondiabetic nephropathy. *Clinical journal of the American Society of Nephrology : CJASN.* 2011;6(8):1845-50.
13. Ito Y, Aten J, Nguyen TQ, Joles JA, Matsuo S, Weening JJ, et al. Involvement of connective tissue growth factor in human and experimental hypertensive nephrosclerosis. *Nephron Experimental nephrology.* 2011;117(1):e9-20.
14. Koitabashi N, Arai M, Niwano K, Watanabe A, Endoh M, Suguta M, et al. Plasma connective tissue growth factor is a novel potential biomarker of cardiac dysfunction in patients with chronic heart failure. *European journal of heart failure.* 2008;10(4):373-9.
15. Jaffa AA, Usinger WR, McHenry MB, Jaffa MA, Lipstiz SR, Lackland D, et al. Connective tissue growth factor and susceptibility to renal and vascular disease risk in type 1 diabetes. *The Journal of clinical endocrinology and metabolism.* 2008;93(5):1893-900.
16. Gomez-Garre D, Martin-Ventura JL, Granados R, Sancho T, Torres R, Ruano M, et al. Losartan improves resistance artery lesions and prevents CTGF and TGF-beta production in mild hypertensive patients. *Kidney international.* 2006;69(7):1237-44.
17. Behnes M, Brueckmann M, Lang S, Weiss C, Ahmad-Nejad P, Neumaier M, et al. Connective tissue growth factor (CTGF/CCN2): diagnostic and prognostic value in acute heart failure. *Clinical research in cardiology : official journal of the German Cardiac Society.* 2014;103(2):107-16.
18. Rickard AJ, Morgan J, Chrissobolis S, Miller AA, Sobey CG, Young MJ. Endothelial cell mineralocorticoid receptors regulate deoxycorticosterone/salt-mediated cardiac remodeling and vascular reactivity but not blood pressure. *Hypertension.* 2014;63(5):1033-40.
19. Leeuwis JW, Nguyen TQ, Theunissen MG, Peeters W, Goldschmeding R, Pasterkamp G, et al. Connective tissue growth factor is associated with a stable atherosclerotic plaque phenotype and is involved in plaque stabilization after stroke. *Stroke; a journal of cerebral circulation.* 2010;41(12):2979-81.
20. Ponticos M. Connective tissue growth factor (CCN2) in blood vessels. *Vascular pharmacology.* 2013;58(3):189-93.
21. Simons PC, Algra A, van de Laak MF, Grobbee DE, van der Graaf Y. Second manifestations of ARterial disease (SMART) study: rationale and design. *European journal of epidemiology.* 1999;15(9):773-81.
22. Levey AS, Coresh J, Greene T, Stevens LA, Zhang YL, Hendriksen S, et al. Using standardized serum creatinine values in the modification of diet in renal disease study equation for estimating glomerular filtration rate. *Annals of internal medicine.* 2006;145(4):247-54.
23. Wilson PW, D'Agostino RB, Levy D, Belanger AM, Silbershatz H, Kannel WB. Prediction of coronary heart disease using risk factor categories. *Circulation.* 1998;97(18):1837-47.
24. Stolk RP, Meijer R, Mali WP, Grobbee DE, van der Graaf Y. Ultrasound measurements of intraabdominal fat estimate the metabolic syndrome better than do measurements of waist circumference. *The American journal of clinical nutrition.* 2003;77(4):857-60.
25. Sokolow M, Lyon TP. The ventricular complex in left ventricular hypertrophy as obtained by unipolar



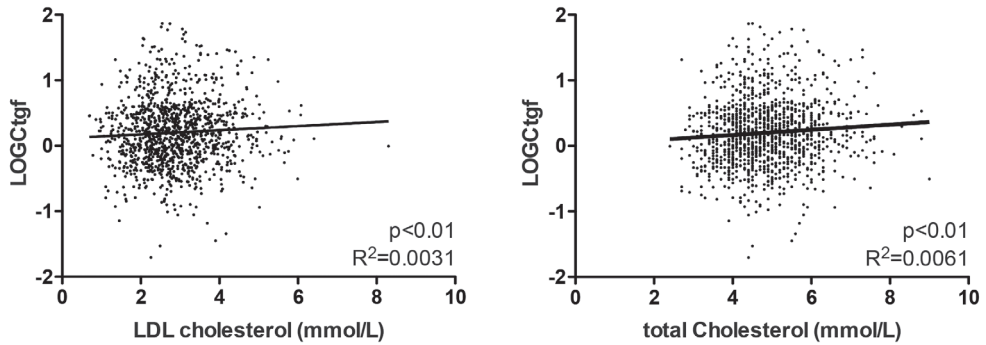
- precordial and limb leads. 1949. *Annals of noninvasive electrocardiology* : the official journal of the International Society for Holter and Noninvasive Electrocardiology, Inc. 2001;6(4):343-68.
26. Casale PN, Devereux RB, Kligfield P, Eisenberg RR, Miller DH, Chaudhary BS, et al. Electrocardiographic detection of left ventricular hypertrophy: development and prospective validation of improved criteria. *Journal of the American College of Cardiology*. 1985;6(3):572-80.
27. Tapp RJ, Shaw JE, Zimmet PZ, Balkau B, Chadban SJ, Tonkin AM, et al. Albuminuria is evident in the early stages of diabetes onset: results from the Australian Diabetes, Obesity, and Lifestyle Study (AusDiab). *American journal of kidney diseases* : the official journal of the National Kidney Foundation. 2004;44(5):792-8.
28. Wolf G. Renal injury due to renin-angiotensin-aldosterone system activation of the transforming growth factor-beta pathway. *Kidney international*. 2006;70(11):1914-9.
29. Yang B, Hodgkinson AD, Shaw NA, Millward BA, Demaine AG. Protective effect of statin therapy on connective tissue growth factor induction by diabetes in vivo and high glucose in vitro. *Growth Factors*. 2013;31(6):199-208.
30. Watts KL, Spiteri MA. Connective tissue growth factor expression and induction by transforming growth factor-beta is abrogated by simvastatin via a Rho signaling mechanism. *Am J Physiol Lung Cell Mol Physiol*. 2004;287(6):L1323-32.
31. Den Hoedt CH, Gerritsen KG, Grooteman MP, Penne EL, Van der Weerd NC, Mazairac AH, et al. Connective tissue growth factor is related to all cause mortality in hemodialysis patients and is lowered by on-line hemodiafiltration. Results from the CONvective TRANsport SStudy. Thesis K Gerritsen: Pharmacokinetics of Connective Tissue Growth Factor. 2012:Chapter 8.
32. Sanchez-Lopez E, Rayego S, Rodrigues-Diez R, Rodriguez JS, Rodriguez-Vita J, Carvajal G, et al. CTGF promotes inflammatory cell infiltration of the renal interstitium by activating NF-kappaB. *Journal of the American Society of Nephrology* : JASN. 2009;20(7):1513-26.
33. Roestenberg P, van Nieuwenhoven FA, Joles JA, Trischberger C, Martens PP, Oliver N, et al. Temporal expression profile and distribution pattern indicate a role of connective tissue growth factor (CTGF/CCN-2) in diabetic nephropathy in mice. *American journal of physiology Renal physiology*. 2006;290(6):F1344-54.
34. Poredos P. Intima-media thickness: indicator of cardiovascular risk and measure of the extent of atherosclerosis. *Vasc Med*. 2004;9(1):46-54.
35. Syeda B, Gottsauner-Wolf M, Denk S, Pichler P, Khorsand A, Glogar D. Arterial compliance: a diagnostic marker for atherosclerotic plaque burden? *American journal of hypertension*. 2003;16(5 Pt 1):356-62.
36. Weber KT, Brilla CG. Structural basis for pathologic left ventricular hypertrophy. *Clinical cardiology*. 1993;16(5 Suppl 2):II10-4.
37. Fan WH, Pech M, Karnovsky MJ. Connective tissue growth factor (CTGF) stimulates vascular smooth muscle cell growth and migration in vitro. *European journal of cell biology*. 2000;79(12):915-23.
38. Wan M, Li C, Zhen G, Jiao K, He W, Jia X, et al. Injury-activated transforming growth factor beta controls mobilization of mesenchymal stem cells for tissue remodeling. *Stem Cells*. 2012;30(11):2498-511.
39. Lee CH, Shah B, Muioli EK, Mao JJ. CTGF directs fibroblast differentiation from human mesenchymal stem/stromal cells and defines connective tissue healing in a rodent injury model. *J Clin Invest*. 2010;120(9):3340-9.
40. Li C, Zhen G, Chai Y, Xie L, Crane JL, Farber E, et al. RhoA determines lineage fate of mesenchymal stem cells by modulating CTGF-VEGF complex in extracellular matrix. *Nat Commun*. 2016;7:11455.
41. Humphreys BD, Lin SL, Kobayashi A, Hudson TE, Nowlin BT, Bonventre JV, et al. Fate tracing reveals the pericyte and not epithelial origin of myofibroblasts in kidney fibrosis. *Am J Pathol*. 2010;176(1):85-97.
42. van Dijk CG, Nieuweboer FE, Pei JY, Xu YJ, Burgisser P, van Mulligen E, et al. The complex mural cell: pericyte function in health and disease. *International journal of cardiology*. 2015;190:75-89.
43. Cicha I, Yilmaz A, Klein M, Raithe D, Brigstock DR, Daniel WG, et al. Connective tissue growth factor is overexpressed in complicated atherosclerotic plaques and induces mononuclear cell chemotaxis in vitro. *Arteriosclerosis, thrombosis, and vascular biology*. 2005;25(5):1008-13.
44. Jedsadayamata A, Chen CC, Kireeva ML, Lau LF, Lam SC. Activation-dependent adhesion of human platelets to Cyr61 and Fisp12/mouse connective tissue growth factor is mediated through integrin alpha(IIb)beta(3). *The Journal of biological chemistry*. 1999;274(34):24321-7.
45. Schober JM, Chen N, Grzeszkiewicz TM, Jovanovic I, Emeson EE, Ugarova TP, et al. Identification of integrin alpha(M)beta(2) as an adhesion receptor on peripheral blood monocytes for Cyr61 (CCN1) and connective tissue growth factor (CCN2): immediate-early gene products expressed in atherosclerotic lesions. *Blood*. 2002;99(12):4457-65.
46. Huang J, Huang H, Wu M, Li J, Xie H, Zhou H, et al. Connective tissue growth factor induces osteogenic differentiation of vascular smooth muscle cells through ERK signaling. *International journal of molecular medicine*. 2013;32(2):423-9.
47. Leask A, Abraham DJ. All in the CCN family: essential matricellular signaling modulators emerge from the bunker. *Journal of cell science*. 2006;119(Pt 23):4803-10.
48. Inoki I, Shiomi T, Hashimoto G, Enomoto H, Nakamura H, Makino K, et al. Connective tissue growth factor binds vascular endothelial growth factor (VEGF) and inhibits VEGF-induced angiogenesis. *FASEB J*. 2002;16(2):219-21.
49. Rodrigues-Diez RR, Garcia-Redondo AB, Orejudo M, Rodrigues-Diez R, Briones AM, Bosch-Panadero E, et al. The C-terminal module IV of connective tissue growth factor, through EGFR/Nox1 signaling, activates the NF-kappaB pathway and proinflammatory factors in vascular smooth muscle cells. *Antioxidants & redox signaling*. 2015;22(1):29-47.
50. Lee YS, Byun J, Kim JA, Lee JS, Kim KL, Suh YL, et al. Monocrotaline-induced pulmonary hypertension correlates with upregulation of connective tissue growth factor expression in the lung. *Experimental & molecular medicine*. 2005;37(1):27-35.

51. Yoshisue H, Suzuki K, Kawabata A, Ohya T, Zhao H, Sakurada K, et al. Large scale isolation of non-uniform shear stress-responsive genes from cultured human endothelial cells through the preparation of a subtracted cDNA library. *Atherosclerosis*. 2002;162(2):323-34.
52. Finckenberg P. Regulation of Connective Tissue Growth Factor (CTGF) in hypertension-induced end organ damage. E-Thesis: University of Helsinki. 2003:1-75.
53. Panek AN, Posch MG, Alenina N, Ghadge SK, Erdmann B, Popova E, et al. Connective tissue growth factor overexpression in cardiomyocytes promotes cardiac hypertrophy and protection against pressure overload. *PLoS one*. 2009;4(8):e6743.
54. Yoon PO, Lee MA, Cha H, Jeong MH, Kim J, Jang SP, et al. The opposing effects of CCN2 and CCN5 on the development of cardiac hypertrophy and fibrosis. *Journal of molecular and cellular cardiology*. 2010;49(2):294-303.
55. Koshman YE, Sternlicht MD, Kim T, O'Hara CP, Koczor CA, Lewis W, et al. Connective tissue growth factor regulates cardiac function and tissue remodeling in a mouse model of dilated cardiomyopathy. *Journal of molecular and cellular cardiology*. 2015.
56. Szabo Z, Magga J, Alakoski T, Ulvila J, Pihola J, Vainio L, et al. Connective tissue growth factor inhibition attenuates left ventricular remodeling and dysfunction in pressure overload-induced heart failure. *Hypertension*. 2014;63(6):1235-40.
57. Fontes MS, Kessler EL, van Stuijvenberg L, Brans MA, Falke LL, Kok B, et al. CTGF knockout does not affect cardiac hypertrophy and fibrosis formation upon chronic pressure overload. *Journal of molecular and cellular cardiology*. 2015;88:82-90.
58. Accornero F, van Berlo JH, Correll RN, Elrod JW, Sargent MA, York A, et al. Genetic Analysis of Connective Tissue Growth Factor as an Effector of Transforming Growth Factor beta Signaling and Cardiac Remodeling. *Molecular and cellular biology*. 2015;35(12):2154-64.
59. Gravning J, Ahmed MS, von Lueder TG, Edvardsen T, Attramadal H. CCN2/CTGF attenuates myocardial hypertrophy and cardiac dysfunction upon chronic pressure-overload. *International journal of cardiology*. 2013;168(3):2049-56.
60. Langsetmo I, Jacob CT, Zhang W, Oliver N, Lin A, Coker G, et al. Anti-CTGF human antibody FG-3019 prevents and reverses diabetes-induced cardiovascular complications in streptozotocin (STZ) treated rats (Abstract). *Diabetes* 2006;55(Suppl 1):A122.
61. Gerritsen KG, Abrahams AC, Peters HP, Nguyen TQ, Koeners MP, den Hoedt CH, et al. Effect of GFR on plasma N-terminal connective tissue growth factor (CTGF) concentrations. *American journal of kidney diseases : the official journal of the National Kidney Foundation*. 2012;59(5):619-27.
62. Sohn M, Tan Y, Wang B, Klein RL, Trojanowska M, Jaffa AA. Mechanisms of low-density lipoprotein-induced expression of connective tissue growth factor in human aortic endothelial cells. *American journal of physiology Heart and circulatory physiology*. 2006;290(4):H1624-34.
63. Cicha I, Goppelt-Strube M, Muehlich S, Yilmaz A, Raaz D, Daniel WG, et al. Pharmacological inhibition of RhoA signaling prevents connective tissue growth factor induction in endothelial cells exposed to non-uniform shear stress. *Atherosclerosis*. 2008;196(1):136-45.

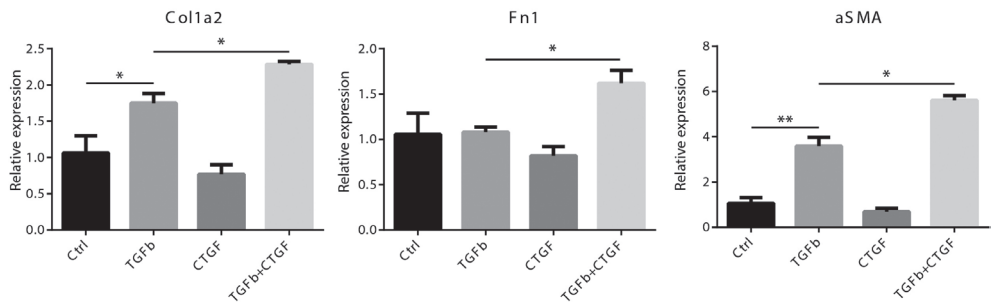
### Acknowledgments

We gratefully acknowledge the contribution of the SMART research nurses, R. van Petersen (data-manager), A.G. Pijl (vascular manager), Danny Kanhai (research physician) and the participants of the SMART Study Group (A. Algra, Julius Center for Health Sciences and Primary Care and Rudolph Magnus Institute of Neuroscience, Department of Neurology; Y. van der Graaf, G.E.H.M. Rutten, D.E. Grobbee, Julius Center for Health Sciences and Primary Care; P.A. Doevendans, Department of Cardiology; F.L. Moll, Department of Vascular Surgery; L.J. Kappelle, Department of Neurology; W.P.Th.M. Mali, Department of Radiology).

**Supplementary material**



**Supplemental Figure 1:** Univariate correlation with regression line comparing logCTGF with LDL cholesterol and total cholesterol respectively.



**Supplemental Figure 2:** Rat pericytes stimulated with 5ng/ml TGFβ1 (R&D systems) for 24hours show an increased expression of Col1a2 and alpha-Smooth Muscle Actin (αSMA). Fibronectin (Fn1) expression was not altered by TGFβ stimulation. Stimulation with 200ng/ml rhCTGF (Biovendor) did not significantly alter Col1a2, Fn1 or αSMA expression compared to TGFβ alone suggesting a synergistic effect on pericytes under pathological conditions. N=3; Error bars represent SEM; \* p<0.05, \*\* p<0.01; Represents ANOVA with Tukey correction for multiple testing.

4



## **Chapter 4:** Diverse origins of the myofibroblast implications for kidney fibrosis

Lucas L. Falke\*<sup>1</sup>, Shima Gholizadeh\*<sup>2</sup>, Roel Goldschmeding<sup>1</sup>, Robbert J. Kok<sup>2</sup> and  
Tri Q. Nguyen<sup>1</sup>

1. Dept. of Pathology, University Medical Center Utrecht, The Netherlands

2. Dept. of Pharmaceutics, Utrecht University, The Netherlands

\* Contributed equally

**Abstract**

Fibrosis is the common end point of chronic kidney disease. The persistent production of inflammatory cytokines and growth factors leads to an ongoing process of extracellular matrix production that eventually disrupts the normal functioning of the organ. During fibrosis, the myofibroblast is commonly regarded as the predominant effector cell. Accumulating evidence has demonstrated a diverse origin of myofibroblasts in kidney fibrosis. Proposed major contributors of myofibroblasts include bone marrow-derived fibroblasts, tubular epithelial cells, endothelial cells, pericytes and interstitial fibroblasts; the published data, however, have not yet clearly defined the relative contribution of these different cellular sources. Myofibroblasts have been reported to originate from various sources, irrespective of the nature of the initial damage responsible for the induction of kidney fibrosis. Here, we review the possible relevance of the diversity of myofibroblast progenitors in kidney fibrosis and the implications for the development of novel therapeutic approaches. Specifically, we discuss the current status of preclinical and clinical antifibrotic therapy and describe targeting strategies that might help support resident and circulating cells to maintain or regain their original functional differentiation state. Such strategies might help these cells resist their transition to a myofibroblast phenotype to prevent, or even reverse, the fibrotic state.

**Key points**

- Myofibroblasts in kidney fibrosis potentially originate from diverse origins such as bone marrow-derived fibroblasts, tubular epithelial cells, endothelial cells, pericytes and interstitial fibroblasts
- Myofibroblasts derive from either one or more sources as shown by independent studies, irrespective of the nature of the initial damage responsible for the induction of kidney fibrosis
- The diversity of myofibroblast progenitors in kidney fibrosis might be relevant in the development of novel therapies
- Some systemic therapies inhibiting myofibroblast accumulation and fibrotic development exist but efficacy and safety during CKD is not clear cut
- Targeting strategies to support resident and circulating cells in maintaining or regaining their original functional differentiation state and resisting transition to a myofibroblast phenotype, might help to prevent fibrosis

## Introduction

The process of fibrosis or scar formation involves a complex interplay between multiple pleiotropic genes, including transforming growth factor  $\beta$  (TGF- $\beta$ ), vascular endothelial growth factor (VEGF), platelet derived growth factor (PDGF), epidermal growth factor and connective tissue growth factor (1, 2). The proliferative response of fibroblasts following injury provides an initial advantage, by helping to maintain tissue integrity and reduce the chance of infection; however, the regenerative potential of the tissue is ultimately limited by this response and the functions of the injured organ are further reduced (3). The proliferative response possibly reflects an ancient evolutionary pressure that has skewed the tissue response to injury towards fibrosis; this process would protect the damaged organ against hazardous external factors, at the expense of long-term regeneration. Less challenging environmental and societal conditions and improved health care make regeneration favourable compared to quick fibrotic repair, as well as the increase in the mean age and lifespan. Understanding the mechanisms behind fibrosis is essential for the development of therapies that can correct or adjust this balance, so as to reduce unnecessary scar formation in pathologies such as kidney disease. The therapeutic potential of interventions that target known profibrotic factors has been extensively studied (1, 4); however, these studies have not yet resulted in the establishment of effective clinically available antifibrotic therapies. (5). Exploration of alternative intervention points for the management of kidney fibrosis is therefore warranted. Myofibroblasts are the key effector cell-type during fibrotic disease; they are the main producers of extracellular matrix (ECM), crosslinking enzymes, and inhibitors of matrix degrading metalloproteinases and increase in number during fibrosis (6). The exact origin of the myofibroblast during chronic kidney disease (CKD) is widely debated. The purpose of this Review is to summarize the evidence for the various potential origins of myofibroblasts in the context of kidney fibrosis. We also discuss the possible clinical implications of the distinct myofibroblast progenitors with respect to drug-targeting strategies.

## Wound healing response

Kidney injury, for example caused by trauma, toxic exposure, or immune complexes, initiates a wound healing response. The early stage of wound healing is characterized by the rupture of platelets and the subsequent formation of a fibrin mesh, which leads to blood coagulation. This mesh recruits neutrophils and monocytes that become polarized macrophages. Macrophages can be polarized towards numerous different subtypes; major subtypes include M1 polarized proinflammatory macrophages and M2

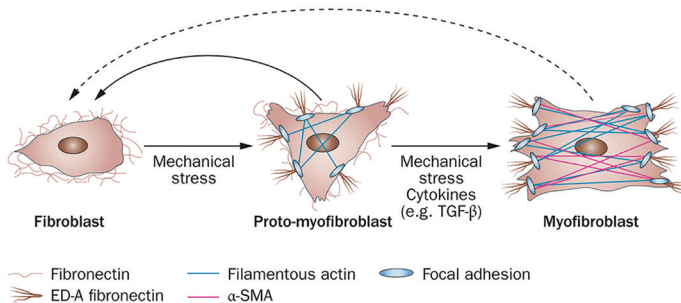


**Figure 1:** Differentiation steps of fibroblasts towards myofibroblast subtypes. Interstitial fibroblasts are characterized by the production of fibronectin and the absence of filamentous-actin,  $\alpha$ SMA and ED-A fibronectin. The protomyofibroblast produces ED-A fibronectin, contains stress fibres and focal adhesions, but does not yet contain the contractile  $\alpha$ SMA thus representing an immature myofibroblast. Mature myofibroblasts show abundant production of ED-A fibronectin and F-actin and are characterized by the presence of  $\alpha$ SMA. The transition from fibroblasts to protomyofibroblasts is reversible (solid line), but it is not known whether myofibroblasts can also redifferentiate into fibroblasts (dotted line).

polarized wound healing-associated macrophages (7). The later stage of the wound healing response can be further subdivided into three phases (8). During the first phase, the macrophage population shifts from an M1 to an M2 phenotype, and from promoting an inflammatory response to promoting tissue regeneration (9). M2 macrophages secrete high levels of growth factors, such as TGF- $\beta$ 1, PDGF, and pro-epidermal growth factor, which induce cellular proliferation and synthesis of the ECM. Under the influence of these growth factors, myofibroblasts become highly abundant in the second phase, start to produce ECM components, and

exert tensile forces to facilitate wound closure (10, 11). Upon repetitive injury, as observed in CKD, the second stage of the wound healing response fails to resolve and fibrosis might ensue during a third phase. The third phase is characterized by protracted excessive deposition of ECM, increased crosslinking of collagen fibres, and decreased degradation of the ECM (10). Figure 1 summarizes the main sequence of events with regard to fibroblast activation. A full overview of the involvement of inflammatory cells, the myofibroblast differentiation sequence and proliferation promoting signals, is provided elsewhere (12-14).

### Techniques to study myofibroblasts

Several approaches can be used to determine the origin of myofibroblasts during disease. The two main methods involve studying the expression of differentiation markers and/or labelling of progenitor cells followed by lineage tracing. The following sections describe both the technical aspects of the methods used and the results that have been obtained thus far with regard to the origins of myofibroblasts during kidney injury. A glossary of terms used throughout this Review can be found in Box 1.

#### Box 1 | Glossary

- Biologic agents: medical term for therapeutic proteins or peptides manufactured in or isolated from a biological source
- Humanized antibody: immunoglobulins that are generated in animals with a full human amino acid sequence, thereby preventing a xenimmune response
- Immunofluorescence/immunohistochemistry: a technique that uses antibodies against specific molecular structures (usually proteins) to identify markers of interest. These antibodies can be detected by using fluorescent or chemical markers
- Lineage tracing: a method used to trace the progeny of a single cell. Furthermore, donor cells or organs *ex vivo* can be labeled and injected into a non-genetically modified wild-type animal. This would be considered as fate tracing of the originally labelled (but not genetically altered) donor cells or organ. For more information see Figure 3
- Marker: an identifiable component expressed on the surface or within a cell that enables specific identification of the cellular subtype. Usually the marker is a specific protein, the expression of which can be identified using either immunofluorescence/immunohistochemistry or immunoelectron microscopy
- Tyrosine kinase inhibitors: small molecules that inhibit the signal domain of receptors on the cell surface

#### Expression of differentiation markers

Numerous studies have attempted to describe the expression of myofibroblast markers and to document any overlap with markers considered to be specific for renal cells (mesenchymal, epithelial, or endothelial) and cells of extra-renal origin (15). A clear definition of the myofibroblast is yet to be agreed on, and therefore researchers currently use distinct but overlapping definitions.

The myofibroblast was first identified as a cell type in fibrotic contractures, with features reminiscent of both fibroblasts and smooth muscle cells (16); cell biologists have now generally accepted that a myofibroblast is a differentiated cell that shows both of these characteristics. A myofibroblast is defined by its ultrastructural features, such as large and expanded endoplasmatic reticula and a fibronexus containing intracellular myofilaments (17). Preparing samples for electron microscopy to visualize such features, however, is labour intensive, time consuming, and costly and therefore immunohistochemical analysis followed by light microscopy of cell-surface markers is often used as an alternative to identify myofibroblasts. Myofibroblasts produce substantial amounts of ECM while additionally exhibiting contractile properties mediated by intermediary filament proteins, such as vimentin (VIM) and aortic smooth muscle actin (ACTA2, commonly known as  $\alpha$ SMA) (18). Myofibroblasts express high levels of  $\alpha$ SMA, a stress fibre protein that facilitates increased contractility; as such,  $\alpha$ SMA is generally accepted as a definitive marker that is capable of identifying all myofibroblasts present in the studied tissue (19). Approximately 75% of collagen-producing cells express  $\alpha$ SMA, indicating that this marker can be used to identify the majority of fibrotic mediator cells, but it is not fully sensitive (20). During fibrosis, interstitial mesenchymal cells and myofibroblasts might comprise a heterogeneous group of cells that shift during disease progression, both in terms of marker expression and function (15). Table 1 provides an overview of the cellular function of these precursor cells and the expression of their defining markers. The expression of most markers overlaps between these interstitial cell types, and consequently it should



**Table 1:** Features of different types of interstitial cells in the kidney

Cell Type	Marker						Feature	
	$\alpha$ SMA	PDGFR $\beta$	S100	NT5E	DES	VIM	Function	Location
Fibroblast	n	y	y	y	n	y	ECM maintenance structural support to the parenchyma	Interstitial In contact with the epithelium and epithelial basal membrane
Myofibroblast	y	y	y	y	n	y	Wound contraction Tissue healing response	Absent under physiological conditions Present in the interstitium under pathological conditions
Pericyte	y	y	n	y	y	y	Vascular stability Production of VEGF-A Chemical and/or mechanical sensation	Interstitial In contact with the endothelium and endothelial basement membrane
VSMC	y	y	y	n	y	y	Regulating vascular wall tonus	Medial layer of blood vessels

\*Owing to the overlap of marker expression, only ultrastructural analysis can discriminate between these four interstitial cell types. Other cell types, such as leucocytes, also express these markers. Abbreviations:  $\alpha$ SMA, aorta smooth muscle actin; DES, desmin; ECM, extracellular matrix; NT5E, 5'-nucleotidase (CD73); PDGFR $\beta$ , platelet-derived growth factor receptor,  $\beta$ ; S100A4, S100 calcium binding protein A4; VEGF, vascular endothelial growth factor A; VIM, vimentin; VSMC, vascular smooth muscle cell; y, yes; n, no.

be noted that no marker has yet been identified that is fully specific for the individual precursors. The majority of fibroblasts express  $\alpha$ SMA, but not all  $\alpha$ SMA-positive cells produce large amounts of collagen. These  $\alpha$ SMA-positive ECM-negative cells might represent leucocytes, thus impairing the specificity of  $\alpha$ SMA as a marker of myofibroblasts. Alternatively, non-ECM-producing  $\alpha$ SMA-positive cells might represent a subset of myofibroblasts that are predominantly contractile (21). Other markers that have been used to identify myofibroblasts include protein S100-A4 (S100A4), Vimentin (VIM), platelet derived growth factor receptor  $\beta$  (PDGFR $\beta$ ) and 5'-nucleotidase (NT5E) (15, 22, 23). S100A4 and VIM were initially considered to be myofibroblast specific; however, these markers have subsequently been identified in macrophages, and thus cannot be used to specifically identify myofibroblasts (24, 25).

Figure 2 illustrates that there is only partial overlap in the cellular expression of  $\alpha$ SMA, VIM and PDGFR $\beta$  during kidney fibrosis; studies of myofibroblasts that employ only one cellular marker should therefore be interpreted with caution. Furthermore, scoring of marker expression using techniques such as immunohistochemistry can be subjective and provides only indirect evidence regarding myofibroblast origin, being at best a static snapshot of the very dynamic fibrotic process.

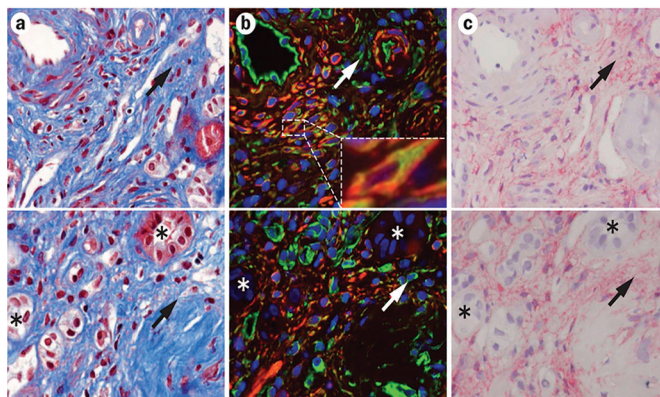


**Figure 2:** Expression of fibroblast markers only partially overlap in kidney fibrosis. A human kidney biopsy sample from a patient with allograft nephropathy was analysed by three staining methods to determine overlap in fibroblast marker expression. The upper and lower panels show a different field of view. **A:** Masson trichrome staining illustrates the extent of interstitial fibrosis. **B:** Co-immunofluorescence for  $\alpha$ SMA (red, TRITC) and VIM (green, FITC). The arrow indicates interstitial cells that are positive for VIM but negative for  $\alpha$ SMA. The insert shows a myofibroblast that is (Figure 2, continued) positive for both  $\alpha$ SMA and VIM. **C:** Immunohistochemistry for PDGFR $\beta$  expression in the corresponding areas to parts a and b. All areas show severe collagen deposition, suggesting that interstitial cells can produce large quantities of extracellular matrix, despite lacking expression of  $\alpha$ SMA. The arrows indicate the same position

(Figure 2, continued) in consecutive microscopic images, as shown in panel b. The asterisks mark tubules. Despite severe interstitial fibrosis, no positive expression for  $\alpha$ SMA, VIM or PDGFR $\beta$  is observed. All images were taken in the same field of view at a magnification of  $\times 400$ . Abbreviations:  $\alpha$ SMA, aorta smooth muscle actin; FITC, fluorescein isothiocyanate; PDGFR $\beta$ , platelet derived growth factor  $\beta$ ; TRITC, tetramethylrhodamine; VIM, vimentin.

### Permanent labelling and lineage tracing

Direct evidence regarding the contribution of specific cell types to the myofibroblast pool during fibrotic kidney disease has been obtained from lineage tracing in animal studies using genetic labelling techniques. Lineage tracing of kidney cells relies on the permanent labelling of parent cells and their subsequent progeny cells, based on the transient expression of specific markers for distinct cell types or cellular compartments (26). This technique can be performed either during development or during the postnatal period of the genetically labelled animals (27). Studies have used Sox2 to label epithelial cells; Foxd1, to label mesenchymal cells; Tie2, to label endothelial cells; and P0 (also known as Mpz) to label neural crest cells (28-30). Using the Cre recombinase system, transient expression can be used to permanently induce tracer protein expression, such as green fluorescent protein (GFP), in these distinct cell types and their progeny (31). An example of how this system could be used to trace Foxd1-positive cells is illustrated in Figure 3.

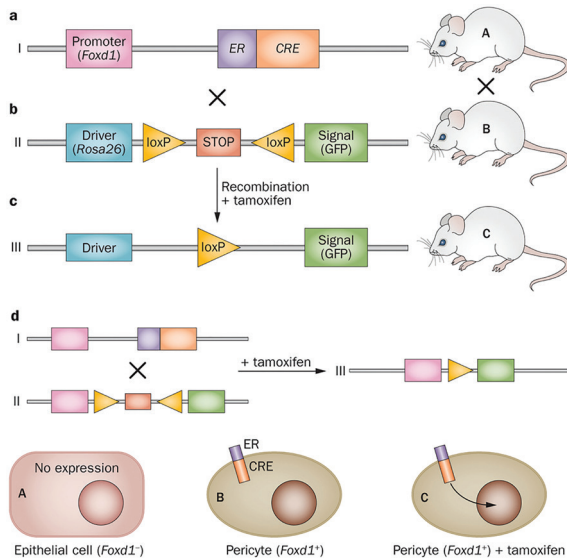


**Figure 3:** Schematic of the Cre-lox system used to trace FOXD1-positive pericytes. **A:** Transgenic mouse “A” contains Cre recombinase capable of recognizing loxP sites, under the control of a specific tracer-marker promoter (in this case Foxd1). The Cre recombinase is only expressed in cells that are positive for the marker. **B:** Transgenic mouse “B” contains a signalling cassette (in this case GFP) that is driven by a ubiquitous driver sequence (Rosa26) that is normally prematurely terminated by an inserted stop codon. The stop sequence is flanked by loxP sites. **C:** Crossbreeding mouse “A” and “B” can produce transgenic mouse “C” in which the tracer or marker promoter driven Cre recombinase recognizes the loxP sites flanking the stop sequence, upon which the latter is excised. This excision allows the driver sequence to complete transcription and translation of the signalling cassette, thus allowing for specific lineage tracing. **D:** An epithelial cell not expressing Foxd1 does not have a tamoxifen-specific modified oestrogen receptor Cre recombinase (ER/Cre) fusion protein expressed at the cell membrane. Consequently, activation of the ER with tamoxifen does not occur and

does not lead to fusion protein translocation to the nucleus and signal protein expression by recombining the stop sequence out of the DNA. In pericytes, however, Foxd1 driven ER/Cre fusion protein expression does occur. Subsequently, tamoxifen injection ultimately leads to permanent signal protein expression allowing for timed FOXD1 specific tracing of pericytes. Abbreviations: FOXD1, forkhead box D1; GFP, green fluorescent protein.

### Origin of interstitial myofibroblasts

#### Interstitial cells of mesodermal origin

The definition of kidney interstitial mesenchymal cells or fibroblasts is not straightforward as it is based on ill-defined morphology, nonspecific marker expression and the absence of markers that define specific cellular functions (15). Pericytes and resident interstitial fibroblasts show overlapping basal expression of several markers that were previously described as being specific for either cell type (15). Table 2 lists the utilized markers of embryonic mesodermal lineage and of differentiated mature cell populations that are relevant for research into the origins of myofibroblasts.

A series of observations have converged on the concept that pericytes—resident interstitial mesenchymal cells supporting capillary endothelial cells—are the main source of myofibroblasts in

**Table 2:** This table lists all published lineage trace experiments to date

Cell type	Traced marker	Model	Results	Ref.
Interstitial fibroblasts (neural crest derived)	P0	UUO	~100% of cortical and medullary resident fibroblasts were of P0 origin. Reduced EPO production	(28)
Pericytes and interstitial fibroblasts	PDGFR $\beta$	UUO COL4A3-KO	Cellular proliferation, with no contribution to fibrosis	(34)
	NG-2	UUO COL4A3-KO	Cellular proliferation, with 6% contribution to fibrosis	(34)
Pericytes, perivascular fibroblasts, VSMCs, and mesangial cells	FOXD1	UUO IR	100% co-expression of FOXD1 and PDGFR $\beta$ in pericytes. ~25% co-expression of $\alpha$ SMA and FOXD1 lineage	(29)
	$\gamma$ GT	UUO	5% contribution to myofibroblasts	(34)
Epithelial cells	SIX2	UUO IR	No contribution to myofibroblasts	(29)
	$\gamma$ GT	UUO	36% contribution to myofibroblasts	(54)
Collecting duct and urothelial cells	HOXB7	UUO IR	No contribution to myofibroblasts	(29)
Endothelial cells	CDH5	UUO	10% contribution to myofibroblasts	(34)
Endothelial cells (and a subpopulation of monocytes)	TIE2 (and CD31 co-expression)	UUO IR COL4A3-KO	30–50% contribution to myofibroblasts	(30)
	TIE2	STZ-induced DN	28% contribution to myofibroblasts	(67)
	TIE2	CRIM1-KO (VEGFA deficiency)	31% co-expression of TIE2 and $\alpha$ SMA 6% coexpression of TIE2, $\alpha$ SMA and F4/80	(68)
Cells of extrarenal origin and/or bone marrow cells	$\alpha$ SMA bone marrow transplant	UUO	35% contribution to myofibroblasts. Contribution to fibrosis is independent of proliferation	(34)
	S100A4 bone marrow transplant	None UUO	12% contribution to interstitial fibroblasts, without fibrogenic stress 15% contribution to myofibroblasts during stress	(54)
	Sex mismatch bone marrow transplant using COL1A2-luciferase	UUO	8.6% contribution of bone marrow-derived cells to myofibroblasts No contribution to COL1A2 synthesis	(75)
	T and B leukocytes	RAG1-KO	COL4A3-KO	Reduced interstitial fibrosis

Abbreviations:  $\alpha$ SMA, aorta smooth muscle actin;  $\gamma$ GT,  $\gamma$ -glutamyl transpeptidase; CDH5, cadherin 5, type 2 (vascular endothelium); COL1A2, collagen type 1,  $\alpha$  2; COL4A3, collagen, type IV,  $\alpha$  3 (Goodpasture antigen); EPO, erythropoietin; FOXD1, forkhead box D1; HOXB7, homeobox B7; IR, ischaemia–reperfusion; KO, knockout; NG-2, neural–glial antigen 2; P0, myelin protein zero; PDGFR $\beta$ , platelet-derived growth factor receptor,  $\beta$  polypeptide; RAG1, recombination activating gene 1; S100A4, S100 calcium binding protein A4; SIX2, SIX homeobox 2; UUO, unilateral ureteral obstruction.; STZ, streptozotocin; DN, diabetic nephropathy.

kidney fibrosis. In an experimental rat model of obstructive nephropathy, an inverse correlation between expression of  $\alpha$ Sma and Nt5e was observed, suggesting the conversion of interstitial mesenchymal cells into myofibroblasts (32). The majority of fibroblasts in a rat model of angiotensin II-induced kidney fibrosis were found to be derived from resident renal interstitial cells (33). These interstitial cells were later identified as perivascular pericytes, which trans-differentiated into collagen-producing myofibroblasts (20). Subsequent Foxd1-driven lineage tracing in mice has provided further support for the notion that pericyte-derived cells account for the vast majority of  $\alpha$ SMA-positive cells in kidney fibrosis (29). Another murine lineage tracing study that used P0-driven Cre recombinase, indicated that a large proportion of the interstitial myofibroblast pool is derived from erythropoietin (EPO)-producing interstitial mesenchymal cells, which are derived from the neural crest during embryogenesis (28). Under conditions of cellular stress, these cells were observed to lose expression of EPO and subsequently transformed into myofibroblasts. Furthermore, a subset of these cells additionally expressed forkhead box protein D1 (FOXD1). An overlap between P0 and FOXD1 was shown in this study, and therefore common ancestry has been suggested. Further elaboration of this observation is made elsewhere (18).

Contradictory to these findings, other studies have suggested that myofibroblasts might be derived from interstitial fibroblasts that are not expressing pericyte markers. Moreover, although pericytes accumulate in the interstitium during CKD, they have not been shown to contribute to the pool of myofibroblasts that express  $\alpha$ SMA or collagen in several genetic mouse models of kidney fibrosis (34). Irrespective of the numerical contribution of pericyte transformation into myofibroblasts, the sequence of pericyte detachment from endothelial cells leading to capillary instability (and an associated subsequent increase in fibrosis), seems to be a hallmark of CKD (35, 36).

Mesangial cells are commonly regarded as glomerular pericytes (37). Research both *in vitro* and *in vivo*, has shown that mesangial cells are capable of transforming into  $\alpha$ SMA-positive cells under profibrotic conditions (38-40). Furthermore, a positive correlation between glomerular  $\alpha$ SMA expression, mesangial expansion, and glomerular type IV collagen expression has been observed in rats with diabetic nephropathy (41).

#### *Epithelial cells*

Epithelial-to-mesenchymal transition (EMT) is a physiological process characterized by the differentiation of epithelial cells towards a more mesenchymal phenotype (42). During development, EMT occurs during gastrulation, whereby ectodermal cells differentiate to form new cells of the mesodermal germ layer (43). Phenotypically, EMT is usually defined as the loss of typical epithelial markers, such as E-cadherin and tight junction protein ZO-1 (TJP1), while gaining mesenchymal markers, such as VIM,  $\alpha$ SMA, and S100A4. Outside of its function during development, EMT contributes to tumour progression and fibrogenesis in various organs, including the lungs, liver, kidneys, and heart.

EMT has been proposed to be important mechanism responsible for the accumulation of interstitial myofibroblasts and collagen production during kidney fibrosis (43). Expression of  $\alpha$ SMA has been detected in tubular and glomerular epithelia in association with disease progression, in both a remnant kidney model and during experimental glomerulonephritis (44, 45). Furthermore, it has been proposed that the EMT might be responsible for the loss of podocytes that occurs in diabetic kidney disease (46); features of EMT have also been observed in human tissue samples obtained by biopsy of patients with various other renal diseases (47-49). Bone morphogenetic protein 7 (BMP7), hepatocyte growth factor (HGF) and EPO are known inhibitors of EMT *in vitro* (50). Injections of BMP7, HGF, and EPO *in vivo* inhibited the increased expression of mesenchymal markers by tubular epithelial cells in murine models of unilateral ureteral obstruction (UUO) and nephrotoxic nephritis-induced CKD (51-53). The possible transition of these cells into interstitial myofibroblasts, however, was not addressed in these studies. In an early lineage tracing study,  $\gamma$ -GT-driven GFP expression in a murine model of UUO indicated that cells of tubular epithelial origin undergoing EMT contributed 36% to the tubulointerstitial myofibroblast pool (54). A later study from the same researchers, using essentially the same mouse model, reported a much smaller contribution of these cells (5%) without providing a clear explanation for the observed difference (34). Subsequent studies have attempted, but not succeeded, to reproduce

the first observation in similar and other *in vivo* models, although EMT of tubular epithelial cells *in vitro* has been confirmed by numerous independent groups (29). An epithelial tracing study using the Cdh16 promoter in a model of obstructive nephropathy failed to identify a contribution of the tubular epithelium to the myofibroblast pool by undergoing EMT (55). An additional report showed that epithelial overexpression of TGF- $\beta$ , driven by Pax8, resulted in tubular autophagy and induced interstitial fibrosis (56). No induction of S100A4 expression, as a marker of fibroblast differentiation, or migration of tubular epithelial cells into the interstitium, however, was observed at an ultrastructural level; in this case it is most likely that interstitial fibrosis occurred by paracrine signalling. Other markers of possible *in situ* EMT, such as Snai1, Twist1, or Snai2 (57), were not addressed in this study (56).

The role of EMT in the context of loss of epithelial and acquisition or reacquisition of certain mesenchymal features and markers by tubular epithelial cells in CKD is largely undisputed. However, the direct contribution of this EMT reminiscent process to the interstitial myofibroblast pool seems unlikely (58, 59).

Numerous studies have demonstrated that EMT is involved in glomerular disease. Extra-capillary lesions that occur in crescentic glomerulonephritis are derived from parietal epithelial cells of the Bowman capsule (60). The contribution of podocytes to glomerulosclerosis has not been studied extensively, although successful podocyte-tracing methods have been described during glomerular injury (61–63). The association between podocytes and glomerulosclerosis has not yet been addressed using a lineage tracing approach, however. Podocyte-mediated production of VEGF is required for glomerular endothelial and mesangial stability; therefore, loss of healthy podocytes might lead to capillary collapse and glomerulosclerosis (64). Furthermore, it has been suggested that  $\alpha$ SMA might not be an appropriate marker for monitoring the fibrotic transition of glomerular epithelial cells. Transgelin could prove to be a more suitable marker for fibrotic effector cell research in glomerulopathies as it seems to be more sensitive and specific than  $\alpha$ SMA with regard to glomerular injury and fibrotic cell activation (65).

### Endothelial cells

The endothelia can transdifferentiate towards a more mesenchymal phenotype, in a similar manner to epithelial cells. This process is known as endothelial-to-mesenchymal transition (EndoMT) (66). EndoMT has been suggested to contribute to the increased number of myofibroblasts during kidney disease (30). Cells, double labelled with the pan endothelial marker platelet endothelial cell adhesion molecule 1 (PECAM-1) and  $\alpha$ SMA, and Tie2-YFP lineage-traced cells, were counted in three different rodent models of kidney disease. From these experiments, the contribution of EndoMT was calculated to be ~40%. Consistent with this observation, EndoMT was subsequently found to give rise to a large proportion of myofibroblasts during experimental diabetic kidney disease (67). In Tie2-GFP mice, cells that are derived from a lineage that once expressed endothelial-specific Tie2, permanently express GFP. Following streptozotocin injection to induce diabetic nephropathy in Tie2-GFP mice, ~10% of  $\alpha$ SMA-positive cells were positive for enhanced GFP, and were thus considered to have derived from Tie2 lineage cells. By analysing GFP overlap with PECAM-1, the specificity of the Tie2 based lineage tracing approach was determined. An additional 80% of this subpopulation of cells was also positive for the expression of PECAM-1, resulting in an 8% computed contribution of endothelial cells to the interstitial myofibroblast pool. Crim1 mutant mice develop renal cysts and fibrosis owing to aberrant capillary formation. Fate tracing of Tie2-positive cells in this mouse model showed that these cells contributed 31% of the interstitial myofibroblasts, composed of 6% cells of monocyte origin, and 25% cells of endothelial origin (68). These studies suggest that endothelium-derived cells contribute to the myofibroblast pool during fibrotic disease. The magnitude of this contribution may vary depending on the model used. Interestingly, in a porcine model of ischaemia-reperfusion injury, an association between complement system activation and EndoMT was identified (69). Accessibility of both the endothelium and the complement system make this an interesting finding for further development of targeted therapeutics; however, causality has yet to be established.

*Cells of extra-renal origin*

In addition to resident kidney cells, circulating cells might also contribute to the interstitial myofibroblast pool in kidney fibrosis. Both mesenchymal stem cells and fibrocytes derived from haematopoietic stem cells are capable of differentiating into collagen-expressing  $\alpha$ SMA-positive myofibroblasts in vitro under profibrotic conditions (70-72). Studies in bone marrow-depleted mice injected with GFP-positive donor bone marrow have indicated that ~15% of myofibroblasts may originate from circulating cells (54).

Transplantation of bone marrow harbouring a red fluorescent protein transgene under the control of the  $\alpha$ Sma promoter indicated that ~35% of interstitial myofibroblasts originated from the bone marrow in both a murine model of obstructive nephropathy and a genetic murine model of Alport syndrome (34). Furthermore, these bone marrow-derived (myo)fibroblasts, actively contributed to fibrosis (73). Data from a rat model of ischaemia–reperfusion injury showed similar results. Injection of human alkaline phosphatase-expressing bone marrow cells showed that >30% of these cells contribute to the interstitial kidney myofibroblast pool (74). Other studies, however, show contradictory data. In human sex-mismatched kidney-allograft recipients (75) and experimental chronic kidney allograft nephropathy, circulating recipient progeny cells were observed as interstitial myofibroblasts (76). Consistently, a mouse model of obstructive nephropathy showed that subsequent to transplantation of sex-mismatched bone marrow, only 9% of myofibroblasts originated from bone marrow cells (77). The same study, however, used Col1a2 promoter-driven luciferase to show that circulating cells did not contribute to collagen production. Transplantation of bone marrow cells expressing GFP under the control of the Col1a2 promoter additionally did not support a contribution of bone marrow-derived cells to collagen production in kidney fibrosis (20). In another study performed by the same research group, mice transplanted with Col1a1-GFP chimeric bone marrow failed to show a direct contribution of bone marrow cells to kidney fibrosis (78). Taken together, these latter two studies show that the direct contribution of bone marrow cells to the interstitial myofibroblast pool, other than through paracrine or endocrine signalling, seems highly unlikely.

*Caveats to lineage experiments*

Although much research has been performed to study the origin of the myofibroblast during CKD, numerous discrepancies exist in the reported data. Several general factors that potentially influence the reliability of the results should be noted and great care should be taken to ensure that future studies are comparable. The choice of mouse strain can be a large influence on fibrotic development (79), as can the duration and severity of the model used. It has been postulated that only during very late and severe stages of kidney disease is the tubular basal membrane sufficiently damaged to allow epithelial cells to infiltrate the interstitium and contribute to the fibrotic process. The infiltration of epithelial cells could be a factor that affects in vitro data, as no basal membrane is present in most culture systems.

Caveats in the use of non-inducible Cre–lox recombination systems have been identified primarily with regard to the sensitivity and specificity of the genetic tracing constructs used. First, it must be shown that the transiently-expressed specific promoter used for tracing experiments is not reactivated later in life or during disease progression, as this process would reduce the specificity of the tracing. By using an inducible Cre, such as an oestrogen receptor fusion protein, specific subsets of cells can express Cre recombinase only when tamoxifen is coadministered. This approach leaves only a small window of opportunity for recombination to occur and thereby increases specificity. In addition, it is essential to demonstrate that artificially truncated or randomly inserted versions of the transgenes are not expressed differentially when compared to the endogenous gene, by assessing both transgenes under physiological and pathological conditions.

The specificity of the promoters used for tracing experiments must be demonstrated. TIE2 is commonly regarded as a marker specific for endothelium; however, it should be noted that although TIE2 is sensitive for endothelial cells, it is not specific as it also marks myeloid-derived cells, such as monocytes (80). In addition, TIE2 is expressed in cells of mesenchymal origin that ultimately give rise to vascular smooth muscle cells and pericytes (81). Numerous cell types that express overlapping markers can bias tracing study results. Critical reviews

describing these shortcomings and discrepancies can be found elsewhere (15, 18, 59, 82, 83).

### Anti-fibrotic therapy

Targeting myofibroblasts is the cornerstone of rational antifibrotic therapy owing to the pivotal role of this cell type in the production of profibrotic mediators and in the deposition of ECM components (84). Molecular medicine has yielded a wide range of targeted agents, including kinase inhibitors and biologic therapies, which can be used for antifibrotic therapy (85, 86). These agents have proven effective in the preclinical setting; however, they have failed to advance into clinical practice, primarily due to a poor balance between antifibrotic efficacy and adverse effects.

#### Direct targeting

Targeted accumulation of antifibrotic therapeutic agents in the kidney, and especially in kidney myofibroblasts, may improve their therapeutic index. Such accumulation can be achieved with the use of nanomedicines, such as nanoparticulate carriers or conjugates that bind to cell-surface receptors on myofibroblasts. Using this approach, nanocarriers can deliver a drug load inside myofibroblast cells when internalization is triggered by binding to the receptor. Hypothetically, this process will increase local antifibrotic activity with lowered systemic drug exposure. Such a strategy has not yet been described for kidney disease, but other studies in liver fibrosis describe nanocarrier-based strategies that might be feasible for targeting kidney myofibroblasts (87, 88).

#### Nanocarriers

Indirect targeting relies upon the delivery of antifibrotic agents into other resident kidney cells, which then subsequently release these drugs in the kidney parenchyma, to provide localized antifibrotic activity on a tissue level rather than a cellular level. Table 3 details the nanocarrier strategies that can be employed for delivering antifibrotic compounds to the kidney through recognition by various cell surface receptors. One of the most appealing approaches to deliver therapeutic compounds to the kidney is through the targeting of tubular epithelial cells. The proximal tubular epithelium is highly active in accumulating compounds from the filtered urine via the multitude of receptors in the luminal brush-border (89).

**Table 3:** Drug targeting to myofibroblasts via surface receptors on kidney cells

Target	Nanocarrier system	Validation
<b>Proximal tubules</b>		
Megalin (LRP2)	Y27632-lysozyme conjugate	Unilateral IR in rats (90)
	SB201290-lysozyme conjugate	Unilateral IR in rats (92)
	LY-364947-lysozyme conjugate	UUO in rats (115)
	Imatinib-lysozyme conjugate	Healthy & UUO mice (114)
	EPAC activator 007-lysozyme conjugate	Unilateral IR in mice (118)
	Mycophenolate-glucosamine conjugate	Unilateral IR in rats (94, 119)
	Prednisolone-glucosamine conjugate	Unilateral IR in rats (93)
Folate receptor 1	Prednisolone-low-molecular weight chitosan conjugate	Healthy mice (120)
	Rapamycin-folate conjugate	PKD in mice (bpc model) (91)
Unknown target	Arg-vasopressin-alkylglycoside conjugate	Healthy rats (121)
<b>Mesangium</b>		
alfa8 integrin	Dye loaded anti-alfa8 immunoliposomes	Lupus-susceptible mice (122)
Thy 1.1.	Mycophenolate loaded OX-7 immunoliposomes	anti-Thy 1.1 GN in rats (123)
<b>Endothelium</b>		
E-selectin	Dexamethasone loaded anti-E-selectin immunoliposomes	anti-GBM in mice (124)
<b>Podocytes</b>		
Podocyte specific antigen*	Anti-podocyte targeted siRNA-protamine polyplexes	UNX in rats (125)

\*Nanocarriers directed to these receptors have been developed for rodents only; human receptor homologues have not yet been identified. Abbreviations: GBM, glomerular basement membrane; IR, ischaemia-reperfusion; OX7, mouse monoclonal anti-Thy1 antibody; PKD, polycystic kidney disease; siRNA, small interfering RNA; Thy1.1, thymocyte differentiation antigen 1.1; UUO, unilateral ureteral obstruction. GN, glomerulonephritis. UNX, Uninephrectomy.

Among these, low density lipoprotein receptor-related protein 2 (commonly known as megalin/cubulin), and folate receptor 1 $\alpha$  have been exploited successfully for drug targeting purposes (90, 91). These receptors can be reached only by filtered compounds, which justifies the investigation of relatively small drug-carrier conjugates that can pass through the glomerular filtration barrier. These drug-targeting approaches rely on the internalization of the nanocarrier and subsequent processing in the lysosomal compartment. This strategy is primarily feasible for small molecule agents that can diffuse over intracellular membranes and further redistribute once liberated from the carrier. Kinase inhibitor-lysozyme conjugates that can perturb the TGF- $\beta$ , p38 MAPK, or Rho kinase signalling pathways have been shown to elicit downstream antifibrotic responses, such as reduced expression of inflammatory and profibrotic mediators (including CCL2 and TGF- $\beta$ 1), when evaluated in rat models of renal inflammation (unilateral renal ischaemia) and fibrosis (UUO) (90, 92). Protection against tubular damage was reported following tubular cell-directed delivery of the Rho kinase inhibitor, Y27632 (90), as well as following tubular delivery of immunosuppressive agents, such as mycophenolic acid and prednisolone, by means of 2-glucosamine-based conjugates (93, 94). Although long-term follow-up studies are lacking, these initial studies show the potential of antifibrotic therapeutic drug delivery in resident kidney cells and the subsequent modulation of profibrotic and antifibrotic mediators.

PDGFR $\beta$  is expressed by the majority of resident cell types in the kidney, and both PDGF ligands and PDGF receptors are overexpressed during fibrosis (95). Higher expression levels of PDGFR $\beta$  on the myofibroblast cell surface compared to normal kidney parenchyma make it an attractive route through which antifibrotic compounds can be accumulated into cells. Interferon- $\gamma$  conjugates have been delivered to PDGFR $\beta$ -expressing fibroblasts by means of cyclic peptide ligands that contain a PDGFR $\beta$  peptide epitope. Chemical conjugation of peptide epitopes, or recombinant expression of a chimeric protein that comprises targeting peptides and the effector domain of interferon- $\gamma$ , are techniques that have been used successfully (87). Targeting myofibroblasts in this way has not yet been explored in kidney fibrosis, but impressive results have already been demonstrated in the context of liver fibrosis. PDGFR $\beta$ -targeted interferon- $\gamma$  derivatives accumulate in activated myofibroblasts upon intravenous administration in mice with CCl<sub>4</sub>-induced liver fibrosis, which subsequently inhibited both early and progressive stages of liver fibrosis (87). In a similar approach, cyclic PDGF $\beta$  peptides and manno-6-phosphate carbohydrate tethers were used to modify human serum albumin, thus obtaining albumin-based nanocarriers directed to fibroblasts (96). This approach has proved successful for the delivery of small molecule antifibrotic agents, such as 15-deoxy-delta12,14-prostaglandin J<sub>2</sub> (88), the angiotensin-receptor blocker losartan and an inhibitor of TGF $\beta$ RI (97, 98).

### **Manipulation of myofibroblast activity**

Indirect approaches to influence renal myofibroblast activity can also be envisioned. Enhancing the production of antifibrotic mediators by kidney resident cells or, inversely, inhibiting the production of profibrotic growth factors or other local mediators, are two possible approaches (1, 84). Fibrosis may also be attenuated by interfering with the recruitment of immune cells into the renal interstitium (12). Several kidney cell types, such as tubular epithelia or endothelia, can be the focus of an indirect myofibroblast targeting strategy, and have been described in more detail in other recent reviews (99-101).

### **Clinical trials**

Numerous preclinical and clinical studies using systemic therapy have been successful in inhibiting myofibroblast accumulation and attenuating kidney fibrosis. An important component of these successful preclinical therapies has been the use of strategies to target the profibrotic TGF- $\beta$  signalling pathway, including with the use of microRNA-29 (102). The pan-TGF- $\beta$  antibody, fresolimumab, has been shown to be well tolerated in a phase I trial among patients with focal segmental glomerulosclerosis (103). The efficacy of this therapy was not studied, but a phase II trial is currently underway among patients with a steroid-resistant form of this condition (104).



Another approach for inhibiting myofibroblast accumulation and attenuating kidney fibrosis is by targeting connective tissue growth factor, a key mediator of profibrotic TGF- $\beta$  activity, using a humanized monoclonal antibody. This human IgG $\kappa$  antibody (known as FG-3,019) has been tested in a phase I clinical trial among patients with microalbuminuric diabetes, and administration of this antibody proved to be well tolerated and significantly decreased albuminuria (105). A trial using the drug nintedanib, a multikinase inhibitor that acts on PDGFR, VEGF receptor and fibroblast growth factor receptor (FGFR) tyrosine kinases, reduced disease progression among patients with idiopathic pulmonary fibrosis (106). Nintedanib was well tolerated and approved by the FDA for idiopathic pulmonary fibrosis in October 2014. Nintedanib may therefore be another potential therapy for kidney fibrosis. Gefitinib, an epidermal growth factor tyrosine kinase inhibitor, has shown promise in the treatment of experimental kidney disease (107). A number of trials assessing the safety and efficacy of gefitinib are currently underway, and if well tolerated, trials studying the therapeutic feasibility in kidney disease might be initiated. A clinical trial investigating the effects of the PDGFR tyrosine kinase inhibitor imatinib, has also shown promising results in patients with nephrogenic systemic fibrosis (108).

Despite some promising data, considerations regarding the limitations of systemic antifibrotic therapy need to be taken into account. Sparse reports exist describing the reversal of renal fibrosis, but it is generally accepted that prevention of ECM deposition is more likely to result in successful treatment. As such, high doses of antifibrotic therapeutics administered during the onset and progression of disease might provide the best results in terms of morbidity and mortality. Indeed, with current therapeutic dosage, adverse events are seen with the majority of tyrosine kinase inhibitors (109, 110). A meta-analysis has shown that targeting VEGF receptors with tyrosine kinase inhibitors increases mortality (111).

Long-term exposure to tolerated doses of biologic therapies might, alternatively, lead to drug resistance as seen during the treatment of oncological disease. Targeting VEGFR leads to a PDGFR/FGFR-mediated escape (112). In addition, long-term exposure of carcinoma cell lines to TGF $\beta$ RI and/or II inhibitors induces drug resistance associated with a more invasive phenotype (113). Whether long-term exposure to antifibrotic drugs, such as tyrosine kinase inhibitors and monoclonal antibodies, during fibrotic kidney disease is well tolerated and effective, remains to be investigated. Emerging data indicates that specific targeting of high-dose antifibrotic therapy to the kidney is preferable over long-term systemic treatment. Anti-fibrotic small molecule drugs can be accumulated in kidney myofibroblasts or other kidney cell types by the above-discussed targeting strategies. To exemplify, the biologic agents galunisertib, indetanib, gefitinib, and imatinib have structural properties that render them good candidates for nanocarrier-based formulations, either using drug-carrier conjugates or by encapsulation in nanoparticles (114, 115).

Furthermore, delivery of antisense or nucleic acid-based therapeutics might also benefit from nanocarrier-based delivery systems, as such hydrophilic agents typically cannot cross cellular or organelle membranes. For example, delivery of microRNA-29 into the kidney has been achieved by local transgene expression following ultrasound microbubble-mediated gene transfer (102). Finally, antibodies or recombinant proteins that target TGF- $\beta$  family members or their receptors are directed to extracellular pharmacological targets; enhancing their accumulation in the kidney should avoid internalization of the therapeutic modality. By contrast, for small molecule inhibitors of TGF- $\beta$  signaling, localized release within the kidney parenchyma seems most appropriate. Renal delivery of recombinant proteins has been investigated recently for the delivery of the antifibrotic protein BMP-7, by means of an injectable hydrogel depot (116).

### Conclusion

This Review summarizes the evidence for a diverse population of myofibroblast progenitors in kidney fibrosis. Data from various research groups have yielded differing results about the nature of the progenitor cells (Figure 4), leading to controversy in this field.

Consequently, a clear understanding of the relative contribution of the different cellular sources to renal myofibroblasts has not yet been achieved. These discrepancies can be explained by several factors, including differences in injury models, the use of different Cre-lox recombination systems, the specificity of chosen promoters, and the lack of a specific myofibroblast cell marker. Targeting myofibroblasts is the cornerstone of rational antifibrotic therapy, in view of the pivotal role of this cell type in the production of profibrotic mediators and its role in the deposition of ECM components. Direct targeting strategies might include support of resident and circulating cells, to help them maintain or regain their original functional differentiation state and resist their transition to a myofibroblast phenotype. In addition, molecular medicine has yielded a wide range of targeted agents, such as kinase inhibitors and biologic therapies, which can be used in antifibrotic approaches. Although clinical trials in patients with kidney fibrosis are scarce, initial studies have shown the potential of antifibrotic therapeutics delivered to resident kidney cells to modulate profibrotic and antifibrotic mediators.

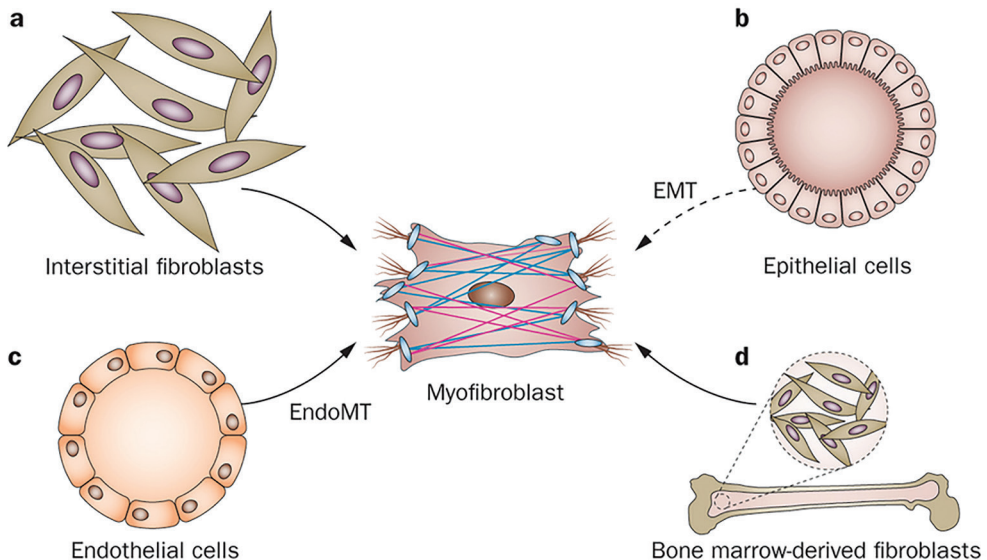


**Figure 4:** Potential origins of myofibroblast progenitors. **A:** Interstitial mesenchymal (fibroblast) cells are commonly regarded as the most profound contributor to the myofibroblast pool during disease. **B:** Epithelial cells were historically indicated as a potential source of myofibroblasts by EMT; however previous research has contradicted this evidence and epithelial progeny has become unlikely. **C:** Endothelial cells have been shown to contribute to some extent to myofibroblasts that contribute to fibrotic development by EndoMT. **D:** Bone marrow derived cells have been shown to incorporate and contribute to myofibroblast numbers. Abbreviations: EMT; epithelial-to-mesenchymal transition; EndoMT, endothelial-to-mesenchymal transition.

## References

1. Kok HM, Falke LL, Goldschmeding R, Nguyen TQ. Targeting CTGF, EGF and PDGF pathways to prevent progression of kidney disease. *Nature reviews Nephrology*. 2014.
2. Hakrrouch S, Moeller MJ, Theilig F, Kaissling B, Sijmonsma TP, Jugold M, et al. Effects of increased renal tubular vascular endothelial growth factor (VEGF) on fibrosis, cyst formation, and glomerular disease. *The American journal of pathology*. 2009;175(5):1883-95.
3. Thannickal VJ. Aging, antagonistic pleiotropy and fibrotic disease. *Int J Biochem Cell Biol*. 2010;42(9):1398-400.
4. Akhurst RJ, Hata A. Targeting the TGFbeta signalling pathway in disease. *Nat Rev Drug Discov*. 2012;11(10):790-811.
5. Ryu JH, Daniels CE. Advances in the management of idiopathic pulmonary fibrosis. *F1000 Med Rep*. 2010;2:28.
6. Duffield JS, Lupher M, Thannickal VJ, Wynn TA. Host responses in tissue repair and fibrosis. *Annu Rev Pathol*. 2013;8:241-76.
7. Novak ML, Koh TJ. Macrophage phenotypes during tissue repair. *Journal of leukocyte biology*. 2013;93(6):875-81.
8. Strutz F, Muller GA. Mechanisms of renal fibrogenesis. *Immunological Renal Diseases*. 2001;2nd edition:73 - 101.
9. Sica A, Mantovani A. Macrophage plasticity and polarization: in vivo veritas. *The Journal of clinical investigation*. 2012;122(3):787-95.
10. Wynn TA, Ramalingam TR. Mechanisms of fibrosis: therapeutic translation for fibrotic disease. *Nat Med*. 2012;18(7):1028-40.
11. Micallef L, Vedrenne N, Billet F, Coulomb B, Darby IA, Desmouliere A. The myofibroblast, multiple origins for major roles in normal and pathological tissue repair. *Fibrogenesis Tissue Repair*. 2012;5 Suppl 1:S5.
12. Meng XM, Nikolic-Paterson DJ, Lan HY. Inflammatory processes in renal fibrosis. *Nature reviews Nephrology*. 2014;10(9):493-503.
13. Tomasek JJ, Gabbiani G, Hinz B, Chaponnier C, Brown RA. Myofibroblasts and mechano-regulation of connective tissue remodelling. *Nature reviews Molecular cell biology*. 2002;3(5):349-63.
14. Meran S, Steadman R. Fibroblasts and myofibroblasts in renal fibrosis. *International journal of experimental pathology*. 2011;92(3):158-67.
15. Boor P, Floege J. The renal (myo-)fibroblast: a heterogeneous group of cells. *Nephrol Dial Transplant*. 2012;27(8):3027-36.
16. Gabbiani G, Majno G. Dupuytren's contracture: fibroblast contraction? An ultrastructural study. *The American journal of pathology*. 1972;66(1):131-46.
17. Eyden B. The myofibroblast: phenotypic characterization as a prerequisite to understanding its functions in translational medicine. *Journal of cellular and molecular medicine*. 2008;12(1):22-37.
18. Duffield JS. Cellular and molecular mechanisms in kidney fibrosis. *The Journal of clinical investigation*. 2014;124(6):2299-306.
19. Hinz B, Phan SH, Thannickal VJ, Galli A, Bochaton-Piallat ML, Gabbiani G. The myofibroblast: one function, multiple origins. *The American journal of pathology*. 2007;170(6):1807-16.
20. Lin SL, Kisseleva T, Brenner DA, Duffield JS. Pericytes and perivascular fibroblasts are the primary source of collagen-producing cells in obstructive fibrosis of the kidney. *The American journal of pathology*. 2008;173(6):1617-27.
21. Hinz B. The myofibroblast: paradigm for a mechanically active cell. *Journal of biomechanics*. 2010;43(1):146-55.
22. Strutz F, Okada H, Lo CW, Danoff T, Carone RL, Tomaszewski JE, et al. Identification and characterization of a fibroblast marker: FSP1. *J Cell Biol*. 1995;130(2):393-405.
23. Leader M, Collins M, Patel J, Henry K. Vimentin: an evaluation of its role as a tumour marker. *Histopathology*. 1987;11(1):63-72.
24. Osterreicher CH, Penz-Osterreicher M, Grivennikov SI, Guma M, Koltsova EK, Datz C, et al. Fibroblast-specific protein 1 identifies an inflammatory subpopulation of macrophages in the liver. *Proceedings of the National Academy of Sciences of the United States of America*. 2011;108(1):308-13.
25. Mor-Vaknin N, Punturieri A, Sitwala K, Markovitz DM. Vimentin is secreted by activated macrophages. *Nature cell biology*. 2003;5(1):59-63.
26. Lewandoski M. Conditional control of gene expression in the mouse. *Nature reviews Genetics*. 2001;2(10):743-55.
27. Dressler GR. Advances in early kidney specification, development and patterning. *Development*. 2009;136(23):3863-74.
28. Asada N, Takase M, Nakamura J, Oguchi A, Asada M, Suzuki N, et al. Dysfunction of fibroblasts of extrarenal origin underlies renal fibrosis and renal anemia in mice. *The Journal of clinical investigation*. 2011;121(10):3981-90.
29. Humphreys BD, Lin SL, Kobayashi A, Hudson TE, Nowlin BT, Bonventre JV, et al. Fate tracing reveals the pericyte and not epithelial origin of myofibroblasts in kidney fibrosis. *The American journal of pathology*. 2010;176(1):85-97.
30. Zeisberg EM, Potenta SE, Sugimoto H, Zeisberg M, Kalluri R. Fibroblasts in kidney fibrosis emerge via endothelial-to-mesenchymal transition. *Journal of the American Society of Nephrology : JASN*. 2008;19(12):2282-7.
31. Sauer B. Inducible gene targeting in mice using the Cre/lox system. *Methods*. 1998;14(4):381-92.

32. Picard N, Baum O, Voetseder A, Kaissling B, Le Hir M. Origin of renal myofibroblasts in the model of unilateral ureter obstruction in the rat. *Histochem Cell Biol*. 2008;130(1):141-55.
33. Faulkner JL, Szyckalski LM, Springer F, Barnes JL. Origin of interstitial fibroblasts in an accelerated model of angiotensin II-induced renal fibrosis. *The American journal of pathology*. 2005;167(5):1193-205.
34. Lebleu VS, Taduri G, O'Connell J, Teng Y, Cooke VG, Woda C, et al. Origin and function of myofibroblasts in kidney fibrosis. *Nat Med*. 2013;19(8):1047-53.
35. Khairoun M, van der Pol P, de Vries DK, Lievers E, Schlagwein N, de Boer HC, et al. Renal ischemia-reperfusion induces a dysbalance of angiopoietins, accompanied by proliferation of pericytes and fibrosis. *Am J Physiol Renal Physiol*. 2013;305(6):F901-10.
36. Kida Y, Duffield JS. Pivotal role of pericytes in kidney fibrosis. *Clin Exp Pharmacol Physiol*. 2011;38(7):467-73.
37. Schlondorff D. The glomerular mesangial cell: an expanding role for a specialized pericyte. *FASEB journal : official publication of the Federation of American Societies for Experimental Biology*. 1987;1(4):272-81.
38. Sam R, Wanna L, Gudehithlu KP, Garber SL, Dunea G, Arruda JA, et al. Glomerular epithelial cells transform to myofibroblasts: early but not late removal of TGF-beta1 reverses transformation. *Transl Res*. 2006;148(3):142-8.
39. Whiteside C, Munk S, Ispanovic E, Wang H, Goldberg H, Kapus A, et al. Regulation of mesangial cell alpha-smooth muscle actin expression in 3-dimensional matrix by high glucose and growth factors. *Nephron Experimental nephrology*. 2008;109(2):e46-56.
40. Alpers CE, Hudkins KL, Gown AM, Johnson RJ. Enhanced expression of "muscle-specific" actin in glomerulonephritis. *Kidney international*. 1992;41(5):1134-42.
41. Matsubara T, Abe H, Arai H, Nagai K, Mima A, Kanamori H, et al. Expression of Smad1 is directly associated with mesangial matrix expansion in rat diabetic nephropathy. *Lab Invest*. 2006;86(4):357-68.
42. Lamouille S, Xu J, Derynck R. Molecular mechanisms of epithelial-mesenchymal transition. *Nature reviews Molecular cell biology*. 2014;15(3):178-96.
43. Kalluri R, Weinberg RA. The basics of epithelial-mesenchymal transition. *The Journal of clinical investigation*. 2009;119(6):1420-8.
44. Ng YY, Fan JM, Mu W, Nikolic-Paterson DJ, Yang WC, Huang TP, et al. Glomerular epithelial-myofibroblast transdifferentiation in the evolution of glomerular crescent formation. *Nephrol Dial Transplant*. 1999;14(12):2860-72.
45. Ng YY, Huang TP, Yang WC, Chen ZP, Yang AH, Mu W, et al. Tubular epithelial-myofibroblast transdifferentiation in progressive tubulointerstitial fibrosis in 5/6 nephrectomized rats. *Kidney international*. 1998;54(3):864-76.
46. Yamaguchi Y, Iwano M, Suzuki D, Nakatani K, Kimura K, Harada K, et al. Epithelial-mesenchymal transition as a potential explanation for podocyte depletion in diabetic nephropathy. *Am J Kidney Dis*. 2009;54(4):653-64.
47. Bariety J, Hill GS, Mandet C, Irinopoulou T, Jacquot C, Meyrier A, et al. Glomerular epithelial-mesenchymal transdifferentiation in pauci-immune crescentic glomerulonephritis. *Nephrol Dial Transplant*. 2003;18(9):1777-84.
48. Rastaldi MP, Ferrario F, Giardino L, Dell'Antonio G, Grillo C, Grillo P, et al. Epithelial-mesenchymal transition of tubular epithelial cells in human renal biopsies. *Kidney international*. 2002;62(1):137-46.
49. Vongwiwatana A, Tasanarong A, Rayner DC, Melk A, Halloran PF. Epithelial to mesenchymal transition during late deterioration of human kidney transplants: the role of tubular cells in fibrogenesis. *Am J Transplant*. 2005;5(6):1367-74.
50. Chen CL, Chou KJ, Lee PT, Chen YS, Chang TY, Hsu CY, et al. Erythropoietin suppresses epithelial to mesenchymal transition and intercepts Smad signal transduction through a MEK-dependent mechanism in pig kidney (LLC-PK1) cell lines. *Exp Cell Res*. 2010;316(7):1109-18.
51. Tasanarong A, Kongkham S, Khositseth S. Dual inhibiting senescence and epithelial-to-mesenchymal transition by erythropoietin preserve tubular epithelial cell regeneration and ameliorate renal fibrosis in unilateral ureteral obstruction. *Biomed Res Int*. 2013;2013:308130.
52. Yang J, Liu Y. Blockage of tubular epithelial to myofibroblast transition by hepatocyte growth factor prevents renal interstitial fibrosis. *Journal of the American Society of Nephrology : JASN*. 2002;13(1):96-107.
53. Zeisberg M, Hanai J, Sugimoto H, Mammoto T, Charytan D, Strutz F, et al. BMP-7 counteracts TGF-beta1-induced epithelial-to-mesenchymal transition and reverses chronic renal injury. *Nat Med*. 2003;9(7):964-8.
54. Iwano M, Plieth D, Danoff TM, Xue C, Okada H, Neilson EG. Evidence that fibroblasts derive from epithelium during tissue fibrosis. *The Journal of clinical investigation*. 2002;110(3):341-50.
55. Li L, Zepeda-Orozco D, Black R, Lin F. Autophagy is a component of epithelial cell fate in obstructive uropathy. *The American journal of pathology*. 2010;176(4):1767-78.
56. Koesters R, Kaissling B, Lehir M, Picard N, Theilig F, Gebhardt R, et al. Tubular overexpression of transforming growth factor-beta1 induces autophagy and fibrosis but not mesenchymal transition of renal epithelial cells. *The American journal of pathology*. 2010;177(2):632-43.
57. Thiery JP, Acloque H, Huang RY, Nieto MA. Epithelial-mesenchymal transitions in development and disease. *Cell*. 2009;139(5):871-90.
58. Galichon P, Finianos S, Hertig A. EMT-MET in renal disease: should we curb our enthusiasm? *Cancer Lett*. 2013;341(1):24-9.
59. Kriz W, Kaissling B, Le Hir M. Epithelial-mesenchymal transition (EMT) in kidney fibrosis: fact or fantasy? *The Journal of clinical investigation*. 2011;121(2):468-74.
60. Smeets B, Uhlig S, Fuss A, Mooren F, Wetzels JF, Floege J, et al. Tracing the origin of glomerular extracapillary lesions from parietal epithelial cells. *Journal of the American Society of Nephrology : JASN*.

2009;20(12):2604-15.

61. Hackl MJ, Burford JL, Villanueva K, Lam L, Susztak K, Schermer B, et al. Tracking the fate of glomerular epithelial cells in vivo using serial multiphoton imaging in new mouse models with fluorescent lineage tags. *Nat Med.* 2013;19(12):1661-6.
62. Schulte K, Berger K, Boor P, Jirak P, Gelman IH, Arkill KP, et al. Origin of parietal podocytes in atubular glomeruli mapped by lineage tracing. *Journal of the American Society of Nephrology : JASN.* 2014;25(1):129-41.
63. Burford JL, Villanueva K, Lam L, Riquier-Brison A, Hackl MJ, Pippin J, et al. Intravital imaging of podocyte calcium in glomerular injury and disease. *The Journal of clinical investigation.* 2014;124(5):2050-8.
64. Eremina V, Cui S, Gerber H, Ferrara N, Haigh J, Nagy A, et al. Vascular endothelial growth factor a signaling in the podocyte-endothelial compartment is required for mesangial cell migration and survival. *Journal of the American Society of Nephrology : JASN.* 2006;17(3):724-35.
65. Sakamaki Y, Sakatsume M, Wang X, Inomata S, Yamamoto T, Gejyo F, et al. Injured kidney cells express SM22alpha (transgelin): Unique features distinct from alpha-smooth muscle actin (alphaSMA). *Nephrology (Carlton).* 2011;16(2):211-8.
66. Piera-Velazquez S, Li Z, Jimenez SA. Role of endothelial-mesenchymal transition (EndoMT) in the pathogenesis of fibrotic disorders. *The American journal of pathology.* 2011;179(3):1074-80.
67. Li J, Qu X, Bertram JF. Endothelial-myofibroblast transition contributes to the early development of diabetic renal interstitial fibrosis in streptozotocin-induced diabetic mice. *The American journal of pathology.* 2009;175(4):1380-8.
68. Phua YL, Martel N, Pennisi DJ, Little MH, Wilkinson L. Distinct sites of renal fibrosis in Crim1 mutant mice arise from multiple cellular origins. *J Pathol.* 2013;229(5):685-96.
69. Curci C, Castellano G, Stasi A, Divella C, Loverre A, Gigante M, et al. Endothelial-to-mesenchymal transition and renal fibrosis in ischaemia/reperfusion injury are mediated by complement anaphylatoxins and Akt pathway. *Nephrol Dial Transplant.* 2014;29(4):799-808.
70. Bellini A, Mattoli S. The role of the fibrocyte, a bone marrow-derived mesenchymal progenitor, in reactive and reparative fibroses. *Lab Invest.* 2007;87(9):858-70.
71. Lee CH, Shah B, Muioli EK, Mao JJ. CTGF directs fibroblast differentiation from human mesenchymal stem/stromal cells and defines connective tissue healing in a rodent injury model. *The Journal of clinical investigation.* 2010;120(9):3340-9.
72. Yang L, Chang N, Liu X, Han Z, Zhu T, Li C, et al. Bone marrow-derived mesenchymal stem cells differentiate to hepatic myofibroblasts by transforming growth factor-beta1 via sphingosine kinase/sphingosine 1-phosphate (S1P)/S1P receptor axis. *The American journal of pathology.* 2012;181(1):85-97.
73. Reich B, Schmidbauer K, Rodriguez Gomez M, Johannes Hermann F, Gobel N, Bruhl H, et al. Fibrocytes develop outside the kidney but contribute to renal fibrosis in a mouse model. *Kidney international.* 2013;84(1):78-89.
74. Broekema M, Harmsen MC, van Luyn MJ, Koerts JA, Petersen AH, van Kooten TG, et al. Bone marrow-derived myofibroblasts contribute to the renal interstitial myofibroblast population and produce procollagen I after ischemia/reperfusion in rats. *Journal of the American Society of Nephrology : JASN.* 2007;18(1):165-75.
75. Grimm PC, Nickerson P, Jeffery J, Savani RC, Gough J, McKenna RM, et al. Neointimal and tubulointerstitial infiltration by recipient mesenchymal cells in chronic renal-allograft rejection. *The New England journal of medicine.* 2001;345(2):93-7.
76. Rienstra H, Boersema M, Onuta G, Boer MW, Zandvoort A, van Riesen M, et al. Donor and recipient origin of mesenchymal and endothelial cells in chronic renal allograft remodeling. *Am J Transplant.* 2009;9(3):463-72.
77. Roufosse C, Bou-Gharios G, Prodromidi E, Alexakis C, Jeffery R, Khan S, et al. Bone marrow-derived cells do not contribute significantly to collagen I synthesis in a murine model of renal fibrosis. *Journal of the American Society of Nephrology : JASN.* 2006;17(3):775-82.
78. Lin SL, Castano AP, Nowlin BT, Lupher ML, Jr., Duffield JS. Bone marrow Ly6Chigh monocytes are selectively recruited to injured kidney and differentiate into functionally distinct populations. *Journal of immunology.* 2009;183(10):6733-43.
79. Eddy AA, Lopez-Guisa JM, Okamura DM, Yamaguchi I. Investigating mechanisms of chronic kidney disease in mouse models. *Pediatr Nephrol.* 2012;27(8):1233-47.
80. De Palma M, Venneri MA, Galli R, Sergi L, Politi LS, Sampaolesi M, et al. Tie2 identifies a hematopoietic lineage of proangiogenic monocytes required for tumor vessel formation and a mesenchymal population of pericyte progenitors. *Cancer cell.* 2005;8(3):211-26.
81. Chang L, Noseda M, Higginson M, Ly M, Patenaude A, Fuller M, et al. Differentiation of vascular smooth muscle cells from local precursors during embryonic and adult arteriogenesis requires Notch signaling. *Proceedings of the National Academy of Sciences of the United States of America.* 2012;109(18):6993-8.
82. Eddy AA. The origin of scar-forming kidney myofibroblasts. *Nat Med.* 2013;19(8):964-6.
83. Zeisberg M, Duffield JS. Resolved: EMT produces fibroblasts in the kidney. *Journal of the American Society of Nephrology : JASN.* 21(8):1247-53.
84. Tampe D, Zeisberg M. Potential approaches to reverse or repair renal fibrosis. *Nature reviews Nephrology.* 2014;10(4):226-37.
85. Distler JH, Distler O. Tyrosine kinase inhibitors for the treatment of fibrotic diseases such as systemic sclerosis: towards molecular targeted therapies. *Annals of the rheumatic diseases.* 2010;69 Suppl 1:i48-51.
86. Prakash J, Poelstra K, van Goor H, Moolenaar F, Meijer DKF, Kok RJ. Novel Therapeutic Targets for the Treatment of Tubulointerstitial Fibrosis. *Current Signal Transduction Therapy.* 2014;3(2):97-111.
87. Bansal R, Prakash J, De Ruiter M, Poelstra K. Targeted recombinant fusion proteins of IFNgamma and mimetic IFNgamma with PDGFbetaR bicyclic peptide inhibits liver fibrogenesis in vivo. *PLoS One.*

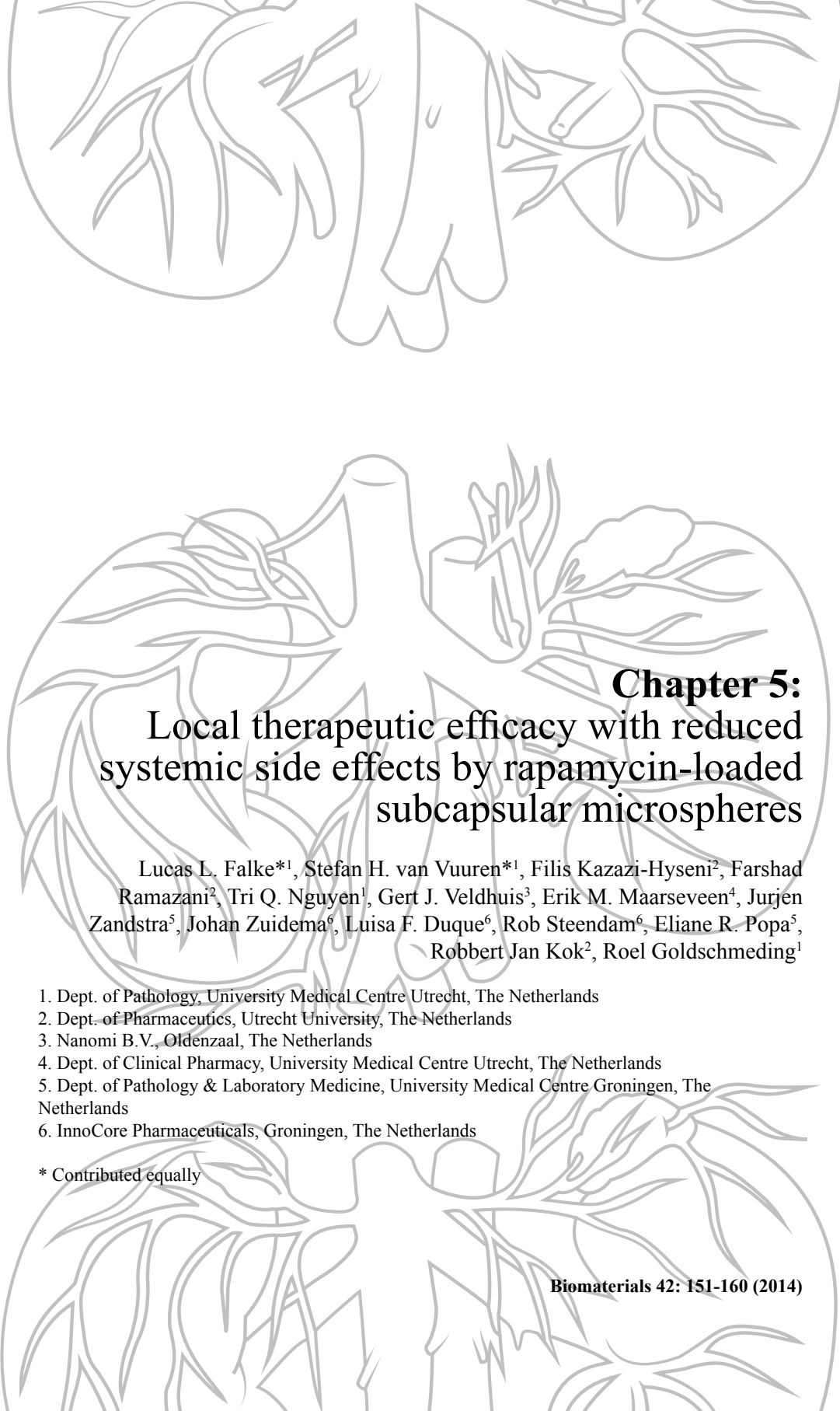
2014;9(2):e89878.

88. Hagens WI, Mattos A, Greupink R, de Jager-Krikken A, Reker-Smit C, van Loenen-Weemaes A, et al. Targeting 15d-prostaglandin J2 to hepatic stellate cells: two options evaluated. *Pharm Res.* 2007;24(3):566-74.
89. Christensen EI, Birn H, Storm T, Weyer K, Nielsen R. Endocytic receptors in the renal proximal tubule. *Physiology* (Bethesda). 2012;27(4):223-36.
90. Prakash J, de Borst MH, Lacombe M, Opdam F, Klok PA, van Goor H, et al. Inhibition of renal rho kinase attenuates ischemia/reperfusion-induced injury. *Journal of the American Society of Nephrology : JASN.* 2008;19(11):2086-97.
91. Shillingford JM, Leamon CP, Vlahov IR, Weimbs T. Folate-conjugated rapamycin slows progression of polycystic kidney disease. *Journal of the American Society of Nephrology : JASN.* 2012;23(10):1674-81.
92. Prakash J, Sandovici M, Saluja V, Lacombe M, Schaapveld RQ, de Borst MH, et al. Intracellular delivery of the p38 mitogen-activated protein kinase inhibitor SB202190 [4-(4-fluorophenyl)-2-(4-hydroxyphenyl)-5-(4-pyridyl)1H-imidazole] in renal tubular cells: a novel strategy to treat renal fibrosis. *The Journal of pharmacology and experimental therapeutics.* 2006;319(1):8-19.
93. Lin Y, Li Y, Wang X, Gong T, Zhang L, Sun X. Targeted drug delivery to renal proximal tubule epithelial cells mediated by 2-glucosamine. *Journal of controlled release : official journal of the Controlled Release Society.* 2013;167(2):148-56.
94. Wang X, Lin Y, Zeng Y, Sun X, Gong T, Zhang Z. Effects of mycophenolic acid-glucosamine conjugates on the base of kidney targeted drug delivery. *International journal of pharmaceutics.* 2013;456(1):223-34.
95. Floege J, Eitner F, Alpers CE. A new look at platelet-derived growth factor in renal disease. *Journal of the American Society of Nephrology : JASN.* 2008;19(1):12-23.
96. Greupink R, Bakker HI, van Goor H, de Borst MH, Beljaars L, Poelstra K. Mannose-6-phosphate/insulin-Like growth factor-II receptors may represent a target for the selective delivery of mycophenolic acid to fibrogenic cells. *Pharm Res.* 2006;23(8):1827-34.
97. Moreno M, Gonzalo T, Kok RJ, Sancho-Bru P, van Beuge M, Swart J, et al. Reduction of advanced liver fibrosis by short-term targeted delivery of an angiotensin receptor blocker to hepatic stellate cells in rats. *Hepatology.* 2010;51(3):942-52.
98. van Beuge MM, Prakash J, Lacombe M, Post E, Reker-Smit C, Beljaars L, et al. Enhanced effectivity of an ALK5-inhibitor after cell-specific delivery to hepatic stellate cells in mice with liver injury. *PLoS One.* 2013;8(2):e56442.
99. Dolman ME, Harmsen S, Storm G, Hennink WE, Kok RJ. Drug targeting to the kidney: Advances in the active targeting of therapeutics to proximal tubular cells. *Adv Drug Deliv Rev.* 2010;62(14):1344-57.
100. Leeuwis JW, Nguyen TQ, Dendooven A, Kok RJ, Goldschmeding R. Targeting podocyte-associated diseases. *Adv Drug Deliv Rev.* 2010;62(14):1325-36.
101. Scindia YM, Deshmukh US, Bagavant H. Mesangial pathology in glomerular disease: targets for therapeutic intervention. *Adv Drug Deliv Rev.* 2010;62(14):1337-43.
102. Qin W, Chung AC, Huang XR, Meng XM, Hui DS, Yu CM, et al. TGF-beta/Smad3 signaling promotes renal fibrosis by inhibiting miR-29. *Journal of the American Society of Nephrology : JASN.* 2011;22(8):1462-74.
103. Trachtman H, Fervenza FC, Gipson DS, Heering P, Jayne DR, Peters H, et al. A phase 1, single-dose study of fresolimumab, an anti-TGF-beta antibody, in treatment-resistant primary focal segmental glomerulosclerosis. *Kidney international.* 2011;79(11):1236-43.
104. A Study of Fresolimumab in Patients With Steroid-Resistant Primary Focal Segmental Glomerulosclerosis(FSGS). <http://clinicaltrials.gov/ct2/show/NCT01665391?term=fresolimumab&rank=3>. 2014.
105. Adler SG, Schwartz S, Williams ME, Arauz-Pacheco C, Bolton WK, Lee T, et al. Phase 1 study of anti-CTGF monoclonal antibody in patients with diabetes and microalbuminuria. *Clinical journal of the American Society of Nephrology : CJASN.* 2010;5(8):1420-8.
106. Richeldi L, du Bois RM, Raghu G, Azuma A, Brown KK, Costabel U, et al. Efficacy and safety of nintedanib in idiopathic pulmonary fibrosis. *The New England journal of medicine.* 2014;370(22):2071-82.
107. Liu N, Guo JK, Pang M, Tolbert E, Ponnusamy M, Gong R, et al. Genetic or pharmacologic blockade of EGFR inhibits renal fibrosis. *Journal of the American Society of Nephrology : JASN.* 2012;23(5):854-67.
108. Elmholdt TR, Buus NH, Ramsing M, Olesen AB. Antifibrotic effect after low-dose imatinib mesylate treatment in patients with nephrogenic systemic fibrosis: an open-label non-randomized, uncontrolled clinical trial. *Journal of the European Academy of Dermatology and Venereology : JEADV.* 2013;27(6):779-84.
109. Illouz F, Braun D, Briet C, Schweizer U, Rodien P. Endocrine side-effects of anti-cancer drugs: thyroid effects of tyrosine kinase inhibitors. *European journal of endocrinology / European Federation of Endocrine Societies.* 2014;171(3):R91-9.
110. Hartmann JT, Haap M, Kopp HG, Lipp HP. Tyrosine kinase inhibitors - a review on pharmacology, metabolism and side effects. *Current drug metabolism.* 2009;10(5):470-81.
111. Hong S, Fang W, Liang W, Yan Y, Zhou T, Qin T, et al. Risk of treatment-related deaths with vascular endothelial growth factor receptor tyrosine kinase inhibitors: a meta-analysis of 41 randomized controlled trials. *OncoTargets and therapy.* 2014;7:1851-67.
112. Casanovas O, Hicklin DJ, Bergers G, Hanahan D. Drug resistance by evasion of antiangiogenic targeting of VEGF signaling in late-stage pancreatic islet tumors. *Cancer cell.* 2005;8(4):299-309.
113. Connolly EC, Saunier EF, Quigley D, Luu MT, De Sapio A, Hann B, et al. Outgrowth of drug-resistant carcinomas expressing markers of tumor aggression after long-term TbetaRI/II kinase inhibition with LY2109761. *Cancer research.* 2011;71(6):2339-49.
114. Dolman ME, van Dorenmalen KM, Pieters EH, Lacombe M, Pato J, Storm G, et al. Imatinib-ULS-lysozyme: a proximal tubular cell-targeted conjugate of imatinib for the treatment of renal diseases. *Journal of controlled release : official journal of the Controlled Release Society.* 2012;157(3):461-8.

115. Prakash J, de Borst MH, van Loenen-Weemaes AM, Lacombe M, Opdam F, van Goor H, et al. Cell-specific delivery of a transforming growth factor-beta type I receptor kinase inhibitor to proximal tubular cells for the treatment of renal fibrosis. *Pharm Res.* 2008;25(10):2427-39.
116. Dankers PY, Hermans TM, Baughman TW, Kamikawa Y, Kieltyka RE, Bastings MM, et al. Hierarchical formation of supramolecular transient networks in water: a modular injectable delivery system. *Advanced materials.* 2012;24(20):2703-9.
117. Lebleu VS, Sugimoto H, Miller CA, Gattone VH, 2nd, Kalluri R. Lymphocytes are dispensable for glomerulonephritis but required for renal interstitial fibrosis in matrix defect-induced Alport renal disease. *Lab Invest.* 2008;88(3):284-92.
118. Stokman G, Qin Y, Booij TH, Ramaiahgari S, Lacombe M, Dolman ME, et al. Epac-Rap signaling reduces oxidative stress in the tubular epithelium. *Journal of the American Society of Nephrology : JASN.* 2014;25(7):1474-85.
119. Wang X, Xiong M, Zeng Y, Sun X, Gong T, Zhang Z. Mechanistic studies of a novel mycophenolic Acid-glucosamine conjugate that attenuates renal ischemia/reperfusion injury in rat. *Molecular pharmaceutics.* 2014;11(10):3503-14.
120. Yuan ZX, Sun X, Gong T, Ding H, Fu Y, Zhang ZR. Randomly 50% N-acetylated low molecular weight chitosan as a novel renal targeting carrier. *J Drug Target.* 2007;15(4):269-78.
121. Suzuki K, Susaki H, Okuno S, Yamada H, Watanabe HK, Sugiyama Y. Specific renal delivery of sugar-modified low-molecular-weight peptides. *The Journal of pharmacology and experimental therapeutics.* 1999;288(2):888-97.
122. Scindia Y, Deshmukh U, Thimmalapura PR, Bagavant H. Anti-alpha8 integrin immunoliposomes in glomeruli of lupus-susceptible mice: a novel system for delivery of therapeutic agents to the renal glomerulus in systemic lupus erythematosus. *Arthritis and rheumatism.* 2008;58(12):3884-91.
123. Suana AJ, Tuffin G, Frey BM, Knudsen L, Muhlfield C, Rodder S, et al. Single application of low-dose mycophenolate mofetil-OX7-immunoliposomes ameliorates experimental mesangial proliferative glomerulonephritis. *The Journal of pharmacology and experimental therapeutics.* 2011;337(2):411-22.
124. Asgeirsdottir SA, Zwiers PJ, Morselt HW, Moorlag HE, Bakker HI, Heeringa P, et al. Inhibition of proinflammatory genes in anti-GBM glomerulonephritis by targeted dexamethasone-loaded AbEsel liposomes. *Am J Physiol Renal Physiol.* 2008;294(3):F554-61.
125. Hauser PV, Pippin JW, Kaiser C, Krofft RD, Brinkkoetter PT, Hudkins KL, et al. Novel siRNA delivery system to target podocytes in vivo. *PLoS One.* 2010;5(3):e9463.

5





## **Chapter 5:** Local therapeutic efficacy with reduced systemic side effects by rapamycin-loaded subcapsular microspheres

Lucas L. Falke\*<sup>1</sup>, Stefan H. van Vuuren\*<sup>1</sup>, Filis Kazazi-Hyseni<sup>2</sup>, Farshad Ramazani<sup>2</sup>, Tri Q. Nguyen<sup>1</sup>, Gert J. Veldhuis<sup>3</sup>, Erik M. Maarseveen<sup>4</sup>, Jurjen Zandstra<sup>5</sup>, Johan Zuidema<sup>6</sup>, Luisa F. Duque<sup>6</sup>, Rob Steendam<sup>6</sup>, Eliane R. Popa<sup>5</sup>, Robbert Jan Kok<sup>2</sup>, Roel Goldschmeding<sup>1</sup>

1. Dept. of Pathology, University Medical Centre Utrecht, The Netherlands
2. Dept. of Pharmaceutics, Utrecht University, The Netherlands
3. Nanomi B.V., Oldenzaal, The Netherlands
4. Dept. of Clinical Pharmacy, University Medical Centre Utrecht, The Netherlands
5. Dept. of Pathology & Laboratory Medicine, University Medical Centre Groningen, The Netherlands
6. InnoCore Pharmaceuticals, Groningen, The Netherlands

\* Contributed equally

**Abstract**

Kidney injury triggers fibrosis, the final common pathway of chronic kidney disease (CKD). The increase of CKD prevalence worldwide urgently calls for new therapies. Available systemic treatment such as rapamycin are associated with serious side effects. To study the potential of local antifibrotic therapy, we administered rapamycin-loaded microspheres under the kidney capsule of ureter-obstructed rats and assessed the local antifibrotic effects and systemic side effects of rapamycin. After 7 days, microsphere depots were easily identifiable under the kidney capsule. Both systemic and local rapamycin treatment reduced intrarenal mTOR activity, myofibroblast accumulation, expression of fibrotic genes, and T-lymphocyte infiltration. Upon local treatment, inhibition of mTOR activity and reduction of myofibroblast accumulation were limited to the immediate vicinity of the subcapsular pocket, while reduction of T-cell infiltration was widespread. In contrast to systemically administered rapamycin, local treatment did not induce off target effects such as weight loss. Thus subcapsular delivery of rapamycin-loaded microspheres successfully inhibited local fibrotic response in UUU with less systemic effects. Therapeutic effect of released rapamycin was most prominent in close vicinity to the implanted microspheres.

## Introduction

Kidney injury triggers inflammation, irrespective of insult type. The inflammatory response encompasses vascular activation (1), infiltration of inflammatory cells into the renal interstitium (2, 3) and production of pro-inflammatory cytokines (1, 4, 5). Inadequate resolution of acute renal inflammation and progression to chronic inflammation set the stage for the development of fibrosis, the final common pathway to chronic kidney disease (CKD). Worldwide rapid increase of CKD incidence urgently calls for new therapies.

Evidence exists that the mTOR pathway plays an important role in the mechanisms underlying the progression of CKD. In all eukaryotic organisms mTOR is present and functions as an intracellular nutrient sensor that controls protein synthesis, cell growth and metabolism (6). There are two mTOR complexes (mTORC1 and mTORC2). The well-known mTOR inhibitor rapamycin inhibits interstitial inflammation, fibrosis, and loss of renal function associated with CKD in a wide variety of animal models (7-13). Rapamycin exclusively inhibits mTORC1, but does not inhibit mTORC2 (14). mTORC1 signalling is activated in myofibroblasts from fibrotic kidneys (15) and rapamycin can ameliorate kidney fibrosis by blocking the mTOR signalling in interstitial myofibroblasts, suggesting a possible role for mTORC1 activation in myofibroblasts in promoting kidney fibrosis (16). Within lymphocytes, where mTOR is involved in the second phase of T-cell activation, rapamycin blocks IL-2-driven T cell cycle progression whilst not influencing T cell survival (17, 18). When rapamycin binds intracellularly to its target, the FKBP12 protein, the signal transduction pathway required for the progression of cytokine-stimulated T cells from the G1 into the S phase is inhibited, thus suppressing interleukin-driven T-cell proliferation.

Rapamycin has great therapeutic potential, but the use of rapamycin and other mTOR inhibitors is associated with many systemic effects. The systemic effects of rapamycin may account for the 20%-40% dropout rate in clinical phase III trials (18). In rats rapamycin induces decreased food intake and concomitant weight loss (19). Although some side effects of rapamycin are easily managed, there is an urgent need for renoprotective approaches that are better tolerated. Targeted treatment for the kidney focuses on nanomedicines and conjugates that accumulate in specific kidney cell types such as podocytes (20) and proximal tubular cells (21). Folate-conjugated rapamycin reduced the progression of polycystic kidney disease in the *bpk*-mutant mice which illustrates the feasibility of such a prodrug approach (22). (23) We now aim to deliver rapamycin locally in the kidney by subcapsular injection of polymeric microspheres. Rapamycin is a hydrophobic compound that can be formulated efficiently in polymeric devices, which has been investigated extensively for drug-eluting stents (24). Various other types of biodegradable implants have been loaded with rapamycin, such as poly(l-lactide-co-trimethylene carbonate) matrices (25), perivascular PLGA wraps (26) and PLGA-PEG based thermosensitive hydrogels (27). Subcapsular injection of a depot under the renal capsule has recently been investigated by Dankers et al who evaluated the biocompatibility of self-assembling hydrogels and the local release of bone-morphogenetic protein 7 (BMP7) in healthy rats (28-32)

We developed rapamycin polymeric microspheres with a multiblock copolymer consisting of amorphous DL-lactide/polyethyleneglycol (PEG)/DL-lactide blocks and crystalline L-lactide blocks. The amorphous PEG-containing blocks favour swelling and gradual erosion of this type of polymeric systems (33). For the present study we used a block copolymer with 20% w/w of the DL-lactide-PEG-DL-lactide block and 80% of the crystalline L-lactide block. We aimed at a rapamycin loading content of 15% w/w which is much higher than previously reported rapamycin microparticles prepared by emulsification methods which typically contain less than 2% rapamycin (34-36), although a high rapamycin loading content was reported for spray-dried rapamycin-PLGA microparticles for pulmonary delivery (37). In order to inflict only minimal damage during the injection under the renal capsule, we need to inject the microspheres via narrow needles. Since monodisperse microspheres have a much better syringibility at high concentration we processed the rapamycin polymeric microspheres by microsieving technology (38). In the present study we explored the feasibility of subcapsular injected microspheres as a drug-eluting depot in the unilateral ureter obstruction (UUO) model in rats. The UUO model is a well-established model for renal fibrosis, in which tubular dilation induces inflammatory and fibrotic cascades discussed above. Local treatment of renal fibrosis with such a depot has not been investigated before, and it is unknown

whether drug released from the depot is efficiently distributed throughout the kidney or only active in close proximity to the injection site. We have evaluated the antifibrotic effects of rapamycin by qPCR and immunostaining of fibrosis and mTOR related markers, and have compared the local and systemic effects of subcapsular delivered rapamycin with daily i.p. injections of rapamycin. We hypothesise that local delivery of rapamycin leads to local therapeutic effects with little systemic consequences.

## Materials and Methods

### *Formulation of rapamycin microspheres*

Polymeric microspheres were prepared using a SynBiosys multiblock copolymer consisting of 20% w/w of poly(DL-lactide-PEG1000) with a molecular weight of 2000 g/mole and 80% w/w poly (L-lactide) with a molecular weight of 4000 g/mole (InnoCore Pharmaceuticals, The Netherlands) (Figure 1A). Microspheres were prepared by a single emulsion membrane emulsification technique using an Iris-20 microsieve membrane (Nanomi BV, The Netherlands), which is a microfabricated membrane with uniform pores. Placebo (drug-free) microspheres were prepared from a 20% w/v polymer solution in dichloromethane.

Prior to emulsification, the SynBiosys solution was filtered through a 0.2 mm PTFE filter. The membrane-emulsified microparticles were collected into an aqueous solution containing 4% polyvinylalcohol (PVA) as emulsifier. The collected dispersion of microparticles was left to stir at room temperature for at least 3 h to evaporate the solvent. The hardened microspheres were concentrated by filtration and washed repeatedly with ultrapure water containing 0.05% Tween20. For rapamycin-loaded SynBiosys microspheres, rapamycin was co-dissolved with the SynBiosys polymer to achieve a 20% w/w which was used to prepare microspheres as described above. Placebo microspheres and rapamycin-loaded microspheres were stored at -20°C until evaluation.

### *In vitro rapamycin release*

Release of rapamycin was studied in triplicate under sink conditions, using 10 mg of rapamycin-loaded microspheres. Samples were suspended in 2.0 ml PBS supplemented with 0.5% SDS and incubated at 37°C under mild shaking using a shaking water bath. After 0, 1, 3 and 5 hours and 1, 2, 5, 8 and 12 days, samples were centrifuged for 1 min at 5000rpm. Subsequently, 1.8 ml of the supernatant was sampled and refreshed with 1.8 ml of fresh buffer. The amount of released rapamycin was determined by HPLC.

### *Unilateral ureteral obstruction*

All experiments were performed with the approval of the Experimental Animal Ethics Committee of the University of Utrecht. Female F344/DuCrI rats, weighing 169-196 grams, were anesthetized by inhalation of isoflurane (4% induction, 1.5-3% maintenance) and underwent unilateral ureteral obstruction (UUO) of the left kidney by permanent ligation of the ureter. Rats were given carprofen analgesia (0.05 mg/kg subcutaneously) during the first 24h after surgery with 12-hour intervals. Rats were housed in standard cages in a room with constant temperature on a 12h light-dark cycle. Animals were fed standard animal chow ad libitum and had free access to water.

### *Rapamycin therapy*

For the analysis of systemic rapamycin therapy, UUO rats were divided in two groups. The first group (n=6) was injected daily intraperitoneally with a vehicle solution (4.8% PEG400, 4.8% TWEEN80, 4.0% ethanol), starting on the day of UUO induction. The second group (n=6) was injected daily intraperitoneally with 2 mg/kg rapamycin in vehicle solution. For subcapsular microsphere injection we created two triangular subcapsular pockets of 25µL on the ventral side on the left kidney with a 26G blunt Hamilton needle (Chrom8 International, the Netherlands), that was also used to inject either placebo microspheres (10mg/50µL; n=6 rats) or rapamycin-loaded microspheres (10 mg microspheres containing 2 mg rapamycin/50µL depot; n=9 rats). The microspheres were dissolved in a sterilized carrier solution consisting of 0.6% carboxymethylcellulose, 5% mannitol and 0.1% tween20. After subcapsular injection of the microspheres, the puncture holes in the renal capsule were sealed with fibrin glue (Tissucol©, Baxter, Utrecht, The Netherlands). Rats were sacrificed 7 days after UUO.

### *Histology and immunohistochemistry (IHC)*

Kidneys were formalin fixed, paraffin-embedded and cut into 3 $\mu$ m sections. Staining for  $\alpha$ -SMA (Sigma, A2457) was performed to assess the accumulation of myofibroblasts. Staining for p-S6 ribosomal protein (Cell Signalling Technology, #2211), a downstream target of mTOR, was used as readout for mTOR activity. Staining for CD3 positive T-Lymphocytes (Dako, A452) was performed to assess the infiltration of CD3 positive T-lymphocytes. Stained sections were scanned (Nikon, Aperio scanscope XT 120) and five 20x random sections per kidney were analysed. In the locally treated groups we scored ten random fields; five at the ventral side of the kidney near the microsphere depot and five at the dorsal side distant from the depot (Fig. 3A). Surface area of  $\alpha$ -SMA positive cells and CD3 positive cells was determined using ImageJ (ImageJ, Rasband, National Institutes of Health, USA). p-S6 was scored blind on intensity of staining (arbitrary scale 0-4).

### *Quantitative PCR*

Total RNA was extracted with TRIzol (Life technologies, California, U.S.) from five frozen tissue sections of 20 $\mu$ m. Subcapsular depots were carefully removed to minimize for possible interference of the microspheres in the PCR reaction. After cDNA synthesis, expression of fibronectin and  $\alpha$ -SMA was assessed by quantitative real time PCR using TaqMan Gene Expression Assays with pre-designed probes and primers (Applied Biosystems, Foster City, CA, USA). PCR was carried out in a LightCycler 480II (Roche, Woerden, The Netherlands) with an initial step at 95°C followed by 40 cycles of 15 seconds at 95°C and 1 minute at 60°C. GAPDH mRNA expression was used as an endogenous control.

### *Rapamycin measurement in plasma, liver and heart*

The analysis of rapamycin was performed using a previously published method with a slight adaption with respect to the matrix: plasma, liver and heart instead of whole blood (39). Briefly, 100mg of organ tissue was homogenized in 200 $\mu$ L PBS using a Precellys 24 tissue homogenizer. 50 $\mu$ L Aliquots plasma or tissue homogenate were diluted with 200  $\mu$ L 0.1 M zinc sulphate and 500  $\mu$ L internal standard solution (deuterated rapamycin-d3). The vials were vortexed for 1 min and centrifuged at 13000 rpm for 5 min. 25  $\mu$ L was injected and analysed with LC-MS/MS using a Thermo Fisher Scientific (Waltham, MA) triple quadrupole Quantum Access LC-MS/MS system. Data acquisition and data processing were performed using Xcalibur software version 2.10 (39).

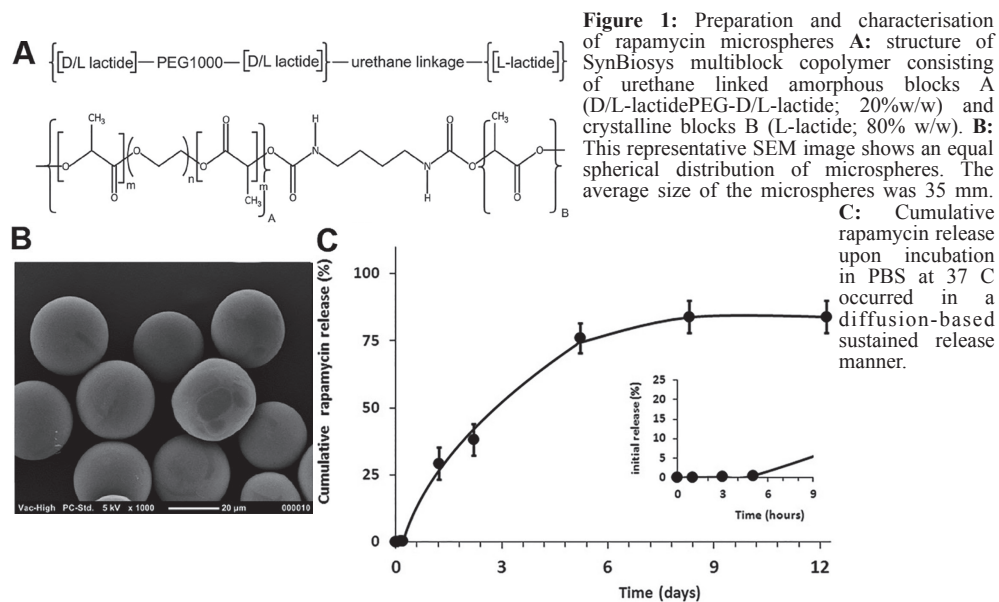
### *Statistics*

Data are represented as mean +/- SEM. Differences between groups were analysed by one-way ANOVA with Bonferroni correction for multiple comparisons. The statistical analysis was performed using GraphPad Prism 5 (GraphPad Software, San Diego, USA).

## Results

### Preparation and characterisation of rapamycin microspheres

Rapamycin-loaded polymeric microspheres were prepared by membrane sieve-technology, yielding monodisperse microspheres with a smooth surface (Fig. 1B). Coulter counter analysis confirmed that rapamycin-loaded microspheres had a narrow size polydispersity (table 1). Rapamycin loading content as determined by UPLC after destruction of the microspheres in acetonitrile was 14% w/w, which corresponded to an encapsulation efficiency of 70%. Additionally, microspheres were characterized for the absence of endotoxin and bacterial contamination, by Limulus amoebocyte lysate assay and by inoculation on blood agar plates respectively. In an in vitro release setup with 1% SDS to provide sink conditions for released rapamycin, we demonstrated that rapamycin was released in a diffusion-related manner, amounting to >80% cumulative release after 7 days (Fig. 1C). No burst release was observed during the first 5 hours. During the 12 days of incubation at 37°C of this experiment, the microspheres remained largely intact as is expected in view of the slow degradation kinetics of the used block copolymer.



Parameter	Level	Method
Rapamycin loading content	14%	UPLC
Encapsulation efficiency	70%	UPLC
Particle size distribution	35 ± 5 μm	Coulter counter
Endotoxin	<0.5 EU/g	Limulus amoebocyte lysate assay
Bacterial contamination	<100 CFU/g	blood agar plate inoculation

### Systemic treatment with rapamycin during 7 days of UUO

Rats injected with intraperitoneal rapamycin injections showed reduced mTOR activity compared to vehicle obstructed kidneys as illustrated by downstream p-S6 staining positivity (Fig. 2A). Furthermore there was a marked reduction in α-SMA area positivity (Fig. 2A). The number of CD3 positive cells was also decreased upon rapamycin administration (Fig. 2A). Upon quantification both p-S6, α-SMA and CD3 showed significant area positivity reduction (Fig. 2B). Body weight of rapamycin treated UUO rats was significantly lower than of vehicle injected UUO rats, indicating that although protecting against obstructive nephropathy, systemic rapamycin treatment is associated with severe unwanted side effects (Fig. 2C).

#### *Subcapsular depot integrity after 7 days of UUO*

Subcapsular depots of rapamycin microspheres were injected directly under the capsule of the ureter-ligated kidney at the moment of the UUO surgical procedure. 7 Days later, at the moment of ing the animals, we inspected the integrity of the subcapsular depots visually. Subcapsular depot integrity was furthermore confirmed in a study with near-infrared labelled microspheres in healthy rats (suppl. Fig 1; Kazazi et al., manuscript in preparation). In both studies, the depots were still detectable under the renal capsule without spread of the microspheres outside of the pockets.

#### *Inhibition of the mTOR pathway*

In rats treated with rapamycin microspheres, SynBiosys, mTOR activity was lower in the renal tissue near the subcapsular pocket compared to placebo microsphere treated rats ( $p < 0.001$ ) (Fig. 3). Placebo-loaded microspheres did not affect mTOR activity. At a larger distance from the subcapsular pockets, i.e. at the dorsal side of the kidney, mTOR pathway activity was still reduced although less pronounced ( $p < 0.05$  vs Veh IP). These results suggest a local effect of the inhibition of mTOR, as could also be observed when inspecting a complete transversal section of the kidney (suppl. Fig. 2).

#### *Antifibrotic and anti-inflammatory effects*

In the entire kidney excluding the subcapsular pocket, mRNA expression of the fibrosis-associated extracellular matrix gene fibronectin was reduced by both subcapsular rapamycin microspheres and systemic daily i.p. injections of rapamycin (Fig. 4). A trend of  $\alpha$ -sma expression reduction was present in rats with systemic rapamycin treatment, but not in rats with local rapamycin treatment (Fig. 4). Staining of tissue sections for  $\alpha$ -SMA revealed a reduction of myofibroblast accumulation of myofibroblasts accumulation near the subcapsular rapamycin microspheres depot ( $p < 0.001$ ), but not distant from the depot. Placebo microspheres did not reduce myofibroblast accumulation nearby or further away from the depot (Fig. 5). Local treatment with rapamycin microspheres reduced the infiltration of CD3 positive T-lymphocytes ( $p < 0.05$ ) compared placebo microspheres both near the rapamycin depot and at more distant parts of the kidney transection (Fig 6).

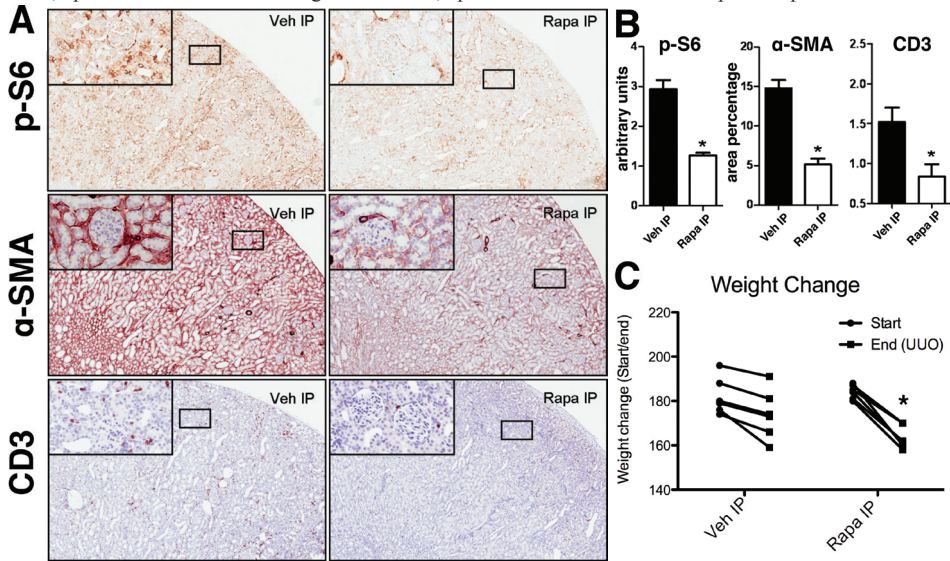
#### *Systemic effects and distribution of rapamycin*

To demonstrate that the action of the subcapsular rapamycin depot is restricted to the treated kidney, we also investigated possible systemic effects. First, we examined the activity of mTOR in the non-obstructed kidney, i.e. the control kidney, which had not received a subcapsular depot. While systemic rapamycin administration strongly inhibited mTOR activity in the non-obstructed kidney ( $p < 0.001$ ), there was only a slight reduction of mTOR activity in the rapamycin microspheres treated group compared to rats injected with vehicle microspheres ( $p < 0.05$ ) (Fig 7A and B). There was no difference between both vehicle treated groups. Additionally, when looking at levels of rapamycin, levels were at the lower limit of detection of 2  $\mu\text{g/L}$  in the rapamycin microspheres group while systemically treated rats had still significantly higher plasma levels at 24h after the last dose as compared to the local treatment (Fig. 7C). Systemic tissue levels of rapamycin were analysed in heart and liver, which showed 5-fold lower levels and 1.5-fold lower levels for the rapamycin microspheres versus systemic treatment (suppl. Fig. 3A&B; liver,  $p < 0.001$ ; heart,  $p < 0.005$ ).

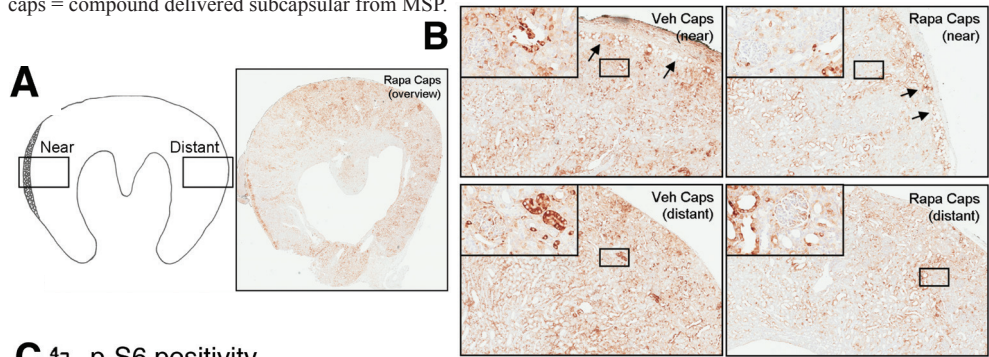
To obtain further evidence to support the predominant local activity of subcapsular rapamycin microspheres, we demonstrated the absence of drug-related weight loss. All animals lost weight during the one-week interval after UUO, due to surgery and the induction of renal disease. Animals treated systemically with rapamycin, however, lost 6% more weight than animals in all the other groups, including the rapamycin microspheres group ( $p < 0.001$ , Fig. 7D and Fig. 2C).



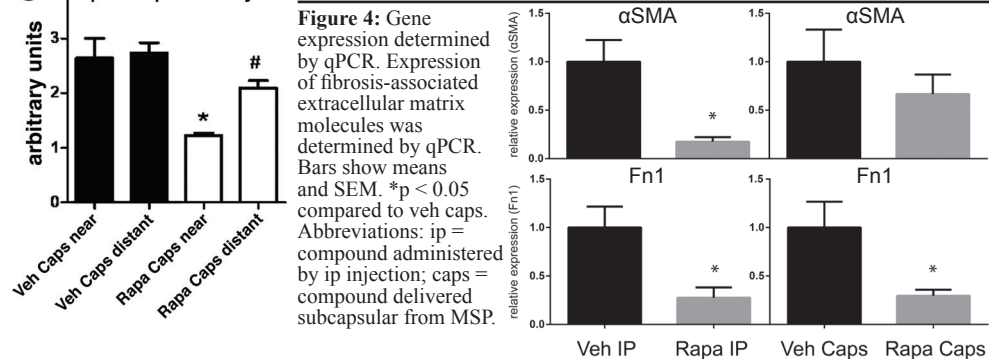
**Figure 2:** Reduction of renal damage and fibrosis by rapamycin. **A:** Representative pictures of kidney sections stained for p-S6,  $\alpha$ -SMA and CD3. **B:** Quantification of positively stained area of kidney sections. Bars represent SEM, \* $p < 0.001$  vs Veh IP. **C:** Weight loss of rats, \* $p < 0.001$  vs Veh IP. Abbrev.: ip = intraperitoneal.



**Figure 3:** mTOR activity in UUO kidneys. **A:** Schematic overview of kidney cross-section demonstrating location of near and distant in respect to the subcapsular pocket (circles represent microspheres, left-hand side of panel). **B:** Visual assessment of staining intensity (4 point scale). Bars demonstrate means and SEM, \* $p < 0.001$  vs Veh IP, Veh caps (near) and Veh caps (distant), # $p < 0.05$  vs Veh IP and Rapa caps (near). **C:** Representative pictures of staining for phospho-S6 ribosomal protein (50x, magnified insert 200x). Arrowheads point towards depot. Abbrev.: caps = compound delivered subcapsular from MSP.



**Figure 4:** Gene expression determined by qPCR. Expression of fibrosis-associated extracellular matrix molecules was determined by qPCR. Bars show means and SEM. \* $p < 0.05$  compared to veh caps. Abbreviations: ip = compound administered by ip injection; caps = compound delivered subcapsular from MSP.



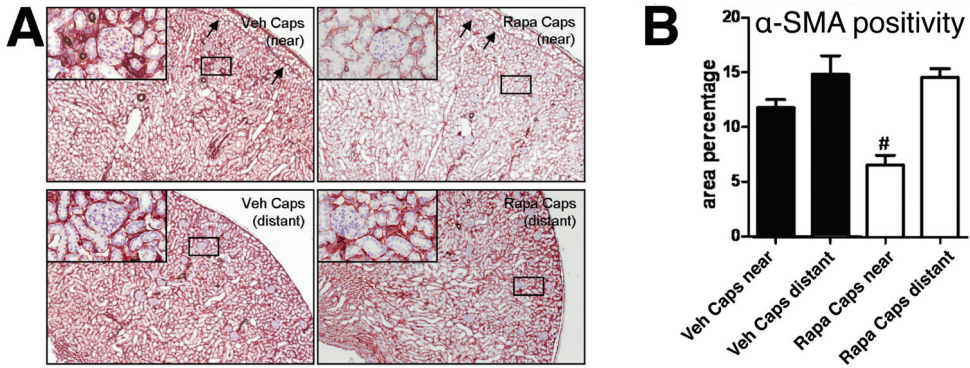


**Figure 5:** Myofibroblast accumulation in UUO kidneys. **A:** Representative pictures of staining for aSMA (50x, magnified insert 200x). **B:** Surface area of positive cells as percentage of total surface area. Bars demonstrate means and SEM, <sup>#</sup>*p* < 0.001 vs Veh IP, *p* < 0.05 vs Veh Caps (near), *p* < 0.001 vs Veh Caps (distant) and Rapa caps distant. Arrowheads point towards depot. Abbrev.: caps = compound delivered subcapsular from MSP.

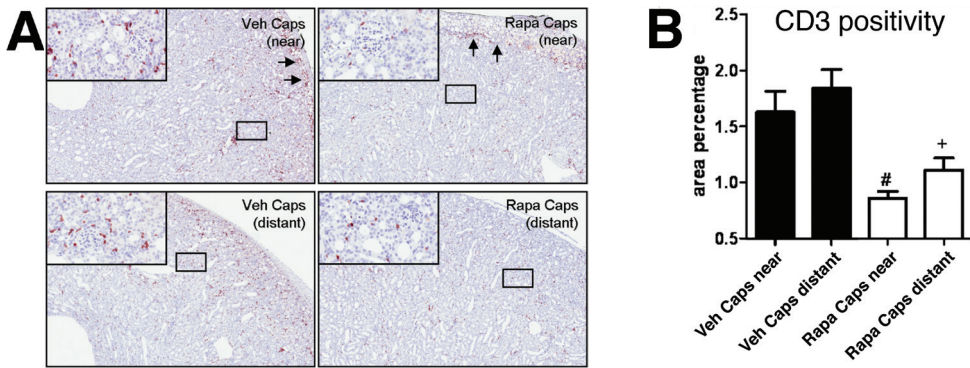


**Figure 6:** T-lymphocyte infiltration in UUO kidneys. **A:** Representative pictures of staining for CD3 (50x, magnified insert 200x). **B:** Surface area of positive cells as percentage of total surface area. Bars demonstrate means and SEM, <sup>#</sup>*p* < 0.05 vs Veh IP, *p* < 0.01 vs Veh Caps (near), Veh Caps (distant) and <sup>+</sup>*p* < 0.01 vs Veh caps (distant). Arrowheads point towards depot. Abbrev.: caps = compound delivered subcapsular from MSP

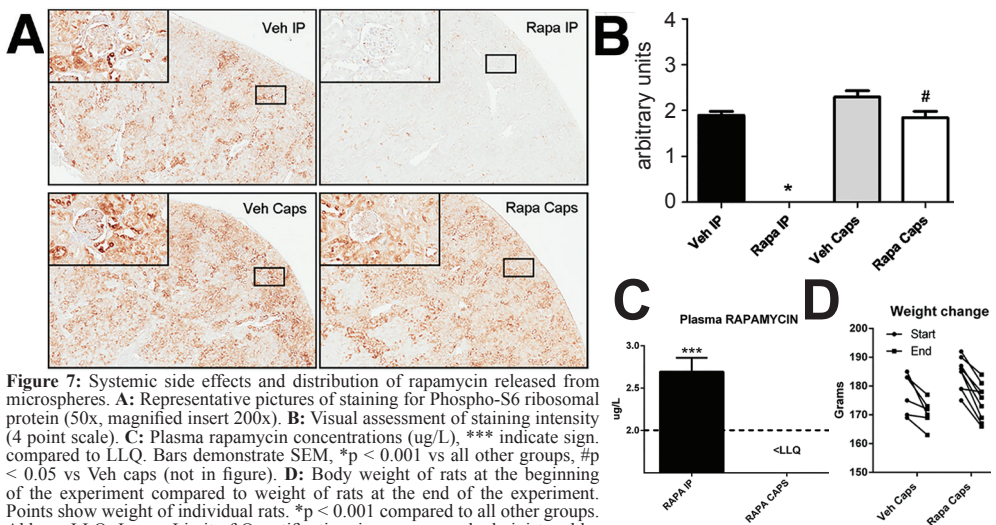


**Figure 7:** Systemic side effects and distribution of rapamycin released from microspheres. **A:** Representative pictures of staining for Phospho-S6 ribosomal protein (50x, magnified insert 200x). **B:** Visual assessment of staining intensity (4 point scale). **C:** Plasma rapamycin concentrations (ug/L), <sup>\*\*\*</sup> indicate sign. compared to LLQ. Bars demonstrate SEM, <sup>\*</sup>*p* < 0.001 vs all other groups, <sup>#</sup>*p* < 0.05 vs Veh caps (not in figure). **D:** Body weight of rats at the beginning of the experiment compared to weight of rats at the end of the experiment. Points show weight of individual rats. <sup>\*</sup>*p* < 0.001 compared to all other groups. Abbrev.: LLQ; Lower Limit of Quantification, ip = compound administered by ip injection; caps = compound delivered subcapsular from MSP.

## Discussion

In the present study we evaluated the feasibility of injecting rapamycin-loaded microspheres under the renal capsule and demonstrated that this polymeric depot is capable of reducing local mTOR activation in obstructed kidneys (Fig. 3). This was associated with less pronounced myofibroblast accumulation and T cell recruitment (Fig. 4-6). The effects of such a treatment were most prominent in close vicinity to the depot although some of the responses were also prominent more distant to the injection site. Moreover, systemic rapamycin levels were low and, as a consequence, no mTOR inhibition or systemic toxicity was observed. Reduction of mTOR-activity was also observed in non-obstructed (contralateral) kidneys from animals treated systemically with rapamycin, but not in animals treated with a subcapsular rapamycin depot. Furthermore, the observed systemic weight loss in the rapamycin i.p. treated group illustrates the severe side-effects of this type of drug. The absence of systemic rapamycin and associated toxicity is an important advantage of our new approach of local subcapsular implantation of rapamycin-loaded microspheres.

Fibroblasts play an important role in maintaining homeostasis of interstitial matrix and adjacent tissues under physiologic conditions through matrix production, cytokine secretion, and direct contact with other cell types (15, 40). Upon activation by profibrotic factors, fibroblasts can be activated to differentiate towards a myofibroblast phenotype by expressing  $\alpha$ -SMA and other markers. Myofibroblasts are commonly regarded as the main effector cell type during fibrosis excreting excessive amounts of ECM and pro fibrotic factors. Rapamycin inhibits kidney fibrosis by blocking mTOR signalling in interstitial myofibroblasts (16). We observed a reduction of myofibroblast accumulation in the entire UUO kidney in systemically treated animals and a more restricted reduction near the subcapsular pocket containing rapamycin-loaded microspheres. These findings match well with the pattern seen by staining for p-S6 as a marker of mTOR signalling activity.

Although immunohistochemical staining is at best semi quantitative it is remarkable that the reduction of p-S6 staining extended over a greater distance from the subcapsular pocket than the reduction of  $\alpha$ -SMA staining. Therefore, the extent of mTOR inhibition in areas more remote from the rapamycin-loaded microspheres in the current formulation appears not to be sufficient to completely inhibit myofibroblast accumulation. This spatially restricted efficacy was also reflected by the fact that, in whole kidney lysates,  $\alpha$ -sma mRNA expression was not significantly reduced in locally treated rats. Additionally, heterogeneous  $\alpha$ -SMA immunohistochemistry suggesting the local penetration of rapamycin might explain the heterogeneous gene expression profile of  $\alpha$ -sma (Fig. 4). In contrast, fibronectin expression was reduced in whole kidney lysates of both locally and systemically treated rats. This suggests that although not sufficiently lowering myofibroblast numbers, local treatment is sufficient to reduce excessive fibronectin expression.

Inhibition of T-lymphocyte infiltration was evident throughout the kidney, including the area's most remote from the pockets containing rapamycin-loaded microspheres. This suggests that a lower dose of rapamycin is enough to inhibit T-lymphocyte activation compared to the dose needed to inhibit the myofibroblast accumulation.

Earlier experiments show that administering drugs in a depot under the renal capsule causes little damage to the renal tissue (28). This was confirmed in this study as the two injected depots did not further damage the obstructed kidney. Biocompatibility of this type of polymeric microspheres is ideally tested in healthy rats, in which the observed inflammatory and fibrotic events can be scored in relation to the foreign body response to the biomaterial. As stents coated with SynBiosys polymers showed good biocompatibility (33) and PLGA microspheres prepared by microsieving also proved safe biomaterials (41), we expect no or only mild foreign body responses to the SynBiosys microspheres injected under the renal capsule.

The observed localized activity of rapamycin near the depot can be considered both a drawback as well as an opportunity of such a localized therapeutic strategy. On one hand, this would require application of multiple depots especially in the much larger kidneys of human patients. Since little is known about fluid streams and about diffusion and conductive transport

of solutes in the kidney interstitium, it remains to be established how the observations made in this study with rapamycin-loaded microspheres in the high pressure ureteral obstruction model would compare to applications involving drugs with other physiochemical characteristics, as well as other models that might more genuinely represent human acute and chronic kidney diseases. Alternatively, the small area of effect as seen in this study might prove of interest in disease where a limited diffusion of therapeutics is warranted such as cancer or other localized disease.

**Conclusion**

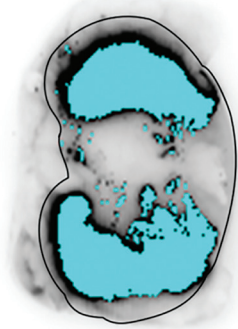
By local administration of rapamycin microspheres under the renal capsule we have obtained proof of principle that, in a model of CKD, subcapsular delivery of drug-loaded microspheres can successfully inhibit inflammatory and fibrotic responses with reduced systemic adverse effects. This novel delivery system offers important opportunities for future development of local drug therapy in kidney diseases and beyond.

## References

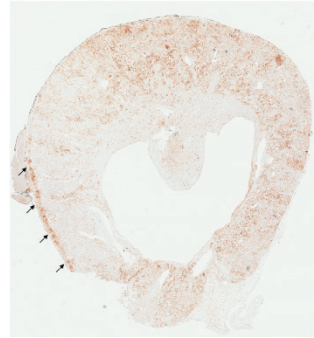
1. Takada M, Nadeau KC, Shaw GD, Marquette KA, Tilney NL. The cytokine-adhesion molecule cascade in ischemia/reperfusion injury of the rat kidney. Inhibition by a soluble P-selectin ligand. *J Clin Invest.* 1997;99(11):2682-90.
2. Friedewald JJ, Rabb H. Inflammatory cells in ischemic acute renal failure. *Kidney Int.* 2004;66(2):486-91.
3. Ysebaert DK, De Greef KE, Vercauteren SR, Ghielli M, Verpooten GA, Eyskens EJ, et al. Identification and kinetics of leukocytes after severe ischaemia/reperfusion renal injury. *Nephrol Dial Transplant.* 2000;15(10):1562-74.
4. Donnahoo KK, Meng X, Ayala A, Cain MP, Harken AH, Meldrum DR. Early kidney TNF-alpha expression mediates neutrophil infiltration and injury after renal ischemia-reperfusion. *Am J Physiol.* 1999;277(3 Pt 2):R922-9.
5. Togel F, Westenfelder C. Recent advances in the understanding of acute kidney injury. *F1000prime reports.* 2014;6:83.
6. Rui L. A link between protein translation and body weight. *J Clin Invest.* 2007;117(2):310-3.
7. Bonegio RG, Fuhro R, Wang Z, Valeri CR, Andry C, Salant DJ, et al. Rapamycin ameliorates proteinuria-associated tubulointerstitial inflammation and fibrosis in experimental membranous nephropathy. *J Am Soc Nephrol.* 2005;16(7):2063-72.
8. Huber TB, Walz G, Kuehn EW. mTOR and rapamycin in the kidney: signaling and therapeutic implications beyond immunosuppression. *Kidney Int.* 2011;79(5):502-11.
9. Kramer S, Wang-Rosenke Y, Scholl V, Binder E, Loof T, Khadzhyrov D, et al. Low-dose mTOR inhibition by rapamycin attenuates progression in anti-thy1-induced chronic glomerulosclerosis of the rat. *Am J Physiol Renal Physiol.* 2008;294(2):F440-9.
10. Lieberthal W, Levine JS. The role of the mammalian target of rapamycin (mTOR) in renal disease. *J Am Soc Nephrol.* 2009;20(12):2493-502.
11. Lock HR, Sacks SH, Robson MG. Rapamycin at subimmunosuppressive levels inhibits mesangial cell proliferation and extracellular matrix production. *Am J Physiol Renal Physiol.* 2007;292(1):F76-81.
12. Schaefer L, Tsalavra W, Babelova A, Baliova M, Minnerup J, Sorokin L, et al. Decorin-mediated regulation of fibrillin-1 in the kidney involves the insulin-like growth factor-I receptor and Mammalian target of rapamycin. *Am J Pathol.* 2007;170(1):301-15.
13. Wu MJ, Wen MC, Chiu YT, Chiou YY, Shu KH, Tang MJ. Rapamycin attenuates unilateral ureteral obstruction-induced renal fibrosis. *Kidney Int.* 2006;69(11):2029-36.
14. Cruzado JM. Nonimmunosuppressive effects of mammalian target of rapamycin inhibitors. *Transplant Rev (Orlando).* 2008;22(1):73-81.
15. Jiang L, Xu L, Mao J, Li J, Fang L, Zhou Y, et al. Rheb/mTORC1 signaling promotes kidney fibroblast activation and fibrosis. *J Am Soc Nephrol.* 2013;24(7):1114-26.
16. Chen G, Chen H, Wang C, Peng Y, Sun L, Liu H, et al. Rapamycin ameliorates kidney fibrosis by inhibiting the activation of mTOR signaling in interstitial macrophages and myofibroblasts. *PLoS One.* 2012;7(3):e33626.
17. Gonzalez J, Harris T, Childs G, Prystowsky MB. Rapamycin blocks IL-2-driven T cell cycle progression while preserving T cell survival. *Blood Cells Mol Dis.* 2001;27(3):572-85.
18. Rostaing L, Kamar N. mTOR inhibitor/proliferation signal inhibitors: entering or leaving the field? *J Nephrol.* 2010;23(2):133-42.
19. Deblon N, Bourgoin L, Veyrat-Durebex C, Peyrou M, Vinciguerra M, Caillon A, et al. Chronic mTOR inhibition by rapamycin induces muscle insulin resistance despite weight loss in rats. *Br J Pharmacol.* 2012;165(7):2325-40.
20. Leeuwis JW, Nguyen TQ, Dendooven A, Kok RJ, Goldschmeding R. Targeting podocyte-associated diseases. *Adv Drug Deliv Rev.* 2010;62(14):1325-36.
21. Dolman ME, Harmsen S, Storm G, Hennink WE, Kok RJ. Drug targeting to the kidney: Advances in the active targeting of therapeutics to proximal tubular cells. *Adv Drug Deliv Rev.* 2010;62(14):1344-57.
22. Shillingford JM, Leamon CP, Vlahov IR, Weimbs T. Folate-conjugated rapamycin slows progression of polycystic kidney disease. *J Am Soc Nephrol.* 2012;23(10):1674-81.
23. Stokman G, Qin Y, Racz Z, Hamar P, Price LS. Application of siRNA in targeting protein expression in kidney disease. *Adv Drug Deliv Rev.* 2010;62(14):1378-89.
24. Khan W, Farah S, Domb AJ. Drug eluting stents: developments and current status. *Journal of controlled release : official journal of the Controlled Release Society.* 2012;161(2):703-12.
25. Jelonek K, Kasperczyk J, Li S, Dobrzynski P, Jarzabek B. Controlled poly(l-lactide-co-trimethylene carbonate) delivery system of cyclosporine A and rapamycin--the effect of copolymer chain microstructure on drug release rate. *International journal of pharmaceuticals.* 2011;414(1-2):203-9.
26. Filova E, Parizek M, Olsovska J, Kamenik Z, Brynda E, Riedel T, et al. Perivascular sirolimus-delivery system. *International journal of pharmaceuticals.* 2011;404(1-2):94-101.
27. Owen SC, Li H, Sanders WG, Cheung AK, Terry CM. Correlation of tissue drug concentrations with in vivo magnetic resonance images of polymer drug depot around arteriovenous graft. *Journal of controlled release : official journal of the Controlled Release Society.* 2010;146(1):23-30.
28. Dankers PY, van Luyn MJ, Huizinga-van der Vlag A, van Gemert GM, Petersen AH, Meijer EW, et al. Development and in-vivo characterization of supramolecular hydrogels for intrarenal drug delivery. *Biomaterials.* 2012;33(20):5144-55.
29. Dankers PY, Hermans TM, Baughman TW, Kamikawa Y, Kieltyka RE, Bastings MM, et al. Hierarchical

- formation of supramolecular transient networks in water: a modular injectable delivery system. *Advanced materials*. 2012;24(20):2703-9.
30. Merani S, Toso C, Emamaullee J, Shapiro AM. Optimal implantation site for pancreatic islet transplantation. *Br J Surg*. 2008;95(12):1449-61.
  31. Cole DR, Waterfall M, McIntyre M, Baird JD. Transplantation of microcapsules (a potential bio-artificial organ): biocompatibility and host reaction. *Journal of Materials Science: Materials in Medicine*. 1993;4(5):437-42.
  32. Lanza RP, Kuhtreiber WM, Ecker D, Staruk JE, Chick WL. Xenotransplantation of porcine and bovine islets without immunosuppression using uncoated alginate microspheres. *Transplantation*. 1995;59(10):1377-84.
  33. Lockwood NA, Hergenrother RW, Patrick LM, Stucke SM, Steendam R, Pacheco E, et al. In vitro and in vivo characterization of novel biodegradable polymers for application as drug-eluting stent coatings. *Journal of biomaterials science Polymer edition*. 2010;21(4):529-52.
  34. Jhunjhunwala S, Raimondi G, Thomson AW, Little SR. Delivery of rapamycin to dendritic cells using degradable microparticles. *Journal of controlled release : official journal of the Controlled Release Society*. 2009;133(3):191-7.
  35. Kauffman KJ, Kanthamneni N, Meenach SA, Pierson BC, Bachelder EM, Ainslie KM. Optimization of rapamycin-loaded acetalated dextran microparticles for immunosuppression. *International journal of pharmaceutics*. 2012;422(1-2):356-63.
  36. Lewis JS, Roche C, Zhang Y, Brusko TM, Wasserfall CH, Atkinson M, et al. Combinatorial delivery of immunosuppressive factors to dendritic cells using dual-sized microspheres. *Journal of materials chemistry B, Materials for biology and medicine*. 2014;2(17):2562-74.
  37. Gupta A, Pant G, Mitra K, Madan J, Chourasia MK, Misra A. Inhalable particles containing rapamycin for induction of autophagy in macrophages infected with *Mycobacterium tuberculosis*. *Molecular pharmaceutics*. 2014;11(4):1201-7.
  38. Kazazi-Hyseni F, Landin M, Lathuile A, Veldhuis GJ, Rahimian S, Hennink WE, et al. Computer Modeling Assisted Design of Monodisperse PLGA Microspheres with Controlled Porosity Affords Zero Order Release of an Encapsulated Macromolecule for 3 Months. *Pharmaceutical research*. 2014;31(10):2844-56.
  39. Koster RA, Dijkers EC, Uges DR. Robust, high-throughput LC-MS/MS method for therapeutic drug monitoring of cyclosporine, tacrolimus, everolimus, and sirolimus in whole blood. *Therapeutic drug monitoring*. 2009;31(1):116-25.
  40. Liu Y. Cellular and molecular mechanisms of renal fibrosis. *Nat Rev Nephrol*. 2011;7(12):684-96.
  41. Zandstra J, Hiemstra C, Petersen AH, Zuidema J, van Beuge MM, Rodriguez S, et al. Microsphere size influences the foreign body reaction. *European cells & materials*. 2014;28:335-47.

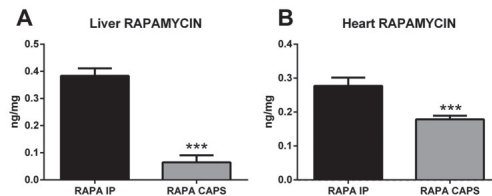
## Supplementary material



**Supplemental figure 1:** Ex vivo Imaging of subcapsular depot in obstructed kidney at day 7 after UUU. IRdye800-labeled polymeric microspheres were injected under the renal capsule of UUU rats and excised 7 days after UUU. Localisation of microspheres was imaged using an Odyssey imager and is displayed in blue. Black line illustrates border of renal tissue and perirenal fat.



**Supplemental figure 2:** Representative picture of staining for phospho-S6 ribosomal protein (1x). Depot is located at left hand-side (ventral side in situ). This figure clearly demonstrates the local effect of mTOR activity inhibition near the depot. Arrows point at depot. Black ink line was added during sacrifice to mark ventral side of kidney.



**Supplemental figure 3:** Rapamycin distribution in liver and heart **A:** concentration of rapamycin (ng) per mg of liver. **B:** concentration of rapamycin (ng) per mg of heart. \*\* $p < 0,005$ ; \*\*\* $p < 0,001$  vs RAPA IP, Abbrev. ip= compound administered by ip injection; caps= compound delivered subcapsular from MSP.

6





## **Chapter 6:** The use of Tamoxifen for Cre-recombination can confound fibrosis outcome in experimental kidney disease

Lucas L. Falke<sup>1</sup>, Roel Broekhuizen<sup>1</sup>, Alwin Huitema<sup>2</sup>, Erik Maarseveen<sup>3</sup>, Tri Q. Nguyen<sup>1</sup>, Roel Goldschmeding<sup>1</sup>

1. Dept. of Pathology, University Medical Center Utrecht, The Netherlands

2. Dept. of Clinical Pharmacy, AVL/Netherlands Cancer Institute, Amsterdam, The Netherlands

3. Dept. of Clinical Pharmacy, University Medical Center Utrecht, The Netherlands

Submitted

**Abstract**

A variety of conditional knock-out mice relying on Tamoxifen-driven ERT2/Cre-mediated recombination are available and have been used to study involvement of specific genes in kidney disease. However, recent data suggest that Tamoxifen itself might attenuate fibrogenesis when administered during experimental models of kidney disease. It has remained unclear whether this still applies also if kidney damage is initiated after a wash-out period has been observed. Here we report that the commonly applied regimen of administration of 4 alternate day doses of 1mg Tamoxifen per mouse until 14 days prior to start of the actual experiment, in this case the induction of obstructive nephropathy by Unilateral Ureteral Obstruction (UUO), still attenuated fibrosis in female obstructed mouse kidneys, whereas this effect was not seen in male obstructed kidneys. Attenuation of fibrosis was accompanied by a reduction in nuclear ER $\alpha$  positivity despite absence of detectable levels of the active tamoxifen metabolite endoxifen throughout the UUO experiment. These results indicate that the Tamoxifen dosing regimen commonly applied in conditional gene targeting experiments might have prolonged confounding effects through attenuation of renal fibrogenesis independent of modulation of the expression of the targeted gene(s)

## Introduction

Tamoxifen is widely used for the induction of genomic recombination in mice (double-)transgenic for floxed genes and Tamoxifen specific estrogen receptors (ER) coupled to Cre-recombinase (Supplemental table 1) (1). Tamoxifen is both an antagonist and agonist of ER signaling, depending on tissue type. In kidneys of both female and male mice, ER $\alpha$  and  $\beta$  are readily detectable (2). The kidney is highly responsive to estrogen in an ER $\alpha$  dependent manner and as such, it is regarded as the most estrogen-sensitive non-reproductive organ (3). Of note, treatment with relatively high doses (10mg/day) of Tamoxifen during experimental obstructive nephropathy, malignant hypertension, or diabetic nephropathy exerted an anti-fibrotic effect (4-6), in association with ER $\alpha$  dependent modulation of TGF $\beta$  signaling (7). However, it is unclear whether also the common study designs involving pretreatment with much lower Tamoxifen doses for genomic recombination prior to the initiation of experimental kidney disease might have confounding protective effects. Therefore, we compared the development of fibrosis in obstructed kidneys of male and female mice undergoing unilateral ureteral obstruction (UUO) after a 14 day wash out period following the last of 4 alternate day injections with Tamoxifen (1mg/mouse) or vehicle-only (corn oil).

## Concise Methods

Animal experiments were performed with approval of animal ethics committee of the university of Utrecht. C57Bl6/J Mice were injected 4 times every other day with either 100ul corn oil vehicle solution or corn oil Tamoxifen solution [10mg/ml] (Sigma Aldrich), and 7 mice were injected per group. 14 days after the last injection, mice were subjected to Unilateral Ureter Obstruction (UUO) by permanent ligation of the left ureter under general isoflurane anesthesia. 14 days after UUO mice were killed and plasma was collected. For measurement of baseline endoxifen levels after two week washout period, an additional 4 mice were killed prior to UUO. The method of Endoxifen measurement, using HPLC in combination with Mass Spectrometry, is extensively described elsewhere (9). FFPE kidneys were cut into 3um sections, deparaffinized, rehydrated and stained with Sirius Red. The percentage of Sirius red positivity was determined by morphometric analysis of 10 kidney cortical fields at 200x magnification using ImageJ. For immunochemistry: antigen retrieval ( $\alpha$ SMA/EDTA, ER $\alpha$ /Citrate) boiling followed by endogenous peroxidase block and primary antibody incubation ( $\alpha$ SMA: 1:200; AbCam, ER $\alpha$ : 1:250; Santa Cruz) was performed after which H-scores were determined (10, 11). ANOVA with Tukey correction for multiple testing was performed unless stated otherwise using GraphPad Prism.

## Results

Mice were pre-treated with 4 doses of 1 mg Tamoxifen or corn oil only on alternate days until two weeks prior to unilateral ureter obstruction (UUO), and killed two weeks after UUO (Figure 1A). Group characteristics are shown in Table 2. First we analyzed Tamoxifen bioavailability by measuring Endoxifen (N-desmethyl-4-hydroxy Tamoxifen) as a stable biologically active downstream metabolite more suitable for measurement (8, 9). In our experimental setup, endoxifen levels were undetectable in plasma and kidney lysate at both 14 days (start of UUO) and 28 days (sacrifice) post injection (LLOQ<0.1ng/ml).

Analysis of Sirius red stained slides showed that collagen deposition was not reduced in obstructed kidneys (OBKs) of Tamoxifen pre-treated male mice (Figure 1B & 1D). In female mice however, pre-treatment with Tamoxifen did result in reduced collagen deposition in OBKs (Figure 1C & 1E). Similarly, also the staining area for  $\alpha$ -Smooth Muscle Actin ( $\alpha$ SMA; a myofibroblast marker) was the same in Tamoxifen and corn oil injected male mice, but reduced in Tamoxifen injected female mice (Figure 2A-D).

To explore a possible role of differential ER expression underlying the gender-associated difference, we analyzed nuclear estrogen receptor- $\alpha$  (ER $\alpha$ ) expression by determining the H-index score, a commonly used weighted quantification method of nuclear ER $\alpha$  positivity (10, 11). In unobstructed kidneys (CLKs), Tamoxifen pre-treatment tended to lower nuclear ER $\alpha$  expression in both male and female mice but this difference was not significant ( $p=0.4$  and  $p=0.3$  resp., Figure 3B & 3D). However, nuclear ER $\alpha$  positivity was significantly increased in OBKs of Tamoxifen pre-treated male mice (Figure 3B), while in Tamoxifen pre-treated female mice the increase was not significant (Figure 3D). Nuclear ER $\alpha$  positivity in vehicle pre-treated OBK's was similar in male and female mice ( $P=0.76$ ; T-test). However, nuclear ER $\alpha$  positivity was significantly lower in female than in male Tamoxifen pre-treated OBKs ( $P=0.0068$ ; T-test).

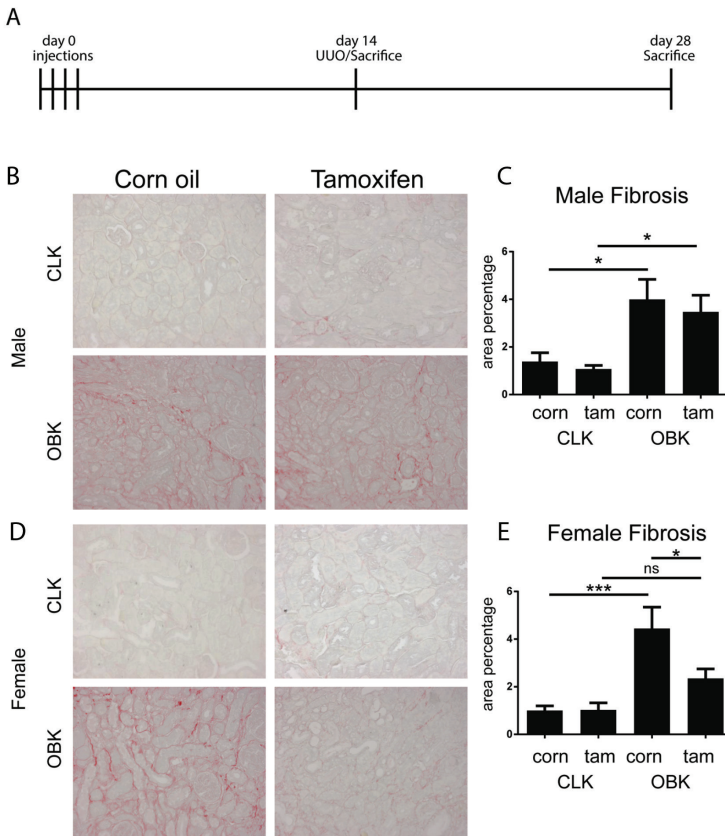


**Figure 1:** Tamoxifen pre-treatment reduces fibrotic development in female mice upon UUO. **A:** experimental setup; **B:** representative micrographs of Sirius Red staining in male CLKs and OBKs; **C:** fibrosis quantification in male mice; **D:** representative micrographs of Sirius Red staining in female CLKs and OBKs; **E:** fibrosis quantification in female mice. 200x magnification \*  $p < 0.05$ , \*\*\* $p < 0.005$ .

**Table 1:** group characteristics

Pre-treatment	Male		Female	
	Corn oil	Tamoxifen	Corn oil	Tamoxifen
Total Tam (mg)	-	4	-	4
Conc. (mg/kgBW)	-	135 (131.1-138.9)	-	186.2 (180.8-191.6)
BW start (g)	28.0 (27.4-28.6)	29.6 (28.8-30.5)	21.9 (20.5-23.3)	21.5 (20.9-22.1)
BW end (g)	28.4 (27.5-29.4)	29.4 (29-29.8)	22.13 (20.9-23.4)	22.43 (21.4-23.5)
BW end/start (g/g)	1.02 (0.99-1.04)	0.99 (0.97-1.02)	1.01 (0.99-1.03)	1.04 (1.01-1.07)
BW end/start (%)	101.6 (99.1-104)	99.2 (96.5-102)	101.2 (99.0-103.4)	104.3 (101.2-107.4)
OBK/CLK (mg/mg)	0.57 (0.54-0.59)	0.55 (0.52-0.57)	0.67 (0.59-0.74)	0.63 (0.58-0.68)
OBK/BW (mg/g)	3.81 (3.5-4.12)	3.25 (3.04-3.45)	4.40 (4.0-4.79)	3.98 (3.42-4.55)

Abbreviations: Tam, Tamoxifen. BW, bodyweight. OBK, obstructed kidney. CLK, contralateral kidney.

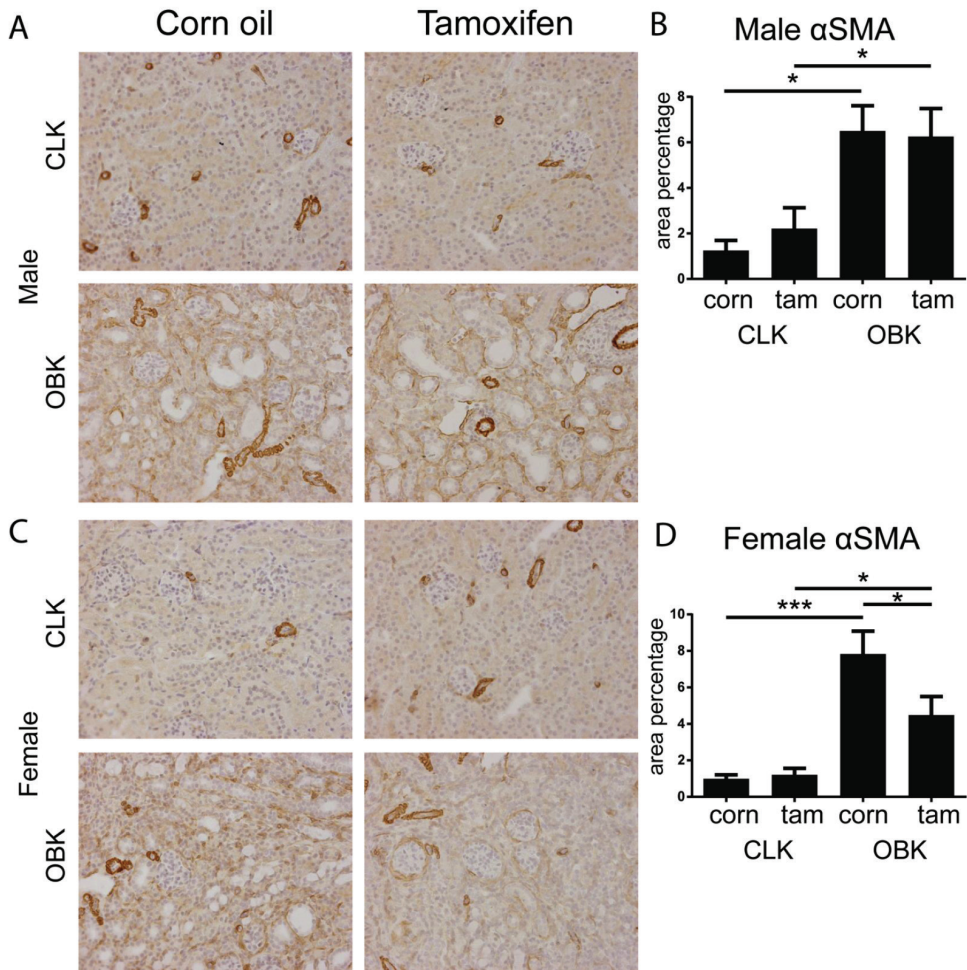


**Figure 2:** Tamoxifen pre-treatment reduces myofibroblast accumulation in female mice upon UUU. **A:** representative micrographs of  $\alpha$  Smooth Muscle Actin staining in male CLKs and OBKs; **B:**  $\alpha$ SMA quantification in male mice; **C:** representative micrographs of  $\alpha$ SMA staining in female CLKs and OBKs; **D:**  $\alpha$ SMA quantification in female mice. 200x magnification \*  $p < 0.05$ , \*\*\* $p < 0.005$ .

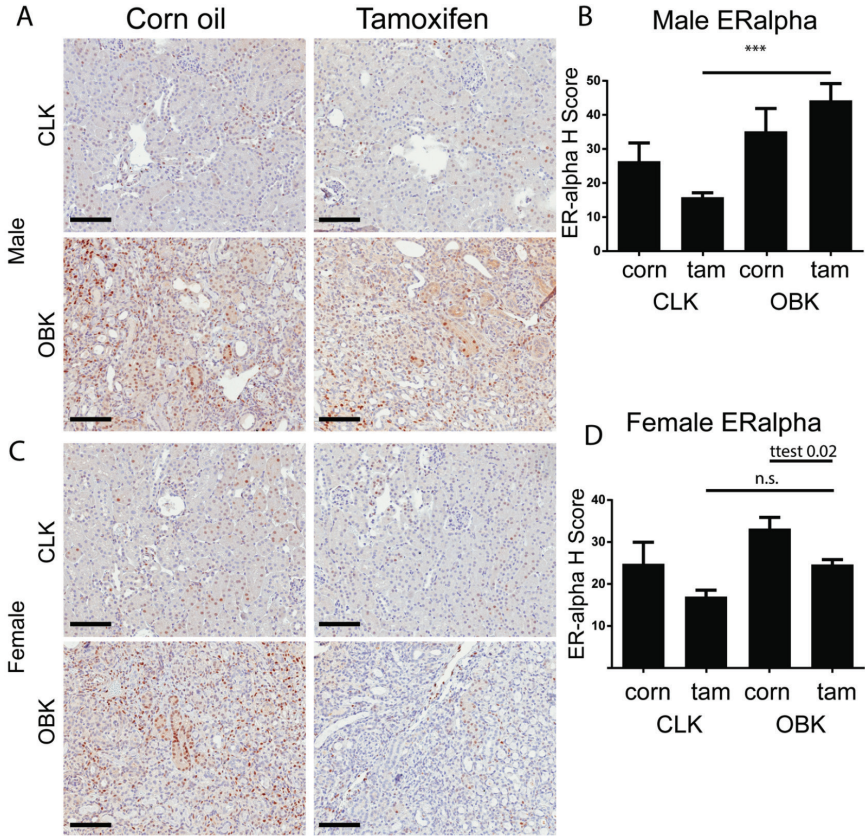


**Figure 3:** Tamoxifen pre-treatment associates with reduced nuclear Estrogen Receptor  $\alpha$  14 days post UUO in female mice. **A:** Representative micrograph of ER $\alpha$  staining in male CLKs and OBKs; **B:** weighted quantification of nuclear ER $\alpha$  positivity in male mice; **C:** Representative micrograph of ER $\alpha$  staining in female CLKs and OBKs; **D:** weighted quantification of nuclear ER $\alpha$  positivity in female mice. 200x magnification \*\*\*p<0.005

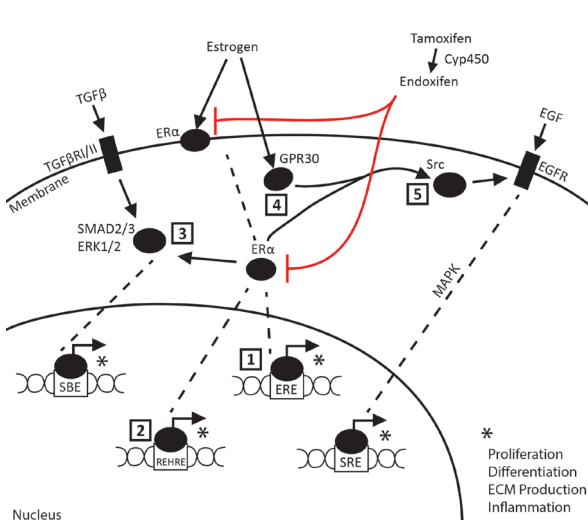


**Figure 4:** Schematic overview of estrogen/Tamoxifen interaction in a fibrogenic context. **1.** Direct nuclear translocation and binding of estrogen/ER $\alpha$  complex to the Estrogen Responsive Element (ERE). **2.** Estrogen/ER $\alpha$  complex binding to the Renin Enhancer Hormone Response Element (REHRE). **3.** Estrogen/ER $\alpha$  complex modulated SMAD2/3 and ERK1/2 binding to SMAD Binding Element (SBE). **4.** ER $\alpha$  independent binding of estrogen to G-protein coupled receptor 30. **5.** Estrogen/GPR30 or estrogen/ER $\alpha$  complex mediated modulation of Src/EGFR interaction leading to downstream alterations in Serum Response Element (SRE) binding to MAPK. \* Complex binding with ERE, REHRE, SBE or SRE respectively leads to modulation of processes involved in fibrogenesis (e.g. proliferation, differentiation, transcription including ECM production or infiltration/migration). Red lines indicate tamoxifen inhibition. Dashed red line indicates Tamoxifen mediated epigenetic alterations resulting in prolonged tamoxifen effects.

## Discussion

This study shows that in male mice, the fibrogenic response upon experimental renal injury is not affected by Tamoxifen pre-treatment with the dosing regimen commonly used for modulation of floxed gene expression. Female mice pre-treated with Tamoxifen, however, showed a hampered fibrogenesis, despite absence of detectable endoxifen in blood and tissue throughout the UUO experiment. This is in line with previous findings that kidneys of male mice are not influenced by ER $\alpha$  Knock Out (KO) (12), and that the sensitivity of female mouse kidneys to acute Ischemia Reperfusion Injury was no longer reduced (compared to male kidneys) upon Tamoxifen administration or ovariectomy (13). Also, using a fixed dose of 4mg per mouse might have higher impact in the 38% lighter female mice (Table 1). However, since already prior to UUO both male and female mice had no detectable endoxifen anymore in the kidney or the blood, it seems unlikely that immediate and direct effects of residual Tamoxifen can fully explain the differential outcome, and that the possibility of sustained, possibly more indirect effects, should be taken into account. As such, the observed sustained reduction of nuclear ER $\alpha$  positivity only in female Tamoxifen treated mice might point to indirect mechanisms reducing ER $\alpha$  mediated fibrogenesis. In line with a sustained effect, the recurrence rate of peritoneal sclerosis was lower after discontinuation of Tamoxifen treatment, as compared to corticosteroid treatment (14)

Deciphering the relative contribution of the various possible pathways is beyond the scope of this report, but a number of different mechanisms have been proposed by which Tamoxifen can have suppressive effects on ER $\alpha$  mediated fibrogenesis is worth mentioning here. These include modulation of TGF $\beta$  and EGF signaling (15-18) and direct induction Renin expression, a protein involved in renal fibrogenesis (19). Since Tamoxifen treatment leads to compensatory increase of endogenous estrogen production, another pathway of possible relevance is activation of G-protein coupled receptor (GPCR; GPR30) signaling upon direct binding of estrogen (20, 21). Figure 4 summarizes a theoretical regulatory network of estrogen/ER $\alpha$  driven fibrogenesis along with tamoxifen/endoxifen intervention potentially explaining reduced fibrogenesis during 14 day UUO.

Prolonged anti-fibrotic effects of Tamoxifen treatment might also relate to mechanisms by which cancer cells have been noted to modulate downstream ER complex signaling through epigenetic regulation in response to Tamoxifen treatment, but it remains unclear how far such mechanisms might be operational in the non-oncological setting of kidney fibrosis (22) (23). Finally, baseline ER $\alpha$  expression increases in female but decreases in male kidneys upon ageing, indicating that studies involving Tamoxifen treatment in older mice might be even more prone to gender-related confounding than observed in the present study in young mice (24).

## Conclusion

We have found that for Tamoxifen-induced manipulation of gene expression in studies addressing kidney fibrosis, the commonly applied protocol with a 14 day washout period between the final dose and start of the actual experiment appears to be appropriate for studies in male mice, but it does not sufficiently prevent confounding anti-fibrotic Tamoxifen effects in female mice. Since (also in female mice) the blood and tissue endoxifen levels had fallen below the detection threshold already before the start of the experiment, a protracted indirect (e.g. epigenetic) effect might be responsible, and it remains to be seen whether longer wash-out periods could suffice to eliminate residual “off target” Tamoxifen effects (also in female mice). Until this has been resolved studies involving Tamoxifen pre-treatment should be limited to male mice, and existing data from such studies in female mice should be interpreted with great caution.

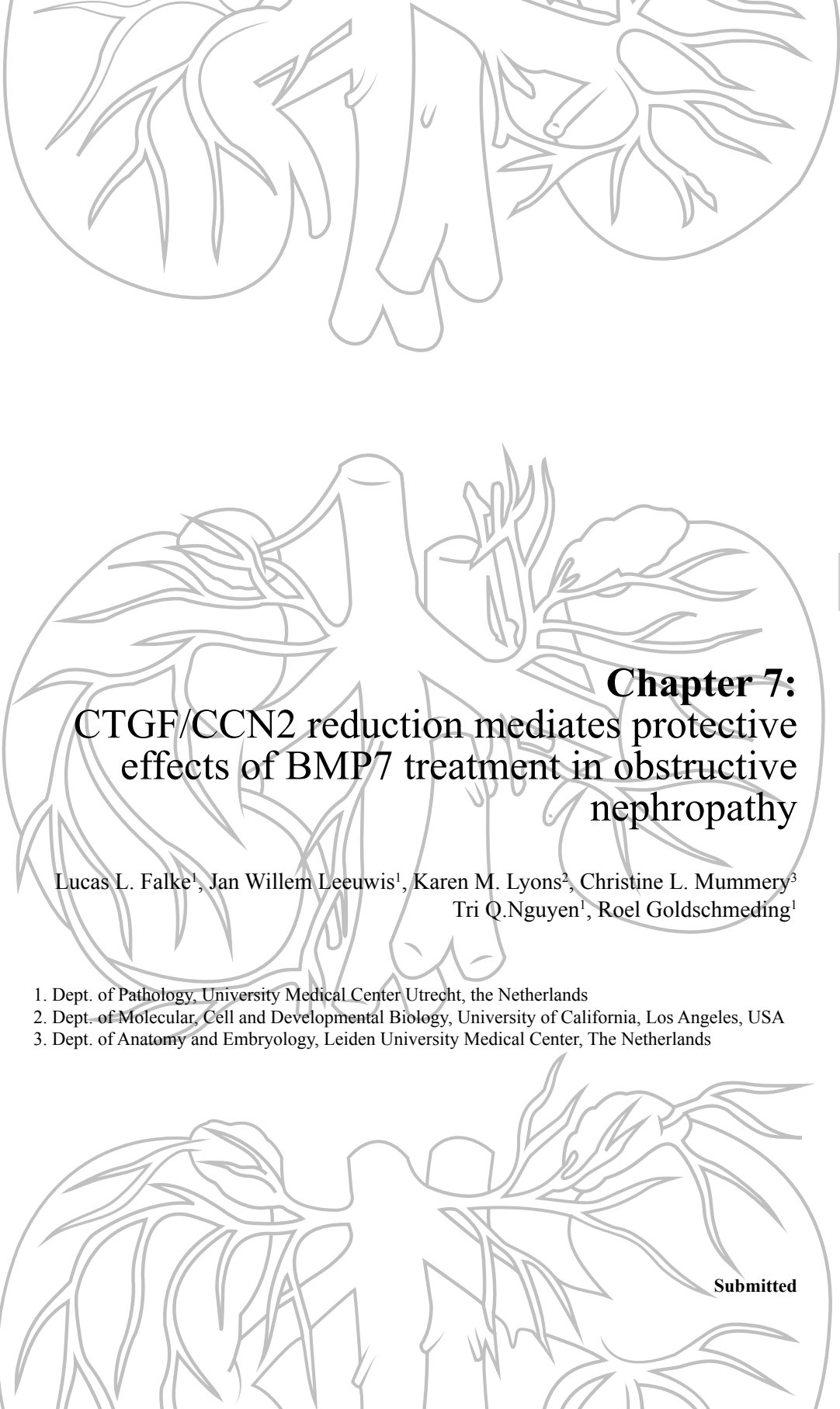
## References:

1. Hayashi S, McMahon AP. Efficient recombination in diverse tissues by a tamoxifen-inducible form of Cre: a tool for temporally regulated gene activation/inactivation in the mouse. *Developmental biology*. 2002;244(2):305-18.
2. Irsik DL, Carmines PK, Lane PH. Classical estrogen receptors and ERalpha splice variants in the mouse. *PLoS one*. 2013;8(8):e70926.
3. Jelinsky SA, Harris HA, Brown EL, Flanagan K, Zhang X, Tunkey C, et al. Global transcription profiling of estrogen activity: estrogen receptor alpha regulates gene expression in the kidney. *Endocrinology*. 2003;144(2):701-10.
4. Mao S, Xu H, Zou L, Xu G, Wu Z, Ding Q, et al. Estrogen preserves split renal function in a chronic complete unilateral ureteral obstruction animal model. *Experimental and therapeutic medicine*. 2014;7(6):1555-62.
5. Delle H, Rocha JR, Cavaglieri RC, Vieira JM, Jr., Malheiros DM, Noronha IL. Antifibrotic effect of tamoxifen in a model of progressive renal disease. *Journal of the American Society of Nephrology : JASN*. 2012;23(1):37-48.
6. Cohen AM, Rosenmann E. Effect of the estrogen antagonist, tamoxifen, on development of glomerulosclerosis in the Cohen diabetic rat. *Diabetes*. 1985;34(7):634-8.
7. Kim D, Lee AS, Jung YJ, Yang KH, Lee S, Park SK, et al. Tamoxifen ameliorates renal tubulointerstitial fibrosis by modulation of estrogen receptor alpha-mediated transforming growth factor-beta1/Smad signaling pathway. *Nephrology, dialysis, transplantation : official publication of the European Dialysis and Transplant Association - European Renal Association*. 2014;29(11):2043-53.
8. Ruddy KJ, Desantis SD, Gelman RS, Wu AH, Punglia RS, Mayer EL, et al. Personalized medicine in breast cancer: tamoxifen, endoxifen, and CYP2D6 in clinical practice. *Breast cancer research and treatment*. 2013;141(3):421-7.
9. Teunissen SF, Jager NG, Rosing H, Schinkel AH, Schellens JH, Beijnen JH. Development and validation of a quantitative assay for the determination of tamoxifen and its five main phase I metabolites in human serum using liquid chromatography coupled with tandem mass spectrometry. *Journal of chromatography B, Analytical technologies in the biomedical and life sciences*. 2011;879(19):1677-85.
10. Wilbur DC, Willis J, Mooney RA, Fallon MA, Moynes R, di Sant'Agnes PA. Estrogen and progesterone receptor detection in archival formalin-fixed, paraffin-embedded tissue from breast carcinoma: a comparison of immunohistochemistry with the dextran-coated charcoal assay. *Modern pathology : an official journal of the United States and Canadian Academy of Pathology, Inc*. 1992;5(1):79-84.
11. Lagiou P, Georgila C, Samoli E, Lagiou A, Zourna P, Minaki P, et al. Estrogen alpha and progesterone receptor expression in the normal mammary epithelium in relation to breast cancer risk. *International journal of cancer Journal international du cancer*. 2009;124(2):440-2.
12. Lane PH. Estrogen receptors in the kidney: lessons from genetically altered mice. *Gender medicine*. 2008;5 Suppl A:S11-8.
13. Tanaka R, Tsutsui H, Ohkita M, Takaoka M, Yukimura T, Matsumura Y. Sex differences in ischemia/reperfusion-induced acute kidney injury are dependent on the renal sympathetic nervous system. *European journal of pharmacology*. 2013;714(1-3):397-404.
14. van der Bilt FE, Hendriksz TR, van der Meijden WA, Brillman LG, van Bommel EF. Outcome in patients with idiopathic retroperitoneal fibrosis treated with corticosteroid or tamoxifen monotherapy. *Clinical kidney journal*. 2016;9(2):184-91.
15. Xu J, Wu RC, O'Malley BW. Normal and cancer-related functions of the p160 steroid receptor co-activator (SRC) family. *Nature reviews Cancer*. 2009;9(9):615-30.
16. Carthy JM, Sundqvist A, Heldin A, van Dam H, Klefsas D, Heldin CH, et al. Tamoxifen Inhibits TGF-beta-Mediated Activation of Myofibroblasts by Blocking Non-Smad Signaling Through ERK1/2. *Journal of cellular physiology*. 2015;230(12):3084-92.
17. Goto N, Hiyoshi H, Ito I, Tsuchiya M, Nakajima Y, Yanagisawa J. Estrogen and antiestrogens alter breast cancer invasiveness by modulating the transforming growth factor-beta signaling pathway. *Cancer science*. 2011;102(8):1501-8.
18. Britton DJ, Hutcheson IR, Knowlden JM, Barrow D, Giles M, McClelland RA, et al. Bidirectional cross talk between ERalpha and EGFR signalling pathways regulates tamoxifen-resistant growth. *Breast cancer research and treatment*. 2006;96(2):131-46.
19. Lu KT, Keen HL, Weatherford ET, Sequeira-Lopez ML, Gomez RA, Sigmund CD. Estrogen Receptor alpha Is Required for Maintaining Baseline Renin Expression. *Hypertension*. 2016.
20. Prossnitz ER, Arterburn JB, Smith HO, Oprea TI, Sklar LA, Hathaway HJ. Estrogen signaling through the transmembrane G protein-coupled receptor GPR30. *Annual review of physiology*. 2008;70:165-90.
21. Ignatov A, Ignatov T, Weissenborn C, Eggemann H, Bischoff J, Semczuk A, et al. G-protein-coupled estrogen receptor GPR30 and tamoxifen resistance in breast cancer. *Breast cancer research and treatment*. 2011;128(2):457-66.
22. Musgrove EA, Sutherland RL. Biological determinants of endocrine resistance in breast cancer. *Nature reviews Cancer*. 2009;9(9):631-43.
23. Feng Q, Zhang Z, Shea MJ, Creighton CJ, Coarfa C, Hilsenbeck SG, et al. An epigenomic approach to therapy for tamoxifen-resistant breast cancer. *Cell research*. 2014;24(7):809-19.
24. Sharma PK, Thakur MK. Estrogen receptor alpha expression in mice kidney shows sex differences during aging. *Biogerontology*. 2004;5(6):375-81.





7



## **Chapter 7:** CTGF/CCN2 reduction mediates protective effects of BMP7 treatment in obstructive nephropathy

Lucas L. Falke<sup>1</sup>, Jan Willem Leeuwis<sup>1</sup>, Karen M. Lyons<sup>2</sup>, Christine L. Mummery<sup>3</sup>  
Tri Q. Nguyen<sup>1</sup>, Roel Goldschmeding<sup>1</sup>

1. Dept. of Pathology, University Medical Center Utrecht, the Netherlands
2. Dept. of Molecular, Cell and Developmental Biology, University of California, Los Angeles, USA
3. Dept. of Anatomy and Embryology, Leiden University Medical Center, The Netherlands

Submitted

**Abstract**

Treatment with rhBMP7 exerts profound protective effects in a wide variety of experimental models of renal disease. However, little is known about how these protective effects are mediated, and which cells in the kidney are targeted by exogenous rhBMP7 treatment. To identify and localize cells in the kidney that respond to exogenous rhBMP7 treatment, we performed Unilateral Ureteral Obstruction (UUO, a widely used obstructive nephropathy model) in mice reporting transcriptional activity downstream of canonical BMP signaling by the expression of GFP under the BMP Responsive Element of the Id1 promoter (BRE:gf<sub>p</sub> mice). We also analysed the impact of rhBMP7 treatment on severity of the UUO phenotype, on TGF $\beta$  signaling, and on expression of CCN2 (CTGF). Despite profound protective effects with respect to morphological damage, macrophage infiltration, and fibrosis, no significant difference in GFP-expression was observed upon rhBMP7 administration. Also TGF $\beta$  signalling was similar in rhBMP7 and vehicle treated mice, but CCN2 expression in obstructed kidneys was significantly reduced by rhBMP7 treatment. Of note, in heterozygous CCN2 mice (CCN2<sup>+/-</sup>) treatment with rhBMP7 did not (further) reduce the severity of kidney damage in the UUO-model. These data suggest that protection against obstructive nephropathy by exogenous rhBMP7 treatment relies primarily on non-canonical BMP signaling, and may be mediated in large part by downregulation of CCN2 expression.

**List of abbreviations**

BMP7	-	Bone Morphogenetic Protein 7
CCN2	-	Cyr61-CTGF-Nov family protein 2
CTGF	-	Connective Tissue Growth Factor
CKD	-	Chronic Kidney Disease
UUO	-	Unilateral Ureteral Obstruction
BW	-	Body Weight
OBK	-	Obstructed Kidney
CLK	-	Contralateral Kidney
GFP	-	Green Fluorescent Protein
TGF $\beta$	-	Transforming Growth Factor $\beta$
LTA	-	Lotus Tetragonolobus Agglutinin

## Introduction

Irrespective of underlying aetiology, chronic kidney disease (CKD) involves structural changes, and ultimately loss of function and fibrosis. Although, there is no effective treatment, several potential targets for intervention in CKD progression have been identified. Transforming Growth Factor beta (TGF $\beta$ ) is generally regarded as the main culprit driving CKD progression (1). Numerous studies targeting TGF $\beta$  in various experimental diseases have yielded favourable results, but recent clinical trials have questioned efficacy of available interventions in human CKD (2, 3)(Clinicaltrial.gov numbers NCT00464321 and NCT01113801).

The administration of recombinant human BMP7 (rhBMP7; Bone Morphogenetic Protein 7) has been proposed as an attractive alternative intervention to stop progression of CKD. Several landmark papers have shown efficacy of BMP7 treatment in a wide range of experimental models of renal disease including diabetic nephropathy, obstructive uropathy, nephron loss and ischemic injury (4-10), and a BMP-mimetic (THR-185) is under study in a phase II clinical trial (Clinicaltrial.gov number NCT01830920). BMP7 treatment is considered to attenuate experimental CKD at least in part by antagonizing TGF $\beta$  (10, 11). BMP7 is required for kidney development and remains highly expressed during adult life (12). Although also several other BMPs are expressed in the kidney throughout development and adulthood, including BMP4 and BMP6, the potential therapeutic effects of BMP7 are considered most potent (10, 13).

Despite all evidence supporting BMP7 efficacy in CKD, the identity and localization of cells responding to exogenous BMP7 treatment remain to be identified. Previous studies in BMP canonical signaling reporter mice (BRE:gf $\beta$  mice) identified glomerular and collecting duct cells to have high endogenous BMP signalling activity (14). Signaling activity in the glomeruli and medulla dropped upon Unilateral Ureteral Obstruction (UUO), but it increased in the proximal tubular compartment. However, if and to what extent exogenous BMP7 therapeutic efficacy might involve restoration of canonical signaling activity in these particular cells or other nephron segments or cell types is still unclear.

CCN2, also known as Connective Tissue Growth Factor (CTGF) is yet another factor involved in CKD progression (15). CCN2 contributes to fibrosis by modulating signaling activity in BMP7, TGF $\beta$ , and other signaling pathways (16, 17). CCN2 expression is increased in essentially all progressive kidney diseases, and CCN2 inhibition decreases loss of function and fibrosis (15, 18, 19). CCN2 can bind to BMP7 thereby inhibiting canonical SMAD1/5/8 signalling, and as such might also be an important determinant of the efficacy of BMP7 treatment (16).

In this study, we set out to shed more light on the mode of action of exogenous BMP7 therapy by analysing distribution of transcriptional activity downstream of canonical BMP signaling, and the associated complex interplay between BMP7, TGF $\beta$ , and CCN2 in rhBMP7 treated BRE-GFP reporter mice subjected to UUO.

## Materials and Methods

### *Animals*

Male BRE:gf<sub>p</sub> mice on a C57Bl6/J background were used for this study. Generation of these mice has been described extensively (20). Briefly, these mice express Green Fluorescent Protein (GFP) under control of the bone morphogenetic protein responsive element (BRE) in the Id1 gene promoter, thus reporting transcriptional activity downstream canonical BMP signaling. CCN2 hemizygous KO mice were used to estimate the relative contribution of CCN2 reduction to the therapeutic effect of exogenous BMP7. CCN2 (hemizygous) KO mice have been described previously (21). Mice were kept on a 12-hour light/day cycle with food and water ad libitum. All work was carried out with approval of the Experimental Animal Ethics Committee of the University of Utrecht.

### *Unilateral Ureteral Obstruction/BMP7 administration*

Mice were subjected to Unilateral Ureteral Obstruction under general isoflurane anaesthesia. The left flank was incised and the ureter was exposed and tied off using silk sutures. Directly after ligation, a depot of 300 µg/kg rhBMP7 (dissolved in PBS; kindly provided by Stryker, Kalamazoo, MI) per mouse was left intraperitoneally (i.p.). Mice received an additional 300 µg/kg rhBMP7 i.p. on day 2, 4 and 6 (n=9). Vehicle (PBS) injected mice were used as control (n=6). 3 mice were used for CCN2 hemizygous groups. At day 7 mice were killed by ketamin, xylazine and atropine overdose. Kidney tissue was fixed in fresh 4% paraformaldehyde solution and embedded in paraffin, or snap frozen and stored at -80°C until further processing.

### *(Immuno)histochemistry*

Sections (3 µm) were cut from paraffin blocks, deparaffinised and rehydrated. For assessment of morphological changes, sections were stained with Periodic Acid Schiff using standard methods. 10 random cortical fields of PAS stained sections were scored on a five-point scale for tubular atrophy or dilatation (0=0-10%, 1=10-25%, 2=25-50%, 3=50-75%, 4=75-100%). For immunohistochemistry, slides were boiled in EDTA or citrate buffer for antigen retrieval where appropriate, and incubated with the following antibodies: anti-GFP (Ab290, Citrate, 1:1000, Abcam, Cambridge, UK), HRP-linked LTA (Citrate, 1:32, Sigma-Aldrich, St. Louis, MO), anti-CCN2 (L20, Citrate, 1:200, Santa-Cruz Biotechnology, Santa Cruz, CA), anti-F4/80 (Fresh Frozen tissue, 1:3000, Serotec/Biorad antibodies, Oxford, UK) or anti-αSMA (Ab5694, EDTA, 1:200, Abcam). The number of proximal tubule cross sections per cortical surface area was counted in 10 random fields per kidney (200x magnified). Percentage of positive cross sectional surface area for GFP, F4/80, and αSMA respectively, were determined by ImageJ analysis in 10 cortical fields photographed at 200x magnification.

### *RT-qPCR*

Full Kidney cortex mRNA was isolated using Trizol and 3000ng of mRNA was reversely transcribed into cDNA. RT-qPCR was performed on a LightCycler480 (Roche, Basel, Switzerland), using commercially available TaqMan primer assays (Thermo Fisher/Life technologies, Waltham, MA): (Yhwaz; Mm03950126\_s1, Ctgf, Mm00515790\_g1; Tgfb1, Mm01178820\_m1; Col1a2, Mm00483888\_m1; Pai1, Mm00435860\_m1). Sybr green GFP primers and probe were designed with Primer Express (Applied Biosystems, Foster City, CA) and purchased from Eurogentec (Maastricht, The Netherlands) (primers) and Applied Biosystems (probe). Yhwaz expression was used as internal reference. Relative expression values were calculated using the ΔΔCT method.

### *Statistics*

All statistical analyses were performed using Graphpad Prism (GraphPad, LaJolla, CA). ANOVA with Tukey post-hoc correction for multiple testing or Student T-test were used where appropriate. A p-value below 0.05 was considered statistically significant.

**Results**

*Exogenous BMP7 does not increase BRE:gfp reporter signal for transcriptional activity downstream of canonical BMP7 signaling*

BRE:gfp mice express GFP under a SMAD binding element in the Id1 promoter region and thereby report transcriptional activity downstream of canonical BMP signaling (20, 22). Body weight, kidneys weights and kidney weight/body weight ratios of rhBMP7 treated BRE:gfp mice were not significantly different from those in vehicle treated mice (See Table). Comparison between direct fluorescent and

Table 1: Weights	Vehicle	rhBMP7	p-value
BW start (g)	25.92 (+/-4.41)	25.88 (+/- 4.32)	0.99
BW end (g)	25.87 (+/- 3.82)	24.84 (+/- 3.52)	0.61
BW end/BW start	1 (+/- 0.05)	0.96 (+/-0.04)	0.15
CLK (mg)	211.6 (+/-48.2)	211 (+/- 47.69)	0.98
OBK (mg)	194.67 +/- 37.33)	199.88(+/- 25.98)	0.76
CLK (mg/g BWs)	8.12 (+/- 0.8)	8.1 (+/- 0.67)	0.96
OBK (mg/g BWs)	7.52 (+/- 0.9)	7.81 (+/-0.96)	0.58
OBK/CLK (mg/mg)	0.91 (+/- 0.08)	0.97 (+/- 0.14)	0.41

Abbreviations: BW, body weight. CLK, contralateral kidney. OBK, obstructed kidney.

immunohistochemical GFP signal detection revealed that IHC detection is more sensitive (Supplemental figure 1A). Using morphometric analysis, percentage positive area of total cortical sections, tubulointerstitial (TI) compartment and glomeruli was analysed in sections where

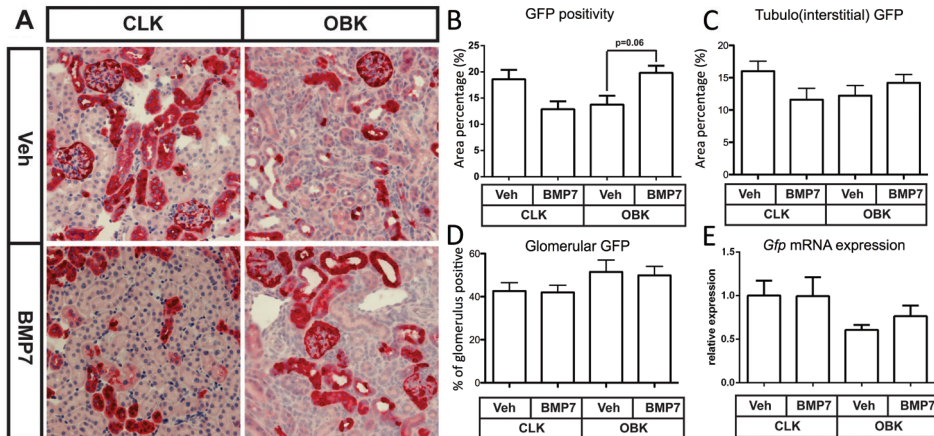


**Figure 1:** rhBMP7 treated BRE:gfp OBKs do not show increased GFP or Id1 expression. **A:** Representative images of GFP immunohistochemistry in CLKs and OBKs 7 days after UUO of both vehicle and BMP7 groups (200x magnified). Panel on the far right shows CLK vehicle binary image illustrating what is regarded as total/ tubulointerstitial area percentage. The red dotted line is a representative depiction of total glomerular area measurement in glomerular GFP area positivity determination. **B-D:** Quantification of total area (B), tubules and interstitium (C) or percentage of the glomeruli (D) positive for GFP. **E:** Cortical Gfp mRNA expression. Error bars represent SEM.

GFP was detected by ImageJ (Supplemental figure 1B). Average total and TI GFP positive area tended to be lower in OBKs than in CLKs, but the observed difference was not significant (Figure 1B and 1C). Remarkably, also the apparently small increase of total cortical GFP positive area in rhBMP7 treated OBKs was not statistically significant (Figure 1B; p=0.06), and totally lost when tubules and glomeruli were analysed separately (Figure 1C and D). Analysis of cortical Gfp mRNA expression revealed a significant decrease upon ureteral obstruction, but also here no effect of BMP7 treatment was observed (Figure 1E).

*BMP7 protects against kidney damage and reduces macrophage infiltration 7 days post-UUO.*

The increase of tubular atrophy and dilatation in OBKs was attenuated in BMP7-treated mice (p<0.005; Figure 2A and 2B). Lotus Tetragonolobus Agglutinin (LTA) staining revealed that the number of LTA+ proximal tubules was decreased in OBKs compared to CLKs, but less so in BMP7 treated mice (Figure 2C and 2D; p<0.05). Macrophage infiltration in OBKs, as assessed by F4/80 IHC, was markedly reduced in the BMP7 treated group (p<0.005; Figure 2E and 2F).

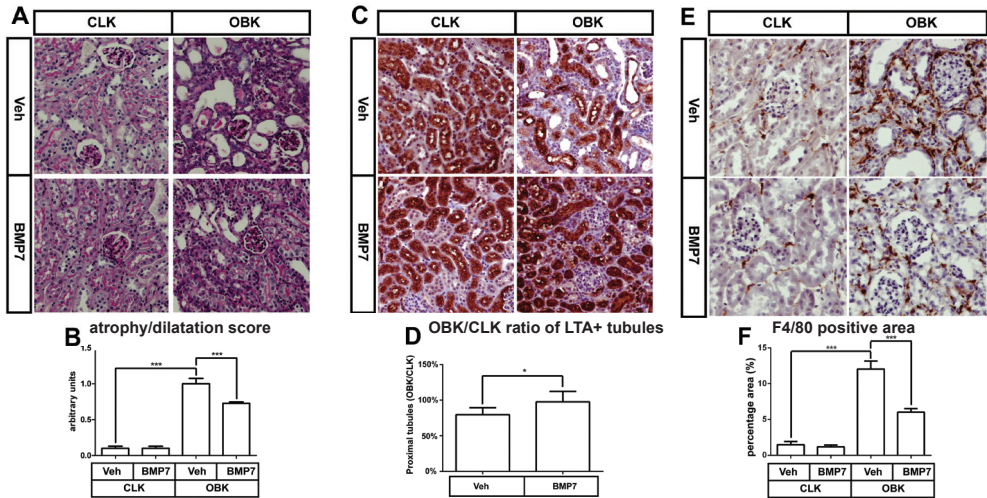


**Figure 2:** rhBMP7 treatment conserves renal morphology and limits macrophage accumulation 7 days after obstructive nephropathy. **A:** Representative images of PAS stained cortical sections in CLKs and OBKs 7 days after UOU of both vehicle and BMP7 treated groups (200x magnified). **B:** Composite of atrophy and dilatation score quantified on PAS stained slides **C:** Representative images of LTA stained cortical sections in CLKs and OBKs of both vehicle and BMP7 treated groups (200x magnified). **D:** Quantification of the average number of LTA+ proximal tubules per HPF corrected for baseline number of proximal tubules per HPF in CLKs (OBK/CLK ratio). **E:** Representative images of F4/80 stained cortical sections in CLKs and OBKs of both vehicle and BMP7 treated groups (200x magnified). **F:** Positive area quantification of F4/80 positive macrophages in CLKs and OBKs of vehicle and rhBMP7 treated kidneys. \* $p < 0.05$ , \*\*\* $p < 0.005$ . Error bar represents SEM. Vehicle  $n = 6$ , rhBMP7  $n = 9$ .

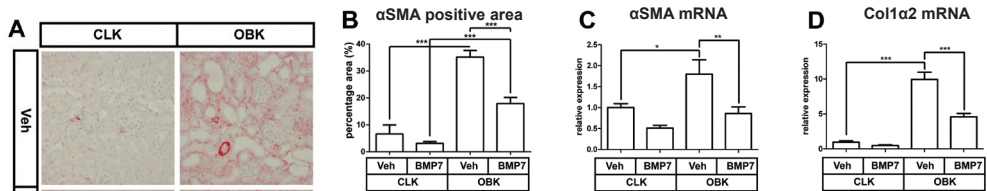


**Figure 3:** rhBMP7 treatment reduces myfibroblast accumulation and associated de novo collagen production. **A:** Representative images of  $\alpha$ SMA in CLKs and OBKs 7 days after UOU of both vehicle and BMP7 treated groups (200x magnified). **B:** Positive area quantification of  $\alpha$ SMA positive myfibroblasts in CLKs and OBKs of vehicle and rhBMP7. **C:**  $\alpha$ Sma mRNA **D:** expression levels in kidney cortex of CLKs and OBKs 7 days after UOU of vehicle and rhBMP7 treated animals. \* $p < 0.05$ , \*\* $p < 0.01$ , \*\*\* $p < 0.005$ . Error bars represent SEM.

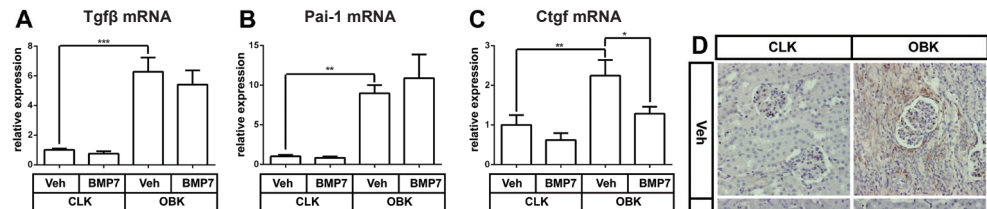


**Figure 4:** rhBMP7 treatment reduces CCN2 expression levels without altering canonical TGF $\beta$  signaling. **A-C:** Cortical mRNA expression levels of Tgf $\beta$ 1 (A), Pai-1 (B) and CCN2 (C) in CLKs and OBKs 7 days after UOU of vehicle and rhBMP7 treated CCN2 $\pm$  mice. **D:** Representative images of CCN2 immunohistochemistry in CLKs and OBKs of both vehicle and rhBMP7 treated groups (200x magnified). \* $p < 0.05$ , \*\* $p < 0.01$ , \*\*\* $p < 0.005$ .



*Fibrogenesis is reduced in BMP7 treated OBKs.*

After 7 days of obstruction, the OBKs of vehicle treated mice showed only a little increase in fibrosis (Suppl. Fig. 2). Accumulation of myofibroblasts in OBKs, as assessed by  $\alpha$ SMA positive surface area, was decreased by BMP7 treatment ( $p < 0.005$ ; Figure 3C and 3D). Furthermore, the increase of mRNA for  $\alpha$ Sma and  $Col1\alpha2$  was reduced by BMP7 treatment ( $p < 0.01$  and  $p < 0.005$  resp.; Figure 3E and 3F).

*BMP7 treatment reduced CCN2 expression but not Tgfb1 expression and transcriptional activity*

Both Tgfb1 and its canonical transcriptional target Pai-1/SerpinE1 were upregulated in OBKs ( $p < 0.005$  and  $p < 0.01$  resp.; Figure 3A and 3B), which was not affected by BMP7 treatment. However, BMP7 blocked the increase of CCN2 expression in OBKs ( $p < 0.05$ ; Figure 3C and 3D).

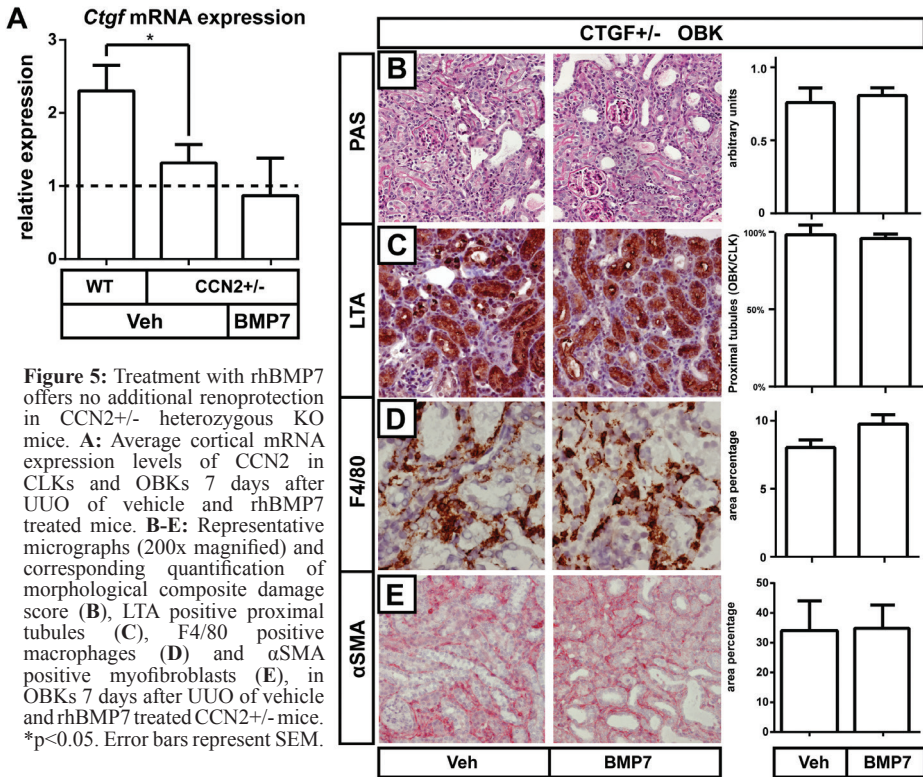


**Figure 5:** Treatment with rhBMP7 offers no additional renoprotection in CCN2+/- heterozygous KO mice. **A:** Average cortical mRNA expression levels of CCN2 in CLKs and OBKs 7 days after UUU of vehicle and rhBMP7 treated mice. **B-E:** Representative micrographs (200x magnified) and corresponding quantification of morphological composite damage score (**B**), LTA positive proximal tubules (**C**), F4/80 positive macrophages (**D**) and  $\alpha$ SMA positive myofibroblasts (**E**), in OBKs 7 days after UUU of vehicle and rhBMP7 treated CCN2+/- mice. \* $p < 0.05$ . Error bars represent SEM.

*In CCN2 hemizygous KO mice, BMP7 treatment did not further reduce damage, macrophage infiltration, and fibrosis of obstructed kidneys*

In good agreement with previous reports, we observed less severe kidney damage, macrophage infiltration, and fibrosis in 7 day OBKs of CCN2 hemizygous KO, than in those of wild type mice. (Supplemental Figure 2A-E). In order to investigate BMP7 induced reno-protection beyond CCN2 reduction, we also treated CCN2+/- UUU mice with rhBMP7. The approximately 50% reduction of CCN2 expression in CTGF+/- mice was not further reduced by rhBMP7 treatment (Figure 5A). In association with this finding, administration of BMP7 to CCN2 hemizygous KO mice also failed to further attenuate renal damage, macrophage infiltration or myofibroblast accumulation (Figure 5B-D), which emphasizes the importance of CCN2 reduction in mediating the protective effect of BMP7 treatment in this model of obstructive nephropathy.

## Discussion

The present study confirms that rhBMP7 treatment reduces the severity of kidney damage, macrophage infiltration, and myofibroblast accumulation in a mouse model of obstructive nephropathy (UO). Remarkably, transcriptional activity downstream of canonical BMP signaling, and also TGF $\beta$  expression and transcriptional activity, appeared not to be altered by rhBMP7 treatment, while the expression of CCN2 was significantly reduced in the obstructed kidneys (OBK) of BMP7-treated mice.

In line with previous observations in the BRE-GFP reporter mouse also used here, the GFP signal was slightly reduced in distal tubuli of obstructed kidneys (Figure 1), but we detected no increase of GFP signal upon rhBMP7-treatment (23). This suggests that the beneficial effects of BMP7 treatment mainly involve non-canonical signaling, rather than transcriptional activity downstream of canonical BMP signaling. However, since no data are available on pharmacokinetics of i.p. injected rhBMP7, we cannot fully exclude that rapid elimination or degradation of de novo synthesized GFP protein within the 24 hour window between the last BMP7 dose and sacrifice might have “quenched” the reporter signal.

The renoprotective effects of rhBMP7 were associated with approximately 50% reduction of CCN2 expression, whereas expression of Tgf $\beta$ 1 and its prototypic canonical transcriptional target Pai-1 remained unaltered (Figure 4). Efficacy of BMP7 therapy without altering TGF $\beta$  signaling has been reported previously in a model of diabetic nephropathy (24). Of note, hemizygous CCN2 deletion (with 50% reduced CCN2 expression), appeared equally effective as rhBMP7 treatment, with similar reduction of morphological damage, macrophage infiltration, and collagen and  $\alpha$ -SMA expression (Supplemental figure 2). This is consistent with previous observations that an approximately 50% reduction of CCN2 expression by genetic deletion or siRNA was sufficient to significantly attenuate models of diabetic nephropathy and obstructive nephropathy (16, 25, 26). Interestingly, administration of rhBMP7 to heterozygous CCN2 mice tended to even further reduce CCN2 expression, but this was not associated with a further decrease in damage and fibrosis. It thus appears that the observed therapeutic effects might relate to a threshold effect of CCN2 reduction rather than on a continuous dose-response relation (Figure 5).

In summary, in the mouse UO model of obstructive nephropathy we observed efficacy of rhBMP7 therapy in the absence of clear evidence for modulation of transcriptional activity downstream of canonical BMP signaling. As a consequence, the BRE-GFP reporter mice failed to reveal the identity of specific phenotypes and localization of cells responding to exogenous BMP7 therapy. Furthermore, efficacy of BMP7 treatment appeared not to require reduction of TGF $\beta$  expression or transcriptional activity, but to be associated with a reduction of CCN2 expression, which by itself could replicate protective effects of rhBMP7 administration. Together, these data suggest that protection against obstructive nephropathy by exogenous BMP7 treatment relates primarily to non-canonical BMP signaling, and may be mediated in large part by downregulation of CCN2 expression.

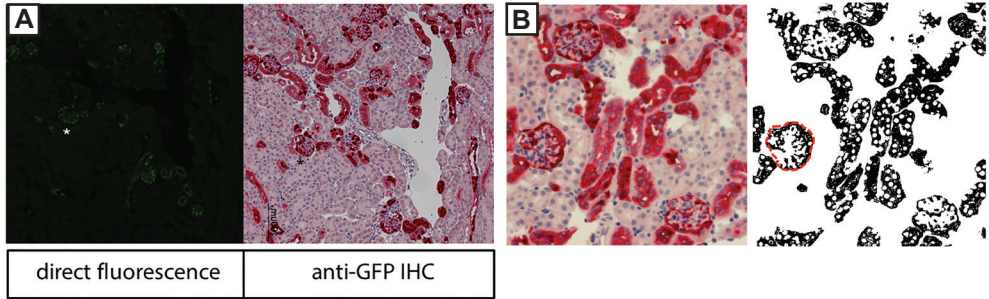
## Acknowledgements

We acknowledge Stryker medical for kindly providing the rhBMP7 used in this study. Furthermore, we thank Roel Broekhuizen for his valuable technical assistance.

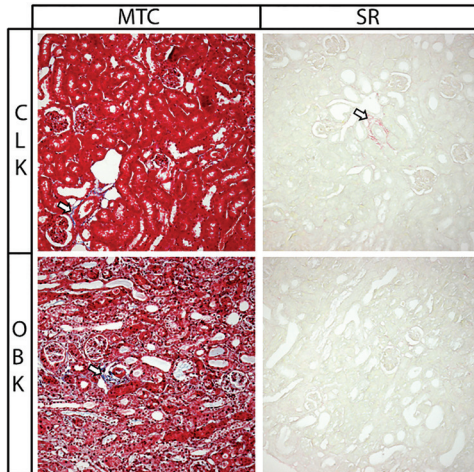
## References

1. Meng XM, Tang PM, Li J, Lan HY. TGF-beta/Smad signaling in renal fibrosis. *Front Physiol.* 2015;6:82.
2. Munoz-Felix JM, Gonzalez-Nunez M, Martinez-Salgado C, Lopez-Novoa JM. TGF-beta/BMP proteins as therapeutic targets in renal fibrosis. Where have we arrived after 25 years of trials and tribulations? *Pharmacol Ther.* 2015;156:44-58.
3. Akhurst RJ, Hata A. Targeting the TGFbeta signalling pathway in disease. *Nat Rev Drug Discov.* 2012;11(10):790-811.
4. Dube PH, Almanzar MM, Frazier KS, Jones WK, Charette MF, Paredes A. Osteogenic Protein-1: gene expression and treatment in rat remnant kidney model. *Toxicol Pathol.* 2004;32(4):384-92.
5. Wang S, Chen Q, Simon TC, Strebeck F, Chaudhary L, Morrissey J, et al. Bone morphogenetic protein-7 (BMP-7), a novel therapy for diabetic nephropathy. *Kidney Int.* 2003;63(6):2037-49.
6. Hruska KA, Guo G, Wozniak M, Martin D, Miller S, Liapis H, et al. Osteogenic protein-1 prevents renal fibrogenesis associated with ureteral obstruction. *Am J Physiol Renal Physiol.* 2000;279(1):F130-43.
7. Morrissey J, Hruska K, Guo G, Wang S, Chen Q, Klahr S. Bone morphogenetic protein-7 improves renal fibrosis and accelerates the return of renal function. *J Am Soc Nephrol.* 2002;13 Suppl 1:S14-21.
8. Vukicevic S, Basic V, Rogic D, Basic N, Shih MS, Shepard A, et al. Osteogenic protein-1 (bone morphogenetic protein-7) reduces severity of injury after ischemic acute renal failure in rat. *J Clin Invest.* 1998;102(1):202-14.
9. Sugimoto H, Grahovac G, Zeisberg M, Kalluri R. Renal fibrosis and glomerulosclerosis in a new mouse model of diabetic nephropathy and its regression by bone morphogenetic protein-7 and advanced glycation end product inhibitors. *Diabetes.* 2007;56(7):1825-33.
10. Zeisberg M, Hanai J, Sugimoto H, Mammoto T, Charytan D, Strutz F, et al. BMP-7 counteracts TGF-beta1-induced epithelial-to-mesenchymal transition and reverses chronic renal injury. *Nat Med.* 2003;9(7):964-8.
11. Wang S, Hirschberg R. BMP7 antagonizes TGF-beta -dependent fibrogenesis in mesangial cells. *Am J Physiol Renal Physiol.* 2003;284(5):F1006-13.
12. Dudley AT, Lyons KM, Robertson EJ. A requirement for bone morphogenetic protein-7 during development of the mammalian kidney and eye. *Genes Dev.* 1995;9(22):2795-807.
13. Dendooven A, van Oostrom O, van der Giezen DM, Leeuwis JW, Snijckers C, Joles JA, et al. Loss of endogenous bone morphogenetic protein-6 aggravates renal fibrosis. *Am J Pathol.* 2011;178(3):1069-79.
14. Leeuwis JW, Nguyen TQ, Chuva de Sousa Lopes SM, van der Giezen DM, van der Ven K, Rouw PJ, et al. Direct visualization of Smad1/5/8-mediated transcriptional activity identifies podocytes and collecting ducts as major targets of BMP signalling in healthy and diseased kidneys. *J Pathol.* 2011;224(1):121-32.
15. Falke LL, Goldschmeding R, Nguyen TQ. A perspective on anti-CCN2 therapy for chronic kidney disease. *Nephrol Dial Transplant.* 2014;29 Suppl 1:i30-i7.
16. Nguyen TQ, Roestenberg P, van Nieuwenhoven FA, Bovenschen N, Li Z, Xu L, et al. CTGF inhibits BMP-7 signaling in diabetic nephropathy. *J Am Soc Nephrol.* 2008;19(11):2098-107.
17. Abreu JG, Ketpura NI, Reversade B, De Robertis EM. Connective-tissue growth factor (CTGF) modulates cell signalling by BMP and TGF-beta. *Nat Cell Biol.* 2002;4(8):599-604.
18. Ren Y, Du C, Yan L, Wei J, Wu H, Shi Y, et al. CTGF siRNA ameliorates tubular cell apoptosis and tubulointerstitial fibrosis in obstructed mouse kidneys in a Sirt1-independent manner. *Drug Des Devel Ther.* 2015;9:4155-71.
19. Ito Y, Aten J, Bende RJ, Oemar BS, Rabelink TJ, Weening JJ, et al. Expression of connective tissue growth factor in human renal fibrosis. *Kidney Int.* 1998;53(4):853-61.
20. Monteiro RM, de Sousa Lopes SM, Bialecka M, de Boer S, Zwijsen A, Mummery CL. Real time monitoring of BMP Smads transcriptional activity during mouse development. *Genesis.* 2008;46(7):335-46.
21. Ivkovic S, Yoon BS, Popoff SN, Safadi FF, Libuda DE, Stephenson RC, et al. Connective tissue growth factor coordinates chondrogenesis and angiogenesis during skeletal development. *Development.* 2003;130(12):2779-91.
22. Korchynskiy O, ten Dijke P. Identification and functional characterization of distinct critically important bone morphogenetic protein-specific response elements in the Id1 promoter. *J Biol Chem.* 2002;277(7):4883-91.
23. Manson SR, Song JB, Guo Q, Liapis H, Austin PF. Cell type specific changes in BMP-7 expression contribute to the progression of kidney disease in patients with obstructive uropathy. *J Urol.* 2015;193(5 Suppl):1860-9.
24. Wang S, de Caestecker M, Kopp J, Mitu G, Lapage J, Hirschberg R. Renal bone morphogenetic protein-7 protects against diabetic nephropathy. *J Am Soc Nephrol.* 2006;17(9):2504-12.
25. Yokoi H, Mukoyama M, Nagae T, Mori K, Suganami T, Sawai K, et al. Reduction in connective tissue growth factor by antisense treatment ameliorates renal tubulointerstitial fibrosis. *Journal of the American Society of Nephrology : JASN.* 2004;15(6):1430-40.
26. Guha M, Xu ZG, Tung D, Lanting L, R. N. Specific down-regulation of connective tissue growth factor attenuates progression of nephropathy in mouse models of type 1 and type 2 diabetes. *FASEB journal : official publication of the Federation of American Societies for Experimental Biology.* 2007;21(12):3355-68.

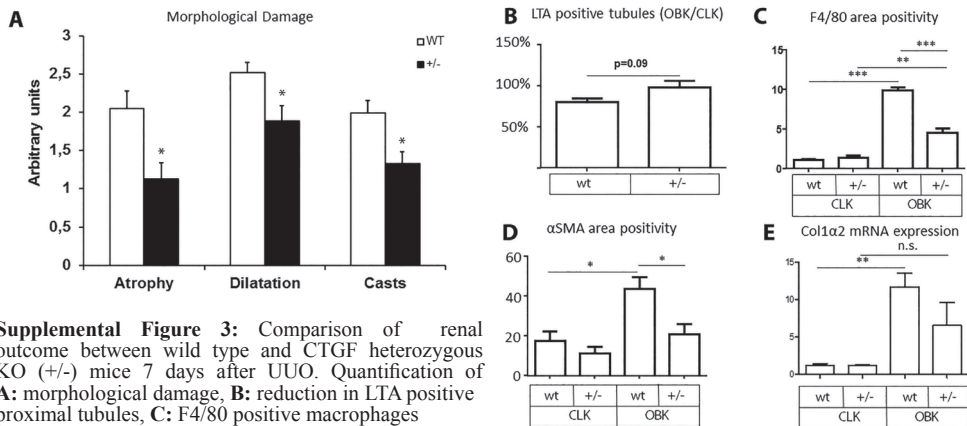
Supplementary material



**Supplemental Figure 1:** A: Comparison between direct GFP fluorescence and immunohistochemically detected GFP in BRE:gf $\beta$  kidney cortex. Asterisk indicates the same glomerulus in consecutive tissue sections. 100x magnified. B: Example of GFP positive area selection with ImageJ.



**Supplemental Figure 2:** Masson Trichrome (MTC) and Sirius Red (SR) histochemical detection of extracellular matrix deposition in CLKs and OBKs. Representative micrographs shown. Arrows indicate intracortical arteries with surrounding collagen deposition. 100x magnified.



**Supplemental Figure 3:** Comparison of renal outcome between wild type and CTGF heterozygous KO (+/-) mice 7 days after UUO. Quantification of A: morphological damage, B: reduction in LTA positive proximal tubules, C: F4/80 positive macrophages D: alphaSMA positive myofibroblasts and E: Col1a2 mRNA expression. \*p<0.05, \*\*p<0.01, \*\*\*p<0.005. Error bar represents SEM.



8



## **Chapter 8:** Targeting CTGF, EGF and PDGF pathways to prevent progression of kidney disease

Lucas L. Falke<sup>\*1</sup>, Helena M. Kok<sup>\*1</sup>, Roel Goldschmeding<sup>1</sup> and Tri Q. Nguyen<sup>1</sup>

1. Department of Pathology, University Medical Centre Utrecht, The Netherlands

\* Contributed equally

**Abstract**

Chronic kidney disease (CKD) is a major health and economic burden with a rising incidence. During progression of CKD, the sustained release of proinflammatory and profibrotic cytokines and growth factors leads to an excessive accumulation of extracellular matrix. Transforming growth factor  $\beta$  (TGF- $\beta$ ) and angiotensin II are considered to be the two main driving forces in fibrotic development. Blockade of the renin–angiotensin–aldosterone system has become the mainstay therapy for preservation of kidney function, but this treatment is not sufficient to prevent progression of fibrosis and CKD. Several factors that induce fibrosis have been identified, not only by TGF- $\beta$ -dependent mechanisms, but also by TGF- $\beta$ -independent mechanisms. Among these factors are the (partially) TGF- $\beta$ -independent profibrotic pathways involving connective tissue growth factor, epidermal growth factor and platelet-derived growth factor and their receptors. In this Review, we discuss the specific roles of these pathways, their interactions and preclinical evidence supporting their qualification as additional targets for novel antifibrotic therapies.

**Review Criteria**

We searched PubMed for original articles published between 1984 and 2014 that focused on one of the three growth factors (CTGF, EGF, PDGF). The search terms used were “CTGF/CCN2”, “EGF”, “PDGF” (either abbreviated or written in full) in combination with “renal fibrosis”, “kidney fibrosis”, “CKD”, “kidney disease” or “intervention”. All selected articles were English-language, full text papers. We also searched reference lists of identified articles for further papers.



## Introduction

Chronic kidney disease (CKD) is a major health and economic burden with a rising incidence and prevalence (1, 2). Almost all variants of CKD are associated with progressive glomerulosclerosis, and tubulointerstitial and vascular fibrosis. Furthermore, acute kidney injury (AKI), if sustained, can also lead to fibrosis. During disease progression, growth factors with proinflammatory and profibrotic activity are released, leading to an excessive accumulation of extracellular matrix (ECM), in which collagen and fibronectin are the most notable components (3). The increase in ECM is driven by myofibroblasts positive for  $\alpha$ -smooth muscle actin (4). Angiotensin II (Ang II) and transforming growth factor  $\beta$  (TGF- $\beta$ ) are considered to be the two main driving forces in fibrotic development as both factors can increase production of ECM as well as myofibroblast numbers (5, 6). Blockade of the renin–angiotensin–aldosterone system has become the mainstay therapy for preservation of kidney function, but this approach is not sufficient to prevent progression of fibrosis and CKD. Much effort has also been put into determining the efficacy of TGF- $\beta$  blockade during fibrotic disease. Despite the impressive results obtained in experimental kidney fibrosis, TGF- $\beta$  inhibition has not yet translated into an effective and safe therapeutic strategy in humans. These failed attempts might relate to possible adverse effects of TGF- $\beta$  inhibition, including autoimmunity, hyperinflammation and increased tumourigenesis (7). Considering the multifunctional biological activities of TGF- $\beta$ , it is important to explore therapeutic strategies that target the downstream effectors of TGF- $\beta$  or the signalling pathways that specifically mediate its fibrogenic action. Several factors have been identified to induce fibrosis, not only by TGF- $\beta$ -dependent mechanisms, but also by TGF- $\beta$ -independent mechanisms. Among these factors are the (partially) TGF- $\beta$ -independent profibrotic pathways involving connective tissue growth factor (CTGF), epidermal growth factor (EGF) and platelet-derived growth factor (PDGF), and their receptors. Evidence from the past few years, mostly obtained in preclinical studies, has indicated important synergistic roles for these three growth factors in the development of kidney fibrosis (Figure 1). In this Review, we will discuss the specific roles of these pathways and their interactions, as well as preclinical evidence supporting their qualification as additional targets for novel antifibrotic therapies.

## CTGF

### *CTGF functions in the kidney*

CTGF (also known as Cyr61, CTGF, NOV family member 2 or CCN2) is the second of six members of the CCN family of matricellular proteins with partially overlapping and partially antagonistic functions (8). The CTGF molecule consists of four distinct, conserved domains that can interact with multiple different extracellular proteins, including growth factors, cell surface molecules such as integrins, and ECM proteins such as fibronectin and proteoglycans (9). Its promoter contains a TGF- $\beta$ -responsive element as well as numerous other regulatory sequences, including a hypoxia-responsive element, and thus can be regarded as an early responder during the onset of fibrotic disease (10). In the healthy kidney, CTGF is expressed in glomerular epithelium, proximal tubules and interstitial fibroblasts (11). No consensus has been reached regarding its major modes of action. Most likely, CTGF acts predominantly by facilitating a fibrosis-oriented regenerative profile through modification of a multitude of signalling pathways. Importantly, CTGF also activates the proinflammatory nuclear factor  $\kappa$ B (NF- $\kappa$ B) pathway in the renal interstitium and induces C-C motif chemokine 2 (12, 13). Thus, CTGF may induce inflammation early in the wound healing response, which if sustained, leads to fibrosis.

Despite failed efforts to identify a true CTGF receptor, many molecular targets have been identified through which CTGF might exert its effects. For instance, many of the functions of TGF- $\beta$  seem to depend on the presence of CTGF both *in vitro* and *in vivo* (14, 15). Direct physical interaction between CTGF and TGF- $\beta$  could increase TGF- $\beta$  binding to TGF- $\beta$  receptor type-2 (16). CTGF also enhances the TGF- $\beta$  signalling pathway by binding and activating the high affinity nerve growth factor receptor (also known as neurotrophic tyrosine kinase receptor type 1 [NTRK1] or tyrosine receptor kinase A [TrkA]).

Binding of CTGF to this receptor induces KLF10 (also known as TIEG-1), which suppresses SMAD7, the major inhibitory Smad of the TGF- $\beta$  signalling pathway (17). In addition, CTGF can directly bind LRP1 and the EGF receptor (EGFR), which leads to activation of profibrotic ERK signalling in the kidney (18-20). Moreover, binding of CTGF to LRP6 activates canonical Wnt signalling and interaction of CTGF with integrins, including  $\alpha\beta 1$  and  $\alpha\beta 3$ , is essential for its role in adherence and migration (21, 22). Interestingly, CTGF inhibits the activity of the antifibrotic and proregenerative bone morphogenetic protein 7 (BMP7), which itself is regarded as a TGF- $\beta$  antagonist (23, 24). Thus, therapeutic inhibition of CTGF could reduce TGF- $\beta$  signalling and increase BMP7 signalling activity in kidney disease.

#### *CTGF as a biomarker in kidney disease*

CTGF is upregulated in the human kidney during a variety of kidney diseases, including diabetic nephropathy, chronic allograft nephropathy, hypertensive nephrosclerosis and crescentic glomerulonephritis (25-27). Upregulation of renal CTGF expression is associated with a rise in plasma CTGF levels, which is an independent predictor of end-stage renal disease and mortality in patients with type 1 diabetic nephropathy (28).

N-terminal CTGF, a proteolytic fragment of full-length CTGF, is freely filtered by the glomerulus, but almost completely resorbed by the proximal tubules in healthy kidneys. However, in the case of elevated plasma CTGF levels and/or renal tubular dysfunction, urine levels of N-terminal CTGF may increase (29, 30). Urinary CTGF level correlates with urinary albumin excretion and glomerular filtration rate, and is as strong a predictor for the progression of diabetic nephropathy as are haemoglobin A1c levels and high blood pressure (31-33). Furthermore, in a large prospective cohort, elevated urinary CTGF predicted tubulointerstitial fibrosis in the kidney allograft (34). Thus, both urine and plasma CTGF could be useful biomarkers of fibrogenesis in CKD (35). Beyond its potential as a biomarker, increased circulating CTGF in patients with CKD might act as a uraemic toxin contributing to cardiovascular risk (30). Increased urinary CTGF can reflect both tubular dysfunction and increased local production in the context of progressive kidney fibrosis, and might also be toxic to tubular epithelium (29).

Several genetic variants in the promoter region of CTGF have been described, including a -20C>G polymorphism, of which the GG allele with higher baseline transcriptional activity is associated with diabetic nephropathy (36). In addition, a -945G>C polymorphism was proposed to determine transcriptional activity downstream of TGF- $\beta$ . Interestingly, increased frequency of this -945G allele was observed in patients with systemic sclerosis, and in these patients this allele was associated with the presence of fibrosing alveolitis (37). However, this particular polymorphism was not associated with susceptibility to diabetic nephropathy (38, 39).

#### *Targeting CTGF in kidney disease*

Constitutional deletion of CTGF causes skeletal deformities associated with pulmonary hypoplasia and vascular abnormalities leading to early postnatal death (40, 41). However, kidney development is not affected in CTGF-knockout mice (9).

A 50% reduction in CTGF expression by antisense oligonucleotides attenuated the progression of CKD and fibrosis after unilateral ureteral obstruction (UUO) in mice (42). Similarly, progression of renal allograft nephropathy in rats was hampered by CTGF reduction (43). In addition, specific downregulation of CTGF with oligonucleotides protected against kidney injury in models of both type 1 and type 2 diabetes mellitus (44). In diabetic mice with genetic hemizygous CTGF deletion, a 50% reduction in CTGF expression was associated with less pronounced mesangial expansion and absence of glomerular basement membrane thickening. Interestingly, reduced CTGF expression in this study was associated with preservation of BMP7 signalling activity (23). By contrast, a 50% reduction in CTGF expression was not sufficient to attenuate kidney damage and fibrosis in more severe models of kidney dysfunction (45). Of note, in these models of severe and prolonged kidney injury, despite a 50% reduction in CTGF expression, levels of this growth factor remained well above baseline levels. Whether further reduction of CTGF to below baseline levels might be protective even in severe models of kidney disease remains to be established. Remarkably, further overexpression of CTGF did not worsen the

phenotype in a severe model of toxic nephropathy, whereas in a mild model of diabetic nephropathy, CTGF overexpression in podocytes aggravated structural and functional damage to the kidney (46, 47).

The fully humanized monoclonal antibody FG-3019, which targets CTGF, is currently in clinical trials for various conditions. In experimental models of fibrosis, FG-3019 reduced deposition of ECM (14). In a phase I clinical study in diabetic patients with microalbuminuria, FG-3019 proved not only to be safe, but also seemed to lower urinary albumin excretion (48). To date, no further clinical studies targeting CTGF in patients with renal disease have been published. Although a phase I clinical trial with FG-3019 in patients with focal segmental glomerulosclerosis and a phase II clinical trial with FG-3019 in patients with type 2 diabetes were terminated, clinical trials with FG-3019 are currently running in patients with idiopathic pulmonary fibrosis, liver fibrosis and pancreatic cancer.

With respect to other members of the CCN family, NOV (CCN3) has been reported to inhibit CTGF-mediated fibrosis by as yet unknown mechanisms, and should be explored in more detail (49). NOV might exert its antifibrotic effects by inhibition of PDGF expression, as has been shown in experimental mesangioliferative nephritis (50).

#### *Clinical perspective*

In preclinical studies, anti-CTGF antibodies were effective in models of kidney injury as well as in other conditions, including pulmonary fibrosis, muscular dystrophy, pancreatic cancer and melanoma. Clinical trials of anti-CTGF antibodies in idiopathic pulmonary fibrosis and pancreatic cancer have been initiated (51-56).

In cardiovascular models, the role of CTGF is still highly controversial and the potential of anti-CTGF therapy has not been studied. Overexpression of CTGF has been implicated in the pathogenesis of myocardial hypertrophy and fibrosis (57, 58). On the other hand, transgenic overexpression of CTGF in cardiomyocytes was protective in models of left ventricular pressure overload and transient coronary occlusion, and high CTGF expression in carotid atherectomies seemed to be associated with a stable plaque phenotype (59-61).

Thus, CTGF seems to be an attractive target for antifibrotic therapy in kidney disease (Table 1), although special caution might be warranted when applying anti-CTGF therapy in patients with cardiovascular comorbidity. However, this concern might only be theoretical, as data from clinical trials have not indicated occurrence of such adverse effects.

**Table 1:** Kidney-specific interventions targeting CTGF

Intervention	Setting	Effects	Ref.
Oligonucleotides (siRNA)	7-day UUO (mouse)	Reduced interstitial fibrosis	(42)
	Type 1 and type 2 diabetes (mouse)	Reduced mesangial expansion Improved renal function	(44)
	Chronic allograft nephropathy (rat)	Reduction in nephropathy	(43)
Transgenic (Hemizygous deletion)	Mild type 1 diabetes (mouse)	Reduced mesangial expansion Reduced GBM thickening Reduced albuminuria	(23)
	14-day UUO severe type 1 diabetes aristolochic-acid-induced nephropathy (mouse)	No effect	(45)
Antibody (FG-3019)	14-day UUO (mouse)	Reduced fibrosis	(14)
	Diabetic patients with microalbuminuria (Phase I trial)	Reduced albuminuria	(48)

Abbreviations: CTGF, connective tissue growth factor. siRNA, small interfering RNA. UUO, unilateral ureteral obstruction. GBM, glomerular basement membrane.

## EGF and EGFR

### *EGFR signalling in the kidney*

EGFR (also known as HER1 or erbB-1) is the first member of a family of four transmembrane tyrosine kinase receptors that also includes erbB-2 (proto-oncogene Neu or HER2), erbB-3 (HER3) and erbB-4 (HER4) (62). Ligand binding causes these receptors to heterodimerize, leading to autophosphorylation and kinase activity responsible for the phosphorylation of downstream mediators. Depending on the ligand–receptor combination, different downstream signalling pathways can be activated (for example MAPK/ERK, PI3K/Akt and JAK/STAT) (63). EGFR-knockout mice are not viable owing to disruption of epithelial development in multiple organs including the kidney (64–66). Interestingly, deletion of EGFR in proximal tubules delayed regeneration of tubular epithelium in mice subjected to renal ischaemia–reperfusion injury, whereas apoptosis was reduced by EGF administration in a model of short-term UO (67, 68). These data indicate that EGFR activation is beneficial during the acute phase of kidney injury. The most prominent ligands of EGFR are EGF, heparin-binding EGF-like growth factor (HB-EGF) and TGF- $\alpha$ . These factors are initially membrane bound and inactive, but are released upon proteolytic cleavage by members of the ADAM family of metalloproteinases (69). Increased expression of both HB-EGF and TGF- $\alpha$  is associated with renal pathophysiology (70, 71). Of note, Ang II, a central mediator of adaptive and maladaptive responses in the kidney, can proteolytically activate pro-TGF- $\alpha$ , and subsequently activate EGFR signalling. This process is called transactivation and is believed to be largely responsible for Ang II-induced fibrosis (72, 73). Whether direct inhibition of EGFR will prove to be more attractive than targeting its ligands or its transactivation remains to be established.

### *EGF and EGFR as biomarkers in kidney disease*

EGFR and its upstream ligands maintain a normal epithelial lining under physiological conditions (74). Of the ligands, EGF is the most widely studied and has the highest affinity for EGFR. This receptor is expressed throughout the kidney epithelium and interstitium (75). During kidney disease, a shift in either ligand or receptor availability might occur. This shift can tilt the physiological balance and lead to kidney disease. The role of the EGF–EGFR signalling axis in kidney disease depends on a variety of factors such as aetiology and disease stage (acute versus chronic) (76).

Because EGF is partially excreted in the urine, it might prove valuable as a prognostic biomarker (77). Patients with AKI caused by an ischaemic insult show reduced levels of urinary EGF. Furthermore, slower recovery of AKI was associated with lower EGF detection in the urine (78). In patients with IgA nephropathy, both renal EGF expression and urinary EGF excretion were reduced at baseline and correlated inversely with disease progression (79, 80). Similarly, in patients with congenital ureteropelvic junction obstruction, urinary EGF levels were decreased (81). In children with chronic kidney failure, the level of urinary EGF correlated with kidney function. However, when corrected for creatinine clearance, EGF levels are still lower in patients with a reduced kidney function. This result indicates that local EGF production is inversely correlated with disease severity, and the level of urinary EGF is not only dependent on kidney function (82). However, the expression of EGFR and its downstream signalling is increased in various types of rapidly progressive glomerulonephritis and allograft nephropathy, and correspond to the extent of fibrosis (70, 83, 84). Increased EGFR signalling is also observed in rat models of type 1 diabetes, polycystic kidney disease and hypertension (85–89). This finding suggests that ligands other than EGF mediate EGFR activation during disease.

HB-EGF is the second member of the EGF family. Upregulation of HB-EGF in response to stress has been described both in vitro (in mesangial cells) and in vivo (in experimental glomerulonephritis), but data supporting these findings are limited (90, 91). The third member of the EGF family, TGF- $\alpha$ , determines genetic susceptibility to CKD in various strains of laboratory mice (71). Furthermore, TGF- $\alpha$  overexpression in rodents leads to polycystic kidney disease. However, TGF- $\alpha$  knockout did not reduce cyst formation in genetically susceptible mice (92). The phenomenon of ADAM17-mediated transactivation explains Ang II-induced activation of the EGFR (73). Upon Ang

II signalling, ADAM17 becomes active and digests pro-TGF- $\alpha$  into a bioactive form, thereby initiating EGFR signalling. In other models of organ fibrosis such as hyperoxia-induced pulmonary fibrosis, a strong correlation between TGF- $\alpha$  and severity of disease exists (93). Additionally, CTGF is also capable of mediating EGFR activation (20).

#### *Targeting EGF/EGFR in experimental models*

Comparing responses to kidney damage in six different inbred mouse strains identified EGFR signalling as the major determinant of CKD susceptibility. The FVB mouse strain showed highest TGF- $\alpha$  expression and EGFR activation, which corresponded to development of the most severe CKD (71). Importantly, kidney-specific overexpression of a dominant negative (nonsignalling) EGFR in mice did not lead to a phenotype under physiological conditions, whereas these mice were resistant to development of fibrosis in models of chronic kidney injury induced by ischaemia–reperfusion and renal ablation (72, 94). Silencing of EGFR expression specifically in proximal tubules impaired fibrotic development after Ang II-induced fibrosis (95).

Waved-2 (Wa-2) mice have a 90% EGFR signal reduction caused by a point mutation in EGFR that inhibits its tyrosine kinase activity (96). The Wa-2 mutation attenuated cyst formation and improved renal function in a genetic mouse model of polycystic kidney disease (97), and reduced ECM deposition and myofibroblast proliferation in the UUO model of obstructive nephropathy (98). Wa-2 mice also showed reduced ECM deposition and myofibroblast activation in a model of chronic renal ischaemia (99).

Erlotinib and gefitinib are EGFR tyrosine kinase inhibiting molecules (100). Other small molecule inhibitors of EGFR signalling include PKI 166, EKI-785, AG 1478 and the antibody cetuximab (101). Gefitinib successfully inhibited development of fibrosis in rodent models of hypertension and UUO (98, 102). In a rat model of diabetic nephropathy, EGFR inhibition with PKI 166 preserved podocyte numbers and reduced albuminuria (85). PKI 166 also protected against early renal morphological changes associated with the onset of diabetic nephropathy (103). Administration of erlotinib prevented the progression of rapidly progressive glomerulonephritis in antglomerular basement membrane nephritis, and restored renal function and reduced sodium retention in nephrotoxic rats (70, 104). However, in the acute phase after ischaemia–reperfusion injury in mice, erlotinib prolonged the time needed for recovery, and gefitinib-mediated EGFR blockade resulted in delayed regeneration in a model of folic-acid-induced nephrotoxicity (67, 105). Regeneration was also impaired in Wa-2 mice in the acute phase after ischaemia, and recovery of renal function in these mice was much slower than in wild-type mice after acute renal injury induced by mercury chloride (99, 106). These observations suggest that during the acute phase of kidney injury, EGFR activation is beneficial, whereas in chronic conditions it seems harmful by enhancing the fibrotic process.

Limiting EGFR activation by tyrosine kinase inhibition and via transgenic silencing led to comparable reductions of several fibrotic parameters in various animal models (Table 2). Inhibition of EGFR ligands was also renoprotective, as illustrated by knockdown of HB-EGF in both an ischaemic and a nephritic mouse model (70, 107). In addition, deletion of TGF- $\alpha$  in hypertensive mice resulted in reduced cell proliferation as well as less interstitial collagen accumulation compared with hypertensive wild-type mice, which is identical to the effects of EGFR deletion in proximal tubules (72). These data indicate that targeting the EGFR axis in kidney disease might be achieved on different levels, all leading to comparable results.

#### *Clinical perspective*

The value of EGFR inhibitors for the treatment of cancer has been clearly established in clinical trials. Although this is not yet the case for application of these drugs in non-neoplastic diseases, the validity of targeting the EGFR axis in antifibrotic therapy in progressive CKD is supported by preclinical studies showing that EGFR inhibition is beneficial during fibrogenic kidney disease, and by the observation that EGFR activation is involved in TGF- $\beta$ -mediated development of fibrosis (95, 108). However, blockade of EGFR during AKI seems to hamper disease resolution and kidney regeneration, as exemplified by a

case report of a patient with lung cancer in whom gefitinib treatment was linked to reduced regeneration and turnover of kidney epithelium and to the development of interstitial fibrosis (109). Targeting EGFR signalling can be achieved by small molecule or antibody-mediated ligand-receptor interaction and downstream signalling thereof, or by prevention of homodimerization or heterodimerization of the receptor by a peptidomimetic (110). Resistance to small-molecule-mediated EGFR blocking therapy during neoplastic disease is a common phenomenon (111). This effect is caused at least in part by genetic adaptation of rapidly dividing tumour cells, and might constitute less of a problem for treatment of fibrotic kidney diseases than for treatment of cancer.

**Table 2:** Kidney-specific intervention targeting EGFR

Intervention	Model	Effects	Ref(s).
<b>Molecular inhibition</b>			
PKI 166	Ischaemia-reperfusion (rat)	Reduced macrophage accumulation Reduced $\alpha$ -SMA expression	(107)
	Diabetic nephropathy (rat)	Attenuated glomerular hypertrophy	(103)
	Diabetic nephropathy (rat)	Podocyte preservation, Reduced albuminuria	(85)
Gefitinib	UUO (mouse)	Reduced fibrosis Reduced $\alpha$ -SMA expression	(98)
	Folic acid (mouse)	Inhibition of epithelial proliferation & differentiation	(105)
	Hypertension (rat)	Reduced collagen I expression	(102)
Erlotinib	Hypertension (mouse)	Reduced interstitial fibrosis	(95)
	Anti-GBM nephritis (mouse)	Reduced crescentic glomeruli	(70)
	Doxorubicin nephrotic syndrome (rat)	Restoration of kidney function	(104)
EKI-785	ARPKD (mouse)	Reduced cystic lesions	(169)
AG 1478	Hypertension (rat)	Reduced glomerular sclerosis Reduced extracellular matrix deposition	(86)
	Anti-GBM nephritis (mouse)	Reduced crescentic lesions Reduced albuminuria	(70)
<b>Transgenic</b>			
Waved-2	Ischaemia-reperfusion (mouse)	Reduced interstitial fibrosis	(99)
	UUO (mouse)	Reduced $\alpha$ -SMA expression Downregulation of profibrotic cytokines	(98)
	Folic acid (mouse)	Inhibition of epithelial proliferation & differentiation	(105)
	Nephrotoxic HgCl <sub>2</sub> injury (mouse)	Delayed regeneration	(106)
Dominant negative EGFR (proximal tubules)	Subtotal nephrectomy ischaemia/reperfusion Ang II injection (mouse)	Reduced tubular cell proliferation Reduced mononuclear cell infiltration Reduced interstitial fibrosis	(72, 94)
	TGF- $\alpha$ knockout	Ang II injection (mouse)	Reduced glomerular sclerosis Reduced interstitial fibrosis Reduced interstitial inflammation
HB-EGF knockout	Subtotal nephrectomy (mouse)	Reduced interstitial fibrosis	(71)
	Ischaemia-reperfusion (mouse)	Reduced macrophage accumulation	(107)
EGFR knockout (proximal tubules)	Anti-GBM nephritis (mouse)	Less kidney damage Prevention of albuminuria	(70)
	Hypertension, diabetic nephropathy (mouse)	Reduced interstitial fibrosis	(95)
EGFR knockout (podocytes)	Anti-GBM nephritis (mouse)	Reduced albuminuria Reduced crescentic glomeruli	(70)

Abbreviations: Ang II, angiotensin II; ARPKD, autosomal recessive polycystic kidney disease; EGFR, epidermal growth factor receptor; GBM, glomerular basement membrane; HB-EGF, heparin-binding epidermal growth factor-like growth factor; SMA, smooth muscle actin; TGF, transforming growth factor; UUO, unilateral ureteral obstruction.

**PDGF and PDGFR***PDGF signalling in the kidney*

PDGF was originally identified as a factor released from platelets that promoted the proliferation and recruitment of mesenchymal cells in the kidney, including fibroblasts, mesangial cells, pericytes and smooth muscle cells (112-115). Four different isoforms of PDGF exist, which can generate five different dimers, namely PDGF-AA, PDGF-BB, PDGF-CC, PDGF-DD and PDGF-AB. PDGF receptor (PDGFR)  $\alpha$  and  $\beta$  chain dimerize as homodimers and heterodimers, constituting PDGFR- $\alpha\alpha$ , PDGFR- $\beta\beta$  and PDGFR- $\alpha\beta$ . Both the PDGFR- $\alpha$  and PDGFR- $\beta$  forms have been studied in experimental models of kidney disease, but a specific function for PDGFR- $\alpha\beta$  has thus far not been identified.

In the kidney, all three PDGFRs are predominantly expressed on mesenchymal cells in glomeruli and the interstitium; PDGFR- $\alpha$  is widely expressed by renal interstitial cells and to some degree by mesangial cells, whereas PDGFR- $\beta$  is expressed predominantly by mesangial cells, glomerular parietal, epithelial and interstitial cells (116, 117). As for PDGF ligands, the PDGF-A chain is normally expressed by mature podocytes and epithelial cells of the distal nephron, including collecting duct cells and urothelium (118), whereas low levels of PDGF-B may be present in mesangial cells (117). Both PDGF-A-deficient and PDGF-B-deficient mice die prenatally. Although PDGF-A-deficient mice do not show renal abnormalities, PDGF-B-deficient mice have severe defective glomerular development due to an absence of mesangial cells (119, 120). Consistently, as mesangial cells are considered to be pericytes of the glomerulus, PDGF-B mutant embryos develop fatal haemorrhages due to disturbed arterial pericyte recruitment (121).

The most likely role of PDGF signalling during fibrotic development is myofibroblast recruitment; aberrant PDGFR signalling induces pericyte–myofibroblast transition *in vivo* (122). Similar to EGFR, PDGFR signalling relies on tyrosine kinase activation (123). Proteolytic activation of PDGF-C and PDGF-D, which is required for receptor binding and activation, can be effectuated by tissue plasminogen activator, urokinase-type activator and plasmin (114, 124). Interestingly, levels of TGF- $\beta$  and hepatocyte growth factor (HGF) are elevated in the tubular fluid of kidneys with glomerular proteinuria, and these growth factors could contribute to interstitial fibrosis by directly increasing PDGF-B expression in proximal tubular epithelial cells (125). This effect seems to be induced more often by TGF- $\beta$  than by HGF, as HGF is commonly regarded as a renoprotective factor (126). Another explanation could be that the bioactive potential of PDGF-B outweighs that of HGF after HGF-mediated PDGF upregulation.

*PDGF as a biomarker in kidney disease*

In fibrotic kidney disease, PDGF-B, PDGF-C, PDGF-D, PDGFR- $\alpha$  and PDGFR- $\beta$  are important components of the PDGFR system. PDGF-B/PDGF-D-mediated PDGFR- $\beta$  signalling and PDGFR- $\beta$  expression are increased in mesangioproliferative glomerulonephritis including IgA nephropathy (117, 127-130). In crescentic glomerulonephritis and lupus nephritis, PDGF-B and PDGFR- $\beta$  expression are increased in the kidney (131-133). PDGF-C is upregulated in podocytes and tubulointerstitial cells in kidneys from patients with membranous nephropathy and transplant glomerulopathy (134). Different isoforms of PDGF, in particular PDGF-D, and PDGFR are also increased in kidney diseases with tubulointerstitial involvement, such as chronic allograft nephropathy and chronic obstructive nephropathy (117, 135, 136).

Serum levels of PDGF-D are elevated in patients with IgA nephropathy. Interestingly, the increase in serum PDGF-D was not accompanied by higher intrarenal PDGF-D mRNA expression, suggesting an extrarenal source of elevated PDGF-D (137). In patients with uncomplicated type 1 diabetes, increased urinary excretion of PDGF-A and PDGF-AB/PDGF-B was associated with hyperfiltration (138).

*Targeting PDGF/PDGFR in kidney disease*

Both immunological blockade of PDGF-D and dominant negative PDGFR- $\beta$  overexpression reduced mesangial proliferation in rodent models (127, 139, 140). Additionally, a reduction in PDGF-B or PDGF-D

availability inhibited tubulointerstitial fibrotic development in models of chronic glomerulonephritis (141-143). In murine diabetic nephropathy, genetic reduction of PDGFR- $\beta$  signalling improved glomerular and interstitial morphology (144). Moreover, by blocking PDGFR- $\beta$  with the molecular compound AG 1295, interstitial fibrosis could be attenuated in rats after UUO (145). Remarkably, reducing PDGF-C expression in a model of mesangioproliferative glomerulonephritis failed to reduce proliferation of the mesangium (146), whereas anti-PDGF-C IgG effectively reduced kidney fibrosis in UUO, and PDGF-C-knockout mice were protected from UUO-induced kidney fibrosis (134, 147). Interestingly, PDGF-C deficiency or antagonism did not protect from liver fibrosis in a model of bile-duct-ligation-induced liver fibrosis, probably because of increased PDGFR- $\beta$  signalling (148).

The clinically available drug imatinib inhibits PDGFR tyrosine kinase activity and has been shown to successfully attenuate anti-glomerular basement membrane nephritis and tubulointerstitial fibrosis (149, 150). Similar results of glomerular protection and interstitial reduction of fibrosis were obtained in murine models of lupus nephritis, cryoglobulinaemia and diabetic nephropathy (151-154). In two rat models of malignant hypertension, imatinib reduced renal damage without showing any effect on systemic blood pressure (155, 156), and in a model of chronic allograft nephropathy, imatinib reduced rejection-mediated interstitial changes to such an extent that the allografted kidneys appeared near normal (157). Imatinib also successfully inhibited myofibroblast recruitment and ECM deposition in models of ischaemia-reperfusion injury and UUO (123, 158). Interestingly, the latter study demonstrated that imatinib might exert its renoprotective effects via inhibition of tyrosine-protein kinase ABL1 (158).

A synthetic nonspecific PDGF blocking molecule, trapidil, was found to protect rats against gentamycin-induced nephrotoxicity, anti-Thy1.1 glomerulonephritis and ischaemic injury (159-162). Paradoxically, however, in rabbits with nephrotoxic nephritis, trapidil treatment resulted in worse histological outcome compared with control animals (163). Also, during the recovery phase of an ischaemic insult, treatment with trapidil led to a decrease in renal function and an increase in mortality in rats (164). These data suggest that, like EGFR, the PDGF/PDGFR axis is involved in the proliferation and regeneration of tubular cells in the acute phase of kidney injury. Once again, however, it needs to be acknowledged that trapidil is not PDGFR specific and mechanisms unrelated to the PDGFR system might exist.

#### *Clinical perspective*

Despite the availability of PDGFR-specific and general tyrosine kinase inhibitors, no clinical trials are currently being performed to investigate the feasibility of anti-PDGF treatment in non-neoplastic kidney disease. However, results of preclinical studies, especially those investigating imatinib and trapidil, are promising and suggest that further exploration of targeting PDGFR signalling in CKD is worthwhile (Table 3). In order to explore this pathway in more detail, however, more specific PDGFR inhibitory agents are required.



**Table 3: Kidney-specific interventions targeting PDGF/PDGFR.**

Intervention	Model	Effects	Ref(s)
<b>Molecular inhibition</b>			
Imatinib	Chronic allograft nephropathy (rat)	Reduced macrophage infiltration Reduced matrix formation	(157)
	Lupus nephritis (mouse)	Decreased matrix formation Delayed onset of proteinuria	(154)
	Type 1 diabetes (mouse)	Reduced albuminuria Reduced glomerulosclerosis Reduced interstitial fibrosis	(154)
	Anti-Thy1.1 nephritis (rat)	Reduced mesangial cell proliferation	(170)
	UNX chronic anti-Thy1.1 nephritis (rat)	Reduced accumulation of matrix proteins Decreased blood pressure Decreased proteinuria	(171)
Trapidil	Anti-Thy1.1 nephritis (rat)	Reduced mesangial proliferation	(161, 162)
	Nephrotoxic nephritis (rabbit)	More severe clinical outcome Worse renal morphology	(163)
	Ischaemia–reperfusion (rat)	Reduced interstitial fibrosis	(159)
	Ischaemia–reperfusion (rat)	Increased mortality Reduced kidney function	(164)
	Gentamycin nephropathy (rat)	Improved renal function Reduced proteinuria	(160)
AG 1295	UUO (rat)	Reduced macrophage accumulation	(145)
<b>Antibody</b>			
PDGF-A/PDGF-B	Anti-Thy1.1 nephritis (rat)	Reduced mesangial proliferation Reduced matrix accumulation	(172)
PDGFR- $\beta$	Anti-Thy1.1 nephritis (rat)	Reduced mesangial proliferation Reduced matrix accumulation	(173)
PDGF-C	UUO (mouse)	Reduced interstitial fibrosis	(147, 148)
CR002 (PDGF-D)	Anti-Thy1.1 nephritis (rat)	Reduced glomerular cell proliferation Reduced infiltration	(140)
	UNX acute anti-Thy1.1 nephritis (rat)	Reduced interstitial fibrosis	(143)
	UNX chronic anti-Thy1.1 nephritis (rat)	Reduced proteinuria Lower expression of collagens	(141)
PDGFR- $\alpha$ and PDGFR- $\beta$	Ischaemia–reperfusion UUO (mouse)	Reduced collagen expression Reduced myofibroblast proliferation	(122)
<b>Oligonucleotide</b>			
Aptamer to PDGF-B	Acute anti-Thy 1.1 nephritis (rat)	Reduced mesangial cell proliferation Reduced matrix accumulation	(174)
	Chronic anti-Thy 1.1 nephritis (rat)	Reduced proteinuria Reduced glomerulosclerosis Reduced interstitial fibrosis	(142)
PDGF-A	Spontaneous hypertension (rat)	Reduced glomerular damage	(175)
<b>Gene transfer</b>			
Dominant negative PDGFR- $\beta$	Anti-Thy1.1 nephritis (rat)	Reduced mesangial cell proliferation Reduced matrix formation	(139)
<b>Transgenic</b>			
PDGF-C knockout	UUO (mouse)	Reduced interstitial fibrosis	(147, 148)

Abbreviations: PDGF, platelet-derived growth factor; PDGFR, PDGF receptor; UNX, unilateral nephrectomy; UUO, unilateral ureteral obstruction.

## Conclusions

Although TGF- $\beta$  is generally considered to be the driving force behind fibrotic processes, alternative factors such as CTGF, PDGFR and EGFR signalling pathways have been identified as feasible targets for treatment of CKD and kidney fibrosis. Interaction between these pathways (Figure 1) is exemplified by observations that induction of CTGF expression by TGF- $\beta$  is partially EGFR dependent,<sup>95, 108</sup> and that Ang II-mediated EGFR transactivation in renal epithelial cells is associated with concomitant TGF- $\beta$  activation (165). Furthermore, CTGF is upregulated by, and is itself a ligand for, EGFR activation, which might constitute a positive feedback loop (20, 166). In addition, TGF- $\beta$  requires both PDGFR and EGFR for its profibrotic activity and dual blockade of PDGF and EGFR pathways with imatinib plus lapatinib prevented fibrosis to a greater extent than either drug alone (167). Numerous studies have demonstrated the successful application of direct or indirect blockade of the CTGF, PDGFR and EGFR signalling pathways to prevent experimental

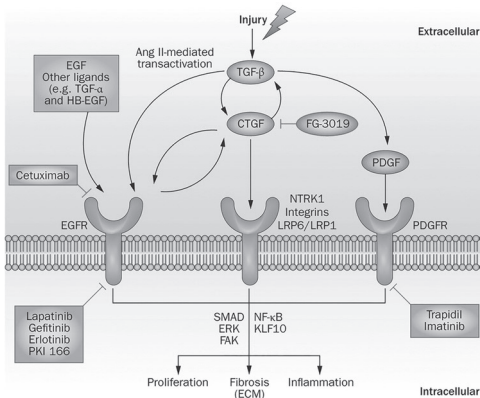


**Figure 1:** Interactions between CTGF, EGF, PDGF and the profibrotic TGF- $\beta$  pathway. TGF- $\beta$  is generally considered to be the driving force behind fibrotic processes in the kidney; however, CTGF, PDGFR and EGFR signalling pathways have also been identified as feasible targets for the treatment of chronic kidney disease and kidney fibrosis. Interaction between these pathways is exemplified by observations that TGF- $\beta$  requires CTGF, PDGFR and EGFR for its profibrotic activity. In addition, CTGF is upregulated by EGFR activation and is itself a ligand for EGFR activation, which might constitute a positive feedback loop. Possible clinical interventions for targeting these pathways are shown in grey boxes. Abbreviations: Ang II, angiotensin II; CTGF, connective tissue growth factor; ECM, extracellular matrix; EGF, epidermal growth factor; EGFR, EGF receptor; HB-EGF, heparin-binding EGF-like growth factor; PDGF, platelet-derived growth factor; PDGFR, PDGF receptor; TGF, transforming growth factor.

kidney fibrosis, but none of these treatment strategies has yet been translated into the clinic. One reason for these failed attempts could be the toxic effects of these drugs in patients, for example, occurrence of adverse effects that have been reported in phase I clinical trials or potential threats based on preclinical observations (Table 4). In conclusion, CTGF, PDGFR and EGFR all seem to constitute valid alternative targets to TGF- $\beta$ , especially if concerns regarding the risks associated with blocking the beneficial anti-inflammatory and tumour-suppressive actions of TGF- $\beta$  prevent clinical implementation of TGF- $\beta$  inhibitors (168). On the basis of current literature, it is difficult to prioritize between these alternative targets. However, considering their substantial interaction, it seems that targeting multiple growth factors might represent the best strategy for treatment of kidney fibrosis.

**Table 4:** Blockade of CTGF, EGF or PDGF pathways—adverse effects and hypothetical threats.

Target	Adverse effects reported in clinical trials	Hypothetical threats based on preclinical observations	Ref(s).
CTGF	Fatigue, headache, dizziness, flushing, anaemia, anxiety, hyperglycaemia, hypoglycaemia	Myocardial dysfunction, unstable atherosclerotic plaque, increased skin fragility	(48, 61, 176, 177)
EGF/EGFR	Interstitial lung disease, cardiomyopathy, skin disorder, nausea, diarrhoea, vomiting, anorexia	Decreased regeneration from acute kidney injury	(109, 178)
PDGF/PDGFR	Thyroid dysfunction, cardiac failure, coronary artery disease, skin disorders, hypertension, thrombocytopenia	Decreased regeneration from acute kidney injury	(164, 179-181)
TKI			

Abbreviations: CTGF, connective tissue growth factor; EGF, epidermal growth factor; EGFR, EGF receptor; PDGF, platelet-derived growth factor; PDGFR, PDGF receptor. TKI, Tyrosine Kinase Inhibitor

## References

1. Couser WG, Remuzzi G, Mendis S, Tonelli M. The contribution of chronic kidney disease to the global burden of major noncommunicable diseases. *Kidney Int.* 2011;80(12):1258-70.
2. Schieppati A, Remuzzi G. Chronic renal diseases as a public health problem: epidemiology, social, and economic implications. *Kidney Int Suppl.* 2005(98):S7-S10.
3. Boor P, Ostendorf T, Floege J. Renal fibrosis: novel insights into mechanisms and therapeutic targets. *Nat Rev Nephrol.* 2010;6(11):643-56.
4. LeBleu VS, Taduri G, O'Connell J, Teng Y, Cooke VG, Woda C, et al. Origin and function of myofibroblasts in kidney fibrosis. *Nat Med.* 2013;19(8):1047-53.
5. Bottinger EP, Bitzer M. TGF-beta signaling in renal disease. *J Am Soc Nephrol.* 2002;13(10):2600-10.
6. Ruster C, Wolf G. Angiotensin II as a morphogenic cytokine stimulating renal fibrogenesis. *J Am Soc Nephrol.* 2011;22(7):1189-99.
7. Akhurst RJ, Hata A. Targeting the TGFbeta signalling pathway in disease. *Nat Rev Drug Discov.* 2012;11(10):790-811.
8. Perbal B. CCN proteins: multifunctional signalling regulators. *Lancet.* 2004;363(9402):62-4.
9. Falke LL, Goldschmeding R, Nguyen TQ. A perspective on anti-CCN2 therapy for chronic kidney disease. *Nephrol Dial Transplant.* 2014;29 Suppl 1:i30-i7.
10. Grotendorst GR, Okochi H, Hayashi N. A novel transforming growth factor beta response element controls the expression of the connective tissue growth factor gene. *Cell Growth Differ.* 1996;7(4):469-80.
11. Ito Y, Aten J, Bende RJ, Oemar BS, Rabelink TJ, Weening JJ, et al. Expression of connective tissue growth factor in human renal fibrosis. *Kidney Int.* 1998;53(4):853-61.
12. Liu SC, Hsu CJ, Fong YC, Chuang SM, Tang CH. CTGF induces monocyte chemoattractant protein-1 expression to enhance monocyte migration in human synovial fibroblasts. *Biochim Biophys Acta.* 2013;1833(5):1114-24.
13. Sanchez-Lopez E, Rayego S, Rodrigues-Diez R, Rodriguez JS, Rodrigues-Diez R, Rodriguez-Vita J, et al. CTGF promotes inflammatory cell infiltration of the renal interstitium by activating NF-kappaB. *J Am Soc Nephrol.* 2009;20(7):1513-26.
14. Wang Q, Usinger W, Nichols B, Gray J, Xu L, Seeley TW, et al. Cooperative interaction of CTGF and TGF-beta in animal models of fibrotic disease. *Fibrogenesis Tissue Repair.* 2011;4(1):4.
15. Yokoi H, Sugawara A, Mukoyama M, Mori K, Makino H, Suganami T, et al. Role of connective tissue growth factor in profibrotic action of transforming growth factor-beta: a potential target for preventing renal fibrosis. *Am J Kidney Dis.* 2001;38(4 Suppl 1):S134-8.
16. Abreu JG, Ketpura NI, Reversade B, De Robertis EM. Connective-tissue growth factor (CTGF) modulates cell signalling by BMP and TGF-beta. *Nat Cell Biol.* 2002;4(8):599-604.
17. Wahab NA, Weston BS, Mason RM. Connective tissue growth factor CCN2 interacts with and activates the tyrosine kinase receptor TrkA. *J Am Soc Nephrol.* 2005;16(2):340-51.
18. Cheng X, Gao W, Dang Y, Liu X, Li Y, Peng X, et al. Both ERK/MAPK and TGF-Beta/Smad signaling pathways play a role in the kidney fibrosis of diabetic mice accelerated by blood glucose fluctuation. *J Diabetes Res.* 2013;2013:463740.
19. Mason RM. Fell-Muir lecture: Connective tissue growth factor (CCN2) -- a pernicious and pleiotropic player in the development of kidney fibrosis. *Int J Exp Pathol.* 2013;94(1):1-16.
20. Rayego-Mateos S, Rodrigues-Diez R, Morgado-Pascual JL, Rodrigues Diez RR, Mas S, Lavoz C, et al. Connective tissue growth factor is a new ligand of epidermal growth factor receptor. *J Mol Cell Biol.* 2013;5(5):323-35.
21. Lau LF, Lam SC. The CCN family of angiogenic regulators: the integrin connection. *Exp Cell Res.* 1999;248(1):44-57.
22. Rooney B, O'Donovan H, Gaffney A, Browne M, Faherty N, Curran SP, et al. CTGF/CCN2 activates canonical Wnt signalling in mesangial cells through LRP6: implications for the pathogenesis of diabetic nephropathy. *FEBS Lett.* 2011;585(3):531-8.
23. Nguyen TQ, Roestenberg P, van Nieuwenhoven FA, Bovenschen N, Li Z, Xu L, et al. CTGF inhibits BMP-7 signaling in diabetic nephropathy. *J Am Soc Nephrol.* 2008;19(11):2098-107.
24. Boon MR, van der Horst G, van der Pluijm G, Tamsma JT, Smit JW, Rensen PC. Bone morphogenetic protein 7: a broad-spectrum growth factor with multiple target therapeutic potency. *Cytokine Growth Factor Rev.* 2011;22(4):221-9.
25. Cheng O, Thuillier R, Sampson E, Schultz G, Ruiz P, Zhang X, et al. Connective tissue growth factor is a biomarker and mediator of kidney allograft fibrosis. *Am J Transplant.* 2006;6(10):2292-306.
26. Ito Y, Aten J, Nguyen TQ, Joles JA, Matsuo S, Weening JJ, et al. Involvement of connective tissue growth factor in human and experimental hypertensive nephrosclerosis. *Nephron Exp Nephrol.* 2011;117(1):e9-20.
27. Kanemoto K, Usui J, Tomari S, Yokoi H, Mukoyama M, Aten J, et al. Connective tissue growth factor participates in scar formation of crescentic glomerulonephritis. *Lab Invest.* 2003;83(11):1615-25.
28. Nguyen TQ, Tarnow L, Jorsal A, Oliver N, Roestenberg P, Ito Y, et al. Plasma connective tissue growth factor is an independent predictor of end-stage renal disease and mortality in type 1 diabetic nephropathy. *Diabetes Care.* 2008;31(6):1177-82.
29. Gerritsen KG, Peters HP, Nguyen TQ, Koeners MP, Wetzels JF, Joles JA, et al. Renal proximal tubular dysfunction is a major determinant of urinary connective tissue growth factor excretion. *Am J Physiol Renal Physiol.* 2010;298(6):F1457-64.
30. Gerritsen KG, Abrahams AC, Peters HP, Nguyen TQ, Koeners MP, den Hoedt CH, et al. Effect of GFR on plasma N-terminal connective tissue growth factor (CTGF) concentrations. *Am J Kidney Dis.* 2012;59(5):619-

- 27.
31. Nguyen TQ, Tarnow L, Andersen S, Hovind P, Parving HH, Goldschmeding R, et al. Urinary connective tissue growth factor excretion correlates with clinical markers of renal disease in a large population of type 1 diabetic patients with diabetic nephropathy. *Diabetes Care*. 2006;29(1):83-8.
32. Riser BL, Cortes P, DeNichilo M, Deshmukh PV, Chahal PS, Mohammed AK, et al. Urinary CCN2 (CTGF) as a possible predictor of diabetic nephropathy: preliminary report. *Kidney Int*. 2003;64(2):451-8.
33. Tam FW, Riser BL, Meeran K, Rambow J, Pusey CD, Frankel AH. Urinary monocyte chemoattractant protein-1 (MCP-1) and connective tissue growth factor (CCN2) as prognostic markers for progression of diabetic nephropathy. *Cytokine*. 2009;47(1):37-42.
34. Metalidis C, van Vuuren SH, Broekhuizen R, Lerut E, Naesens M, Bakker SJ, et al. Urinary connective tissue growth factor is associated with human renal allograft fibrogenesis. *Transplantation*. 2013;96(5):494-500.
35. Dendooven A, Gerritsen KG, Nguyen TQ, Kok RJ, Goldschmeding R. Connective tissue growth factor (CTGF/CCN2) ELISA: a novel tool for monitoring fibrosis. *Biomarkers*. 2011;16(4):289-301.
36. Wang B, Carter RE, Jaffa MA, Nakerakanti S, Lackland D, Lopes-Virella M, et al. Genetic variant in the promoter of connective tissue growth factor gene confers susceptibility to nephropathy in type 1 diabetes. *J Med Genet*. 2010;47(6):391-7.
37. Fonseca C, Lindahl GE, Ponticos M, Sestini P, Renzoni EA, Holmes AM, et al. A polymorphism in the CTGF promoter region associated with systemic sclerosis. *N Engl J Med*. 2007;357(12):1210-20.
38. Dendooven A, Nguyen TQ, Brosens L, Li D, Tarnow L, Parving HH, et al. The CTGF -945GC polymorphism is not associated with plasma CTGF and does not predict nephropathy or outcome in type 1 diabetes. *J Negat Results Biomed*. 2011;10:4.
39. Patel SK, Wai B, Macisaac RJ, Grant S, Velkoska E, Ord M, et al. The CTGF gene -945 G/C polymorphism is not associated with cardiac or kidney complications in subjects with type 2 diabetes. *Cardiovasc Diabetol*. 2012;11:42.
40. Baguma-Nibasheka M, Kablar B. Pulmonary hypoplasia in the connective tissue growth factor (Ctgf) null mouse. *Dev Dyn*. 2008;237(2):485-93.
41. Ivkovic S, Yoon BS, Popoff SN, Safadi FF, Libuda DE, Stephenson RC, et al. Connective tissue growth factor coordinates chondrogenesis and angiogenesis during skeletal development. *Development*. 2003;130(12):2779-91.
42. Yokoi H, Mukoyama M, Nagae T, Mori K, Suganami T, Sawai K, et al. Reduction in connective tissue growth factor by antisense treatment ameliorates renal tubulointerstitial fibrosis. *J Am Soc Nephrol*. 2004;15(6):1430-40.
43. Luo GH, Lu YP, Song J, Yang L, Shi YJ, Li YP. Inhibition of connective tissue growth factor by small interfering RNA prevents renal fibrosis in rats undergoing chronic allograft nephropathy. *Transplant Proc*. 2008;40(7):2365-9.
44. Guha M, Xu ZG, Tung D, Lanting L, Natarajan R. Specific down-regulation of connective tissue growth factor attenuates progression of nephropathy in mouse models of type 1 and type 2 diabetes. *Faseb J*. 2007;21(12):3355-68.
45. Falke LL, Dendooven A, Leeuwis JW, Nguyen TQ, van Geest RJ, van der Giezen DM, et al. Hemizygous deletion of CTGF/CCN2 does not suffice to prevent fibrosis of the severely injured kidney. *Matrix Biol*. 2012;31(7-8):421-31.
46. Yokoi H, Mukoyama M, Mori K, Kasahara M, Suganami T, Sawai K, et al. Overexpression of connective tissue growth factor in podocytes worsens diabetic nephropathy in mice. *Kidney Int*. 2008;73(4):446-55.
47. Fragiadaki M, Witherden AS, Kaneko T, Sonnyal S, Pusey CD, Bou-Gharios G, et al. Interstitial fibrosis is associated with increased COL1A2 transcription in AA-injured renal tubular epithelial cells in vivo. *Matrix Biol*. 2011;30(7-8):396-403.
48. Adler SG, Schwartz S, Williams ME, Arauz-Pacheco C, Bolton WK, Lee T, et al. Phase I study of anti-CTGF monoclonal antibody in patients with diabetes and microalbuminuria. *Clin J Am Soc Nephrol*. 2010;5(8):1420-8.
49. Riser BL, Najmabadi F, Perbal B, Peterson DR, Rambow JA, Riser ML, et al. CCN3 (NOV) is a negative regulator of CCN2 (CTGF) and a novel endogenous inhibitor of the fibrotic pathway in an in vitro model of renal disease. *Am J Pathol*. 2009;174(5):1725-34.
50. van Roeyen CR, Boor P, Borkham-Kamphorst E, Rong S, Kunter U, Martin IV, et al. A novel, dual role of CCN3 in experimental glomerulonephritis: pro-angiogenic and antimesangioproliferative effects. *Am J Pathol*. 2012;180(5):1979-90.
51. Morales MG, Gutierrez J, Cabello-Verrugio C, Cabrera D, Lipson KE, Goldschmeding R, et al. Reducing CTGF/CCN2 slows down mdx muscle dystrophy and improves cell therapy. *Hum Mol Genet*. 2013;22(24):4938-51.
52. Wang X, Wu G, Gou L, Liu Z, Wang X, Fan X, et al. A novel single-chain-Fv antibody against connective tissue growth factor attenuates bleomycin-induced pulmonary fibrosis in mice. *Respirology*. 2011;16(3):500-7.
53. Lipson KE, Wong C, Teng Y, Spong S. CTGF is a central mediator of tissue remodeling and fibrosis and its inhibition can reverse the process of fibrosis. *Fibrogenesis Tissue Repair*. 2012;5 Suppl 1:S24.
54. Aikawa T, Gunn J, Spong SM, Klaus SJ, Kore M. Connective tissue growth factor-specific antibody attenuates tumor growth, metastasis, and angiogenesis in an orthotopic mouse model of pancreatic cancer. *Mol Cancer Ther*. 2006;5(5):1108-16.
55. Finger EC, Cheng CF, Williams TR, Rankin EB, Bedogni B, Tachiki L, et al. CTGF is a therapeutic target for metastatic melanoma. *Oncogene*. 2013.
56. Neesse A, Frese KK, Bapiro TE, Nakagawa T, Sternlicht MD, Seeley TW, et al. CTGF antagonism with mAb FG-3019 enhances chemotherapy response without increasing drug delivery in murine ductal pancreas cancer. *Proc Natl Acad Sci U S A*. 2013;110(30):12325-30.

57. Panek AN, Posch MG, Alenina N, Ghadge SK, Erdmann B, Popova E, et al. Connective tissue growth factor overexpression in cardiomyocytes promotes cardiac hypertrophy and protection against pressure overload. *PLoS One*. 2009;4(8):e6743.
58. Yoon PO, Lee MA, Cha H, Jeong MH, Kim J, Jang SP, et al. The opposing effects of CCN2 and CCN5 on the development of cardiac hypertrophy and fibrosis. *J Mol Cell Cardiol*. 2010;49(2):294-303.
59. Ahmed MS, Gravning J, Martinov VN, von Lueder TG, Edvardsen T, Czibik G, et al. Mechanisms of novel cardioprotective functions of CCN2/CTGF in myocardial ischemia-reperfusion injury. *Am J Physiol Heart Circ Physiol*. 2011;300(4):H1291-302.
60. Gravning J, Orn S, Kaasboll OJ, Martinov VN, Manhenke C, Dickstein K, et al. Myocardial connective tissue growth factor (CCN2/CTGF) attenuates left ventricular remodeling after myocardial infarction. *PLoS One*. 2012;7(12):e52120.
61. Leeuwis JW, Nguyen TQ, Theunissen MG, Peeters W, Goldschmeding R, Pasterkamp G, et al. Connective tissue growth factor is associated with a stable atherosclerotic plaque phenotype and is involved in plaque stabilization after stroke. *Stroke*. 2010;41(12):2979-81.
62. Schlessinger J. Ligand-induced, receptor-mediated dimerization and activation of EGF receptor. *Cell*. 2002;110(6):669-72.
63. Holbro T, Hynes NE. ErbB receptors: directing key signaling networks throughout life. *Annu Rev Pharmacol Toxicol*. 2004;44:195-217.
64. Miettinen PJ, Berger JE, Meneses J, Phung Y, Pedersen RA, Werb Z, et al. Epithelial immaturity and multiorgan failure in mice lacking epidermal growth factor receptor. *Nature*. 1995;376(6538):337-41.
65. Sibilina M, Wagner EF. Strain-dependent epithelial defects in mice lacking the EGF receptor. *Science*. 1995;269(5221):234-8.
66. Threadgill DW, Dlugosz AA, Hansen LA, Tennenbaum T, Lichti U, Yee D, et al. Targeted disruption of mouse EGF receptor: effect of genetic background on mutant phenotype. *Science*. 1995;269(5221):230-4.
67. Chen J, Chen JK, Harris RC. Deletion of the epidermal growth factor receptor in renal proximal tubule epithelial cells delays recovery from acute kidney injury. *Kidney Int*. 2012;82(1):45-52.
68. Kennedy WA, 2nd, Buttyan R, Garcia-Montes E, D'Agati V, Olsson CA, Sawczuk IS. Epidermal growth factor suppresses renal tubular apoptosis following ureteral obstruction. *Urology*. 1997;49(6):973-80.
69. Huovila AP, Turner AJ, Peltto-Huikko M, Karkkainen I, Ortiz RM. Shedding light on ADAM metalloproteinases. *Trends Biochem Sci*. 2005;30(7):413-22.
70. Bollee G, Flamant M, Schordan S, Fligny C, Rumpel E, Milon M, et al. Epidermal growth factor receptor promotes glomerular injury and renal failure in rapidly progressive crescentic glomerulonephritis. *Nat Med*. 2011;17(10):1242-50.
71. Laouari D, Burtin M, Phelep A, Martino C, Pillebout E, Montagutelli X, et al. TGF- $\alpha$  mediates genetic susceptibility to chronic kidney disease. *J Am Soc Nephrol*. 2011;22(2):327-35.
72. Lautrette A, Li S, Alili R, Sunnarborg SW, Burtin M, Lee DC, et al. Angiotensin II and EGF receptor cross-talk in chronic kidney diseases: a new therapeutic approach. *Nat Med*. 2005;11(8):867-74.
73. Shah BH, Catt KJ. TACE-dependent EGF receptor activation in angiotensin-II-induced kidney disease. *Trends Pharmacol Sci*. 2006;27(5):235-7.
74. Melenhorst WB, Mulder GM, Xi Q, Hoenderop JG, Kimura K, Eguchi S, et al. Epidermal growth factor receptor signaling in the kidney: key roles in physiology and disease. *Hypertension*. 2008;52(6):987-93.
75. Yoshioka K, Takemura T, Murakami K, Akano N, Matsubara K, Aya N, et al. Identification and localization of epidermal growth factor and its receptor in the human glomerulus. *Lab Invest*. 1990;63(2):189-96.
76. Tang J, Liu N, Zhuang S. Role of epidermal growth factor receptor in acute and chronic kidney injury. *Kidney Int*. 2013;83(5):804-10.
77. Jørgensen PE, Rasmussen TN, Skov Olsen P, Raaberg L, Seier Poulsen S, Nexø E. Renal uptake and excretion of epidermal growth factor from plasma in the rat. *Regul Pept*. 1990;28(3):273-81.
78. Kwon O, Ahn K, Zhang B, Lockwood T, Dhamija R, Anderson D, et al. Simultaneous monitoring of multiple urinary cytokines may predict renal and patient outcome in ischemic AKI. *Ren Fail*. 2010;32(6):699-708.
79. Ranieri E, Gesualdo L, Petrarulo F, Schena FP. Urinary IL-6/EGF ratio: a useful prognostic marker for the progression of renal damage in IgA nephropathy. *Kidney Int*. 1996;50(6):1990-2001.
80. Stangou M, Alexopoulos E, Papagianni A, Pantzaki A, Bantis C, Dovas S, et al. Urinary levels of epidermal growth factor, interleukin-6 and monocyte chemoattractant protein-1 may act as predictor markers of renal function outcome in immunoglobulin A nephropathy. *Nephrology (Carlton)*. 2009;14(6):613-20.
81. Grandaliano G, Gesualdo L, Bartoli F, Ranieri E, Monno R, Leggio A, et al. MCP-1 and EGF renal expression and urine excretion in human congenital obstructive nephropathy. *Kidney Int*. 2000;58(1):182-92.
82. Tsau Y, Chen C. Urinary epidermal growth factor excretion in children with chronic renal failure. *Am J Nephrol*. 1999;19(3):400-4.
83. Nakopoulou L, Stefanaki K, Boletis J, Papadakis J, Kostakis A, Vosnides G, et al. Immunohistochemical study of epidermal growth factor receptor (EGFR) in various types of renal injury. *Nephrol Dial Transplant*. 1994;9(7):764-9.
84. Sis B, Sarioglu S, Celik A, Zeybel M, Soylu A, Bora S. Epidermal growth factor receptor expression in human renal allograft biopsies: an immunohistochemical study. *Transpl Immunol*. 2004;13(3):229-32.
85. Advani A, Wiggins KJ, Cox AJ, Zhang Y, Gilbert RE, Kelly DJ. Inhibition of the epidermal growth factor receptor preserves podocytes and attenuates albuminuria in experimental diabetic nephropathy. *Nephrology (Carlton)*. 2011;16(6):573-81.
86. Benter IF, Canatan H, Benboubetra M, Yousif MH, Akhtar S. Global upregulation of gene expression associated with renal dysfunction in DOCA-salt-induced hypertensive rats occurs via signaling cascades involving epidermal growth factor receptor: a microarray analysis. *Vascul Pharmacol*. 2009;51(2-3):101-9.

87. Gilbert RE, Cox A, McNally PG, Wu LL, Dziadek M, Cooper ME, et al. Increased epidermal growth factor in experimental diabetes related kidney growth in rats. *Diabetologia*. 1997;40(7):778-85.
88. Guh JY, Lai YH, Shin SJ, Chuang LY, Tsai JH. Epidermal growth factor in renal hypertrophy in streptozotocin-diabetic rats. *Nephron*. 1991;59(4):641-7.
89. Torres VE, Sweeney WE, Jr., Wang X, Qian Q, Harris PC, Frost P, et al. EGF receptor tyrosine kinase inhibition attenuates the development of PKD in Han:SPRD rats. *Kidney Int*. 2003;64(5):1573-9.
90. Mishra R, Leahy P, Simonson MS. Gene expression profiling reveals role for EGF-family ligands in mesangial cell proliferation. *Am J Physiol Renal Physiol*. 2002;283(5):F1151-9.
91. Paizis K, Kirkland G, Khong T, Katerelos M, Fraser S, Kanellis J, et al. Heparin-binding epidermal growth factor-like growth factor is expressed in the adhesive lesions of experimental focal glomerular sclerosis. *Kidney Int*. 1999;55(6):2310-21.
92. Nemo R, Murcia N, Dell KM. Transforming growth factor alpha (TGF-alpha) and other targets of tumor necrosis factor-alpha converting enzyme (TACE) in murine polycystic kidney disease. *Pediatr Res*. 2005;57(5 Pt 1):732-7.
93. Waheed S, D'Angio CT, Wagner CL, Madtes DK, Finkelstein JN, Paxhia A, et al. Transforming growth factor alpha (TGF(alpha)) is increased during hyperoxia and fibrosis. *Exp Lung Res*. 2002;28(5):361-72.
94. Terzi F, Burtin M, Hekmati M, Federici P, Grimber G, Briand P, et al. Targeted expression of a dominant-negative EGF-R in the kidney reduces tubulo-interstitial lesions after renal injury. *J Clin Invest*. 2000;106(2):225-34.
95. Chen J, Chen JK, Nagai K, Plieth D, Tan M, Lee TC, et al. EGFR signaling promotes TGFbeta-dependent renal fibrosis. *J Am Soc Nephrol*. 2012;23(2):215-24.
96. Luetteke NC, Phillips HK, Qiu TH, Copeland NG, Earp HS, Jenkins NA, et al. The mouse waved-2 phenotype results from a point mutation in the EGF receptor tyrosine kinase. *Genes Dev*. 1994;8(4):399-413.
97. Richards WG, Sweeney WE, Yoder BK, Wilkinson JE, Woychik RP, Avner ED. Epidermal growth factor receptor activity mediates renal cyst formation in polycystic kidney disease. *J Clin Invest*. 1998;101(5):935-9.
98. Liu N, Guo JK, Pang M, Tolbert E, Ponnusamy M, Gong R, et al. Genetic or pharmacologic blockade of EGFR inhibits renal fibrosis. *J Am Soc Nephrol*. 2012;23(5):854-67.
99. Tang J, Liu N, Tolbert E, Ponnusamy M, Ma L, Gong R, et al. Sustained activation of EGFR triggers renal fibrogenesis after acute kidney injury. *Am J Pathol*. 2013;183(1):160-72.
100. Roengvoraphoj M, Tsongalis GJ, Dragnev KH, Rigas JR. Epidermal growth factor receptor tyrosine kinase inhibitors as initial therapy for non-small cell lung cancer: focus on epidermal growth factor receptor mutation testing and mutation-positive patients. *Cancer Treat Rev*. 2013;39(8):839-50.
101. Hoekstra R, Dumez H, Eskens FA, van der Gaast A, Planting AS, de Heus G, et al. Phase I and pharmacologic study of PKI166, an epidermal growth factor receptor tyrosine kinase inhibitor, in patients with advanced solid malignancies. *Clin Cancer Res*. 2005;11(19 Pt 1):6908-15.
102. Francois H, Placier S, Flamant M, Tharaux PL, Chansel D, Dussaule JC, et al. Prevention of renal vascular and glomerular fibrosis by epidermal growth factor receptor inhibition. *Faseb J*. 2004;18(7):926-8.
103. Wassef L, Kelly DJ, Gilbert RE. Epidermal growth factor receptor inhibition attenuates early kidney enlargement in experimental diabetes. *Kidney Int*. 2004;66(5):1805-14.
104. Bou Matar RN, Klein JD, Sands JM. Erlotinib preserves renal function and prevents salt retention in doxorubicin treated nephrotic rats. *PLoS One*. 2013;8(1):e54738.
105. He S, Liu N, Bayliss G, Zhuang S. EGFR activity is required for renal tubular cell dedifferentiation and proliferation in a murine model of folic acid-induced acute kidney injury. *Am J Physiol Renal Physiol*. 2013;304(4):F356-66.
106. Wang Z, Chen JK, Wang SW, Moeckel G, Harris RC. Importance of functional EGF receptors in recovery from acute nephrotoxic injury. *J Am Soc Nephrol*. 2003;14(12):3147-54.
107. Mulder GM, Nijboer WN, Seelen MA, Sandovici M, Bos EM, Melenhorst WB, et al. Heparin binding epidermal growth factor in renal ischaemia/reperfusion injury. *J Pathol*. 2010;221(2):183-92.
108. Samarakoon R, Dobberfuhr AD, Cooley C, Overstreet JM, Patel S, Goldschmeding R, et al. Induction of renal fibrotic genes by TGF-beta1 requires EGFR activation, p53 and reactive oxygen species. *Cell Signal*. 2013;25(11):2198-209.
109. Masutani K, Fujisaki K, Maeda H, Toyonaga J, Inoshima I, Takayama K, et al. Tubulointerstitial nephritis and IgA nephropathy in a patient with advanced lung cancer treated with long-term gefitinib. *Clin Exp Nephrol*. 2008;12(5):398-402.
110. Banappagari S, Corti M, Pincus S, Satyanarayanajois S. Inhibition of protein-protein interaction of HER2-EGFR and HER2-HER3 by a rationally designed peptidomimetic. *J Biomol Struct Dyn*. 2012;30(5):594-606.
111. Vlacich G, Coffey RJ. Resistance to EGFR-targeted therapy: a family affair. *Cancer Cell*. 2011;20(4):423-5.
112. Alpers CE, Seifert RA, Hudkins KL, Johnson RJ, Bowen-Pope DF. Developmental patterns of PDGF B-chain, PDGF-receptor, and alpha-actin expression in human glomerulogenesis. *Kidney Int*. 1992;42(2):390-9.
113. Boor P, Ostendorf T, Floege J. PDGF and the progression of renal disease. *Nephrol Dial Transplant*. 2014;29 Suppl 1:i45-i54.
114. Fredriksson L, Li H, Eriksson U. The PDGF family: four gene products form five dimeric isoforms. *Cytokine Growth Factor Rev*. 2004;15(4):197-204.
115. Ross R, Glomset J, Kariya B, Harker L. A platelet-dependent serum factor that stimulates the proliferation of arterial smooth muscle cells in vitro. *Proc Natl Acad Sci U S A*. 1974;71(4):1207-10.
116. Alpers CE, Seifert RA, Hudkins KL, Johnson RJ, Bowen-Pope DF. PDGF-receptor localizes to mesangial, parietal epithelial, and interstitial cells in human and primate kidneys. *Kidney Int*. 1993;43(2):286-94.
117. Floege J, Eitner F, Alpers CE. A new look at platelet-derived growth factor in renal disease. *J Am Soc*

Nephrol. 2008;19(1):12-23.

118. Alpers CE, Hudkins KL, Ferguson M, Johnson RJ, Rutledge JC. Platelet-derived growth factor A-chain expression in developing and mature human kidneys and in Wilms' tumor. *Kidney Int.* 1995;48(1):146-54.
119. Bostrom H, Willetts K, Pekny M, Leveen P, Lindahl P, Hedstrand H, et al. PDGF-A signaling is a critical event in lung alveolar myofibroblast development and angiogenesis. *Cell.* 1996;85(6):863-73.
120. Leveen P, Pekny M, Gebre-Medhin S, Swolin B, Larsson E, Betsholtz C. Mice deficient for PDGF B show renal, cardiovascular, and hematological abnormalities. *Genes Dev.* 1994;8(16):1875-87.
121. Lindahl P, Johansson BR, Leveen P, Betsholtz C. Pericyte loss and microaneurysm formation in PDGF-B-deficient mice. *Science.* 1997;277(5323):242-5.
122. Chen YT, Chang FC, Wu CF, Chou YH, Hsu HL, Chiang WC, et al. Platelet-derived growth factor receptor signaling activates pericyte-myofibroblast transition in obstructive and post-ischemic kidney fibrosis. *Kidney Int.* 2011;80(11):1170-81.
123. Chen PH, Chen X, He X. Platelet-derived growth factors and their receptors: structural and functional perspectives. *Biochim Biophys Acta.* 2013;1834(10):2176-86.
124. Reigstad LJ, Varhaug JE, Lillehaug JR. Structural and functional specificities of PDGF-C and PDGF-D, the novel members of the platelet-derived growth factors family. *FEBS J.* 2005;272(22):5723-41.
125. Wang SN, Hirschberg R. Growth factor ultrafiltration in experimental diabetic nephropathy contributes to interstitial fibrosis. *Am J Physiol Renal Physiol.* 2000;278(4):F554-60.
126. Liu Y. Hepatocyte growth factor in kidney fibrosis: therapeutic potential and mechanisms of action. *Am J Physiol Renal Physiol.* 2004;287(1):F7-16.
127. Floege J, van Roeyen C, Boor P, Ostendorf T. The role of PDGF-D in mesangioproliferative glomerulonephritis. *Contrib Nephrol.* 2007;157:153-8.
128. Hudkins KL, Gilbertson DG, Carling M, Tameda S, Hughes SD, Holdren MS, et al. Exogenous PDGF-D is a potent mesangial cell mitogen and causes a severe mesangial proliferative glomerulopathy. *J Am Soc Nephrol.* 2004;15(2):286-98.
129. Iida H, Seifert R, Alpers CE, Gronwald RG, Phillips PE, Pritzl P, et al. Platelet-derived growth factor (PDGF) and PDGF receptor are induced in mesangial proliferative nephritis in the rat. *Proc Natl Acad Sci U S A.* 1991;88(15):6560-4.
130. van Roeyen CR, Eitner F, Boor P, Moeller MJ, Raffetseder U, Hanssen L, et al. Induction of progressive glomerulonephritis by podocyte-specific overexpression of platelet-derived growth factor-D. *Kidney Int.* 2011;80(12):1292-305.
131. Gesualdo L, Di Paolo S, Milani S, Pinzani M, Grappone C, Ranieri E, et al. Expression of platelet-derived growth factor receptors in normal and diseased human kidney. An immunohistochemistry and in situ hybridization study. *J Clin Invest.* 1994;94(1):50-8.
132. Matsuda M, Shikata K, Makino H, Sugimoto H, Ota K, Akiyama K, et al. Gene expression of PDGF and PDGF receptor in various forms of glomerulonephritis. *Am J Nephrol.* 1997;17(1):25-31.
133. Waldherr R, Noronha IL, Niemir Z, Kruger C, Stein H, Stumm G. Expression of cytokines and growth factors in human glomerulonephritides. *Pediatr Nephrol.* 1993;7(4):471-8.
134. Eitner F, Ostendorf T, Kretzler M, Cohen CD, Eriksson U, Grone HJ, et al. PDGF-C expression in the developing and normal adult human kidney and in glomerular diseases. *J Am Soc Nephrol.* 2003;14(5):1145-53.
135. Liu G, Changsirikulchai S, Hudkins KL, Banas MC, Kowalewska J, Yang X, et al. Identification of platelet-derived growth factor D in human chronic allograft nephropathy. *Hum Pathol.* 2008;39(3):393-402.
136. Tameda S, Hudkins KL, Topouzis S, Gilbertson DG, Ophascharoensuk V, Truong L, et al. Obstructive uropathy in mice and humans: potential role for PDGF-D in the progression of tubulointerstitial injury. *J Am Soc Nephrol.* 2003;14(10):2544-55.
137. Boor P, Eitner F, Cohen CD, Lindenmeyer MT, Consortium E, Mertens PR, et al. Patients with IgA nephropathy exhibit high systemic PDGF-DD levels. *Nephrol Dial Transplant.* 2009;24(9):2755-62.
138. Har R, Scholey JW, Daneman D, Mahmud FH, Dekker R, Lai V, et al. The effect of renal hyperfiltration on urinary inflammatory cytokines/chemokines in patients with uncomplicated type 1 diabetes mellitus. *Diabetologia.* 2013;56(5):1166-73.
139. Nakamura H, Isaka Y, Tsujie M, Akagi Y, Sudo T, Ohno N, et al. Electroporation-mediated PDGF receptor-IgG chimera gene transfer ameliorates experimental glomerulonephritis. *Kidney Int.* 2001;59(6):2134-45.
140. Ostendorf T, van Roeyen CR, Peterson JD, Kunter U, Eitner F, Hamad AJ, et al. A fully human monoclonal antibody (CR002) identifies PDGF-D as a novel mediator of mesangioproliferative glomerulonephritis. *J Am Soc Nephrol.* 2003;14(9):2237-47.
141. Boor P, Konieczny A, Villa L, Kunter U, van Roeyen CR, LaRochelle WJ, et al. PDGF-D inhibition by CR002 ameliorates tubulointerstitial fibrosis following experimental glomerulonephritis. *Nephrol Dial Transplant.* 2007;22(5):1323-31.
142. Ostendorf T, Kunter U, Grone HJ, Bahlmann F, Kawachi H, Shimizu F, et al. Specific antagonism of PDGF prevents renal scarring in experimental glomerulonephritis. *J Am Soc Nephrol.* 2001;12(5):909-18.
143. Ostendorf T, Rong S, Boor P, Wiedemann S, Kunter U, Haubold U, et al. Antagonism of PDGF-D by human antibody CR002 prevents renal scarring in experimental glomerulonephritis. *J Am Soc Nephrol.* 2006;17(4):1054-62.
144. Suzuki H, Usui I, Kato I, Oya T, Kanatani Y, Yamazaki Y, et al. Deletion of platelet-derived growth factor receptor-beta improves diabetic nephropathy in Ca(2+)-calmodulin-dependent protein kinase IIalpha (Thr286Asp) transgenic mice. *Diabetologia.* 2011;54(11):2953-62.
145. Ludewig D, Kosmehl H, Sommer M, Bohmer FD, Stein G. PDGF receptor kinase blocker AG1295 attenuates interstitial fibrosis in rat kidney after unilateral obstruction. *Cell Tissue Res.* 2000;299(1):97-103.
146. Boor P, van Roeyen CR, Kunter U, Villa L, Bucher E, Hohenstein B, et al. PDGF-C mediates glomerular

capillary repair. *Am J Pathol.* 2010;177(1):58-69.

147. Eitner F, Bucher E, van Roeyen C, Kunter U, Rong S, Seikrit C, et al. PDGF-C is a proinflammatory cytokine that mediates renal interstitial fibrosis. *J Am Soc Nephrol.* 2008;19(2):281-9.
148. Martin IV, Borkham-Kamphorst E, Zok S, van Roeyen CR, Eriksson U, Boor P, et al. Platelet-derived growth factor (PDGF)-C neutralization reveals differential roles of PDGF receptors in liver and kidney fibrosis. *Am J Pathol.* 2013;182(1):107-17.
149. Iyoda M, Shibata T, Kawaguchi M, Yamaoka T, Akizawa T. Preventive and therapeutic effects of imatinib in Wistar-Kyoto rats with anti-glomerular basement membrane glomerulonephritis. *Kidney Int.* 2009;75(10):1060-70.
150. Iyoda M, Shibata T, Wada Y, Kuno Y, Shindo-Hirai Y, Matsumoto K, et al. Long- and short-term treatment with imatinib attenuates the development of chronic kidney disease in experimental anti-glomerular basement membrane nephritis. *Nephrol Dial Transplant.* 2013;28(3):576-84.
151. Iyoda M, Hudkins KL, Becker-Herman S, Wietecha TA, Banas MC, Guo S, et al. Imatinib suppresses cryoglobulinemia and secondary membranoproliferative glomerulonephritis. *J Am Soc Nephrol.* 2009;20(1):68-77.
152. Lassila M, Jandeleit-Dahm K, Seah KK, Smith CM, Calkin AC, Allen TJ, et al. Imatinib attenuates diabetic nephropathy in apolipoprotein E-knockout mice. *J Am Soc Nephrol.* 2005;16(2):363-73.
153. Sadanaga A, Nakashima H, Masutani K, Miyake K, Shimizu S, Igawa T, et al. Amelioration of autoimmune nephritis by imatinib in MRL/lpr mice. *Arthritis Rheum.* 2005;52(12):3987-96.
154. Zoja C, Corna D, Rottoli D, Zanchi C, Abbate M, Remuzzi G. Imatinib ameliorates renal disease and survival in murine lupus autoimmune disease. *Kidney Int.* 2006;70(1):97-103.
155. Graciano ML, Mitchell KD. Imatinib ameliorates renal morphological changes in Cyp11a1-Ren2 transgenic rats with inducible ANG II-dependent malignant hypertension. *Am J Physiol Renal Physiol.* 2012;302(1):F60-9.
156. Schellings MW, Baumann M, van Leeuwen RE, Duisters RF, Janssen SH, Schroen B, et al. Imatinib attenuates end-organ damage in hypertensive homozygous TGR(mRen2)27 rats. *Hypertension.* 2006;47(3):467-74.
157. Savikko J, Taskinen E, Von Willebrand E. Chronic allograft nephropathy is prevented by inhibition of platelet-derived growth factor receptor: tyrosine kinase inhibitors as a potential therapy. *Transplantation.* 2003;75(8):1147-53.
158. Wang S, Wilkes MC, Leof EB, Hirschberg R. Imatinib mesylate blocks a non-Smad TGF-beta pathway and reduces renal fibrogenesis in vivo. *FASEB J.* 2005;19(1):1-11.
159. Avlan D, Tamer L, Ayaz L, Polat A, Ozturk C, Ozturhan H, et al. Effects of trapidil on renal ischemia-reperfusion injury. *J Pediatr Surg.* 2006;41(10):1686-93.
160. Buyukafsar K, Yazar A, Dusmez D, Ozturk H, Polat G, Levent A. Effect of trapidil, an antiplatelet and vasodilator agent on gentamicin-induced nephrotoxicity in rats. *Pharmacol Res.* 2001;44(4):321-8.
161. Futamura A, Izumino K, Nakagawa Y, Takata M, Inoue H, Iida H. Effect of the platelet-derived growth factor antagonist trapidil on mesangial cell proliferation in rats. *Nephron.* 1999;81(4):428-33.
162. Razaque MS, Cheng M, Taguchi T. Suppression of mesangial-cell proliferation by trapidil in glomerulonephritis induced by anti-thymocyte serum in rats. *J Int Med Res.* 1995;23(6):458-66.
163. Shinkai Y, Cameron JS. Trial of platelet-derived growth factor antagonist, trapidil, in accelerated nephrotic nephritis in the rabbit. *Br J Exp Pathol.* 1987;68(6):847-52.
164. Nakagawa T, Sasahara M, Haneda M, Kataoka H, Nakagawa H, Yagi M, et al. Role of PDGF B-chain and PDGF receptors in rat tubular regeneration after acute injury. *Am J Pathol.* 1999;155(5):1689-99.
165. Chen J, Chen JK, Neilson EG, Harris RC. Role of EGF receptor activation in angiotensin II-induced renal epithelial cell hypertrophy. *J Am Soc Nephrol.* 2006;17(6):1615-23.
166. Urtasun R, Latasa MU, Demartis MI, Balzani S, Goni S, Garcia-Irigoyen O, et al. Connective tissue growth factor autocrine in human hepatocellular carcinoma: oncogenic role and regulation by epidermal growth factor receptor/yes-associated protein-mediated activation. *Hepatology.* 2011;54(6):2149-58.
167. Andrianifahanana M, Wilkes MC, Gupta SK, Rahimi RA, Repellin CE, Edens M, et al. Profibrotic TGFbeta responses require the cooperative action of PDGF and ErbB receptor tyrosine kinases. *FASEB J.* 2013;27(11):4444-54.
168. Nguyen TQ, Goldschmeding R. Bone morphogenetic protein-7 and connective tissue growth factor: novel targets for treatment of renal fibrosis? *Pharm Res.* 2008;25(10):2416-26.
169. Sweeney WE, Chen Y, Nakanishi K, Frost P, Avner ED. Treatment of polycystic kidney disease with a novel tyrosine kinase inhibitor. *Kidney Int.* 2000;57(1):33-40.
170. Hirai T, Masaki T, Kuratsune M, Yorioka N, Kohno N. PDGF receptor tyrosine kinase inhibitor suppresses mesangial cell proliferation involving STAT3 activation. *Clin Exp Immunol.* 2006;144(2):353-61.
171. Wang-Rosenke Y, Khadzhyrov D, Loof T, Mika A, Kawachi H, Neumayer HH, et al. Tyrosine kinases inhibition by Imatinib slows progression in chronic anti-thy1 glomerulosclerosis of the rat. *BMC Nephrol.* 2013;14:223.
172. Johnson RJ, Raines EW, Floege J, Yoshimura A, Pritzl P, Alpers C, et al. Inhibition of mesangial cell proliferation and matrix expansion in glomerulonephritis in the rat by antibody to platelet-derived growth factor. *J Exp Med.* 1992;175(5):1413-6.
173. Takahashi T, Abe H, Arai H, Matsubara T, Nagai K, Matsuura M, et al. Activation of STAT3/Smad1 is a key signaling pathway for progression to glomerulosclerosis in experimental glomerulonephritis. *J Biol Chem.* 2005;280(8):7100-6.
174. Floege J, Ostendorf T, Janssen U, Burg M, Radeke HH, Vargese C, et al. Novel approach to specific growth factor inhibition in vivo: antagonism of platelet-derived growth factor in glomerulonephritis by aptamers. *Am J Pathol.* 1999;154(1):169-79.
175. Kishioka H, Fukuda N, Wen-Yang H, Nakayama M, Watanabe Y, Kanmatsuse K. Effects of PDGF A-chain antisense oligodeoxynucleotides on growth of cardiovascular organs in stroke-prone spontaneously



- hypertensive rats. *Am J Hypertens*. 2001;14(5 Pt 1):439-45.
176. Quan T, Shao Y, He T, Voorhees JJ, Fisher GJ. Reduced expression of connective tissue growth factor (CTGF/CCN2) mediates collagen loss in chronologically aged human skin. *J Invest Dermatol*. 2010;130(2):415-24.
177. Gravning J, Ahmed MS, von Lueder TG, Edvardsen T, Attramadal H. CCN2/CTGF attenuates myocardial hypertrophy and cardiac dysfunction upon chronic pressure-overload. *Int J Cardiol*. 2013;168(3):2049-56.
178. Pastore S, Lulli D, Girolomoni G. Epidermal growth factor receptor signalling in keratinocyte biology: implications for skin toxicity of tyrosine kinase inhibitors. *Arch Toxicol*. 2014;88(6):1189-203.
179. Fallahi P, Ferrari SM, Vita R, Di Domenicantonio A, Corrado A, Benvenega S, et al. Thyroid dysfunctions induced by tyrosine kinase inhibitors. *Expert Opin Drug Saf*. 2014;13(6):723-33.
180. Hartmann JT, Haap M, Kopp HG, Lipp HP. Tyrosine kinase inhibitors - a review on pharmacology, metabolism and side effects. *Curr Drug Metab*. 2009;10(5):470-81.
181. Korashy HM, Rahman AF, Kassem MG. Dasatinib. *Profiles Drug Subst Excip Relat Methodol*. 2014;39:205-37.

9

## **Chapter 9:** **Hemizygous deletion of CTGF/CCN2 does not suffice to prevent fibrosis of the severely injured kidney**

Lucas L. Falke\*<sup>1</sup>, Amélie Dendooven\*<sup>1</sup>, Jan Willem Leeuwis<sup>1</sup>, Tri Q. Nguyen<sup>1</sup>  
Rob J. van Geest<sup>2</sup>, Dionne M. van der Giezen<sup>1</sup>, Roel Broekhuizen<sup>1</sup>, Karen Lyons<sup>3</sup>  
Reinout Stoop<sup>4</sup>, Hans Kemperman<sup>5</sup>, Reinier Schlingemann<sup>2</sup>  
Jaap A. Joles<sup>6</sup>, Roel Goldschmeding<sup>1</sup>

1. Dept. of Pathology, University Medical Center Utrecht, The Netherlands
2. Dept. of Ophthalmology, Academic Medical Center Amsterdam, The Netherlands
3. Dept. of Molecular and Cell Biology, University of California Los Angeles, USA
4. Dept. of Metabolic Health Research, TNO, Leiden, The Netherlands
5. Dept. of Clinical Chemistry and Haematology, University Medical Center Utrecht, The Netherlands
6. Dept. of Nephrology and Hypertension, University Medical Center Utrecht, The Netherlands

\* Contributed equally

**Abstract**

**Background:** Connective Tissue Growth Factor (CTGF/CCN2) is an important mediator of kidney fibrosis. Previous observations indicated that attenuation of CTGF expression sufficed to alleviate early kidney damage. However, little is known about the role of CTGF in fibrosis of severely damaged and more chronically injured kidneys. Therefore, we examined the effects of CTGF haploinsufficiency on the progression of renal scarring in long-term STZ-induced diabetic nephropathy, in a more advanced stage of obstructive nephropathy following unilateral ureteric obstruction (UUO), and in severe aristolochic acid (AA)-induced tubulotoxic nephritis.

**Methods:** Wild-type (WT, CTGF<sup>+/+</sup>) and hemizygous CTGF<sup>+/-</sup> C57Bl/6 mice were studied. In the diabetes experiment, streptozotocin-injected and control mice were followed for 6 months, with regular blood pressure, glycaemia and albuminuria recordings. In the UUO experiment, the left ureter was obstructed for 14 days with the contralateral kidney serving as control. For the AA experiment, mice were followed for 25 days after 5 intraperitoneal injections with AA and compared to control mice injected with buffer alone. Organs were harvested for histology, mRNA and protein measurements. Collagen content was determined by HPLC and expressed as hydroxyproline/proline ratio.

**Results:** CTGF expression was significantly increased in the damaged as compared to control kidneys. In all three models, CTGF levels in the damaged kidneys of CTGF<sup>+/-</sup> mice averaged about 50% of those in damaged WT kidneys. After 6 months of diabetes, albuminuria was increased 2.5-fold in WT mice, compared to 1.5-fold in CTGF<sup>+/-</sup> mice, mesangial matrix was expanded 5-fold in WT and 4.4-fold in CTGF<sup>+/-</sup> mice and the glomerular basement membrane was thickened 1.3-fold in WT and 1.5-fold in CTGF<sup>+/-</sup> mice (all differences between WT and CTGF<sup>+/-</sup> mice are NS). Tubular damage and interstitial fibrosis scores were also not different between Wt and CTGF<sup>+/-</sup> mice in the diabetes (1.8 vs. 1.7), UUO (2.8 vs. 2.6), and AA (1.4 vs. 1.2) models, as was the case for macrophage influx and collagen content in these three models.

**Conclusion:** Unlike in mild and relatively early STZ-induced diabetic nephropathy, scarring of severely and chronically damaged kidneys is not attenuated by a 50% reduction of CTGF to (near) normal levels. This suggests that CTGF is either redundant in severe and chronic kidney disease, or that it is a limiting factor only at subnormal concentrations requiring further reduction by available or emerging therapies to prevent fibrosis of the severely injured kidney.

**Key points**

- Loss of one CTGF allele reduces CTGF level by 50% in healthy and diseased mice.
- 50% reduction of CTGF does not reduce fibrosis in 3 models of severe renal injury.
- CTGF appears not to be limiting at 50% reduced levels in severe kidney disease.
- A 50% reduction of CTGF attenuates mild, but not severe models of kidney injury.

## Introduction

Over the recent years, Connective Tissue Growth Factor, recently renamed Cyr61/CTGF/Nov family protein number 2 (CTGF/CCN2) (1), has emerged as a critical profibrotic factor in the pathogenesis of various diseases such as cardiomyopathy, fibrotic skin disorders, systemic sclerosis, biliary atresia, liver fibrosis, sarcoidosis and idiopathic pulmonary fibrosis (for an extensive review see (2)). CTGF is upregulated by various stimuli including TGF- $\beta$ 1 and influences downstream Smad, PKC, Akt/ERK and other signaling pathways (3-6).

Although CTGF is also expressed in podocytes, parietal epithelial cells and occasional interstitial fibroblasts in the healthy kidney, its expression is greatly increased in renal diseases, including diabetic nephropathy (7, 8). Studying (semi-)quantitative aspects of the contribution of CTGF increase to renal fibrosis is particularly relevant also with respect to possible future application of anti-CTGF therapies, including inhibitory oligonucleotides and a recently developed monoclonal human anti-CTGF antibody (FG-3019) that proved to be safe and effective in the treatment of microalbuminuric renal disease of patients with diabetes (9).

Previously, we demonstrated the beneficial effects of genetic CTGF lowering by 50% in a 16-week STZ model of diabetic nephropathy (10). In that study, early and mild diabetes-induced albuminuria, glomerular basement membrane thickening, and mesangial matrix increase were all attenuated in CTGF $^{+/-}$  mice expressing approximately 50% of CTGF levels as compared to wild-type mice. However, this particular model lacked interstitial fibrosis, which in human patients is known to correlate better with progressive renal function decline than glomerular parameters (11-13). Beneficial effects of reduced CTGF expression on renal damage have also been reported when using antisense oligonucleotides to neutralize or inhibit CTGF expression in models of diabetes and unilateral ureter obstruction (UUO). However, also in those studies, only relatively mild and early changes were addressed, lacking tubulointerstitial fibrosis in the diabetes model and evaluating obstructed kidneys “already” at day 7 post UUO (14, 15).

We hypothesized that phenotypes of WT and CTGF $^{+/-}$  mice might diverge more profoundly with increased severity and duration of kidney injury. To investigate this hypothesis, we chose three essentially unrelated models. We applied a long-term (26-week) STZ-induced model of type 1 diabetes to study a more advanced stage of STZ-induced diabetic nephropathy, including presence of tubulointerstitial fibrosis, which is one of the key criteria for the ‘ideal’ diabetic mouse model that the Animal Models of Diabetic Complications Consortium (AMDCC) recently proposed (16, 17). A 14-day UUO model was used representing a later stage of interstitial fibrosis and tubular atrophy (18), and in a 25-day AA nephropathy model we studied the sequelae of severe acute toxic tubular damage (19, 20).

## Materials and methods

### *Animal experiments*

Generation of CTGF heterozygous knockout mice has been described elsewhere (21). CTGF<sup>+/-</sup> mice, in which exon 1 of one CTGF allele has been replaced by a neomycin resistance gene, were crossed back on a C57BL/6 background (Harlan, Horst, The Netherlands). Mice of the 8th generation or later were used for the present study, and compared with WT littermates. Genotyping was performed on 100 ng DNA isolated from earmarks following a standard procedure using the following primers: 5'-TGT GTA GGACTTCATTCAGTTCT3-', 5'-GTCTGTGATCGCAGCTCACTC-3' and 5'-ATGGCCGCTTTTCTGGATTC-3', resulting in a 400 bp product for the wild-type, and a 560 bp product for the CTGF-neomycin construct. All mice were housed in a temperature- and humidity-controlled room with a 12-hour light/dark cycle.

Diabetes was induced in CTGF<sup>+/-</sup> mice (n = 22) and wild-type mice (n = 28) by a single intraperitoneal injection of 200 mg/kg streptozotocin (STZ), concentration 30 mg/ml, dissolved in 100 mM sodium citrate buffer, pH 4.5) (Sigma-Aldrich, St. Louis, MO, USA). Control animals were injected with buffer alone (CTGF<sup>+/-</sup> n = 17, wild-type n = 17). Hyperglycemia was determined 3 days after injection by measurement of blood glucose levels (Medisense Precision Xtra; Abbott, Bedford, IN). Non-responders were injected with a second dose of STZ. Animals were kept on standard laboratory chow with daily addition of mash food. Slow release insulin pellets (Linshin, Scarborough, Canada) were implanted to stabilize the condition of the STZ-induced diabetic animals 5 days after STZ injection. Mice were monitored daily for weight loss and clinical condition. Blood was withdrawn by cheek puncture for glucose measurement at 1, 3, and 6 months, and on indication whenever there was significant weight loss (> 1 g). Blood glucose levels of more than 25 mmol/l warranted reimplantation of a slow release insulin pellet. Mice typically needed a new insulin pellet after 4–6 weeks of diabetes. Blood pressure was determined by the non-invasive tail cuff method using pulse detection with photoelectric sensors (IITC Life Sciences, Woodlands Hills, USA). Mice were killed 26 weeks after induction of diabetes by KXA injection. HbA1C was measured on the automated HA8140 HPLC analyzers (Menarini Diagnostics, Florence, Italy).

For the UUO experiment, male CTGF<sup>+/-</sup> (n = 7) and WT mice (n = 7) were anaesthetized by inhalation of isoflurane/oxygen. Under aseptic conditions, a small incision was made in the flank, the left ureter was permanently ligated at two points, and the wound was stitched. Mice were killed 14 days after surgery by KXA injection. Contralateral non-obstructed kidneys were used as internal control.

For the AA experiment, male CTGF<sup>+/-</sup> mice (n = 6) and WT mice (n = 6) were injected intraperitoneally with aristolochic acid I sodium salt (5 mg/kg body weight dissolved in distilled water) (A9451, Sigma-Aldrich Company Ltd., Gillingham, UK) once a day for 5 consecutive days. Control mice were injected with buffer alone (n = 4). Mice were killed 25 days after the initial injection by KXA injection. Urine collection was performed by means of metabolic cages. Albumin levels were determined by sandwich ELISA using a goat-anti-mouse albumin antibody (Bethyl Laboratories, Inc., Montgomery, TX, USA). Urinary creatinine excretion was determined by enzymatic assays (J2L Elitech, Labarthe Inard, France). The experiments were performed with the approval of the Experimental Animal Ethics Committee of the University of Utrecht. All animals were used for analysis unless stated otherwise.

### *Histology*

Renal tissue was paraffin-embedded and cut into 3 µm sections. Periodic acid Schiff (PAS) staining was performed to assess morphology. Two skilled observers blinded to the identity of the slides scored mesangial matrix index (MMI) (only in the STZ experiment) and tubular atrophy (TA). For mesangial matrix index, 30 random glomeruli were scored per mouse on a 200 × magnification using the following semiquantitative scale: 0 = 0%MMI, 1 = 0-25%, 2 = 25-50%, 3 = 50-75% and 4 = 75-100%. Tubular atrophy (TA) was scored in 10 randomly selected cortical areas on × 100 magnification. The following semiquantitative scale was used: 0: no TA; 1: 0–5% TA (0-5% of tubuli in the field shows atrophy); 2: 5–10% TA; 3: 25–50% TA; 4: 50–75% TA; 5: 75–100% TA. The mean of the ten fields scored was used for further

statistical analysis. Photographs were taken on a Nikon Eclipse E800 microscope with a Nikon DXM1200 digital camera using the Nikon ACT-1 software version 2.70 (Nikon Netherlands, Lijnden, Netherlands).

#### *Electron microscopy*

Tissue samples were fixed in Karnovsky solution. Upon embedding, samples were rinsed with 0.1 M Na-cacodylate buffer, followed by fixation with 1% osmiumtetroxide, and dehydrated with acetone and embedded in Epon. Ultrathin sections of 95 nm were cut and mounted on copper one-hole specimen support grids. Sections were stained with uranyl acetate and lead citrate to provide contrast. Ultrathin sections were photographed using a transmission electron microscope (JEM-1200 EX; JEOL, Peabody, MA). GBM thickness was measured in five random glomeruli per mouse at 10 perpendicular cross-sections of GBM per glomerulus at a magnification of 5000 and analyzed by computer image analysis (ImageJ; National Institutes of Health, [www.rsb.info.nih.gov/ij/](http://www.rsb.info.nih.gov/ij/)). GBM thickness was defined as the distance between the inner and the outer lamina rara.

#### *Immunohistochemistry*

Immunohistochemistry was performed on 3  $\mu$ m formalin-fixed and paraffin embedded (FFPE) kidney slides injected with endogenous peroxidase block and heat-based antigen retrieval in citrate buffer (pH 6). For  $\alpha$ -smooth muscle actin ( $\alpha$ SMA) immunostaining, sections were incubated with 1/200 rabbit polyclonal anti- $\alpha$ SMA antibody (ab5694, Abcam, Cambridge, UK), followed by incubation with goat-anti-rabbit BrightVision-PO (Klinipath, Duiven, The Netherlands). Bound antibody was visualized with NovaRed (Vector Laboratories, Burlingame, CA, USA). In the diabetes experiment, per animal, ten 200  $\times$  high power fields were scored as 0 (no/minor interstitial staining) or 1 (moderate/heavy interstitial staining). The average score per animal was used for statistical analysis. In the UUO and AA experiments, amount of  $\alpha$ SMA positivity was scored on a scale of 1 to 10 on ten 200  $\times$  high power fields. Scoring was performed by two independent observers. For CTGF immunohistology, after heat-based antigen retrieval in citrate buffer (pH 6), sections were incubated with a 1/800 dilution of goat polyclonal anti-CTGF antibody (sc-14939, Santa Cruz Biotechnology, Heidelberg, Germany) for 60 min, followed by rabbit anti-goat IgG (Dako, Glostrup, Denmark) and goat-anti-rabbit Powervision-HRP (Klinipath). Infiltration of macrophages was determined in frozen kidney sections, which were fixed with acetone, blocked, and incubated with a rat antibody against the mouse macrophage antigen F4/80 (Serotec Benelux, Oxford, UK). Sections were then incubated with horseradish peroxidase (HRP)-conjugated rabbit anti-rat (Dako, Glostrup, Denmark) and goat anti-rabbit Powervision-HRP (Klinipath, Duiven, The Netherlands), developed with Nova Red (Vector Laboratories, Burlingame, CA, USA) and counterstained with hematoxylin. The number of F4/80 positive cells per high power field (field area 0.245 mm<sup>2</sup>) was counted in a blinded fashion in the STZ experiment. Only cells positive for F4/80 in both the nucleus and the cytoplasm were counted as truly positive cells. In the UUO and AA experiments, staining intensity was digitally measured (% positive area), for the large number of macrophages in obstructed kidneys precluded accurate counting.

#### *Quantitative PCR*

Total RNA was extracted from 30 mg frozen renal cortex using RNeasy columns (Qiagen, Venlo, The Netherlands). After cDNA synthesis, expression of CTGF was assessed by quantitative real-time PCR using TaqMan Gene Expression Assays with commercially pre-designed probe and primers (Applied Biosystems, Foster City, CA, USA) (Product nr; Mm00515790\_g1). Tata-box binding protein (TBP) (Product nr; Mm00446973\_g1) was used as internal reference gene.

#### *Western blot analysis*

Sections of renal cortex were homogenized in lysis buffer (20 mM Tris at pH 7.4, 150 mM NaCl, 1% Triton X-100, 0.1% SDS, 10% glycerol, 1 mM EDTA, 1 mM EGTA, 0.5% sodium deoxycholate, 50 mM NaF, 2 mM Na<sub>3</sub>VO<sub>4</sub>) containing 5% Protease Inhibitor Cocktail (Sigma, St Louis, MO, USA). Protein quantity was determined by BCA protein assay kit (Pierce, Rockford, IL, USA). Samples were run on

10% sodium dodecyl sulfate polyacrylamide gels (SDS-PAGE) and transferred onto PVDF membranes. Following blocking, membranes were incubated with polyclonal antibody (1:200) specifically directed against CTGF (sc-14939, Santa Cruz Biotechnology, Heidelberg, Germany) overnight, washed, and incubated with horseradish peroxidase-conjugated secondary antibody. For detection, membranes were incubated with ECL Advance Western Blotting Detection Kit (GE Healthcare, Diegem, Belgium) and scanned by making use of the Chemidoc XRS imaging system (Biorad, Hercules, CA). Actin antibody (Sigma-Aldrich) was used for loading control. Densitometric analysis was performed using Imagemlab software version 3.0.1 (Biorad, Hercules, CA). The average intensity of the 38 kDa CTGF bands was divided by the average intensity of the corresponding beta-actin bands.

#### *Hydroxyproline assay*

Renal tissue from FFPE sections was deparaffinated, hydrolyzed and dissolved in lysis buffer. Samples underwent pre-column derivatization with  $\sigma$ -phtaldialdehyde (Sigma-Aldrich) and then 9-fluorenylmethylchloroformate (Fluka) to form fluorescent adducts of proline and hydroxyproline. The fluorescent adducts were separated and determined by reverse-phase HPLC followed by fluorometric detection. The ratio of hydroxyproline to proline was used as a measure for quantification of total tissue collagen content.

#### *Statistical analysis*

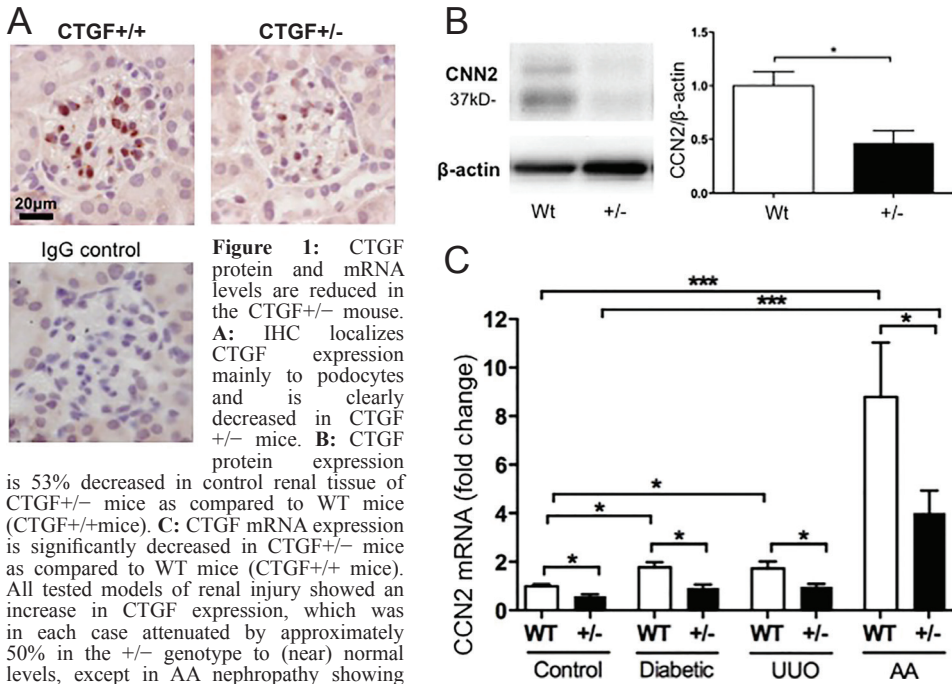
Data are presented as mean  $\pm$  SEM. Differences between groups were analyzed by Chi-Square test and two-way ANOVA with Bonferroni correction for multiple comparisons where appropriate. The statistical analysis was performed using GraphPad Prism software for Mac, version 5 (GraphPad Software, San Diego, CA, USA). For all comparisons, a value of  $P < 0.05$  was considered to be significant (two-tailed).



**Results**

*CTGF mRNA and protein levels are reduced in the CTGF<sup>+/-</sup> mouse*

Compared to wild-type (WT, CTGF<sup>+/+</sup>) mice, CTGF<sup>+/-</sup> mice showed significantly less CTGF protein expression. In WT mice, podocytes stained strongly for CTGF as evaluated by immunohistochemistry, and this intensity was attenuated in CTGF<sup>+/-</sup> mice (Figure 1A). Quantification by western blotting on renal cortex lysates confirmed these results: there was a significant, 53% reduction in CTGF expression in CTGF<sup>+/-</sup> mice as compared to WT mice ( $P < 0.05$ ) (Figure 1B). CTGF mRNA was equally reduced in CTGF<sup>+/-</sup> mice as compared to WT mice and this reduction was comparable to the protein reduction. In each tested animal model of renal disease, CTGF mRNA was clearly upregulated (up to 8.8-fold in AA nephropathy,  $P < 0.001$ ), and CTGF reduction in renal cortex of CTGF<sup>+/-</sup> mice as compared to WT mice was approximately 50% in all three disease models ( $P < 0.05$ ) (Figure 1C).



is 53% decreased in control renal tissue of CTGF<sup>+/-</sup> mice as compared to WT mice (CTGF<sup>+/+</sup> mice). C: CTGF mRNA expression is significantly decreased in CTGF<sup>+/-</sup> mice as compared to WT mice (CTGF<sup>+/+</sup> mice). All tested models of renal injury showed an increase in CTGF expression, which was in each case attenuated by approximately 50% in the +/- genotype to (near) normal levels, except in AA nephropathy showing almost 9-fold increase of CTGF expression in WT and approximately 4.5-fold increase in CTGF<sup>+/-</sup> mice. \* $P < 0.05$ , \*\*\* $P < 0.001$

*Clinical characteristics of mice in long-term STZ-induced diabetic nephropathy*

Induction of diabetes in WT and CTGF<sup>+/-</sup> mice on a C57BL/6 background by intraperitoneal injection of high-dose streptozotocin (200 mg/kg) resulted in characteristic features of diabetic nephropathy (DN), including persistent hyperglycemia, increased glycosylated hemoglobin levels, increased kidney-to-body-weight ratio, hyperfiltration and increased plasma urea levels. Blood pressure was not significantly elevated in STZ-induced diabetic vs. control mice (Table 1). After 6 months, the mean survival rate of STZ-induced diabetic mice was 70% with no significant difference between WT and CTGF<sup>+/-</sup> mice. Of all injected mice, 25.9% did not respond to STZ and were excluded from further analysis. The amount of non-responders was not significantly different between WT and CTGF<sup>+/-</sup> mice.

*Experimental long-term diabetes induces typical diabetic glomerular pathology*

In the diabetes model, we observed glomerular pathology with diffuse mesangial matrix increase and nodular accentuation in some glomeruli (Figure 2A). Examination of glomerular histology by means of PAS staining showed an increased mesangial matrix index (MMI) in STZ-induced diabetic mice as compared to control mice ( $12.1 \pm 1.08$  vs.  $2.6 \pm 0.34$  in controls,  $P < 0.001$ ), and MMI was 1.4-fold higher in STZ-induced diabetic CTGF<sup>+/-</sup> as compared to WT mice ( $P < 0.05$ , Figure 2A). Glomerular basement membrane (GBM) thickness as measured by electron microscopy was significantly increased in STZ-induced diabetic kidneys as compared to control kidneys ( $137.6 \pm 5.2$  nm vs.  $98.1 \pm 2.9$  nm in controls,  $P < 0.001$ , Figure 2B).

**Table 1.** Characteristics of control and STZ-induced diabetic WT and CTGF<sup>+/-</sup> mice

	Ctrl WT	Ctrl +/-	STZ WT	STZ +/-
N (% male)	8 (50)	7 (43)	9 (56)	7 (57)
Body weight (g)	28.8 (5.4)	29.1 (8.3)	24.2 (2.7)*	24.2 (2.4)*
Kidney weight (mg)	149 (8.0)	147 (8.7)	157 (7.6)	172.4 (11)
Kidney weight/body weight (mg/g)	5.2 (0.6)	5.1 (0.3)	5.9 (0.9)*	7.0 (0.5)*
Plasma glucose (mmol/l)	11.0 (0.6)	10.6 (0.5)	25.7 (0.3)*	24.6 (1.4)*
HbA1c (%)	3.7 (0.6)	3.7 (0.4)	6.4 (1.4)*	6.3 (1.2)*
Plasma creatinine (umol/l)	14.1 (2.1)	21.5 (2.9)	20.3 (2.8)	25.2 (3.8)
Plasma ureum (mmol/l)	7.3 (0.5)	6.7 (0.8)	12.9 (0.8)*	11.5 (1.9)*
Urine (ml/24 h)	1.6 (0.4)	1.4 (0.1)	14.6 (4.4)*	16.8 (3.9)*
Blood pressure (mmHg)	106 (6.1)	109 (3.6)	115 (8.5)	116 (6.0)

Data are means (SEM). \* $P < 0.05$  STZ-induced diabetic versus control mice. No significant differences between CTGF WT and CTGF<sup>+/-</sup> mice. Abbreviations: Ctrl, Vehicle control. WT, CTGF<sup>+/+</sup> wild type. STZ, streptozotocin induced diabetes.

*STZ-induced diabetic CTGF<sup>+/-</sup> mice are not protected from albuminuria, tubulointerstitial damage, fibrosis, and renal inflammation*

Albuminuria is increased in STZ-induced diabetic as compared to control mice, both in male and female mice and especially beyond 3 months of diabetes, but there was no attenuation of albuminuria in STZ-induced diabetic CTGF<sup>+/-</sup> mice (Figure 3).

Tubular injury associated with DN in human patients is characterized by flattening of tubular epithelial cells and thickening of the tubular basement membrane. Areas of tubular atrophy are typically found in close proximity with surrounding interstitial fibrosis. In the diabetes model, tubular atrophy and interstitial fibrosis were both clearly present. Tubular atrophy scoring revealed a significant increase in STZ-induced diabetic mice as compared to control mice ( $1.7 \pm 0.7$  vs.  $0.1 \pm 0.3$  in controls,  $P < 0.001$ ), but tubular atrophy was not attenuated in diabetic CTGF<sup>+/-</sup> mice (Figure 4A).

The mesenchymal marker  $\alpha$ -smooth muscle actin ( $\alpha$ SMA) (staining interstitial myofibroblasts) was clearly expressed in interstitial areas in STZ-induced diabetic mice ( $0.50 \pm 0.06$  vs.  $0.14 \pm 0.03$  in control mice,  $P < 0.05$ ) but could not distinguish between WT and CTGF<sup>+/-</sup> mice (Figure 4B). As a quantitative measure of collagen content, hydroxyproline/proline ratio (Hyp/prol ratio) was measured in renal cortical lysates by HPLC technology. Kidneys from STZ-induced diabetic mice showed a significantly increased collagen content ( $0.78 \pm 0.09$  vs.  $1.17 \pm 0.06$  Hyp/prol ratio,  $P < 0.01$ ), though there was no difference between CTGF<sup>+/-</sup> mice and WT mice (Figure 4C).

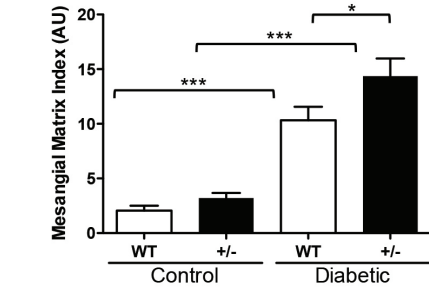
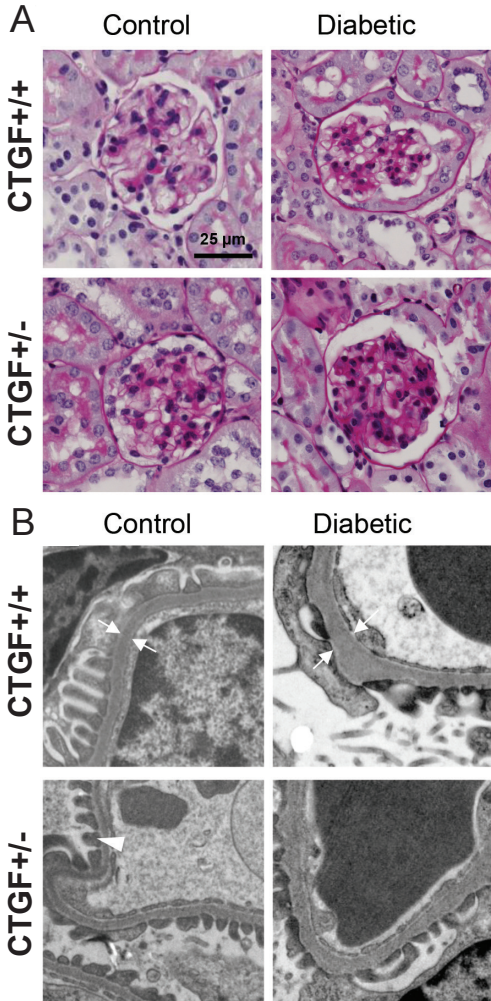


**Figure 2:** Experimental long-term diabetes induces typical diabetic glomerular pathology. **A:** Mesangial matrix increase is clearly visible in PAS-stained slides of diabetic glomeruli. Semi quantitative evaluation confirms a significant mesangial matrix increase (MMI) between STZ-induced diabetic and control mice, and a slightly but significantly higher increase in CTGF<sup>+/-</sup> as compared to WT mice.

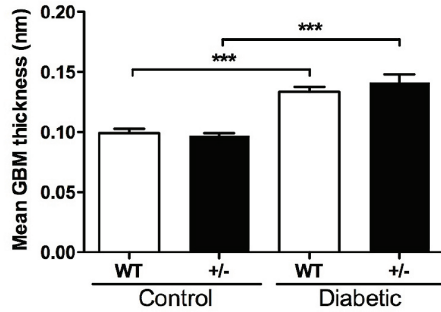


**Figure 2 (Continued): B:** Glomerular basement membrane (GBM) thickness measured by EM is equally increased in WT and CTGF<sup>+/-</sup> STZ-induced diabetic as compared to control glomeruli (arrows indicate GBM, arrowhead indicates podocytes foot process). \*P < 0.05, \*\*\*P < 0.001.

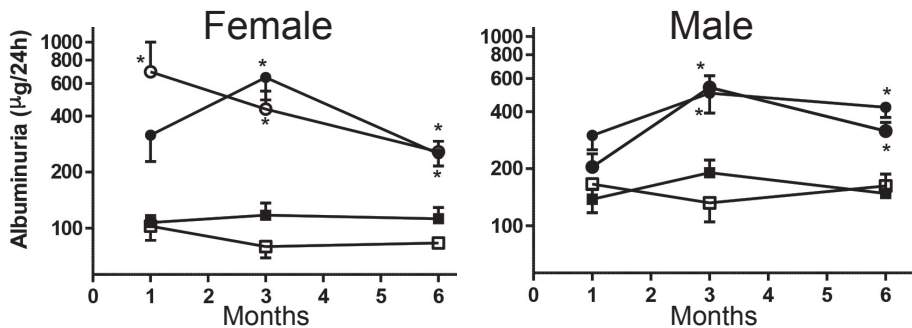


**Figure 3:** Albuminuria is not attenuated in STZ-induced diabetic CTGF<sup>+/-</sup> mice. Both female (A) and male (B) mice were studied at different time points. Generally, albuminuria was higher in male mice. There was an equal increase in albuminuria in male as well as female WT and CTGF<sup>+/-</sup> STZ-induced diabetic mice as compared to control mice. \*P < 0.05.

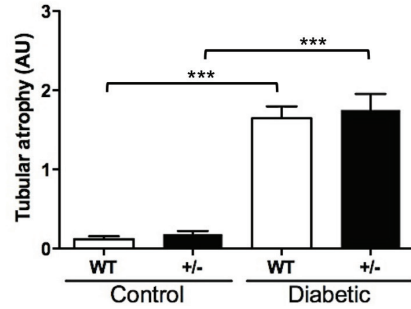
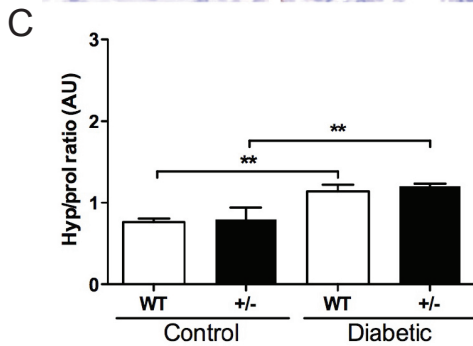
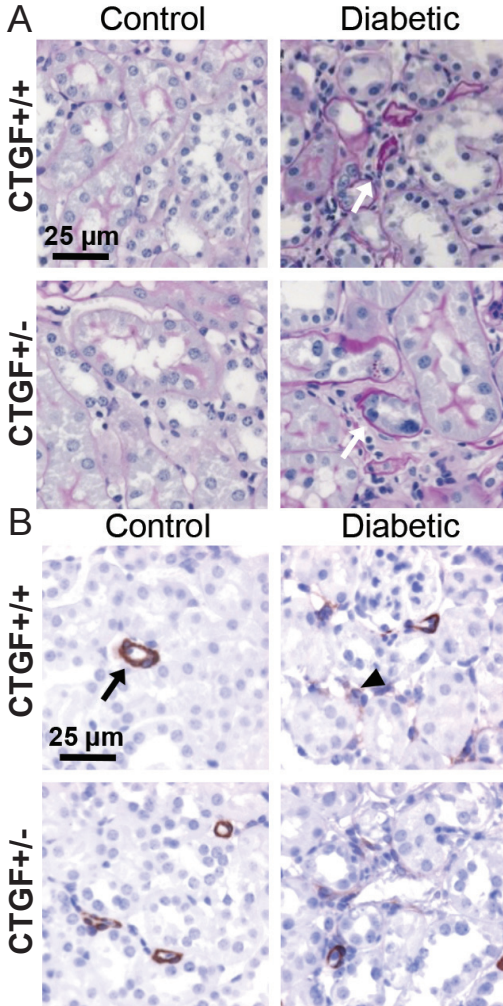


**Figure 4:** STZ-induced diabetic CTGF<sup>+/-</sup> mice are not protected from tubulointerstitial damage and fibrosis in long-term diabetes. **A:** Tubular atrophy, as evidenced by flattening of tubular cells and increased thickness of the tubular basement membrane, is observed in WT as well as CTGF<sup>+/-</sup> STZ-induced diabetic mice (arrows), but not in control mice.

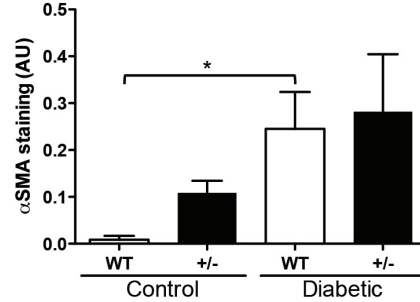


**Figure 4 (Continued): B:** Staining for  $\alpha$ -smooth muscle actin can be seen in control mice only marking the media of (small) arteries (arrow:  $\alpha$ -smooth muscle actin staining in glomerular arteriole). In STZ-induced diabetic WT as well as in STZ-induced diabetic CTGF<sup>+/-</sup> mice,  $\alpha$ -smooth muscle actin staining is increased and observed also in interstitial areas (arrowhead). **C:** Hydroxyproline/proline ratio's reflect the equal increase of renal collagen contents of STZ-induced diabetic as compared to control kidney in WT and CTGF<sup>+/-</sup> mice. (AU: arbitrary units). \*P < 0.05, \*\*P < 0.01, \*\*\*P < 0.001.

F4/80 positive macrophages were more widespread in STZ-induced diabetic mice as compared to control mice: STZ-induced diabetic mice showed an approximate 1.5-fold increase in presence of F4/80 positive cells in the kidney ( $133.9 \pm 15.4$  vs.  $80.5 \pm 7.9$  per HPF in control mice,  $P < 0.01$ ). No statistical significant difference in cellular infiltration between STZ-induced diabetic WT mice and diabetic CTGF<sup>+/-</sup> mice was detected (Figure 5A).

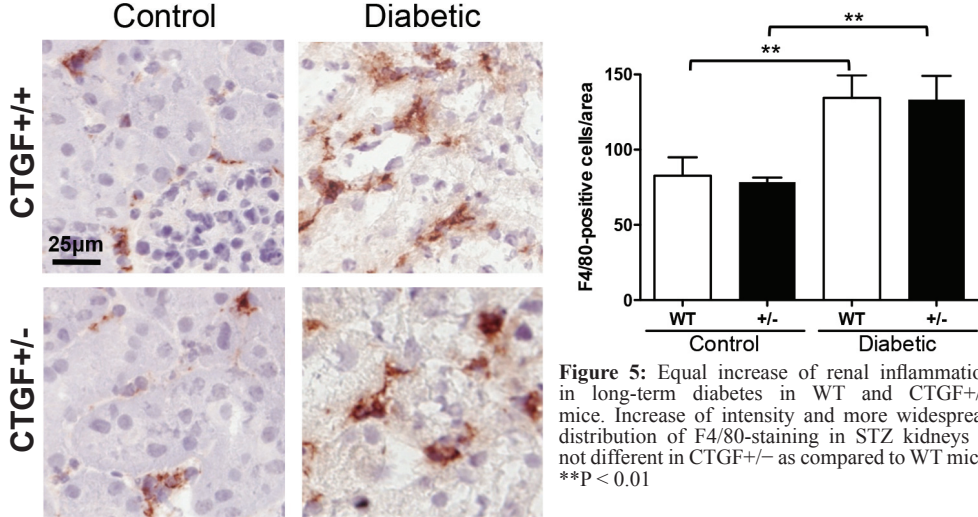


**Figure 5:** Equal increase of renal inflammation in long-term diabetes in WT and CTGF<sup>+/-</sup> mice. Increase of intensity and more widespread distribution of F4/80-staining in STZ kidneys is not different in CTGF<sup>+/-</sup> as compared to WT mice. \*\* $P < 0.01$

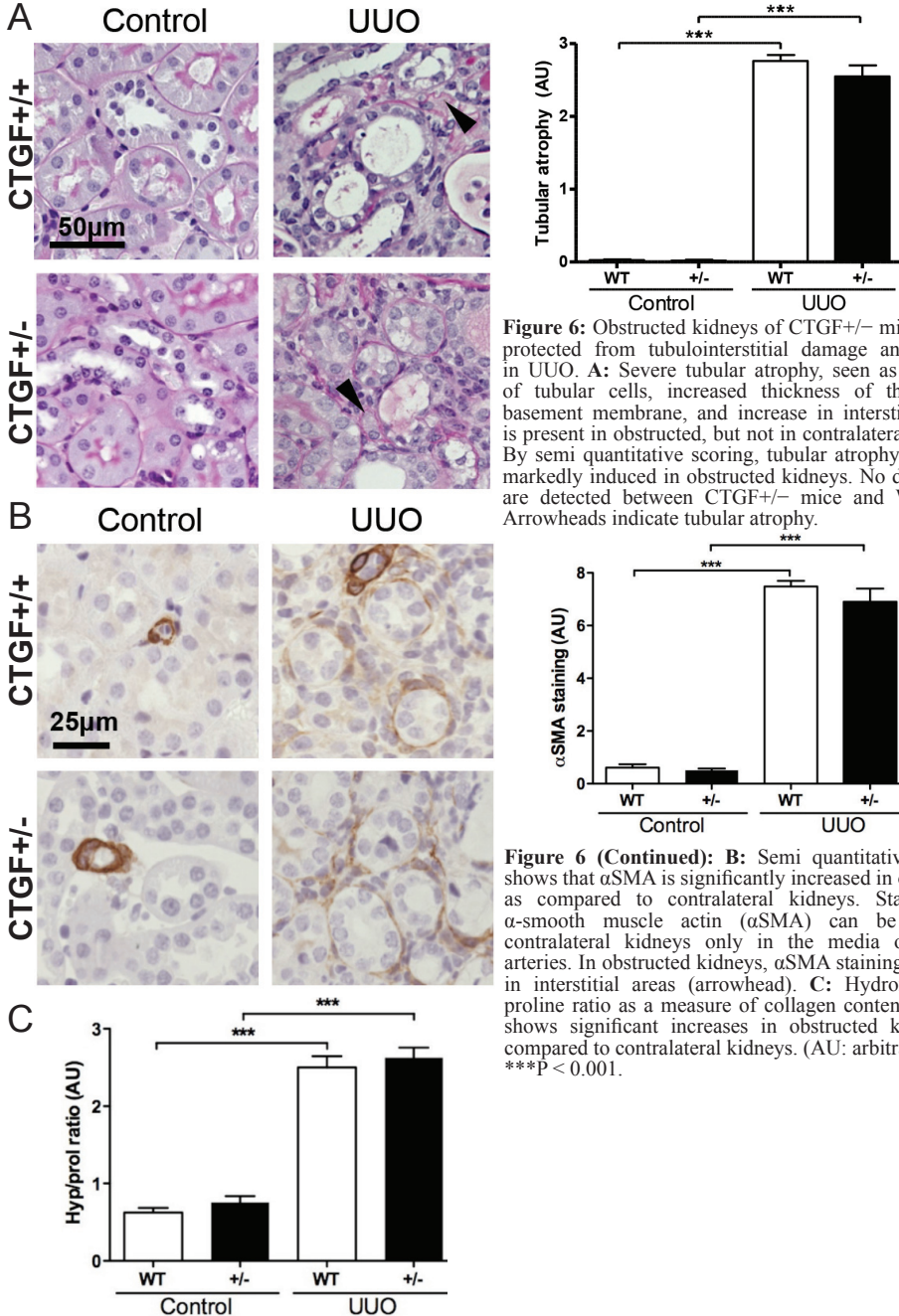
*CTGF<sup>+/-</sup> mice are not protected from tubulointerstitial damage, fibrosis, and renal inflammation induced by UO*

After 14 days of unilateral ureteric obstruction, tubular atrophy and interstitial fibrosis were markedly increased in obstructed kidneys, and clearly more severe as compared to the tubular atrophy seen in STZ-induced diabetic animals. Tubular atrophy scoring revealed a significant increase in obstructed as compared to contralateral kidneys ( $2.8 \pm 0.4$  vs.  $0.2 \pm 0.5$  in controls,  $P < 0.001$ ), but tubular atrophy was not attenuated in obstructed kidneys of CTGF<sup>+/-</sup> mice (Figure 6A). In interstitial areas of obstructed kidneys,  $\alpha$ SMA staining was intense ( $7.19 \pm 0.56$  vs.  $0.13 \pm 0.09$  in control mice,  $P < 0.001$ ) but not different between WT and CTGF<sup>+/-</sup> mice (Figure 6B). The Hyp/prol ratio, showed a 3.7-fold increase in obstructed as compared to contralateral kidneys ( $0.69 \pm 0.07$  vs.  $2.56 \pm 0.14$ ,  $P < 0.001$ ), which is a larger increase than seen in STZ kidneys or kidneys from mice injected with AA (Figure 4 and Figure 8). Again, no significant differences could be detected between both genotypes (Figure 6C). As compared to contralateral kidneys, there was a more than 4-fold increase in F4/80 staining intensity in obstructed kidneys ( $37.7 \pm 2.2$  vs.  $8.8 \pm 2.7$  in contralateral kidneys,  $P < 0.01$ ). No statistical significant difference in cellular infiltration between WT mice and CTGF<sup>+/-</sup> mice was detected (Figure 7A).

*The aristolochic acid model of nephropathy induces profound tubular damage and renal fibrosis, which is not attenuated in CTGF<sup>+/-</sup> mice*

Twenty-five days after the first AA injection, both WT and CTGF<sup>+/-</sup> mice showed loss of renal function as evident by plasma urea levels which were 6.1-fold elevated as compared to controls ( $6.3 \pm 0.9$  vs.  $37.9 \pm 7.3$  mmol/l,  $P < 0.05$ ). Histologically, profound tubular dilation and atrophy of proximal tubular epithelium were seen in AA mice (tubular atrophy scoring  $1.3 \pm 0.3$  vs.  $0.2 \pm 0.01$ ,  $P < 0.05$ ). Semiquantitative scoring however could not detect differences between CTGF<sup>+/-</sup> mice and WT mice (Figure 8A). In interstitial areas,  $\alpha$ SMA staining was clearly induced ( $6.77 \pm 0.55$  vs.  $0.48 \pm 0.08$  in control mice,  $P < 0.05$ ) but this was not different between WT and CTGF<sup>+/-</sup> (Figure 8B). Collagen content as measured by HPLC (Hyp/proline ratio) showed a 70% increase of levels in renal tissue of AA-injected mice ( $0.69 \pm 0.07$  vs.  $2.56 \pm 0.14$  in control mice,  $P < 0.05$ ),

although no significant differences could be detected between both genotypes (Figure 8C). The increase in collagen content in this model is larger than the increase seen in diabetic nephropathy, but smaller than the increase seen in the UUO model. As compared to contralateral kidneys, there was a 3-fold increase in macrophage influx in AA kidneys ( $37.7 \pm 2.2$  vs.  $8.8 \pm 2.7$  in control kidneys,  $P < 0.001$ ), but no difference between WT mice and CTGF<sup>+/-</sup> mice was detected (Figure 8D).



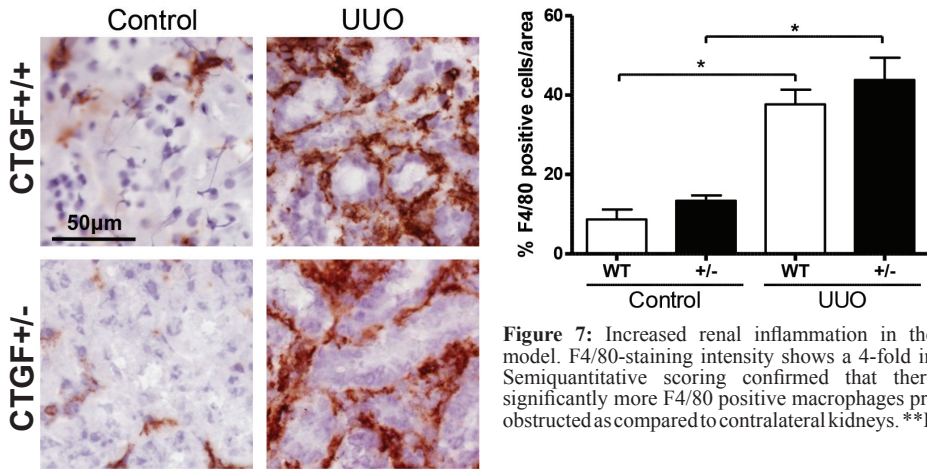


**Figure 7:** Increased renal inflammation in the UUU model. F4/80-staining intensity shows a 4-fold increase. Semiquantitative scoring confirmed that there were significantly more F4/80 positive macrophages present in obstructed as compared to contralateral kidneys. \*\*P<0.01.

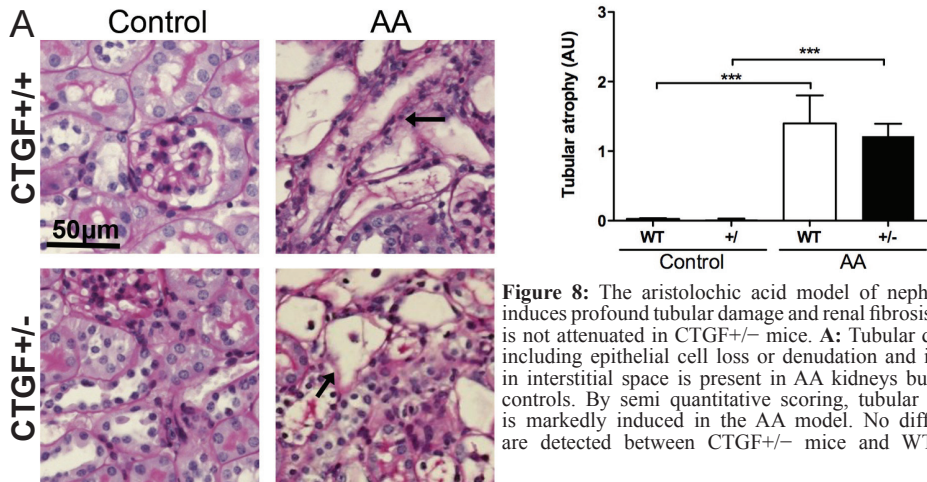


**Figure 8:** The aristolochic acid model of nephropathy induces profound tubular damage and renal fibrosis, which is not attenuated in CTGF<sup>+/-</sup> mice. **A:** Tubular damage, including epithelial cell loss or denudation and increase in interstitial space is present in AA kidneys but not in controls. By semi quantitative scoring, tubular atrophy is markedly induced in the AA model. No differences are detected between CTGF<sup>+/-</sup> mice and WT mice.

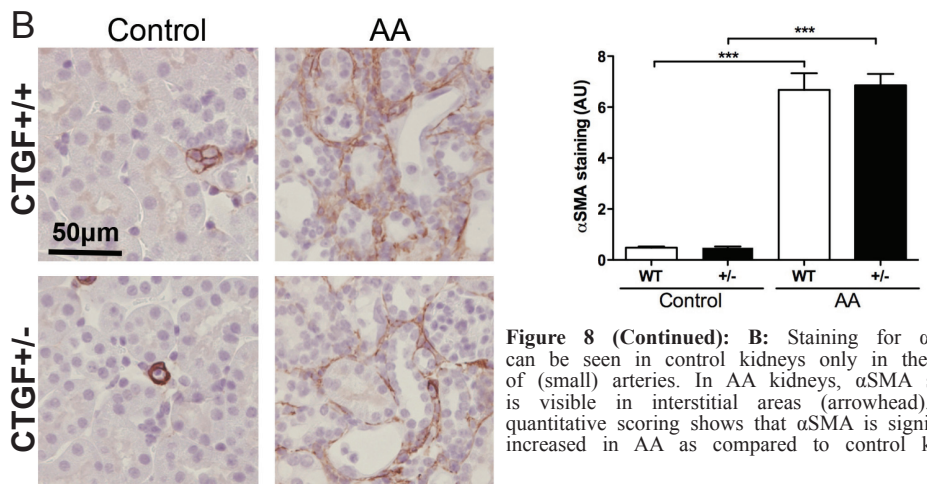


**Figure 8 (Continued): B:** Staining for  $\alpha$  SMA can be seen in control kidneys only in the media of (small) arteries. In AA kidneys,  $\alpha$ SMA staining is visible in interstitial areas (arrowhead). Semi quantitative scoring shows that  $\alpha$ SMA is significantly increased in AA as compared to control kidneys.

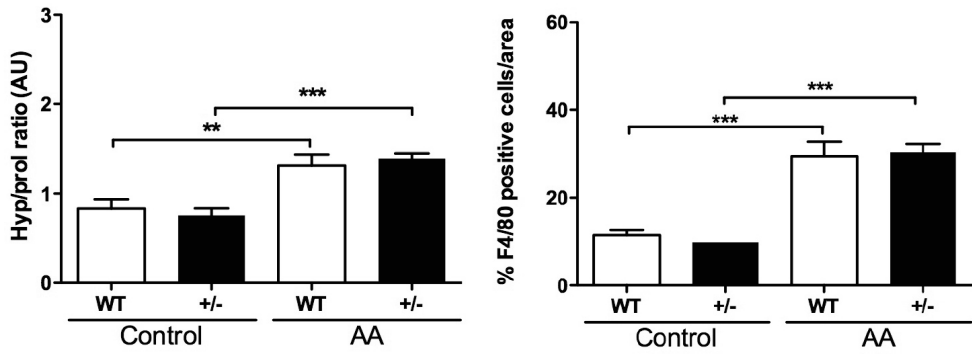


**Figure 8 (Continued):** C: Collagen content measured by hydroxyproline/proline ratio (Hyp/pro) is significantly increased (by 70%) in AA kidneys as compared to controls, but there were no differences between CTGF<sup>+/-</sup> mice and WT mice. D: Significantly more F4/80 positive macrophages present in AA as compared to control animals. (AU: arbitrary units). \*\*P < 0.01, \*\*\*P < 0.001



## Discussion

The major finding in this study is that WT and CTGF<sup>+/-</sup> mice do not present major differences in renal phenotype in three models of severe and chronic renal damage. There were no important differences in structural and functional read-outs between both genetic strains, indicating that the level of CTGF expression was not a limiting factor in the here studied experimental models of kidney disease.

In the 6 months STZ induced diabetes experiment, relatively pronounced histological alterations occurred, including mesangial matrix expansion, increase in glomerular basement membrane thickness, nodular glomerulosclerosis, tubulointerstitial damage with myofibroblast activation ( $\alpha$ SMA positivity), increase in renal collagen content (hydroxyproline/proline ratio) and increase in inflammation as measured by macrophage influx. These changes were accompanied by a significant rise in albuminuria and plasma urea in STZ-induced diabetic mice. For none of these histological and functional parameters, a clear difference was seen between hemizygous CTGF<sup>+/-</sup> mice and WT mice, the only exception being mesangial matrix expansion, which was slightly more increased in STZ-induced diabetic CTGF<sup>+/-</sup> as compared to WT mice. The significance of this is unknown, since it did not translate into differences in albuminuria, and it was unrelated to glomerular basement membrane thickness. Remarkably, separate evaluation of ocular manifestations of long-term diabetes did reveal a significantly attenuated phenotype of retinal damage in these same CTGF<sup>+/-</sup> mice (R.J. van Geest et al., unpublished), in line with the known harmful profibrotic role CTGF plays in the diabetic eye, despite not influencing angiogenesis (22, 23). A recent study that targets CTGF with siRNA in diabetic retinopathy in rats confirms the deleterious effects of CTGF in development of retinofibrosis (24). Furthermore, in a milder model of STZ induced nephropathy also conducted with the same CTGF<sup>+/-</sup> mouse strain, a significant lowering of albuminuria could be observed (10). This suggests different mechanisms and/or contextual determinants of quantitative CTGF effects that still await clarification.

In the UUO and AA experiments, extensive tubulointerstitial damage was seen. Semiquantitative tubular atrophy scoring showed a mean of 2.7 and of 1.8 on a scale of 5 in obstructed and AA-damaged kidneys, respectively, indicating that approximately 50% and 35% of renal parenchyma showed scarring. Both in the UUO and the AA nephropathy experiments, there was pronounced interstitial  $\alpha$ SMA positivity, reflecting presence of activated myofibroblasts, which was associated with significant interstitial inflammation, evidenced by 2- and 4-fold increases in F4/80 positivity as compared to control kidneys. Thus, these two models of tubulointerstitial renal disease have not revealed any significant effect of 50% reduced CTGF levels in CTGF<sup>+/-</sup> mice. For AA nephropathy, this is in line with a recent report where tubulointerstitial injury, fibrosis and loss of kidney function were not aggravated in transgenic mice overexpressing CTGF under the Col1A2 promoter as compared to WT mice, showing that further increase of CTGF above the levels occurring in injured WT mice do not aggravate the renal response to injury in AA nephropathy (19). Of note, the 3 to 4-fold increase of CTGF expression in WT and CTGF overexpressing mice in this report, is lower than the 8-fold increase we observed in our study, which might relate to the earlier time of evaluation (52 days in the paper by Fragiadaki et al., compared to 25 days in our study) and to the different mouse strains (CBA/C57BL10 vs. C57Bl/6).

Two other studies have already evaluated the effect CTGF attenuation by targeting its transcription. Yokoi et al. demonstrated attenuation of fibrosis in a 7-day rat UUO model after CTGF blockade by antisense oligodeoxynucleotide treatment, which reduced CTGF expression to  $\pm$  50% of normal levels (15), while Guha et al. tested antisense oligonucleotides in a low-dose STZ model with 16 weeks of hyperglycemia (14). A major difference between experimental set-ups in those studies as compared to the studies presented here is the 7 days longer obstruction in our UUO-study and 2 months longer duration of our diabetes model. Remarkably, at the earlier time-points addressed in these papers, attenuation of CTGF expression translated into almost linear reduction of e.g. fibronectin,  $\alpha$ SMA and collagen expression, suggesting that in the initial phase of fibrotic renal disease, CTGF is a crucial and limiting factor determining renal response to injury. In a more recent publication, the monoclonal anti-CTGF antibody FG-3019 was used to inhibit fibrosis in mice subjected to UUO (25). Duration of

the experiment was 14 days, which makes the set-up of this study very well comparable to our 14-day UUU experiment. Hydroxyproline/proline ratios were 15 to 20% lower in mice injected with doses of resp. 30 mg/kg and 10 mg/kg FG-3019 every other day. Remarkably, there was no linear dose–response relationship, since the lower 10 mg/kg dose was the most effective in reducing renal collagen content. It was not reported to what extent FG-3019 treatment reduced CTGF levels, and no other gene, protein or histological read-outs of fibrosis apart from the hydroxyproline/proline ratios were reported. This makes it again difficult to accurately compare the morphological phenotype between this study and our study.

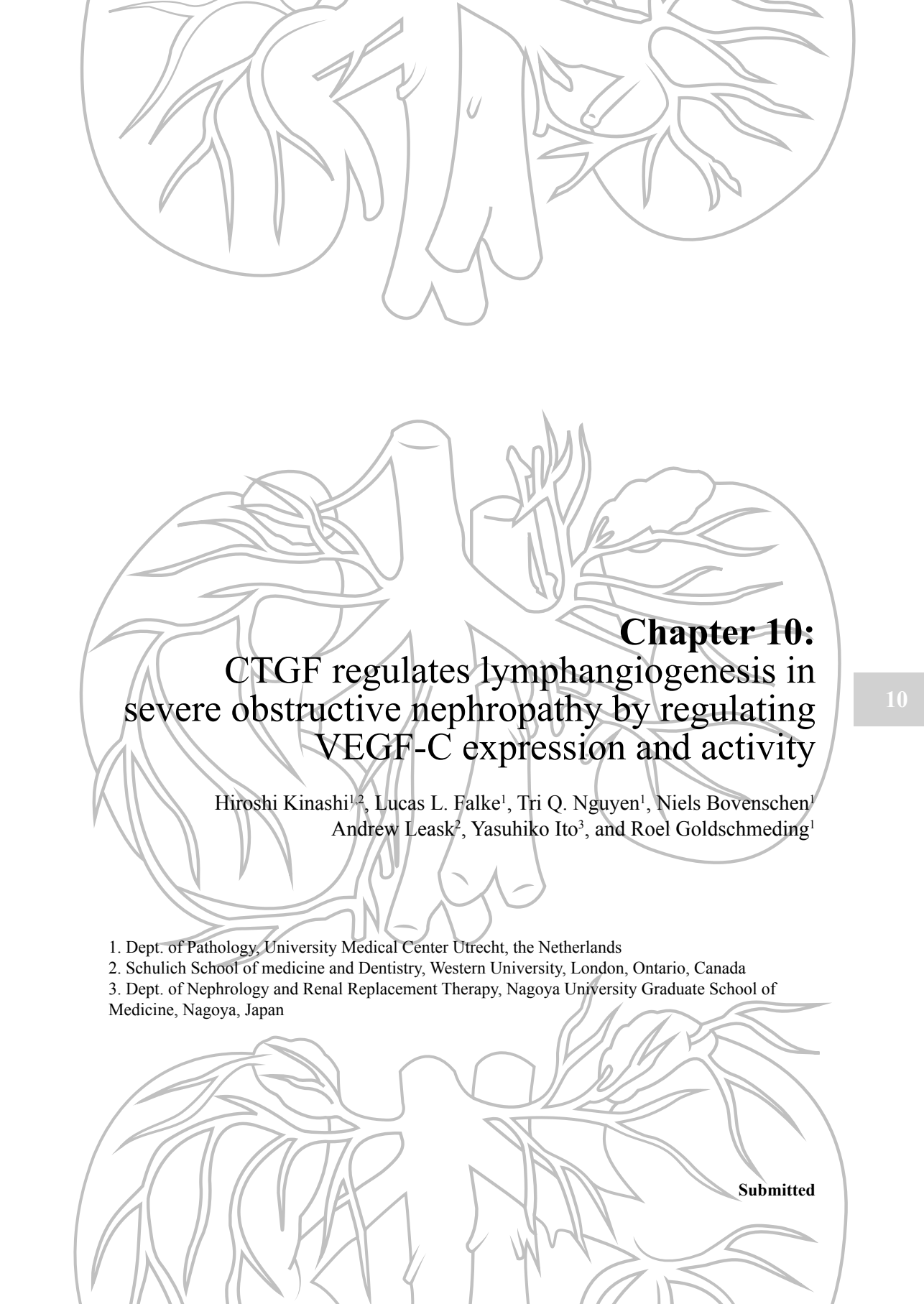
One possible explanation for the lack of differences between damaged WT and CTGF<sup>+/-</sup>-kidneys in the present study might be that CTGF is redundant with, or overruled by other factors in the fibrotic response to chronic or more severe acute kidney damage. Alternatively, there might be a threshold level below the 50% knockdown we observed. It might well be that a further reduction of CTGF does attenuate adverse remodelling and loss of kidney function. In light of this it is important to realize how the relatively reduced CTGF level in damaged CTGF<sup>+/-</sup> kidneys compared to the absolute levels in normal control kidneys. In AA nephropathy, the CTGF<sup>+/-</sup> kidneys still contained > 4-fold higher CTGF levels than WT control kidneys, which makes it less surprising that there is still fibrosis. In contrast, in the diabetes and UUU models, renal CTGF levels of hemizygous knock-out mice were comparable to or even below those in WT control kidneys. This might seem to suggest that the disease phenotype in these mice should be explained largely by CTGF-independent factors. However, considering the modulatory action of CTGF in many different signalling pathways, also smaller, even normal amounts of CTGF in concert with other factors, such as CCN family members, might still be a critical determinant of the renal response to chronic and severe injury. To test these hypotheses, further reduction of CTGF availability in these models will be necessary. Since homozygous CTGF deletion is lethal early after birth, these experiments will have to rely on alternative approaches, including inducible knockout of floxed CTGF alleles using a gene recombination knockdown system. Since 50% CTGF reduction did not appear to limit fibrosis in severe models of kidney fibrosis, CTGF therapy comes into a new perspective. Whether CTGF reduction might prove enough to combat fibrosis or organ failure in other fibrotic diseases under severe conditions, such as cardiomyopathy, fibrotic skin disorders, systemic sclerosis, biliary atresia, liver fibrosis, sarcoidosis and idiopathic pulmonary fibrosis is also an objective worthwhile investigating.

In conclusion, unlike in mild and relatively early STZ induced nephropathy, reduction of CTGF by 50% to (near) normal levels may by itself not be sufficient to inhibit fibrosis in severe and chronic kidney diseases. Future studies aiming at further reduction of CTGF availability to levels below those of normal controls will be needed to determine whether CTGF is redundant in severe and chronic kidney disease, or whether it is a rate limiting factor of fibrosis in low concentrations that might be effective when reduced by available or emerging therapies.

**References**

1. Brigstock DR, Goldschmeding R, Katsube KI, Lam SC, Lau LF, Lyons K, et al. Proposal for a unified CCN nomenclature. *Mol Pathol.* 2003;56(2):127-8.
2. Nguyen TQ, Goldschmeding R. Bone morphogenetic protein-7 and connective tissue growth factor: novel targets for treatment of renal fibrosis? *Pharm Res.* 2008;25(10):2416-26.
3. Chen MM, Lam A, Abraham JA, Schreiner GF, Joly AH. CTGF expression is induced by TGF- $\beta$  in cardiac fibroblasts and cardiac myocytes: a potential role in heart fibrosis. *J Mol Cell Cardiol.* 2000;32(10):1805-19.
4. Chen Y, Shi-Wen X, van Beek J, Kennedy L, McLeod M, Renzoni EA, et al. Matrix contraction by dermal fibroblasts requires transforming growth factor- $\beta$ /activin-linked kinase 5, heparan sulfate-containing proteoglycans, and MEK/ERK: insights into pathological scarring in chronic fibrotic disease. *Am J Pathol.* 2005;167(6):1699-711.
5. Leask A, Abraham DJ. All in the CCN family: essential matricellular signaling modulators emerge from the bunker. *J Cell Sci.* 2006;119(Pt 23):4803-10.
6. Mason RM. Connective tissue growth factor (CCN2), a pathogenic factor in diabetic nephropathy. What does it do? How does it do it? *J Cell Commun Signal.* 2009;3(2):95-104.
7. Ito Y, Aten J, Bende RJ, Oemar BS, Rabelink TJ, Weening JJ, et al. Expression of connective tissue growth factor in human renal fibrosis. *Kidney Int.* 1998;53(4):853-61.
8. Kobayashi T, Okada H, Inoue T, Kanno Y, Suzuki H. Tubular expression of connective tissue growth factor correlates with interstitial fibrosis in type 2 diabetic nephropathy. *Nephrol Dial Transplant.* 2006;21(2):548-9.
9. Adler SG, Schwartz S, Williams ME, Arauz-Pacheco C, Bolton WK, Lee T, et al. Phase 1 study of anti-CTGF monoclonal antibody in patients with diabetes and microalbuminuria. *Clin J Am Soc Nephrol.* 2010;5(8):1420-8.
10. Nguyen TQ, Roestenberg P, van Nieuwenhoven FA, Bovenschen N, Li Z, Xu L, et al. CTGF inhibits BMP-7 signaling in diabetic nephropathy. *J Am Soc Nephrol.* 2008;19(11):2098-107.
11. Cameron JS. Tubular and interstitial factors in the progression of glomerulonephritis. *Pediatr Nephrol.* 1992;6(3):292-303.
12. Risdon RA, Sloper JC, De Wardener HE. Relationship between renal function and histological changes found in renal-biopsy specimens from patients with persistent glomerular nephritis. *Lancet.* 1968;2(7564):363-6.
13. Schainuck LI, Striker GE, Cutler RE, Benditt EP. Structural-functional correlations in renal disease. II. The correlations. *Hum Pathol.* 1970;1(4):631-41.
14. Guha M, Xu ZG, Tung D, Lanting L, Natarajan R. Specific down-regulation of connective tissue growth factor attenuates progression of nephropathy in mouse models of type 1 and type 2 diabetes. *FASEB J.* 2007;21(12):3355-68.
15. Yokoi H, Mukoyama M, Nagae T, Mori K, Suganami T, Sawai K, et al. Reduction in connective tissue growth factor by antisense treatment ameliorates renal tubulointerstitial fibrosis. *J Am Soc Nephrol.* 2004;15(6):1430-40.
16. Breyer MD, Bottinger E, Brosius FC, 3rd, Coffman TM, Harris RC, Heilig CW, et al. Mouse models of diabetic nephropathy. *J Am Soc Nephrol.* 2005;16(1):27-45.
17. Brosius FC, 3rd, Alpers CE, Bottinger EP, Breyer MD, Coffman TM, Gurley SB, et al. Mouse models of diabetic nephropathy. *J Am Soc Nephrol.* 2009;20(12):2503-12.
18. Chevalier RL, Forbes MS, Thornhill BA. Ureteral obstruction as a model of renal interstitial fibrosis and obstructive nephropathy. *Kidney Int.* 2009;75(11):1145-52.
19. Fragiadaki M, Witherden AS, Kaneko T, Sonnylal S, Pusey CD, Bou-Gharios G, et al. Interstitial fibrosis is associated with increased COL1A2 transcription in AA-injured renal tubular epithelial cells in vivo. *Matrix Biol.* 2011;30(7-8):396-403.
20. Lebeau C, Debelle FD, Arlt VM, Pozdzik A, De Prez EG, Phillips DH, et al. Early proximal tubule injury in experimental aristolochic acid nephropathy: functional and histological studies. *Nephrol Dial Transplant.* 2005;20(11):2321-32.
21. Ivkovic S, Yoon BS, Popoff SN, Safadi FF, Libuda DE, Stephenson RC, et al. Connective tissue growth factor coordinates chondrogenesis and angiogenesis during skeletal development. *Development.* 2003;130(12):2779-91.
22. Kuiper EJ, Roestenberg P, Ehlken C, Lambert V, van Treslong-de Groot HB, Lyons KM, et al. Angiogenesis is not impaired in connective tissue growth factor (CTGF) knock-out mice. *J Histochem Cytochem.* 2007;55(11):1139-47.
23. Kuiper EJ, van Zijderveld R, Roestenberg P, Lyons KM, Goldschmeding R, Klaassen I, et al. Connective tissue growth factor is necessary for retinal capillary basal lamina thickening in diabetic mice. *J Histochem Cytochem.* 2008;56(8):785-92.
24. Winkler JL, Kedees MH, Guz Y, Teitelman G. Inhibition of connective tissue growth factor by small interfering ribonucleic acid prevents increase in extracellular matrix molecules in a rodent model of diabetic retinopathy. *Mol Vis.* 2012;18:874-86.
25. Wang Q, Usinger W, Nichols B, Gray J, Xu L, Seeley TW, et al. Cooperative interaction of CTGF and TGF- $\beta$  in animal models of fibrotic disease. *Fibrogenesis Tissue Repair.* 2011;4(1):4.

10



## **Chapter 10:** **CTGF regulates lymphangiogenesis in severe obstructive nephropathy by regulating VEGF-C expression and activity**

Hiroshi Kinashi<sup>1,2</sup>, Lucas L. Falke<sup>1</sup>, Tri Q. Nguyen<sup>1</sup>, Niels Bovenschen<sup>1</sup>  
Andrew Leask<sup>2</sup>, Yasuhiko Ito<sup>3</sup>, and Roel Goldschmeding<sup>1</sup>

1. Dept. of Pathology, University Medical Center Utrecht, the Netherlands

2. Schulich School of medicine and Dentistry, Western University, London, Ontario, Canada

3. Dept. of Nephrology and Renal Replacement Therapy, Nagoya University Graduate School of  
Medicine, Nagoya, Japan

Submitted

**Abstracts**

Increased lymphangiogenesis occurs in various types of kidney disease, and the number of renal lymphatic vessels is related to the degree of renal interstitial fibrosis. Vascular endothelial growth factor-C (VEGF-C) is the main driver of lymphangiogenesis. Transforming growth factor- $\beta$  (TGF- $\beta$ ) plays a key role in renal lymphangiogenesis by promoting VEGF-C production. Connective tissue growth factor (CTGF; CCN-2), another TGF- $\beta$  responsive gene, is an important mediator of kidney fibrosis and has been shown to interact with VEGF-A. A possible CTGF interaction with VEGF-C and involvement thereof in lymphangiogenesis has not been explored. We used inducible CTGF ubiquitous knockout (CTGF<sup>-/-</sup>) mice to investigate the involvement of CTGF in fibrosis and associated lymphangiogenesis in severe obstructive nephropathy. In vitro, we investigated the possible involvement of CTGF in VEGF-C expression downstream of TGF- $\beta$ , and in regulation of VEGF-C lymphangiogenic activity. The increase of lymphatic vessels and VEGF-C in obstructed wild-type kidneys was significantly reduced in CTGF<sup>-/-</sup> mice. In vitro, rhCTGF induced VEGF-C production in HK-2 cells, and CTGF siRNA suppressed TGF- $\beta$ 1-induced VEGF-C upregulation. Furthermore, CTGF bound directly to VEGF-C, with similar affinity as to VEGF-A. Interestingly, VEGF-C-induced capillary-like tube formation by human lymphatic endothelial cells was suppressed by full-length CTGF, but not by its physiological cleavage products.

We conclude that CTGF can regulate fibrosis-associated lymphangiogenesis in the kidney by stimulating VEGF-C expression and modulating VEGF-C activity through direct physical interaction.

## Introduction

Chronic kidney disease (CKD) is a major health problem with rising incidence and prevalence for which currently no effective therapy other than renal replacement therapy exists (1). Both hemodialysis and renal transplantation are accompanied by a major economic and health burden, and the number of transplantable donor kidneys does not match the need (2, 3). Therefore, increasing effort is being put in the development of therapeutic interventional strategies to prevent CKD occurrence or limit progression to end stage renal disease. One potential strategy focuses on lymphangiogenesis.

The lymphatic vasculature is essential for the maintenance of tissue fluid balance, immune surveillance, and absorption of fatty acids in the gut. Lymphatic vessels normally drain, filter, and return extravasated tissue fluid, cells, and proteins back to the circulation through the thoracic and lymphatic ducts (4). Lymphangiogenesis has been observed in various diseases, including tumor metastasis (5), inflammatory disease (6), heart disease (7), and renal diseases such as transplant rejection (8-10). Signaling of vascular endothelial growth factor (VEGF)-C through the VEGF receptor (VEGFR)-3 is central to lymphangiogenesis (11, 12). In addition, lymphangiogenesis is associated with fibrotic disease. We previously reported that lymphangiogenesis was observed in various types of human kidney diseases, and the number of renal lymphatics was related to the degree of renal interstitial fibrosis (13). During obstructive nephropathy, transforming growth factor- $\beta$  (TGF- $\beta$ ) increases VEGF-C expression, which leads to lymphangiogenesis (14, 15). We also demonstrated a similar mechanism of lymphangiogenesis in peritoneal fibrosis in association with peritoneal dialysis (16).

The matricellular and multimodular protein connective tissue growth factor (CTGF; CCN-2) is a major contributor to CKD development and progression (17). TGF- $\beta$  induces CTGF expression in multiple cell types including mesangial cells and renal tubular epithelial cells. CTGF plays a role in the development and progression of glomerulosclerosis and tubulointerstitial fibrosis as part of TGF- $\beta$ -dependent and TGF- $\beta$ -independent pathways (18, 19). Additionally CTGF modulates TGF- $\beta$  signaling by direct physical interaction (20). A 50% reduction of CTGF reduced fibrotic development in relatively mild models of renal disease (21, 22). We also found, that 50% reduction of CTGF was not enough to reduce fibrosis in severe models of renal disease (23), but it should be noted that under these circumstances, the 50% reduced CTGF expression was still well above physiological baseline levels. Besides its major regulatory role during fibrosis, CTGF is also an important regulator of angiogenesis (24). Paradoxically, CTGF binding to VEGF-A, a strong angiogenic growth factor, reduces *in vitro* tube formation by vascular endothelial cells and inhibits angiogenesis (25, 26). However, little is known about the possible role of CTGF in lymphangiogenesis and regulation of VEGF-C expression and activity remains to be elucidated.

In the present study, we address the hypotheses that that 1) CTGF reduction well below baseline levels during a severe model of renal disease will result in reduction of fibrosis in a severe model of (obstructive) kidney disease, and 2) CTGF plays a major role in fibrosis associated lymphangiogenesis in this model. To this aim, we assessed fibrosis, lymphangiogenesis, and VEGF-C expression in severe obstructive nephropathy induced by unilateral ureteral obstruction for 14 days in wild type (WT) and inducible ubiquitous CTGF knock-out mice (Rosa26-MER; CTGF<sup>fl/fl</sup>) in which near complete CTGF-deletion was achieved by repeated tamoxifen administration 2 weeks earlier. In addition, we analyzed CTGF effects on VEGF-C production in cultured human renal proximal tubular epithelial cells (HK-2). The interaction of CTGF with VEGF-C was studied by surface plasmon resonance (SPR) and human lymphatic microvascular endothelial cell culture.

## Materials and Methods

### *Experimental animal model*

The animal experiment was performed with the approval of the Experimental Animal Ethics Committee of the University of Utrecht. Generation of floxCTGF mice has been extensively described elsewhere (27). Briefly: LoxP sites flank exon 4 of the CTGF gene and genetic recombination leads to an early frameshift. By crossing floxCTGF mice with ROSA26-ERT2CRE mice for several generations, ROSA26-ERT2CRE/floxCTGF mice were created. Both strains were of C57Black6/J background. ROSA26-ERT2CRE/floxCTGF mice were injected with corn oil (n = 5) for WT mice or tamoxifen (n = 9) for CTGF<sup>-/-</sup> mice. Mice received 4 intraperitoneal injections of 100  $\mu$ l (10mg/ml) tamoxifen every other day over the course of one week. Two weeks after the last injection, the ureter of the left kidney was obstructed in all mice (UUO) as extensively described elsewhere (23). 14 days after ligation, mice were sacrificed and organs were harvested for analysis. Unobstructed contralateral kidneys (CLKs) serve as control. Tissue was processed for western blot, IHC, and qPCR.

### *Immunohistochemistry*

For staining and IHC in mouse kidney specimens, 3 $\mu$ m formalin-fixed paraffin sections were deparaffinized and rehydrated. PAS and Masson's trichrome staining was performed using standard procedures. For IHC, after blocking endogenous peroxidase activity, heat-based antigen retrieval was performed in EDTA buffer (pH=9) for  $\alpha$ -SMA or in citrate buffer (pH=6) for LYVE-1 and VEGF-C. Slides were incubated for 1 h at room temperature with the following antibodies: rabbit anti- $\alpha$ SMA antibody (1:200, Abcam, Cambridge, UK), rabbit anti-mouse LYVE-1 antibody (1:500, Acris Antibodies GmbH, Herford, Germany), or rabbit anti-VEGF-C antibody (1:100, Zymed Laboratories, San Francisco, CA), followed by the incubation with Brightvision Poly-HRP-anti-rabbit IgG (Immunologic BV, Duiven, Netherlands). Bound antibody was visualized with 3,3'-diaminobenzidine or NovaRed (Vector Laboratories, Burlingame, CA). Stained sections were counterstained with hematoxylin. To determine positive area percentage of Masson's trichrome,  $\alpha$ -SMA, and VEGF-C stained slides, 10 random fields per section were chosen and photographed. Positive staining areas were quantitated using Image J software (NIH, USA) with appropriate thresholding. LYVE-1-positive lymphatic vessels were identified and counted in whole renal cortex areas of slides. The number of LYVE-1-positive vessels was corrected by renal cortex area measured by Image J.

### *Western blot*

Frozen mouse renal cortex was homogenized in NP-40 lysis buffer containing sodium orthovanadate, sodium fluoride and protease inhibitor cocktail (Sigma, St. Louis, MO). Protein quantity was determined by BCA protein assay kit (Pierce, Rockford, IL). Samples were run on 10% SDS-PAGE gels and transferred onto polyvinylidene difluoride membranes. After blocking, membranes were incubated with a CTGF antibody (Santa Cruz Biotechnology) overnight, washed, and incubated with horseradish peroxidase-conjugated secondary antibody. Actin antibody (MP Biomedicals, Santa Ana, CA) was used on the same blot for loading control. For detection, membranes were incubated with chemiluminescence substrate (GE Healthcare, Little Chalfont, England) and imaged.

### *HK-2 cell culture*

HK-2 cells (human renal proximal tubular epithelial cell line) were cultured in Dulbecco's modified eagle's medium with 10% fetal calf serum, penicillin and streptomycin in humidified air with 5% CO<sub>2</sub> at 37 °C. HK-2 cells were plated at a density of  $1 \times 10^5$  cells in 6-well plates. After a 1-day incubation, culture medium was replaced with serum-free medium for 24 h to render cells quiescent. Subsequently, cells were incubated in serum-free medium supplemented with 0, 2.5, 5, or 10 nM FL-CTGF (FibroGen, South San Francisco, CA). Cells were harvested after 8 h incubation for qPCR analysis. In CTGF inhibition studies, 1 day after seeding cells in 6-well plates, cells were transfected with Lipofectamine RNAiMAX (Invitrogen, Carlsbad, CA) and 20



nM CTGF siRNA or Non-targeting siRNA (GE Healthcare). After 6 h incubation, culture medium was replaced with serum-free medium and incubated for 24 h. Subsequently, cells were incubated in serum-free medium alone or medium with 10 ng/ml TGF- $\beta$ 1 (R&D System, Minneapolis, MN). Cells and cell supernatants were harvested after 8 or 24 h incubation for qPCR and ELISA.

#### *Quantitative PCR*

Total RNA was extracted from frozen mouse renal cortex or from cultured cells using TRIzol (Life technologies, Carlsbad, CA). After cDNA synthesis, expression of target genes was assessed by qPCR using TaqMan Gene Expression Assays (mouse CTGF, Mm00515790\_g1; mouse *Coll1a2*, Mm00483888\_m1; mouse LYVE-1, Mm00475056\_m1; mouse VEGF-C, Mm00437313\_m1; human CTGF, Hs00170014\_m1; human VEGF-C, Hs00153458\_m1; human PAI-1, Hs00167155\_m1, Applied Biosystems, Foster City, CA). TATA-box binding protein (TBP, Mm00446971\_m1) and glyceraldehydes-3-phosphate dehydrogenase (GAPDH, Hs99999905\_m1) were used as internal reference. Samples were run on a Lightcycler 480 (Roche, Basel, Switzerland) and relative expression was determined using double delta Ct analysis.

#### *VEGF-C ELISA*

VEGF-C protein levels in cell culture supernatants were measured using the Human VEGF-C Assay Kit (IBL, Takasaki, Japan), according to the manufacturer's instruction. Samples were frozen at the time of collection and stored at -80°C. Samples were not subjected to freeze-thaw cycles.

#### *Surface Plasmon Resonance analysis*

Real-time binding experiments were performed with Biacore T100 (GE Healthcare, Uppsala, Sweden). rhVEGF-C (R&D Systems) was immobilized (1360 RU) on a CM5 sensor-chip surface. Association of rhCTGF was assessed in 10mM HEPES (pH 7.4), 150mM NaCl, 3mM EDTA, 0.005% surfactant P20 for 200 seconds, at a flow rate of 20 $\mu$ l/min at 25°C. Dissociation was allowed for 10 min in the same buffer flow. Sensor chips were regenerated using several pulses of 20mM HEPES (pH 7.4), 1M NaCl at a flow rate of 20 $\mu$ l/min. One control flow-channel was routinely activated and blocked in the absence of protein. Data was corrected for aspecific binding. Specific binding at equilibrium was plotted against [CTGF] from which Kd values were calculated using BIAevaluation Software 3.1 (GE Healthcare).

#### *Capillary-like tube formation assay*

HMVEC-dLy Neo (Neonatal normal human dermal lymphatic microvascular endothelial cells) were purchased from Lonza (Walkersville, MD) and were maintained in EGM-2MV BulletKit (Lonza) in humidified air with 5% CO<sub>2</sub> at 37 °C. 400 $\mu$ l aliquots of Growth Factor Reduced Matrigel Matrix (Corning, Bedford, MA) were added to each well of 6-well plates, and were incubated at 37 °C for 30 min. Cells were plated at a density of 2  $\times$  10<sup>5</sup> /ml in serum free medium and added to the wells (1ml per well) and treated with 500 ng/ml recombinant VEGF-C (R&D). Cells were supplemented with equivalent amount (25nM) of FL-CTGF, or N-CTGF, or C-CTGF (FibroGen) in the presence of VEGF-C. After 6 h of incubation at 37 °C, 10 randomly selected 1700  $\times$  1360- $\mu$ m fields were photographed in each well, and the number of capillary-like tube formation was counted. Control cells were incubated without any treatment and data was expressed as a percentage of the controls.

#### *Statistical Analyses*

Values are expressed as means  $\pm$  s.e. Differences between two groups were analyzed by Student T test. Comparisons among groups were performed by one-way ANOVA followed by Tukey's HSD multiple comparison test. Differences were considered to be statistically significant if P<0.05. All analyses were performed using SPSS software (SPSS, Chicago, IL).

## Results

### *Near complete deletion of CTGF reduced tubulointerstitial fibrosis 14 days after UUO*

In order to investigate the effect of CTGF reduction on renal fibrosis 14 days after UUO, we made use of conditional CTGF<sup>-/-</sup> mice. In WT mice, CTGF mRNA expression was increased 2.2-fold in obstructed kidneys (OBK) compared to contralateral kidneys (CLK) ( $p < 0.05$ ). CTGF<sup>-/-</sup> mice showed more than 90% reduction of CTGF mRNA expression in both CLK ( $P < 0.05$ ) and OBK ( $P < 0.001$ ) compared to WT mice (Figure 1A). CTGF<sup>-/-</sup> mice also showed a decreased expression of CTGF protein levels in both CLK and OBK compared to WT mice by western blot analysis (Figure 1B). Periodic acid Schiff (PAS) staining showed no morphological abnormalities in CLK of either WT or CTGF<sup>-/-</sup> mice. Renal cortex of both WT and CTGF<sup>-/-</sup> OBK showed tubular dilatation, atrophy, and casts (Figure 2A). Analysis of extracellular matrix accumulation by Masson's trichrome (MTC) staining revealed that WT OBK shows a significant increase of tubulointerstitial fibrosis compared to WT CLK ( $P < 0.001$ , Figure 2A and 2B). The percentage MTC positive area was significantly decreased in CTGF<sup>-/-</sup> OBK compared to WT OBK ( $P < 0.01$ , Figure 2A and 2B). Collagen type 1 alpha 2 (Coll1 $\alpha$ 2) mRNA expression was significantly increased in WT OBK compared to WT CLK ( $P < 0.001$ , Figure 2D), but significantly decreased in CTGF<sup>-/-</sup> OBK compared to WT OBK ( $P < 0.001$ , Figure 2d). Staining for Alpha-smooth muscle actin ( $\alpha$ -SMA), a myofibroblast marker, showed a significant increase in WT OBK compared to WT CLK ( $P < 0.001$ , Figure 2A, C), and was significantly decreased in CTGF<sup>-/-</sup> OBK compared to WT OBK ( $P < 0.01$ , Figure 2A, C). During the experimental period, body weight was maintained better in CTGF<sup>-/-</sup> mice ( $97.9 \pm 2.6\%$ ) than in WT mice ( $93.2 \pm 2.5\%$ ;  $P < 0.01$ , Supplementary Figure 1).

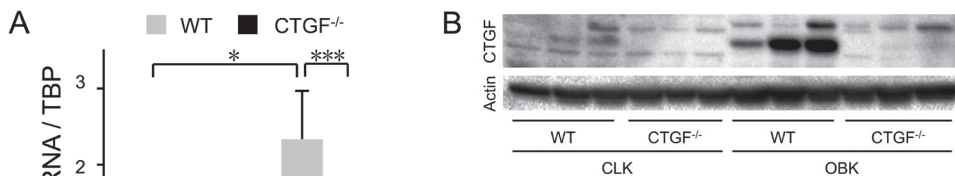


**Figure 1:** Expression of CTGF was dramatically decreased in CTGF knockout (CTGF<sup>-/-</sup>) mouse kidneys. **A:** RT-qPCR analysis showed that CTGF messenger RNA (mRNA) expression was significantly decreased in both of contralateral (CLK) and obstructed (OBK) kidneys of CTGF<sup>-/-</sup> mice compared to wild-type (WT) mice. Data are means  $\pm$  s.e. (N = 5 for WT mice and N = 9 for CTGF<sup>-/-</sup> mice). TATA-box binding protein (TBP) was used as an internal control. \* $P < 0.05$ , \*\*\* $P < 0.001$ . **B:** Both of CLK and OBK lysates showed the decreased expression of CTGF protein levels in CTGF<sup>-/-</sup> mice compared to WT mice by western blot analysis. Actin was shown as a loading control.

### *Lymphangiogenesis and VEGF-C expression are reduced in CTGF<sup>-/-</sup> OBK*

Next, we investigated whether near total reduction of CTGF was associated with a reduction in lymphangiogenesis. Lymphatic endothelial hyaluronan receptor-1 (LYVE-1) is specifically expressed in lymph vessels (28). LYVE-1 positive lymphatic vessels were seen only adjacent to renal blood vessels in CLK of both WT and CTGF<sup>-/-</sup> mice (Figure 3A). LYVE-1-positive lymphatic vessels were observed in the injured cortical tubulointerstitial area in OBK of both groups (Figure 3A). Quantification showed that the density of LYVE-1-positive lymphatic vessels in the renal cortex was significantly increased in OBK of WT mice compared to WT CLK ( $P < 0.005$ , Figure 3A and 3B). Compared to OBK of WT mice however, CTGF<sup>-/-</sup> had a significantly lower lymphatic vessel density ( $P < 0.05$ , Figure 3A and B). VEGF-C Immunohistochemistry (IHC) was barely detectable in CLK of both WT and CTGF<sup>-/-</sup> mice, and levels rose significantly in OBK of WT mice ( $P < 0.005$ , Figure 3A and 3C). However, VEGF-C area positivity was significantly reduced in CTGF<sup>-/-</sup> OBK compared to WT OBK ( $P < 0.005$ , Figure 3A and 3C). qPCR analysis showed that LYVE-1 and VEGF-C mRNA expression were increased 20.3- and 2.2-fold respectively in WT OBK compared to WT CLK. CTGF<sup>-/-</sup> OBK showed a significant decrease of both LYVE-1 and VEGF-C mRNA expression compared to WT OBK ( $P < 0.05$ , Figure 3D and 3E).

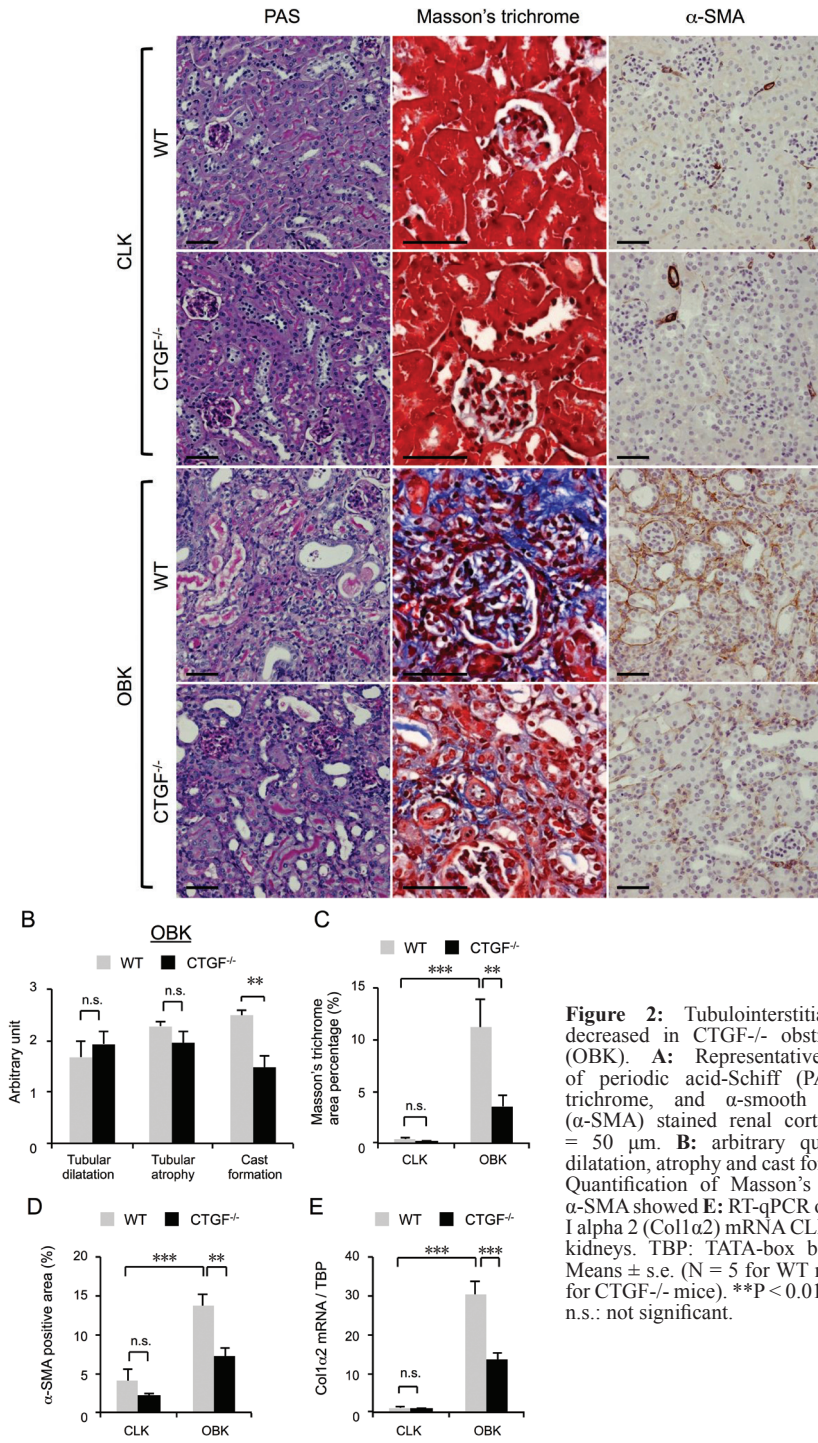
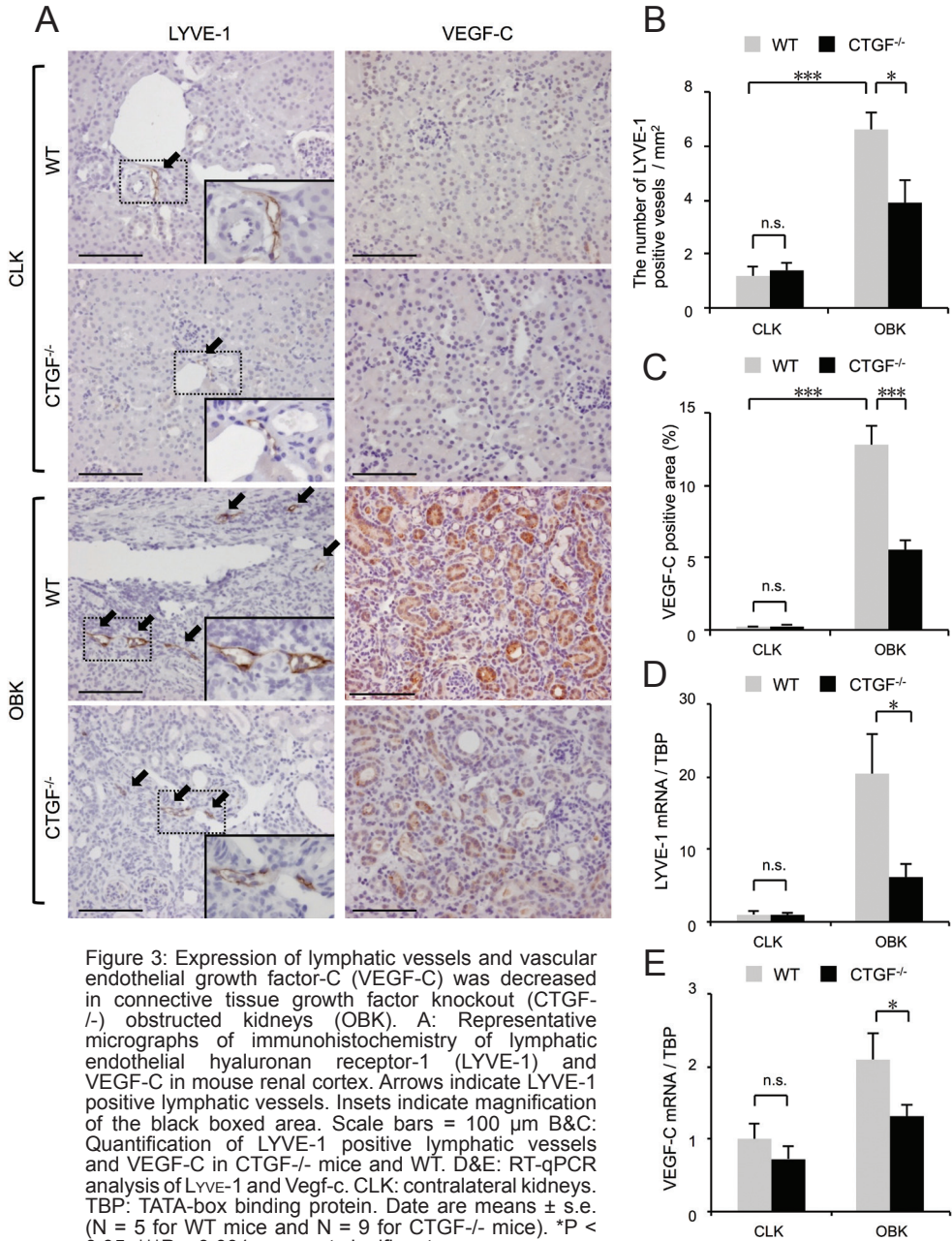


**Figure 2:** Tubulointerstitial fibrosis is decreased in CTGF<sup>-/-</sup> obstructed kidneys (OBK). **A:** Representative micrographs of periodic acid-Schiff (PAS), Masson's trichrome, and  $\alpha$ -smooth muscle actin ( $\alpha$ -SMA) stained renal cortex. Scale bars = 50  $\mu$ m. **B:** arbitrary quantification of dilatation, atrophy and cast formation. **C&D:** Quantification of Masson's trichrome and  $\alpha$ -SMA showed **E:** RT-qPCR of collagen type I alpha 2 (Col1a2) mRNA CLK: contralateral kidneys. TBP: TATA-box binding protein. Means  $\pm$  s.e. (N = 5 for WT mice and N = 9 for CTGF<sup>-/-</sup> mice). \*\*P < 0.01, \*\*\*P < 0.001, n.s.: not significant.



*CTGF induces VEGF-C production in proximal tubular cells*

We investigated CTGF-induced VEGF-C expression in HK-2 cells to assess the role of CTGF in renal lymphangiogenic signaling. Recombinant human full-length (FL)-CTGF dose-dependently upregulated VEGF-C mRNA expression in HK-2 cells 8h after incubation ( $P < 0.05$ , Figure 4A). We inhibited CTGF expression by the transfection of CTGF short-interfering RNA (siRNA) in HK-2 cells with or without TGF- $\beta$ 1 treatment. Non-targeting siRNA was used as a control siRNA. CTGF mRNA expression was significantly increased by TGF- $\beta$ 1 8h ( $P < 0.001$ ), and CTGF siRNA significantly reduced CTGF expression in both control ( $P < 0.05$ ) and TGF- $\beta$ 1 treatment condition ( $P < 0.001$ ) compared to control siRNA (Figure 4B). TGF- $\beta$ 1 treatment significantly upregulated VEGF-C mRNA expression ( $P < 0.001$ , Figure 4C). Although CTGF siRNA did not affect VEGF-C mRNA expression in control condition, it significantly suppressed VEGF-C upregulation treated with TGF- $\beta$ 1 ( $P < 0.05$ , Figure 4C). VEGF-C protein levels in supernatants of HK-2 cells determined by enzyme-linked immunosorbent assay (ELISA) showed that upregulated VEGF protein levels treated with TGF- $\beta$ 1 after 24h of incubation ( $P < 0.001$ ) was significantly decreased by CTGF siRNA compared to control siRNA ( $P < 0.01$ , Figure 4D). The upregulation of the canonical TGF- $\beta$  transcriptional target Plasminogen activator inhibitor-1 (PAI-1) was also significantly suppressed by CTGF siRNA ( $P < 0.05$ , supplementary Figure 2).

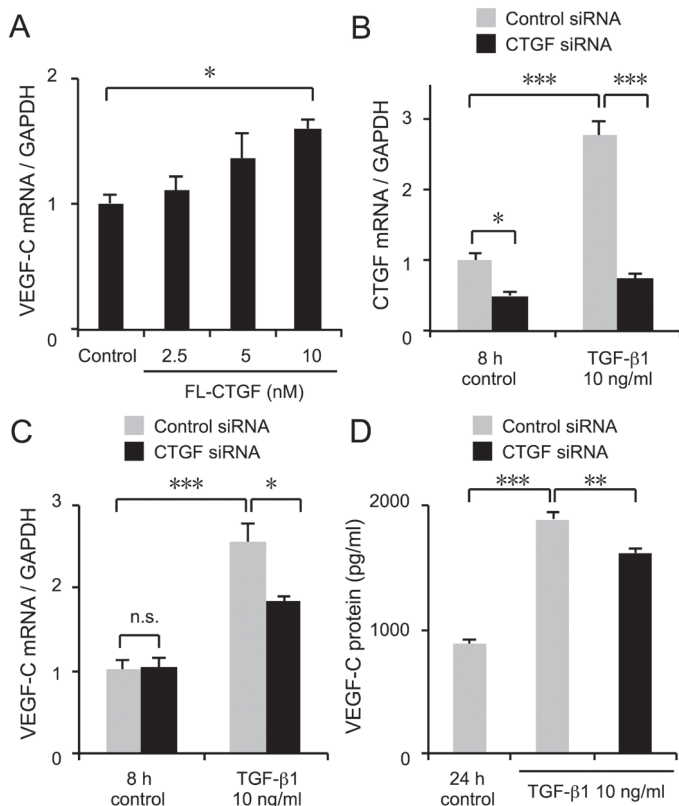


**Figure 4:** CTGF induced VEGF-C production in cultured human renal proximal tubular epithelial cells (HK-2). **A:** HK-2 cells were treated with recombinant human full-length CTGF (FL-CTGF). **B-D:** HK-2 cells were transfected with CTGF small interfering RNA (siRNA) and treated with transforming growth factor- $\beta$ 1 (TGF- $\beta$ 1). Non-targeting siRNA was used as a control siRNA. CTGF (**A**) and VEGF-C (**A&C**) messenger RNA (mRNA) was determined by quantitative real-time PCR. (**A-C**) Glyceraldehyde-3-phosphate dehydrogenase (GAPDH) was used as an internal control. (**D**) VEGF-C protein level in the supernatant was determined by enzyme-linked immunosorbent assay. Data are means  $\pm$  s.e. (N = 4). \* $P < 0.05$ , \*\* $P < 0.01$ , \*\*\* $P < 0.001$ , n.s.: not significant.

*CTGF directly binds to VEGF-C*

To analyze the binding of CTGF to VEGF-C, we used surface plasmon resonance. CTGF displayed time dependent association followed by dissociation with immobilized VEGF-C ( $K_d = 243 \text{ nM} \pm 24$ ; Figure 5A and 5B). Additionally, we tested NH<sub>2</sub>- and COOH-terminal proteolytic CTGF fragment (N-CTGF and C-CTGF) binding to VEGF-C. This showed that C-CTGF binds to VEGF-C with similar

affinity as FL-CTGF ( $K_d=239\text{nM}\pm\text{SD } 14$ ). No association was observed for N-terminal CTGF.

*CTGF suppressed VEGF-C-induced tube formation by human dermal lymphatic microvascular endothelial cells (HMVEC-dLy)* HMVEC-dLy were plated on Matrigel surface and incubated for 6 hours. Cell growth was assessed by formation of the number of capillary-like tubes. HMVEC-dLy efficiently formed tube structures with VEGF-C treatment ( $P<0.001$ , Figure 6A, 6B, 6F). Remarkably, the addition of FL-CTGF significantly suppressed VEGF-C-induced tube formation ( $P<0.01$ , Figure 6b, c, f). In contrast, equivalent amounts of N-CTGF and C-CTGF had no significant effect on VEGF-C-induced tube formation (Figure 6B-D and 6F).

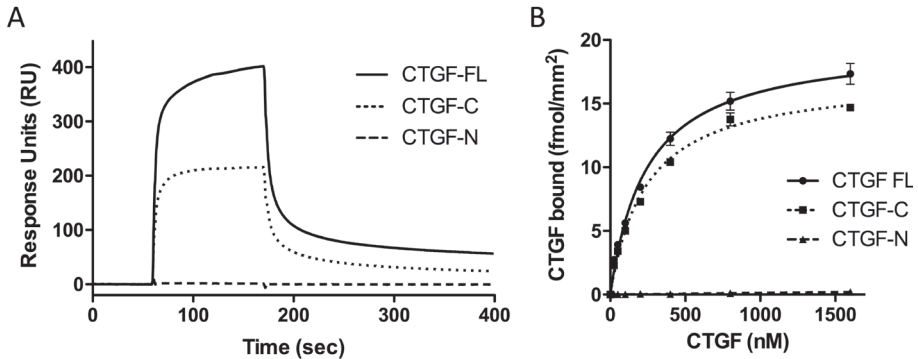


**Figure 5:** Full length and C terminal Connective tissue growth factor (CTGF) directly binds to vascular endothelial growth factor-C (VEGF-C). **A:** Physical interaction between CTGF and VEGF-C was demonstrated by Surface Plasmon Resonance. Purified full length (FL), C-terminal and N-terminal CTGF were run over VEGF-C sensor chips. Association and subsequent dissociation were monitored by a change in resonance units. **B:** Binding at equilibrium was plotted against indicated CTGF concentrations, from which half maximal binding ( $K_d$ ) was calculated. Mean $\pm$ SD shown,  $n=3$ .

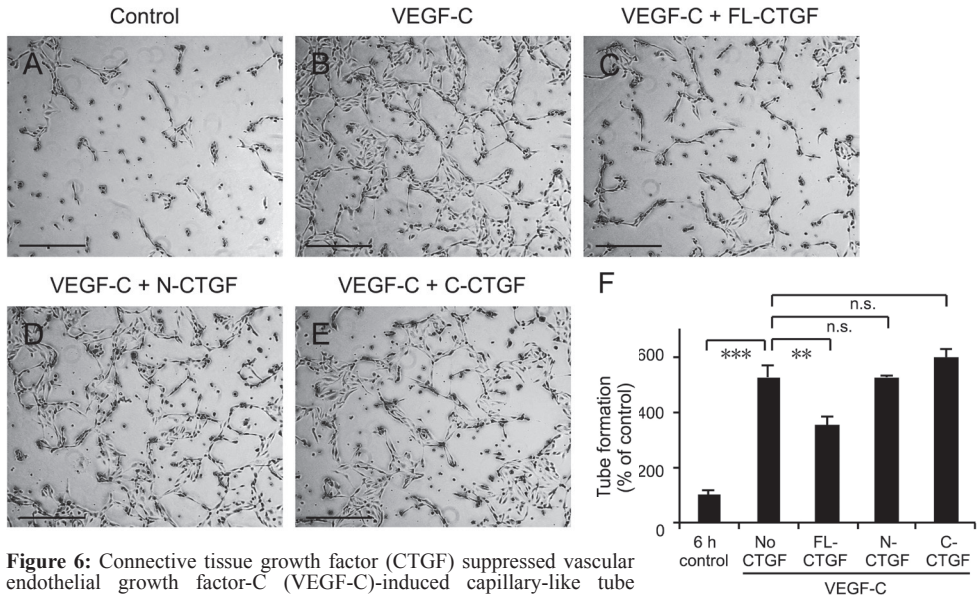


**Figure 6:** Connective tissue growth factor (CTGF) suppressed vascular endothelial growth factor-C (VEGF-C)-induced capillary-like tube formation in human dermal lymphatic microvascular endothelial cells (HMVEC-dLy). (A&B) VEGF-C efficiently induced capillary-like tube formation in HMVEC-dLy seeded on Matrigel in serum free medium for 6 h (a and b). HMVEC-dLy were treated with recombinant human full-length CTGF (FL-CTGF) (C) or NH2-terminal fragment of CTGF (N-CTGF) (D) or COOH-terminal fragment of CTGF (C-CTGF) (e) in the presence of VEGF-C. Scale bars = 400  $\mu\text{m}$ . **F:** Tube formation was quantified by counting the number of tubes. FL-CTGF suppressed VEGF-C-induced tube formation. N-CTGF and C-CTGF had no significant effect on tube formation induced by VEGF-C. Data are means  $\pm$  s.e. ( $N = 3$ ). \*\* $P < 0.01$ , \*\*\* $P < 0.001$ , n.s.: not significant.

## Discussion

In this study, we show that tubulointerstitial fibrosis and lymphangiogenesis in severe obstructive nephropathy is suppressed by a reduction of CTGF expression well below physiological baseline levels. Several reports show that reduction of CTGF expression by approximately 50% reduces fibrosis in mild to moderately severe models of obstructive (22), diabetic nephropathy (21), allograft nephropathy (29), and in the remnant kidney model (30). However, 50% reduction of CTGF expression in hemizygous CTGF knockout (CTGF<sup>+/-</sup>) does not suffice to reduce fibrosis in severe models of kidney injury, including 14 days UUO (23). Of note, CTGF expression in these models remained significantly elevated compared to baseline control levels. We here show that, unlike 50% reduction in CTGF <sup>+/-</sup> mice, stronger reduction of CTGF expression to levels well below baseline does significantly attenuate tubulointerstitial fibrosis and  $\alpha$ -SMA expression also in the 14 day UUO model of severe chronic kidney disease.

In addition, we found that near total reduction of CTGF also suppressed lymphangiogenesis, most likely as a result of decreased expression of VEGF-C, suggesting that CTGF might also be involved in regulation of VEGF-C expression and lymphangiogenesis. In line with this, we found that CTGF co-stimulation enhanced TGF- $\beta$ 1 induced VEGF-C expression in HK-2 cells, while CTGF siRNA significantly suppressed TGF- $\beta$ 1 induced VEGF-C. Thus, inhibition of CTGF might be a promising therapeutic approach targeting both fibrosis and lymphangiogenesis. TGF- $\beta$ 1 induced VEGF-C expression also occurs during dialysis associated peritoneal fibrosis (16), and might also be largely CTGF mediated, especially since peritoneal fibrosis is associated with high levels of CTGF (31).

Induction of lymphangiogenesis via release of VEGF-C/D is correlated with a poor prognosis in a number of solid tumors (32), and blocking VEGFR-3 signaling inhibited tumor lymphangiogenesis as well as lymph node metastasis in animal models (33, 34). Interestingly, WNT1-inducible-signaling pathway protein-1 (WISP-1), another member of the CCN (CTGF/Cyr61/Nov) family, was shown to promote lymphangiogenesis via upregulation of VEGF-C expression in oral squamous cell carcinoma (35). A therapeutic monoclonal human antibody against CTGF, FG-3019, reduced tumor progression in two mouse models of pancreatic cancer and melanoma (36, 37), and is currently under clinical investigation in a phase 1/2 trial of chemotherapy in pancreatic cancer patients (Clinicaltrials.gov reference number NCT02210559). Considering the now apparent role of CTGF in lymphangiogenesis, the anti-metastatic effect of CTGF reduction might be due at least in part to reduction of tumor lymphangiogenesis.

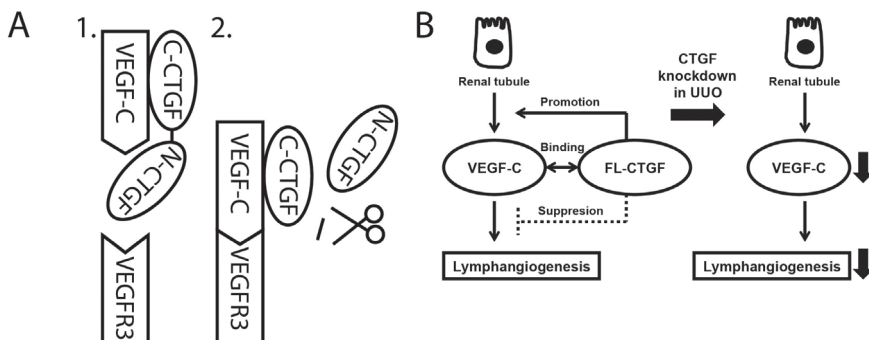


**Figure 7:** Connective tissue growth factor (CTGF) plays a significant role in renal lymphangiogenesis. **A:** Situation 1: Full length (C&N terminal) CTGF binds VEGF-C via the C terminal domain and the attached N terminal domain inhibits binding of VEGF-C to the VEGFR3 via steric interference. Situation 2: Upon proteolytic cleavage of FL-CTGF, only the C-terminal part of CTGF binds VEGF-C and N-terminal steric interference is no longer present. **B:** Full-length CTGF (FL-CTGF) promotes vascular endothelial growth factor-C (VEGF-C) production in renal tubular epithelial cells. FL-CTGF binds to VEGF-C, and suppresses VEGF-C-induced lymphangiogenesis. NH<sub>2</sub>-terminal fragment and COOH-terminal fragment of CTGF have no influence on VEGF-C function. CTGF knockdown suppresses VEGF-C expression and lymphangiogenesis in the unilateral ureteral obstruction (UUO) model.

With respect to by which mechanisms CTGF might modulate lymphangiogenic activity of VEGF-C, we observed direct binding of FL-CTGF to VEGF-C, and suppression of VEGF-C-induced lymphatic endothelial cell growth in FL-CTGF co-stimulated cultures. In vivo as well as in vitro, CTGF is readily cleaved by proteolysis of its hinge region, leading to dissociation of a C- and an N-terminal CTGF fragment (CTGF-N and CTGF-C). In our SPR analysis, the CTGF-N did not bind to VEGF-C at all, but the CTGF-C bound VEGF-C with similar affinity as FL-CTGF. Unlike FL-CTGF, however, CTGF-C did not suppress in vitro lymphatic capillary tube formation endothelial. This suggests that FL-CTGF binds to VEGF-C through its C-terminal part, and that inhibition of VEGF-C activity is due to steric interference by the other, N-terminal half of the FL-CTGF molecule, e.g. with VEGF-C binding to VEGFR3. Thus, upon proteolytic cleavage of the CTGF hinge region, C-terminal CTGF can still bind or remain bound to VEGF-C, but the cleaved off N-terminal part can no longer inhibit VEGF-C interaction with VEGFR3 (Figure 7A). Thus CTGF is required for VEGF-C expression, but also negatively influences VEGF-C signaling via direct physical interaction.

This would be similar to previous observations regarding CTGF interaction with VEGF-A. It has been shown that FL-CTGF can bind to VEGF-A, and inhibit VEGF-A-induced angiogenesis in vitro and in vivo (26, 38). Some matrix metalloproteinases can cleave FL-CTGF in complex with VEGF-A into N-CTGF and C-CTGF, upon which the two CTGF fragments dissociate, thereby releasing the angiogenic activity of VEGF-A that was inhibited while bound to FL-CTGF (25, 39). All VEGF members share a VEGF homology domain (40), and possibly this domain is recognized by C-CTGF.

Whether and how inhibition of lymphangiogenesis might reduce progression of fibrosis remains illusive. It has been speculated that lymphatic vessels not only drain inflammatory infiltrate but also maintain the immune response by producing lymphatic chemokines that attract inflammatory cells (9). Observations regarding effects of blocking lymphangiogenesis have been ambiguous. For instance, in a renal transplantation model, sirolimus inhibited lymphangiogenesis, which was associated with attenuated development of chronic kidney allograft injury (41). In contrast, VEGF-C treatment attenuated lung allograft rejection by inducing lymphangiogenesis, probably by facilitating clearance of detrimental hyaluronan from the lung allografts (8). During aspiration pneumonia increased lymphangiogenesis is observed, and treatment with VEGFR inhibitor or VEGFR-3 specific inhibitor improved inflammation and oxygen saturation (42). Blocking of lymphangiogenesis by soluble VEGFR-3 also improved ultrafiltration failure in a mouse peritoneal fibrosis model (43). Interestingly, Yazdani S et al. reported that specific blocking of lymphangiogenesis by anti-VEGFR-3 antibody did not prevent inflammation, interstitial fibrosis, and proteinuria in a rat model of proteinuric nephropathy (44). They also showed that macrophage depletion by clodronate liposomes did not prevent lymphangiogenesis in this model. This is in stark contrast to another report showing that treatment with clodronate liposomes markedly reduced the number of macrophages and lymphangiogenesis induced by UO (14, 45). Thus the requirement for lymphangiogenesis and efficacy of therapeutic intervention varies depending on organ and etiology of disease, and further studies are needed to understand the role of renal lymphangiogenesis in a variety of kidney diseases.

In conclusion, near total silencing of CTGF expression suppressed fibrosis, and lymphangiogenesis in severe obstructive nephropathy, and CTGF promoted VEGF-C production in renal tubular cells with or without TGF- $\beta$  treatment. FL-CTGF directly bound to VEGF-C, and suppressed VEGF-C-induced in vitro lymphatic capillary tube formation. However, the former VEGF-C expression inducing effect of CTGF is potentially more profound than the latter physical inhibition of VEGF-C signaling, since CTGF-/- OBK showed less lymphatic vessels compared to WT OBK (Figure 7B). Thus, CTGF plays a significant role in renal lymphangiogenesis through the interaction with VEGF-C. Further clarification of the mechanism of lymphangiogenesis in kidney fibrosis might lead to additional interventional strategies to combat chronic kidney disease.

#### **Disclosure & Acknowledgements**

R.G. received research supports from FibroGen, a company invested in developing anti-CTGF therapy. We are grateful for the assistance of Roel Broekhuizen (Dept. of Pathology, UMC Utrecht, the Netherlands).

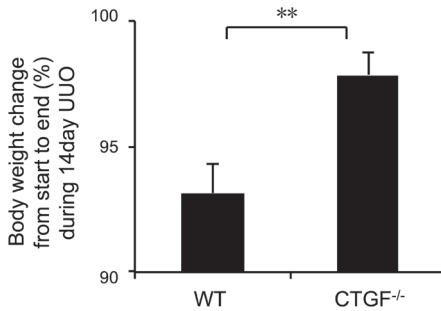


## References

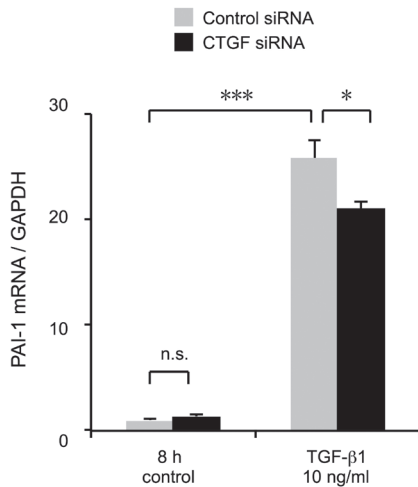
1. Fung E, Kurella Tamura M. Epidemiology and Public Health Concerns of CKD in Older Adults. *Adv Chronic Kidney Dis.* 2016;23(1):8-11.
2. Ghanta M, Jim B. Renal Transplantation in Advanced Chronic Kidney Disease Patients. *Med Clin North Am.* 2016;100(3):465-76.
3. Thomas B, Wulf S, Bikbov B, Perico N, Cortinovis M, Courville de Vaccaro K, et al. Maintenance Dialysis throughout the World in Years 1990 and 2010. *J Am Soc Nephrol.* 2015;26(11):2621-33.
4. Norrmen C, Tammela T, Petrova TV, Alitalo K. Biological basis of therapeutic lymphangiogenesis. *Circulation.* 2011;123(12):1335-51.
5. Alitalo A, Detmar M. Interaction of tumor cells and lymphatic vessels in cancer progression. *Oncogene.* 2012;31(42):4499-508.
6. Kim H, Kataru RP, Koh GY. Inflammation-associated lymphangiogenesis: a double-edged sword? *J Clin Invest.* 2014;124(3):936-42.
7. Dashkevich A, Hagl C, Beyersdorf F, Nykanen AI, Lemstrom KB. VEGF Pathways in the Lymphatics of Healthy and Diseased Heart. *Microcirculation.* 2016;23(1):5-14.
8. Cui Y, Liu K, Monzon-Medina ME, Padera RF, Wang H, George G, et al. Therapeutic lymphangiogenesis ameliorates established acute lung allograft rejection. *J Clin Invest.* 2015;125(11):4255-68.
9. Kerjaschki D, Regele HM, Moosberger I, Nagy-Bojarski K, Watschinger B, Soleiman A, et al. Lymphatic neoangiogenesis in human kidney transplants is associated with immunologically active lymphocytic infiltrates. *J Am Soc Nephrol.* 2004;15(3):603-12.
10. Yazdani S, Navis G, Hillebrands JL, van Goor H, van den Born J. Lymphangiogenesis in renal diseases: passive bystander or active participant? *Expert Rev Mol Med.* 2014;16:e15.
11. Coso S, Bovay E, Petrova TV. Pressing the right buttons: signaling in lymphangiogenesis. *Blood.* 2014;123(17):2614-24.
12. Zheng W, Aspelund A, Alitalo K. Lymphangiogenic factors, mechanisms, and applications. *J Clin Invest.* 2014;124(3):878-87.
13. Sakamoto I, Ito Y, Mizuno M, Suzuki Y, Sawai A, Tanaka A, et al. Lymphatic vessels develop during tubulointerstitial fibrosis. *Kidney Int.* 2009;75(8):828-38.
14. Lee AS, Lee JE, Jung YJ, Kim DH, Kang KP, Lee S, et al. Vascular endothelial growth factor-C and -D are involved in lymphangiogenesis in mouse unilateral ureteral obstruction. *Kidney Int.* 2013;83(1):50-62.
15. Suzuki Y, Ito Y, Mizuno M, Kinashi H, Sawai A, Noda Y, et al. Transforming growth factor-beta induces vascular endothelial growth factor-C expression leading to lymphangiogenesis in rat unilateral ureteral obstruction. *Kidney Int.* 2012;81(9):865-79.
16. Kinashi H, Ito Y, Mizuno M, Suzuki Y, Terabayashi T, Nagura F, et al. TGF-beta1 promotes lymphangiogenesis during peritoneal fibrosis. *J Am Soc Nephrol.* 2013;24(10):1627-42.
17. Falke LL, Goldschmeding R, Nguyen TQ. A perspective on anti-CCN2 therapy for chronic kidney disease. *Nephrol Dial Transplant.* 2014;29 Suppl 1:i30-i7.
18. Gupta S, Clarkson MR, Duggan J, Brady HR. Connective tissue growth factor: potential role in glomerulosclerosis and tubulointerstitial fibrosis. *Kidney Int.* 2000;58(4):1389-99.
19. Phanish MK, Winn SK, Dockrell ME. Connective tissue growth factor-(CTGF, CCN2)--a marker, mediator and therapeutic target for renal fibrosis. *Nephron Exp Nephrol.* 2010;114(3):e83-92.
20. Abreu JG, Ketpura NI, Reversade B, De Robertis EM. Connective-tissue growth factor (CTGF) modulates cell signalling by BMP and TGF-beta. *Nat Cell Biol.* 2002;4(8):599-604.
21. Guha M, Xu ZG, Tung D, Lanting L, Natarajan R. Specific down-regulation of connective tissue growth factor attenuates progression of nephropathy in mouse models of type 1 and type 2 diabetes. *FASEB J.* 2007;21(12):3355-68.
22. Yokoi H, Mukoyama M, Nagae T, Mori K, Suganami T, Sawai K, et al. Reduction in connective tissue growth factor by antisense treatment ameliorates renal tubulointerstitial fibrosis. *J Am Soc Nephrol.* 2004;15(6):1430-40.
23. Falke LL, Dendooven A, Leeuwis JW, Nguyen TQ, van Geest RJ, van der Giezen DM, et al. Hemizygous deletion of CTGF/CCN2 does not suffice to prevent fibrosis of the severely injured kidney. *Matrix Biol.* 2012;31(7-8):421-31.
24. Pi L, Shenoy AK, Liu J, Kim S, Nelson N, Xia H, et al. CCN2/CTGF regulates neovessel formation via targeting structurally conserved cystine knot motifs in multiple angiogenic regulators. *FASEB J.* 2012;26(8):3365-79.
25. Hashimoto G, Inoki I, Fujii Y, Aoki T, Ikeda E, Okada Y. Matrix metalloproteinases cleave connective tissue growth factor and reactivate angiogenic activity of vascular endothelial growth factor 165. *J Biol Chem.* 2002;277(39):36288-95.
26. Inoki I, Shiomi T, Hashimoto G, Enomoto H, Nakamura H, Makino K, et al. Connective tissue growth factor binds vascular endothelial growth factor (VEGF) and inhibits VEGF-induced angiogenesis. *FASEB J.* 2002;16(2):219-21.
27. Liu S, Shi-wen X, Abraham DJ, Leask A. CCN2 is required for bleomycin-induced skin fibrosis in mice. *Arthritis Rheum.* 2011;63(1):239-46.
28. Banerji S, Ni J, Wang SX, Clasper S, Su J, Tammi R, et al. LYVE-1, a new homologue of the CD44 glycoprotein, is a lymph-specific receptor for hyaluronan. *J Cell Biol.* 1999;144(4):789-801.
29. Luo GH, Lu YP, Song J, Yang L, Shi YJ, Li YP. Inhibition of connective tissue growth factor by small interfering RNA prevents renal fibrosis in rats undergoing chronic allograft nephropathy. *Transplant Proc.* 2008;40(7):2365-9.

30. Okada H, Kikuta T, Kobayashi T, Inoue T, Kanno Y, Takigawa M, et al. Connective tissue growth factor expressed in tubular epithelium plays a pivotal role in renal fibrogenesis. *J Am Soc Nephrol.* 2005;16(1):133-43.
31. Mizutani M, Ito Y, Mizuno M, Nishimura H, Suzuki Y, Hattori R, et al. Connective tissue growth factor (CTGF/CCN2) is increased in peritoneal dialysis patients with high peritoneal solute transport rate. *Am J Physiol Renal Physiol.* 2010;298(3):F721-33.
32. Sleeman JP, Thiele W. Tumor metastasis and the lymphatic vasculature. *Int J Cancer.* 2009;125(12):2747-56.
33. He Y, Rajantie I, Pajusola K, Jeltsch M, Holopainen T, Yla-Herttuala S, et al. Vascular endothelial cell growth factor receptor 3-mediated activation of lymphatic endothelium is crucial for tumor cell entry and spread via lymphatic vessels. *Cancer Res.* 2005;65(11):4739-46.
34. Quagliata L, Klusmeier S, Cremers N, Pytowski B, Harvey A, Pettis RJ, et al. Inhibition of VEGFR-3 activation in tumor-draining lymph nodes suppresses the outgrowth of lymph node metastases in the MT-450 syngeneic rat breast cancer model. *Clin Exp Metastasis.* 2014;31(3):351-65.
35. Lin CC, Chen PC, Lein MY, Tsao CW, Huang CC, Wang SW, et al. WISP-1 promotes VEGF-C-dependent lymphangiogenesis by inhibiting miR-300 in human oral squamous cell carcinoma cells. *Oncotarget.* 2016;7(9):9993-10005.
36. Finger EC, Cheng CF, Williams TR, Rankin EB, Bedogni B, Tachiki L, et al. CTGF is a therapeutic target for metastatic melanoma. *Oncogene.* 2014;33(9):1093-100.
37. Neesse A, Frese KK, Bapiro TE, Nakagawa T, Sternlicht MD, Seeley TW, et al. CTGF antagonism with mAb FG-3019 enhances chemotherapy response without increasing drug delivery in murine ductal pancreas cancer. *Proc Natl Acad Sci U S A.* 2013;110(30):12325-30.
38. Pi L, Chung PY, Sriram S, Rahman MM, Song WY, Scott EW, et al. Connective tissue growth factor differentially binds to members of the cystine knot superfamily and potentiates platelet-derived growth factor-B signaling in rabbit corneal fibroblast cells. *World J Biol Chem.* 2015;6(4):379-88.
39. Dean RA, Butler GS, Hamma-Kourbali Y, Delbe J, Brigstock DR, Courty J, et al. Identification of candidate angiogenic inhibitors processed by matrix metalloproteinase 2 (MMP-2) in cell-based proteomic screens: disruption of vascular endothelial growth factor (VEGF)/heparin affinity regulatory peptide (pleiotrophin) and VEGF/Connective tissue growth factor angiogenic inhibitory complexes by MMP-2 proteolysis. *Mol Cell Biol.* 2007;27(24):8454-65.
40. Hoeben A, Landuyt B, Highley MS, Wildiers H, Van Oosterom AT, De Bruijn EA. Vascular endothelial growth factor and angiogenesis. *Pharmacol Rev.* 2004;56(4):549-80.
41. Palin NK, Savikko J, Koskinen PK. Sirolimus inhibits lymphangiogenesis in rat renal allografts, a novel mechanism to prevent chronic kidney allograft injury. *Transpl Int.* 2013;26(2):195-205.
42. Nihei M, Okazaki T, Ebihara S, Kobayashi M, Niu K, Gui P, et al. Chronic inflammation, lymphangiogenesis, and effect of an anti-VEGFR therapy in a mouse model and in human patients with aspiration pneumonia. *J Pathol.* 2015;235(4):632-45.
43. Terabayashi T, Ito Y, Mizuno M, Suzuki Y, Kinashi H, Sakata F, et al. Vascular endothelial growth factor receptor-3 is a novel target to improve net ultrafiltration in methylglyoxal-induced peritoneal injury. *Lab Invest.* 2015;95(9):1029-43.
44. Yazdani S, Hijmans RS, Poosti F, Dam W, Navis G, van Goor H, et al. Targeting tubulointerstitial remodeling in proteinuric nephropathy in rats. *Dis Model Mech.* 2015;8(8):919-30.
45. Jung YJ, Lee AS, Nguyen-Thanh T, Kang KP, Lee S, Jang KY, et al. Hyaluronan-induced VEGF-C promotes fibrosis-induced lymphangiogenesis via Toll-like receptor 4-dependent signal pathway. *Biochem Biophys Res Commun.* 2015;466(3):339-45.

**Supplementary material**

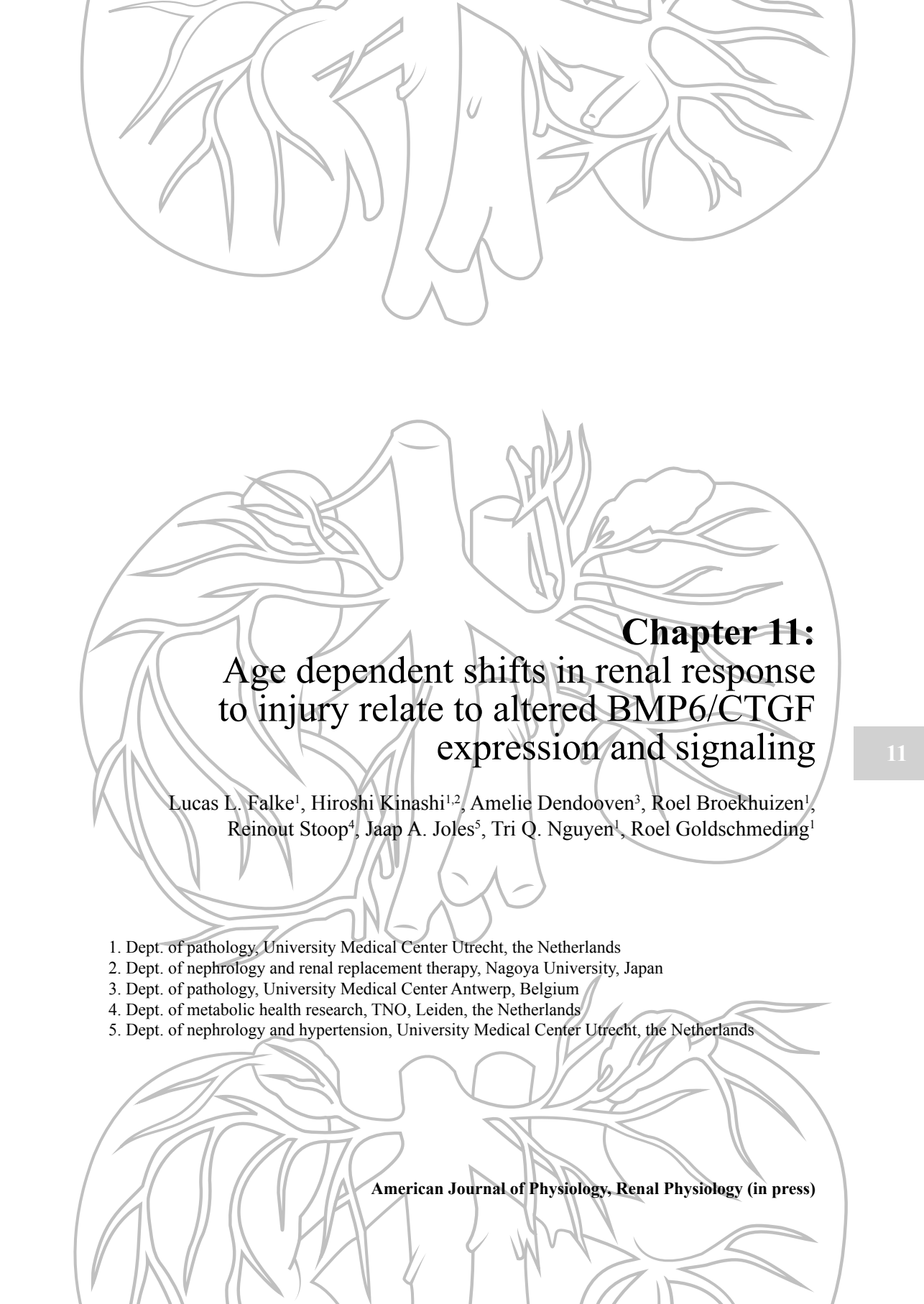


**Supplementary Figure 1.** Connective tissue growth factor knockout (CTGF<sup>-/-</sup>) mice showed a beneficial effect for maintaining body weight during 14-days unilateral ureteral obstruction (UUO) model. Percentage of mouse body weight 14 days after UUO is shown. CTGF<sup>-/-</sup> mice (97.9±2.6 %) showed a beneficial effect for maintaining body weight during an experimental period compared with wild-type (WT) mice (93.2±2.5 %). Data are means ± s.e. (N = 5 for WT mice and N = 9 for CTGF<sup>-/-</sup> mice). \*\*P < 0.01.



**Supplementary Figure 2.** Connective tissue growth factor short-interfering RNA (CTGF siRNA) suppressed plasminogen activator inhibitor-1 (PAI-1) messenger RNA (mRNA) expression in cultured human renal proximal tubular epithelial cells (HK-2) treated with transforming growth factor-β1 (TGF-β1). HK-2 cells were transfected with CTGF siRNA and treated with TGF-β1. Non-targeting siRNA was used as a control siRNA. PAI-1 mRNA expression was determined by quantitative real-time PCR. Glyceraldehyde-3-phosphate dehydrogenase (GAPDH) was used as an internal control. PAI-1 mRNA expression was significantly increased by TGF-β1 treatment after 8 h incubation. TGF-β1-induced PAI-1 mRNA upregulation was significantly suppressed by CTGF siRNA. Data are means ± s.e. (N = 4). \*P < 0.05, \*\*\*P < 0.001, n.s.: not significant.

11



## **Chapter 11:** Age dependent shifts in renal response to injury relate to altered BMP6/CTGF expression and signaling

Lucas L. Falke<sup>1</sup>, Hiroshi Kinashi<sup>1,2</sup>, Amelie Dendooven<sup>3</sup>, Roel Broekhuizen<sup>1</sup>,  
Reinout Stoop<sup>4</sup>, Jaap A. Joles<sup>5</sup>, Tri Q. Nguyen<sup>1</sup>, Roel Goldschmeding<sup>1</sup>

1. Dept. of pathology, University Medical Center Utrecht, the Netherlands
2. Dept. of nephrology and renal replacement therapy, Nagoya University, Japan
3. Dept. of pathology, University Medical Center Antwerp, Belgium
4. Dept. of metabolic health research, TNO, Leiden, the Netherlands
5. Dept. of nephrology and hypertension, University Medical Center Utrecht, the Netherlands

**Abstract**

Age is associated with an increased prevalence of chronic kidney disease (CKD), which, through progressive tissue damage and fibrosis, ultimately leads to loss of kidney function. Although much effort is put into studying CKD development experimentally, age has rarely been taken into account. Therefore, we investigated the effect of age on the development of renal tissue damage and fibrosis in a mouse model of obstructive nephropathy (i.e. unilateral ureter obstruction; UUU). We observed that after 14 days, obstructed kidneys of old mice had more tubulointerstitial atrophic damage but less fibrosis than those of young mice. This was associated with reduced connective tissue growth factor (CTGF), and higher BMP6 expression and pSMAD1/5/8 signaling, while TGF- $\beta$  expression and transcriptional activity were no different in obstructed kidneys of old and young mice. In vitro, CTGF bound to and inhibited BMP6 activity.

In summary, our data suggest that in obstructive nephropathy atrophy increases and fibrosis decreases with age, and that this relates to increased BMP signaling, most likely due to higher BMP6 and lower CTGF expression.

**Abbreviations:**

BMP (6/7)	- Bone Morphogenetic Protein (family member 6 or 7)
CTGF	- Connective Tissue Growth Factor
TGF $\beta$	- Transforming Growth Factor $\beta$
UUO	- Unilateral Ureter Obstruction
CLK	- Contralateral Kidney
OBK	- Obstructed Kidney
CKD	- Chronic Kidney Disease
KW	- Kidney Weight
BW	- Body Weight

## Introduction

Chronic kidney disease (CKD) primarily affects the aging population (11, 37, 42). Decline of kidney function with age might result from multifactorial changes in kidney physiology primarily due to “senescence” itself, and a more adverse response to injury (1, 5, 22, 43, 45, 47). As such, it has been proposed that the aging kidney increasingly accumulates extracellular matrix, leading to glomerulosclerosis and interstitial fibrosis (1, 25) and ultimately to loss of renal mass and reduced glomerular and tubular function (17, 51). Parameters such as diabetes, vitamin D deficiency, alterations in Renin Angiotensin and Aldosterone (RAAS) signaling, oxidative stress by reactive oxygen species (ROS) production and advanced glycation end (AGE) products are thought to underlie these morphological and functional changes of the kidney parenchyma (8). Furthermore, the age associated gradual decline in Klotho, a transmembrane FGF23 co-receptor expressed in the convoluted distal tubule under physiological condition renders kidneys more susceptible to injury, dysregulation of mineral homeostasis and fibrosis (28).

In young mice, kidney response to injury is profoundly influenced by the Transforming Growth Factor  $\beta$ -superfamily (TGF  $\beta$ ), including TGF $\beta$ 1, Bone Morphogenetic Protein 7 (BMP7), and BMP6 (14, 35). Canonical signaling of the TGF  $\beta$  superfamily is accomplished via Activin like kinase (ALK) activation and subsequent downstream SMAD phosphorylation. Activation of ALK4, 5 or 7 by TGF $\beta$  leads to fibrosis associated SMAD2/3 phosphorylation. ALK1-3 or 6 activation by BMP's leads to renoprotection associated SMAD1/5/8 phosphorylation (10). Under specific conditions, TGF $\beta$  has been shown to activate ALK1 (36). Upon injury, TGF $\beta$  levels rise and BMP levels drop rapidly (34). The shift in these factors is regarded as major early event in ensuing tissue damage with subsequent fibrosis following injury.

Connective Tissue Growth Factor is another immediate early factor shown to greatly influence the response to kidney injury. CTGF is a matricellular protein involved in various fibrosis associated phenomena such as extracellular matrix production, proliferation and myofibroblast differentiation (19). Although no exclusive CTGF receptor has been identified, CTGF has been known to interact with TGF $\beta$  and BMP7 thereby modulating signaling in favor of pro-fibrotic TGF $\beta$  whilst inhibiting BMP7 signaling (2, 35). As such, TGF $\beta$ , BMP6 and 7, and CTGF are regarded as major factors influencing the renal response to injury. The age associated production of reaction oxygen species (ROS) is related to increased levels of pro-fibrotic growth factors (41), but little is known about the impact of aging on the regulation of these factors in the kidney. It has been reported that pro-fibrotic TGF $\beta$  signaling generally increases with age, which might at least in part be due to the gradual decline of Klotho (15).

The effect of ageing on renal CTGF expression is largely unknown, but CTGF/CCN2 was found to be reduced in aged skin in association with loss of collagen (39). Interestingly, conditional overexpression of CTGF prevented age-related degenerative changes in epiphyseal cartilage of rats (27). In contrast, ageing is associated with increased cardiac CTGF expression in mice (40, 48), suggesting that age related differential expression of CTGF is context dependent.

Reports on age-associated changes in expression and signaling of the (anti-fibrotic) BMPs are scarce, but it has been noted that BMP7 expression declines in aging cartilage (3), while increased expression of BMP6 was found in Alzheimer brains (12), and early aging in Klotho-deficient mice was associated with increased BMP-signaling and vascular calcification (23). To the best of our knowledge, there are no previous data on age-related changes in renal BMP expression and signaling. Based on our find in the current study, we hypothesize that old and young kidneys respond differently to injury in association with differential TGF $\beta$ /BMP/CTGF signaling.

Unilateral Ureter Obstruction (UUO) is a commonly used model of renal injury characterized by inflammation, extensive morphological damage and fibrosis (7, 29). Upon obstruction, the quick rise in TGF $\beta$  levels and subsequent phosphorylation of SMAD2/3 and PAI1 upregulation are regarded as key events ultimately leading to fibrosis (26, 44). We studied morphological damage and fibrosis following 14 days of UUO and observed a shift from a largely fibrotic phenotype in young, to a more atrophic phenotype of tubulointerstitial damage in old kidneys, although BMP7 and TGF $\beta$  were not different.

This phenotypic shift might derive from a synergistic effect of the observed decrease of CTGF and increase of BMP6, even more so since we noted in vitro that CTGF directly binds to BMP6 and inhibits its signaling activity. Together these findings provide further understanding of the age associated response to injury, and might help to identify better diagnostic methods and therapeutic interventions in the aging population.



## Materials and Methods

### *Animals*

Two groups of C57Bl6/J mice (16 week old (n=6; Young) and 50 week old (n=6; Old)) were housed under standard conditions and subjected to UUO. Under general isoflurane anesthesia the left ureter was ligated with silk suture through the left flank, after which the wound was closed and stitched. One young and one old mouse deteriorated in condition rapidly after surgery and both were sacrificed within a week. These mice were excluded from further analysis. After 13 days the remaining mice were housed in metabolic cages for 16 hours for urine collection. At day 14 they were killed and organs and plasma were collected for analysis. Animal experiments were carried out with approval of the Experimental Animal Ethics Committee of the University of Utrecht conform Dutch law.

### *Immunohistochemistry*

Fresh kidney tissue was fixed in buffered 4% paraformaldehyde solution and embedded in paraffin. 3 $\mu$ m sections were cut, embedded on object slides and incubated in a stove at 60°C for 16 hours. Sections were deparaffinised and rehydrated in xylene, 100% & 70% ethanol respectively, after which the sections were rinsed in de-mineralized water.

Periodic acid Schiff and Masson-trichrome staining was performed using standard procedures. For quantification of morphological damage, 10 arbitrary cortical fields per kidney were scored in PAS-stained sections with regards to atrophy and dilatation (0=<1%, 1=1-25%, 2=25-50%, 3=50-75%, 4=75-100%).

For immunohistochemistry, antigen retrieval consisted of 20 minute boiling in either citrate buffer (pH=6), EDTA buffer (pH=9) or 10 minute pepsin digestion depending upon primary antibody. Slides were incubated with the following antibodies:  $\alpha$ SMA (EDTA, 1:200, Abcam, Cambridge, UK), CTGF (Citrate, 1:200, Santa-Cruz Biotechnology, Santa Cruz, CA), pSMAD2/3 (Pepsin, 1:400, Santa-Cruz Biotech.), or pSMAD1/5/8 (Citrate, 1:50, Cell signaling tech., Danvers, MA). To determine positive area percentages of Masson-trichrome and CTGF stained slides, 10 random fields per section were chosen and photographed. Using Photoshop (version 12.0) positive staining areas were selected and quantitated using ImageJ software (NIH, Baltimore, MD).

### *Hydroxyproline-, urea-, protein- and SA- $\beta$ -Galactosidase assay.*

Hydroxyproline: Paraffin sections were analyzed for hydroxyproline levels as a measurement of collagen content using HPLC (18); proline ratio was taken as a measure of relative abundance of collagen. Plasma urea: Plasma urea levels were measured by colorimetric assay using standard procedures (DiaSys, Holzheim, Germany). Urinary protein: Urinary protein was measured by BCA assay (BioRad, Hercules, CA). Senescence Associated- $\beta$ -Galactosidase: SA- $\beta$ -gal activity was detected as described (13).

### *Western blot*

Snap frozen renal cortex was homogenized and lysed using NP-40 lysis buffer containing Na-Orthovanadate, Na-Fluoride and complete protease inhibitor cocktail. Lysates were spun down and pellets were discarded. Total protein concentration in the supernatant was measured using BCA (Pierce Thermo, Rockford, IL). 20 $\mu$ g of protein was boiled with Laemli/DTT and run for 90 minutes on 10% SDS-PAGE gels (BioRad). Gels were subsequently blotted for 90 minutes on PVDF membrane using a wet blotting transfer system (BioRad). For p-Smad1/5/8 analysis membranes were incubated with primary antibody (pSMAD1/5/8, 1:2000, CST; SMAD1/5/8, 1:1000, Santa-Cruz) in TBS-Tween containing 3%BSA overnight. After thorough rinsing membranes were incubated with secondary HRP conjugated antibody and imaged using chemiluminescence substrate (GE healthcare lifescience, Buckinghamshire, UK).

*RT-qPCR*

RNA was isolated from both tissue homogenate and cell cultures using TRIzol (Life technologies, Carlsbad, CA). RNA was reversely transcribed to cDNA using standard procedures. Expression of target genes was determined using commercially available pre-designed TaqMan probes (Bmp6, Mm00432095\_m1; Bmp7, Mm00432102\_m1; Col1a2, Mm00483888\_m1; Ctgf, Mm00515790\_g1; Hsp47, Mm00438058\_g1; Klotho, Mm00502002\_m1; Pai1, Mm00435860\_m1; Tgfβ1, Mm01178820\_m1; Id1: Mm00775963\_g1; Tbp: Mm01277042\_m1; Thermo Fisher, Waltham, MA). Samples were run on a Lightcycler 480 (Roche, Basel, Switzerland) and relative expression was determined by the  $\Delta\Delta CT$  method. Application of GeNorm identified TATA box binding protein (tbp) as the most stable reference gene (out of gapdh, yhwaz, actb and tbp).

*Solid-phase BMP6/CTGF binding assay*

Microtiter plates were coated with fixed concentration of 200ng/ml full length rhCTGF (BioVendor, Modrice, Czech republic) at 4°C overnight. Plates were rinsed and blocked with 1% BSA for 2h. After rinsing, a range of 0-1000ng/ml rhBMP6 (R&D Systems) was added. Bound BMP6 was detected by using a BMP6 antibody (Santa Cruz).

*Cell culture*

HK-2 cells were maintained in DMEM (Gibco/Thermo, Waltham, MA) with 10% FCS, penicillin and streptomycin in humidified air with 5% CO<sub>2</sub> at 37 °C. HK-2 cells were plated at a density of  $1 \times 10^5$  cells in 6-well plates. Cells were serum starved for 24 hours and subsequently incubated with serum-free medium alone, 50 ng/ml rhBMP-6 (R&D Systems, Minneapolis, MN) with or without 400 ng/ml rhCTGF. Cells were harvested after 1 h for Western blot analysis and after 2 h for quantitative PCR.

*Statistics*

Data was analyzed using GraphPad Prism version 6.02 (Graphpad software inc., La Jolla, CA). All data was statistically tested with Student-T test for two groups, or two-way ANOVA followed by post-hoc Tukey correction for multiple testing when more groups were compared, unless stated otherwise.  $p < 0.05$  was considered statistically significant. Error bars represent SEM.

**Results***General characteristics*

To investigate potential age related differential responses to injury, we performed UUO in both groups for 14 days. Post UUO, kidney weight loss, diuresis, plasma urea and proteinuria were similar at both ages (data not shown). However, old mice lost more body weight compared to young mice (Figure 1A). Old contralateral kidneys (50 weeks) showed sporadic senescence associated- $\beta$ -Galactosidase activity whereas this was not detected in any of sections from kidneys of young mice (16 weeks) (data not shown). Glomerulosclerosis, a phenomenon associated with ageing, was not seen in old CLKs (Figure 1B).

*Ureteral ligation induces a more severe morphological phenotype in aged kidneys*

To assess the extent of injury, dilatation and atrophy (two hallmarks of UUO induced renal damage) were scored. Morphological interstitial damage after obstruction was more severe in old Obstructed Kidneys (OBK), as exemplified by higher kidney tubular morphological damage scores for dilatation and atrophy in old OBKs compared to young OBKs (Figure 1B and 1C).

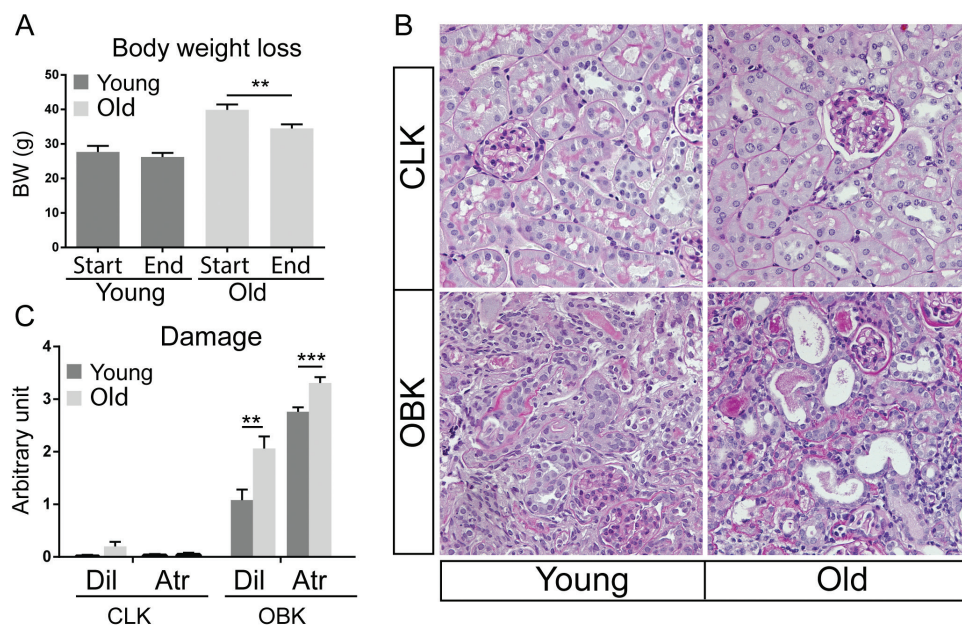


**Figure 1:** Unilateral Ureter Obstruction (UUO) causes more morphological damage in old kidneys. **A:** Total body weight (BW) prior to UUO (Start) and after sacrifice (End). **B:** Representative micrographs of PAS stained slides of contralateral kidney (CLK) and obstructed kidney (OBK) in both age groups (200x). **C:** Quantification of microscopically observed atrophy and dilatation observed; Error bars represent SEM; \*\* $p < 0.01$ , \*\*\* $p < 0.005$ . Statistics used in A: two-way ANOVA with Sidak correction for multiple comparison, C&E: non-paired two-way ANOVA with Tukey correction.

*Development of fibrosis is reduced in aged kidneys*

Since fibrosis is a second major phenomenon occurring during UUO mediated renal injury, we studied the level of ECM deposition and associated myofibroblast accumulation in obstructed kidney of both age groups. Quantification of Masson Trichrome (MTC) staining, a staining for fibrillary collagen, showed a reduced area positivity (%) in old OBKs compared to young OBKs (Figure 2A). An increase in MTC positive surface area in young OBKs was observed, whereas no significant increase was seen in old OBKs compared to CLKs (Figure 2B). Furthermore, myofibroblast numbers as assessed by  $\alpha$  Smooth Muscle Actin ( $\alpha$ SMA) were also lower in old OBKs compared to young OBKs (Figure 2A lower panels B&C). No difference was observed in CLKs (data not shown). Old OBKs show a reduced

Col1a2 up regulation compared to young OBKs (Figure 2D). Correspondingly, a significant increase in the message for collagen chaperone Hsp47 was seen in young kidneys upon obstruction whereas this was not observed in old obstructed kidneys (Figure 2E). Hydroxyproline levels were higher in old CLKs compared to young CLKs, but were similar in OBKs of both age groups (Figure 2F). Fold increase (OBK/CLK) of hydroxyproline was reduced in old compared to young kidneys (Figure 2 F; right panel). Taken together this suggests a decreased de novo synthesis of collagen in old compared to young kidneys upon ureteral obstruction.

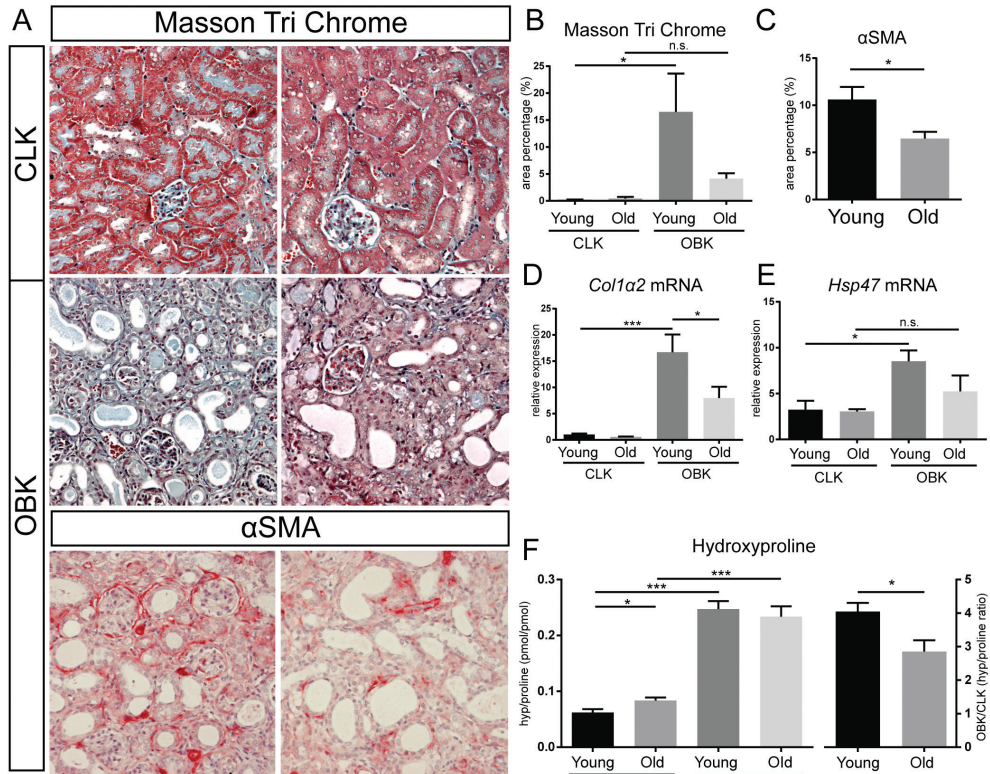


**Figure 2:** Old kidneys show less ECM deposition upon UUU. **A:** Representative micrographs of Masson-Trichrome (MTC) and αSMA stained kidneys of both age groups (200x); **B:** Morphometric quantification of fibrosis as seen with MTC staining. **C:** Morphometric quantification of myofibroblasts as seen with αSMA staining. **D:** Col1a2 expression levels in CLK and OBK; **E:** Hsp47 expression levels in CLK and in OBKs. **F:** Hydroxyproline/proline ratio; Error bars represent SEM; \* p<0.05, \*\*\*p<0.005. Statistics used in B-D: non-paired two-way ANOVA with Tukey correction.

*Age is associated with an altered pro-fibrotic/regenerative balance*

To gain insight in potential underlying differences in pro-fibrotic signaling resulting in the altered phenotype, we studied several important known mediators of ageing or fibrosis. For assessment of pro-regenerative gene expression, we investigated Klotho, Bmp6 and Bmp7 mRNA expression levels (Figure 3 A-C). The renoprotective factor Klotho is strongly associated with aging, and interacts with the TGFβ pathway during fibrogenesis in the kidney (4, 31, 50). Despite the 38 week age difference, Klotho expression was not differentially regulated in unobstructed CLKs of 50 week and 12 week old mice (Figure 3A). Also, Klotho was similarly down regulated in OBKs of both age groups, and no significant change in Klotho expression was observed between old and young OBKs (Figure 3A). In young mice, obstructed kidneys had significantly reduced gene expression levels of Bmp6 and Bmp7 (Figure 3B&C). In old and young OBKs, Bmp7 expression was similarly suppressed (Figure 3B). However, unlike young OBKs, old OBKs showed no reduction of Bmp6 expression (Figure 3C).

The increase of TGF $\beta$ 1 as a key pro-fibrotic regulator, and PAI-1 as important downstream mediator of TGF $\beta$ 1 in kidney fibrosis (24), were not different in old and young OBKs ( $P=0.96$ ,  $P=0.36$  respectively; Figure 3D&E). To further evaluate downstream signaling of TGF $\beta$ 1 we performed pSMAD2/3 IHC on kidney cortex. However, the number of cortical cells showing TGF $\beta$  associated nuclear SMAD2/3 phosphorylation was not significantly different between old and young OBKs ( $P=0.95$ ; Data not shown). CTGF greatly influences the fibrotic/regenerative balance by positively modulating TGF $\beta$  and negatively modulating BMP signaling, and is commonly regarded as pro-fibrotic (2, 35). In CLKs, *Ctgf* mRNA expression levels were identical in old and young mice (Figure 3F). In OBKs mean *Ctgf* gene expression tended to be higher in young OBK as compared to old OBK, and compared to young CLK ( $P=0.07$ ); the mean increase vs. age-matched CLK was 7 fold in young OBKs, compared to 3.5 fold in old OBKs (Figure 3F). This increase was significant in young OBKs but not in old OBKs ( $p=0.013$  vs  $0.54$  respectively). Furthermore, CTGF IHC showed a decrease in CTGF positive area both in CLK and OBK old kidneys compared to CLK and OBK young kidneys respectively (Figure 3G&H:  $P<0.05$ ), while the increase in OBK compared to CLK was significant only in young mice. Signal loss occurred mainly in cortical tubules. *Bmp6/Ctgf* ratio's in individual OBKs was significantly higher in old than in young OBKs (12.1 SEM 2.6 vs 4.1 SEM 0.4;  $p<0.05$ ).

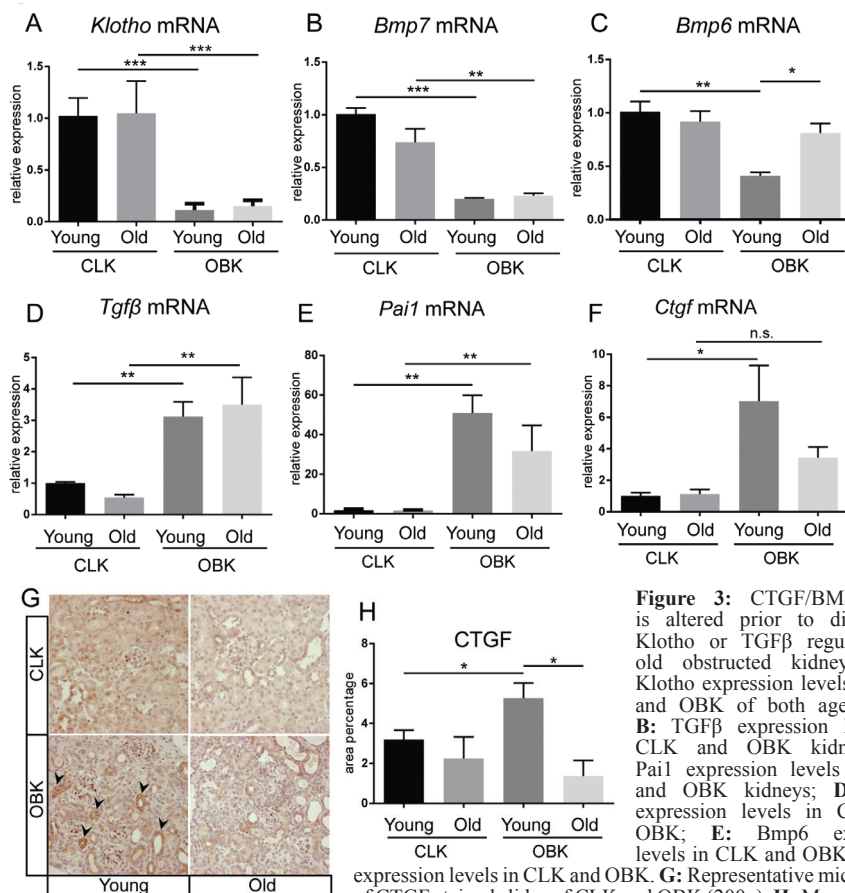


**Figure 3:** CTGF/BMP6 ratio is altered prior to differential Klotho or TGF $\beta$  regulation in old obstructed kidneys. **A:** Klotho expression levels in CLK and OBK of both age groups; **B:** TGF $\beta$  expression levels in CLK and OBK kidneys; **C:** *Bmp6* expression levels in CLK and OBK kidneys; **D:** *Bmp7* expression levels in CLK and OBK; **E:** *Bmp6* expression levels in CLK and OBK. **F:** *Ctgf* expression levels in CLK and OBK. **G:** Representative micrographs of CTGF stained slides of CLK and OBK (200x). **H:** Morphometric quantification of CTGF positive staining area. Arrowheads indicate positive tubular staining; Error bars represent SEM; \*  $p<0.05$ , \*\* $p<0.01$ , \*\*\* $p<0.005$ . Statistics used A-F & H: non-paired two-way ANOVA with Tukey correction.

*Canonical BMP signaling is better preserved in cortical tubular epithelium of old mice*

Given the increased BMP6/CTGF ratio, we next studied whether this resulted in an increase in canonical BMP signaling. In old OBKs, pSMAD1/5/8 signal was better preserved compared to young OBKs (Figure 4A & 4B). Immunostaining for pSMAD1/5/8 shows that glomerular and interstitial pSMAD1/5/8 is similar in young and old OBKs (Figure 4C & 4D). However, preservation of pSMAD1/5/8 signal occurred in the tubuli.

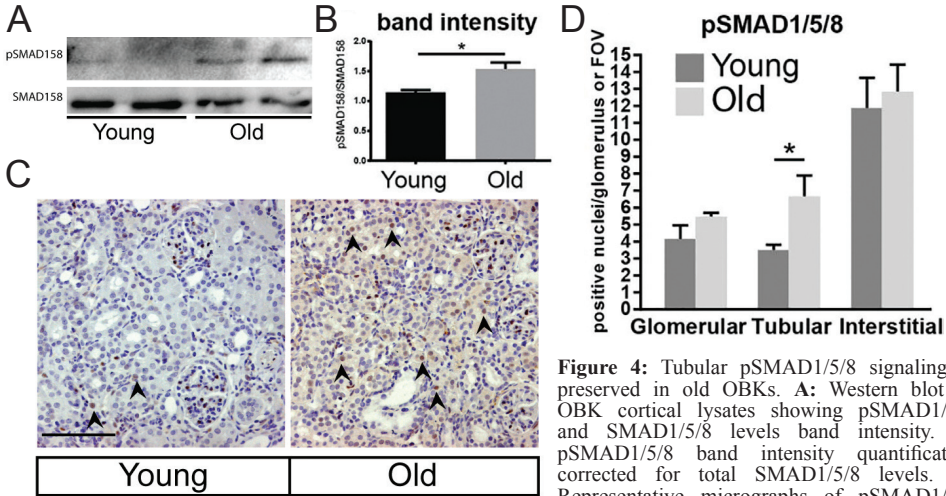


**Figure 4:** Tubular pSMAD1/5/8 signaling is preserved in old OBKs. **A:** Western blot of OBK cortical lysates showing pSMAD1/5/8 and SMAD1/5/8 levels band intensity. **B:** pSMAD1/5/8 band intensity quantification corrected for total SMAD1/5/8 levels. **C:** Representative micrographs of pSMAD1/5/8

OBKs (200x magnified). Arrowheads indicate pSMAD1/5/8 positive tubular cells. **D:** Quantification of the number of cortical pSMAD158 positive nuclei in glomerular, tubular and interstitial cells; Error bars represent SEM; \* p<0.05, \*\*p<0.01, \*\*\*p<0.005. Statistics used A&C: non-paired two-way ANOVA with Tukey correction, E: Student-T test.

*CTGF binds BMP6 and inhibits canonical downstream signaling*

CTGF inhibits canonical BMP7 signaling in proximal tubular (HK-2) cells via direct interaction (35). Whether CTGF holds similar potential with regards to BMP6 is unknown. By solid phase assay we observed concentration dependent binding of rhBMP6 in rhCTGF coated microtiter plates (Figure 5A). Stimulating HK-2 cells with rhBMP6 increased downstream transcriptional Id1 expression significantly (p<0.05) (Figure 5B). When co-stimulating HK-2 cells with rhBMP6 and rhCTGF however, this increase was significantly less profound (Figure 5B). Consistently, Western blot analysis showed increased SMAD1/5/8 phosphorylation upon rhBMP6 stimulation, which was less profound when

rhBMP6 was pre-incubated with rhCTGF prior to stimulation (Figure 5C). Thus, in vivo the increased BMP6 expression and associated SMAD1/5/8 phosphorylation might be further complemented by reduced physical inhibition by CTGF.

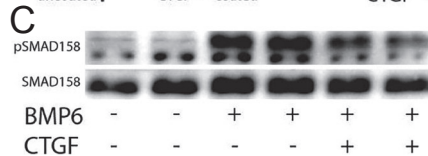
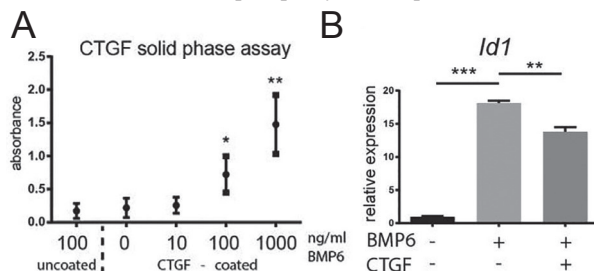


**Figure 5:** CTGF binds BMP6 and inhibits canonical BMP signaling **A:** Absorbance levels of CTGF/BMP6 solid phase assay. **B:** Western blot of HK-2 cell lysate 1 hour after stimulation with rhBMP6 and/or rhCTGF. Upper panel pSMAD1/5/8, Lower panel SMAD1/5/8. **C:** Id1 expression levels of HK-2 cells stimulated with rhBMP6 and/or rhCTGF; Error bars represent SEM; \* p<0.05, \*\*p<0.01, \*\*\*p<0.005. Statistics: non-paired two-way ANOVA with Tukey correction.

## Discussion

In this study, we revealed an age related differential response to persistent renal injury. We show that age-associated changes in the fibrotic response to kidney injury, occur already prior to the appearance of typical senescence markers like SA- $\beta$ -Gal activity, Klotho loss, and spontaneous glomerulosclerosis. In particular, increased morphological damage and a reduced fibrotic response were observed in 1-year-old mice without alteration of canonical TGF $\beta$  transcriptional activity. Instead, a decrease of CTGF and increase of BMP6 expression was found, associated with increased downstream pSMAD1/5/8 activity in cortical tubules, which might at least in part explain the observed reduced fibrogenesis to kidney injury in aging.

In human diagnostics and experimental animal research interstitial fibrosis and tubular atrophy (IFTA) is often assessed together and thought to “go hand in hand” (21). We show that following injury in the aged kidney, the proportion of fibrosis and atrophy can be shifted in favour of atrophy suggesting ramifications for clinical assessment of IFTA in the ageing kidney. Previously, it has been shown that renal damage in response to Ischemia Reperfusion Injury (IRI), in terms of GFR loss, morphological injury, and fibrosis, is increased in ageing (9, 46). Inverse correlations have been reported previously (38). Age-related acceleration of progressive kidney senescence and CKD development, after the initial acute injury has subsided, is becoming a widely recognized phenomenon, and considered to be due to decrease of reparative capacity (20). It remains to be established whether, in addition to decreased regenerative capacity, also the observed “weaker” but possibly more persistent fibrotic renal response to injury might be involved in more progressive loss of function upon transient injury in old kidneys.

The kidney is a major contributor to Klotho production and Klotho loss is strongly associated with ageing and the renal response to damage (6, 16, 30, 31, 33). Klotho is an important inhibitor of TGF $\beta$ , one of the most important mediators of fibrotic renal response to damage and ageing (34, 43). However, we found that at the age of 50 weeks Klotho and Tg $\beta$  expression were not yet affected by ageing but diminished and increased, respectively, to a similar extent in young obstructed kidneys. Thus the observed differential renal damage response occurred prior to the well-established changes of baseline Klotho and TGF $\beta$  expression at a more advanced age.

Interestingly, expression of the well-established anti-fibrotic and pro-regenerative BMP7-gene was also not different in old as compared to young OBKs, but the older OBKs had an increased BMP6/CTGF ratio, resulting from retained BMP6 expression and suppressed CTGF expression. The finding that preserved Bmp6 expression in old OBK was associated with less fibrosis is congruent with our previous observation that loss of BMP6, together with the ensuing overexpression of CTGF, aggravated renal fibrosis and myofibroblast ( $\alpha$ SMA) accumulation (14). This study by Dendooven et al. also showed that the level of tubular dilatation was unaltered suggesting BMP6 to be unrelated to dilatation. We propose that direct BMP6-effects might mainly attenuate fibrosis, while the other morphological differences observed might be secondary to this.

In our experiment, the increased BMP6 expression might at least partially account for the 50% reduction of CTGF in old OBK. Figure 5 shows that CTGF directly interacts with BMP6 and as such inhibits canonical signaling. Since old OBKs show less CTGF but more BMP6 expression, this increased BMP6/CTGF ratio might underlie the found pSMAD158 increase in cortical tubules, especially since we have an indication that the inhibitory effects of CTGF on pSMAD158 might be due to direct physical interaction with BMP6.

In the cortex, mainly distal tubules and collecting ducts display canonical BMP signaling, and it has been noted previously that upon UUO, signaling decreases (32). The phenomenon of epithelial to mesenchymal transition (EMT) is a large contributor to the development of renal fibrosis (49). Possibly the increase in tubular pSMAD1/5/8 seen in figure 4 reflects reduced EMT rate underlying the reduction in fibrosis.

Previously, we reported that a 50% reduction of CTGF as such is not sufficient to hamper the phenotype observed in 14 day UUO and other severe models of CKD (18). In conjunction with the present observations this might suggest that, at least in the UUO model, BMP6/CTGF balance is more

important for fibrosis control than the absolute CTGF level.

One might speculate that, in conjunction with less pronounced fibrosis, increase of morphological damage in terms of atrophy and dilatation in old OBKs, might result from less fibrogenic growth factor activity, with the resulting reduction of matrix deposition hampering generation of sufficient structural support to withstand increased pressure developing upon obstruction. As previously mentioned, there are many factors playing a role in the process of renal aging. However, the production of pro-fibrotic cytokines is a common end point (e.g. TGF $\beta$ ). Since there is no differential regulation of TGF $\beta$  or downstream PAII expression, the observed effects might have different drivers than the usual suspects of aging.

In conclusion, our studies have revealed an age-dependent shift in renal response to injury, developing a more atrophic and less fibrotic phenotype. This change is associated with altered BMP6/CTGF balance and already occurs before mice have lived through half of their life span and before the appearance of classical signs of senescence namely spontaneous loss of Klotho, increase in TGF $\beta$  expression and SA- $\beta$ -Gal. Figure 6 depicts a proposed mechanism distilled from the observations presented in this manuscript. While most experimental studies addressing CKD have been performed in young rodents, these might not appropriately reflect renal response to injury in ageing patients. This should be taken into account when interpreting existing and designing future studies addressing CKD progression in the ageing population.

#### Disclosures

RG has performed contract research for, and received research support, from FibroGen Inc.; a company involved in development of anti-CTGF therapy. RG has been employed by FibroGen Inc. from August 2008 till August 2009.

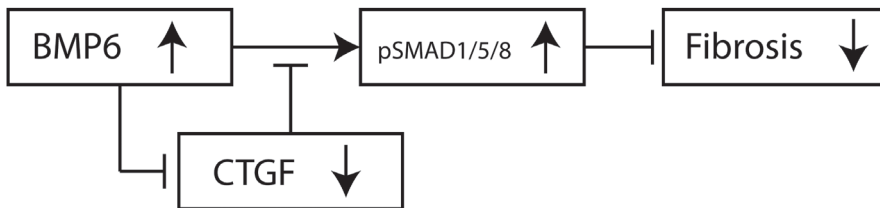


**Figure 6:** Proposed model for age associated change in the response to renal injury In the aged kidneys there is an increased expression of BMP6 that in itself is capable of reducing CTGF expression. Both the increase of BMP6 and the reduction of CTGF lead to increased levels of pSMAD1/5/8 (partially due to loss of physical binding to and inhibition of BMP6 by CTGF). The increase in pSMAD1/5/8 leads to reduced fibrosis, possibly via inhibition of EMT.



## References

1. Prakash S, O'Hare AM. Interaction of aging and chronic kidney disease. *Semin Nephrol.* 2009;29(5):497-503.
2. Rosner M, Abdel-Rahman E, Williams ME. Geriatric nephrology: responding to a growing challenge. *Clin J Am Soc Nephrol.* 2010;5(5):936-42.
3. Coresh J, Astor BC, Greene T, Eknoyan G, Levey AS. Prevalence of chronic kidney disease and decreased kidney function in the adult US population: Third National Health and Nutrition Examination Survey. *Am J Kidney Dis.* 2003;41(1):1-12.
4. Frenkel-Denkberg G, Gershon D, Levy AP. The function of hypoxia-inducible factor 1 (HIF-1) is impaired in senescent mice. *FEBS letters.* 1999;462(3):341-4.
5. Tanaka T, Kato H, Kojima I, Ohse T, Son D, Tawakami T, et al. Hypoxia and expression of hypoxia-inducible factor in the aging kidney. *The journals of gerontology Series A, Biological sciences and medical sciences.* 2006;61(8):795-805.
6. Abrass CK, Adcox MJ, Raugi GJ. Aging-associated changes in renal extracellular matrix. *Am J Pathol.* 1995;146(3):742-52.
7. Ruiz-Torres MP, Bosch RJ, O'Valle F, Del Moral RG, Ramirez C, Masseroli M, et al. Age-related increase in expression of TGF-beta1 in the rat kidney: relationship to morphologic changes. *Journal of the American Society of Nephrology : JASN.* 1998;9(5):782-91.
8. Schmitt R, Cantley LG. The impact of aging on kidney repair. *American journal of physiology Renal physiology.* 2008;294(6):F1265-72.
9. Bolignano D, Mattace-Raso F, Sijbrands EJ, Zoccali C. The aging kidney revisited: A systematic review. *Ageing Res Rev.* 2014;14C:65-80.
10. Hewitson TD. Renal tubulointerstitial fibrosis: common but never simple. *American journal of physiology Renal physiology.* 2009;296(6):F1239-44.
11. Epstein M. Aging and the kidney. *Journal of the American Society of Nephrology : JASN.* 1996;7(8):1106-22.
12. Zhou XJ, Rakheja D, Yu X, Saxena R, Vaziri ND, Silva FG. The aging kidney. *Kidney international.* 2008;74(6):710-20.
13. Choudhury D, Levi M. Kidney aging--inevitable or preventable? *Nature reviews Nephrology.* 2011;7(12):706-17.
14. Kim JH, Hwang KH, Park KS, Kong ID, Cha SK. Biological Role of Anti-aging Protein Klotho. *J Lifestyle Med.* 2015;5(1):1-6.
15. Dendooven A, van Oostrom O, van der Giezen DM, Leeuwis JW, Snijckers C, Joles JA, et al. Loss of endogenous bone morphogenetic protein-6 aggravates renal fibrosis. *Am J Pathol.* 2011;178(3):1069-79.
16. Nguyen TQ, Roestenberg P, van Nieuwenhoven FA, Bovenschen N, Li Z, Xu L, et al. CTGF inhibits BMP-7 signaling in diabetic nephropathy. *Journal of the American Society of Nephrology : JASN.* 2008;19(11):2098-107.
17. Conidi A, Cazzola S, Beets K, Coddens K, Collart C, Cornelis F, et al. Few Smad proteins and many Smad-interacting proteins yield multiple functions and action modes in TGFbeta/BMP signaling in vivo. *Cytokine Growth Factor Rev.* 2011;22(5-6):287-300.
18. Oh SP, Seki T, Goss KA, Imamura T, Yi Y, Donahoe PK, et al. Activin receptor-like kinase 1 modulates transforming growth factor-beta 1 signaling in the regulation of angiogenesis. *Proceedings of the National Academy of Sciences of the United States of America.* 2000;97(6):2626-31.
19. Meng XM, Chung AC, Lan HY. Role of the TGF-beta/BMP-7/Smad pathways in renal diseases. *Clin Sci (Lond).* 2013;124(4):243-54.
20. Falke LL, Goldschmeding R, Nguyen TQ. A perspective on anti-CCN2 therapy for chronic kidney disease. *Nephrology, dialysis, transplantation : official publication of the European Dialysis and Transplant Association - European Renal Association.* 2014;29 Suppl 1:i30-i7.
21. Abreu JG, Ketpura NI, Reversade B, De Robertis EM. Connective-tissue growth factor (CTGF) modulates cell signalling by BMP and TGF-beta. *Nat Cell Biol.* 2002;4(8):599-604.
22. Richter K, Kietzmann T. Reactive oxygen species and fibrosis: further evidence of a significant liaison. *Cell and tissue research.* 2016.
23. Doi S, Zou Y, Togao O, Pastor JV, John GB, Wang L, et al. Klotho inhibits transforming growth factor-beta1 (TGF-beta1) signaling and suppresses renal fibrosis and cancer metastasis in mice. *The Journal of biological chemistry.* 2011;286(10):8655-65.
24. Quan T, Shao Y, He T, Voorhees JJ, Fisher GJ. Reduced expression of connective tissue growth factor (CTGF/CCN2) mediates collagen loss in chronologically aged human skin. *The Journal of investigative dermatology.* 2010;130(2):415-24.
25. Itoh S, Hattori T, Tomita N, Aoyama E, Yutani Y, Yamashiro T, et al. CCN family member 2/connective tissue growth factor (CCN2/CTGF) has anti-aging effects that protect articular cartilage from age-related degenerative changes. *PLoS one.* 2013;8(8):e71156.
26. Reed AL, Tanaka A, Sorescu D, Liu H, Jeong EM, Sturdy M, et al. Diastolic dysfunction is associated with cardiac fibrosis in the senescence-accelerated mouse. *Am J Physiol Heart Circ Physiol.* 2011;301(3):H824-31.
27. van Almen GC, Verhesen W, van Leeuwen RE, van de Vrie M, Eurlings C, Schellings MW, et al. MicroRNA-18 and microRNA-19 regulate CTGF and TSP-1 expression in age-related heart failure. *Aging cell.* 2011;10(5):769-79.
28. Abula K, Muneta T, Miyatake K, Yamada J, Matsukura Y, Inoue M, et al. Elimination of BMP7 from the

- developing limb mesenchyme leads to articular cartilage degeneration and synovial inflammation with increased age. *FEBS letters*. 2015;589(11):1240-8.
29. Crews L, Adame A, Patrick C, Delaney A, Pham E, Rockenstein E, et al. Increased BMP6 levels in the brains of Alzheimer's disease patients and APP transgenic mice are accompanied by impaired neurogenesis. *The Journal of neuroscience : the official journal of the Society for Neuroscience*. 2010;30(37):12252-62.
  30. Gomez D, Kessler K, Michel JB, Vranckx R. Modifications of chromatin dynamics control Smad2 pathway activation in aneurysmal smooth muscle cells. *Circulation research*. 2013;113(7):881-90.
  31. Chevalier RL, Forbes MS, Thornhill BA. Ureteral obstruction as a model of renal interstitial fibrosis and obstructive nephropathy. *Kidney international*. 2009;75(11):1145-52.
  32. Klahr S. Urinary tract obstruction. *Semin Nephrol*. 2001;21(2):133-45.
  33. Inazaki K, Kanamaru Y, Kojima Y, Sueyoshi N, Okumura K, Kaneko K, et al. Smad3 deficiency attenuates renal fibrosis, inflammation, and apoptosis after unilateral ureteral obstruction. *Kidney international*. 2004;66(2):597-604.
  34. Samarakoon R, Overstreet JM, Higgins SP, Higgins PJ. TGF-beta1 --> SMAD/p53/USF2 --> PAI-1 transcriptional axis in ureteral obstruction-induced renal fibrosis. *Cell and tissue research*. 2012;347(1):117-28.
  35. Falke LL, Dendooven A, Leeuwis JW, Nguyen TQ, van Geest RJ, van der Giezen DM, et al. Hemizygous deletion of CTGF/CCN2 does not suffice to prevent fibrosis of the severely injured kidney. *Matrix Biol*. 2012;31(7-8):421-31.
  36. Debacq-Chainiaux F, Erusalimsky JD, Campisi J, Toussaint O. Protocols to detect senescence-associated beta-galactosidase (SA-beta-gal) activity, a biomarker of senescent cells in culture and in vivo. *Nature protocols*. 2009;4(12):1798-806.
  37. Zhou L, Li Y, Zhou D, Tan RJ, Liu Y. Loss of Klotho contributes to kidney injury by derepression of Wnt/beta-catenin signaling. *Journal of the American Society of Nephrology : JASN*. 2013;24(5):771-85.
  38. Kuro-o M, Matsumura Y, Aizawa H, Kawaguchi H, Suga T, Utsugi T, et al. Mutation of the mouse klotho gene leads to a syndrome resembling ageing. *Nature*. 1997;390(6655):45-51.
  39. Arking DE, Krebsova A, Macek M, Sr., Macek M, Jr., Arking A, Mian IS, et al. Association of human aging with a functional variant of klotho. *Proceedings of the National Academy of Sciences of the United States of America*. 2002;99(2):856-61.
  40. He W, Tan R, Dai C, Li Y, Wang D, Hao S, et al. Plasminogen activator inhibitor-1 is a transcriptional target of the canonical pathway of Wnt/beta-catenin signaling. *The Journal of biological chemistry*. 2010;285(32):24665-75.
  41. Forbes MS, Thornhill BA, Minor JJ, Gordon KA, Galarreta CI, Chevalier RL. Fight-or-flight: murine unilateral ureteral obstruction causes extensive proximal tubular degeneration, collecting duct dilatation, and minimal fibrosis. *American journal of physiology Renal physiology*. 2012;303(1):F120-9.
  42. Shimizu MH, Araujo M, Borges SM, de Tolosa EM, Seguro AC. Influence of age and vitamin E on post-ischemic acute renal failure. *Experimental gerontology*. 2004;39(5):825-30.
  43. Clements ME, Chaber CJ, Ledbetter SR, Zuk A. Increased cellular senescence and vascular rarefaction exacerbate the progression of kidney fibrosis in aged mice following transient ischemic injury. *PLoS one*. 2013;8(8):e70464.
  44. Pulskens WP, Rampanelli E, Teske GJ, Butter LM, Claessen N, Luirink IK, et al. TLR4 promotes fibrosis but attenuates tubular damage in progressive renal injury. *Journal of the American Society of Nephrology : JASN*. 2010;21(8):1299-308.
  45. Ferenbach DA, Bonventre JV. Mechanisms of maladaptive repair after AKI leading to accelerated kidney ageing and CKD. *Nature reviews Nephrology*. 2015;11(5):264-76.
  46. Duce JA, Podvin S, Hollander W, Kipling D, Rosene DL, Abraham CR. Gene profile analysis implicates Klotho as an important contributor to aging changes in brain white matter of the rhesus monkey. *Glia*. 2008;56(1):106-17.
  47. Lindberg K, Amin R, Moe OW, Hu MC, Erben RG, Ostman Wernerson A, et al. The kidney is the principal organ mediating klotho effects. *Journal of the American Society of Nephrology : JASN*. 2014;25(10):2169-75.
  48. Koh N, Fujimori T, Nishiguchi S, Tamori A, Shiomi S, Nakatani T, et al. Severely reduced production of klotho in human chronic renal failure kidney. *Biochemical and biophysical research communications*. 2001;280(4):1015-20.
  49. Buendia P, Carracedo J, Soriano S, Madueno JA, Ortiz A, Martin-Malo A, et al. Klotho Prevents NFkappaB Translocation and Protects Endothelial Cell From Senescence Induced by Uremia. *The journals of gerontology Series A, Biological sciences and medical sciences*. 2015;70(10):1198-209.
  50. Leeuwis JW, Nguyen TQ, Chuva de Sousa Lopes SM, van der Ven K, Rouw PJ, et al. Direct visualization of Smad1/5/8-mediated transcriptional activity identifies podocytes and collecting ducts as major targets of BMP signalling in healthy and diseased kidneys. *The Journal of pathology*. 2011;224(1):121-32.
  51. Zeisberg M, Kalluri R. The role of epithelial-to-mesenchymal transition in renal fibrosis. *J Mol Med (Berl)*. 2004;82(3):175-81.

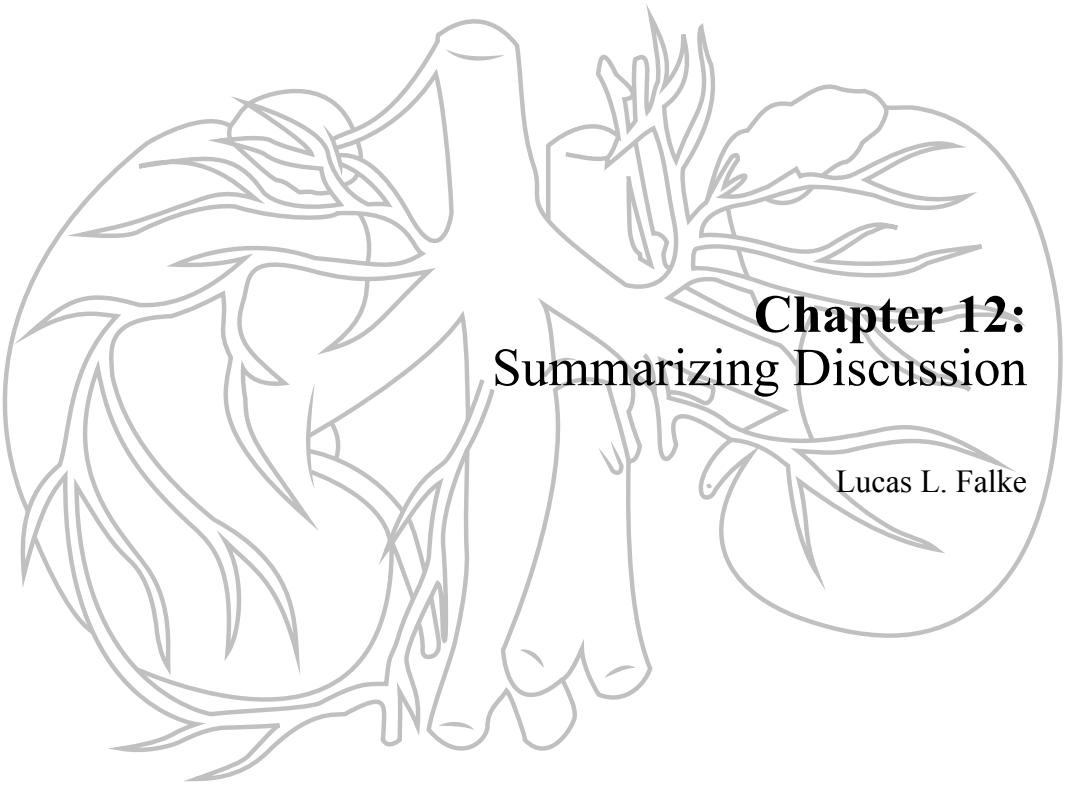


12



## **Chapter 12: Summarizing Discussion**

Lucas L. Falke



In the previous chapters of this thesis several modifiers of the renal response to injury were explored. Special attention was given to CTGF mediated modulation of renal pathophysiological responses. In this summarizing discussion, first the clinical concerns and caveats regarding Chronic Kidney Disease (CKD) care are defined. This is followed by a summarization of the means studied in this thesis to identify and combat CKD in the patient at risk. The third section of this final chapter aims to integrate findings thus comprising a concise perspective to base further research on.

#### *Identifying patients at risk*

CKD has several underlying aetiologies including but not limited to cardiovascular and hypertensive disease, diabetes, polycystic kidney disease, obstructive nephropathy, vasculitis, or intrinsic glomerular/tubulointerstitial disease. Furthermore, in recent years it has become clear that Acute Kidney Injury (AKI) predisposes to and is a major cause of CKD and associated renal fibrosis later in life (1, 2). After acute kidney injury, two outcomes may present themselves; 1) complete remission of AKI accompanied by regeneration of the kidney parenchyma, or 2) development of CKD over time. Subsequently, CKD can 1) stabilize or regress, although this is very rare, 2) progress towards end stage renal disease (ESRD) requiring renal replacement therapy, or 3) cause death mainly due to cardiovascular complications prior to ESRD (3). As such, CKD development can be regarded as a pre-final distinctive end-point that requires successful intervention to prevent renal replacement therapy dependency. A logical starting point is to identify which patients will recover, will remain stable, or will develop CKD and require intensive follow up after AKI (4). In **Chapter 2**, we showed in patients with delayed graft function (DGF, a form of AKI) 7 days after renal transplantation, that a novel histological damage score predicts the speed of recovery, and the quality of kidney function 6 months later. By developing this reproducible histological scoring system we eventually hope to broaden the clinicians arsenal in determining the prognosis and, if prognosis is poor, the means to identify patients who need (more intensive or modified) treatment. Since our patient cohort was selected for the exploratory nature of this paper, actual clinical value of our scoring method still has to be evaluated in a larger cohort including biopsies of AKI cases with a wider range of underlying aetiologies. Furthermore, we were unable to see a clear association between proliferative markers CD133 or Ki67 and the duration and level of restoration after transplantation induced AKI and associated DGF. This signifies the complexity of the balance between damage and regeneration, a relationship potentially further complicated by cell cycle arrest (5). Additionally, **Chapter 3** shows that plasma CTGF levels (pCTGF) predict cardiovascular morbidity and mortality after patients presented themselves initially with cardiovascular disease. pCTGF levels were, after correction for a variety of possible confounding variables such as renal function, co-morbidities and medication, independent predictors.

#### *Novel tools to combat renal disease in the patient at risk*

After identifying patients at risk, the greatest challenge in combating CKD is to find ways to prevent or reverse its progression, and to facilitate regeneration of functional kidney parenchyma.

As discussed in **Chapter 4**, the myofibroblast holds a central role in fibrosis and is a prime target in combating CKD. The myofibroblast is scarcely present under physiological conditions and much effort has been undertaken to understand its origin. Current understanding with regards to myofibroblast origin is reviewed in this chapter. From the reviewed literature, we conclude that most likely renal interstitial fibroblasts, as well as bone marrow derived cells, endothelial cells, and pericytes can all contribute to myofibroblasts accumulating in CKD. Furthermore, a broad array of interventional strategies, including nanomedicine and targeted therapies, is currently under development to target these cell types specifically, and is also discussed. As an example of these developments,

**Chapter 5** shows conceptual proof that the use of a local surgical deposit of rapamycin loaded microspheres reduces infiltration and myofibroblast accumulation for up to 8 days, without the systemic side effects seen with intraperitoneal administration.

**Chapter 6** shows that in female mice Tamoxifen, a selective estrogen receptor modulator (SERM) often used in experimental animal models to induce Cre mediated genetic recombination,

exerts anti-fibrotic properties by itself when administered up to two weeks prior to ureteral ligation for the induction of obstructive nephropathy (UUO). Applying a commonly used Tamoxifen injection regimen we found that despite the built in 14 day washout period, female mice had a reduced level of myofibroblast accumulation and associated fibrosis after unilateral ureter obstruction.

In the study presented in **Chapter 7**, it is shown that rhBMP7 is capable of reducing renal damage, myofibroblast accumulation, early fibrotic development and macrophage infiltration during obstructive nephropathy. This was associated with a decrease in CTGF expression, but not with evident changes in transcriptional activity downstream of canonical BMP signalling, nor with changes in TGF $\beta$ . To test whether the reduction of CTGF contributed significantly to rhBMP7-mediated renoprotection, we repeated the experiment in heterozygous CTGF $\pm$  mice. This revealed that rhBMP7 did not further reduce the severity of obstructive nephropathy in CTGF $\pm$  mice, suggesting that rhBMP7 efficacy in wild type mice was mediated in large part by reduction of CTGF.

CTGF is an immediate early gene increased from start to finish during renal disease (6), and plasma level of CTGF is an independent predictor of ESRD and mortality in diabetic nephropathy (7). As described in the Introduction and **Chapter 8**, a wide variety of CKD associated signals increase CTGF levels. Currently, PubMed holds 647 hits when “CTGF” and “Kidney” are cross-referenced. Combined, these papers depict CTGF as an interwoven mediator of many pathophysiological phenomena known to occur during CKD, as was briefly noted in the introduction.

Previous work, including chapter 6 has shown that an approximate CTGF reduction of 50% protects against fibrosis in mild models of fibrotic disease (8, 9). Whether this level of reduction is sufficient to reduce fibrosis in severe models of renal disease is unknown. **Chapter 9** shows that this is not the case: in models of advanced diabetic nephropathy or unilateral ureter obstruction, and in severe aristolochic acid nephropathy, the ECM and myofibroblast accumulation, and also macrophage infiltration were similar in wild type and CTGF $\pm$  mice. Furthermore, no difference in renal function was observed between CTGF $\pm$  and wild type mice with DN or AAN.

In addition to the previous chapter, we show in **Chapter 10** that a near total reduction of CTGF is sufficient to reduce fibrosis in a severe model of unilateral ureter obstruction. Furthermore, we describe that lymphangiogenesis, a process associated with fibrotic development, was reduced in CTGF KO mice. This was associated with reduced VEGF-C levels. In vitro analysis revealed that CTGF stimulates VEGF-C production but also binds and inhibits VEGF-C mediated lymphangiogenesis.

In **Chapter 11** of this thesis, the differential response to injury in young and old mice is studied. We found that aged animals have increased morphological damage in response to UUO. However, a reduction in fibrosis was observed. This was associated with an increased ratio between reno-protective BMP6 and CTGF. Furthermore, we found that CTGF can bind BMP6 thereby inhibiting downstream signalling of the latter. Together these data suggest that upon ageing, the fibrotic response in the kidney upon ureteral obstruction is reduced in a CTGF dependent manner.

#### *Clinical Relevance and Future perspectives*

Although several methods to predict CKD to ESRD progression have been developed (10), no effective method to accurately predict GFR in the context of CKD exists. The histological damage score we developed for patients suffering from post-transplantation DGF in chapter 2 correlates to eGFR 6 months later (renal outcome). Our histological damage score potentially also holds predictive value for CKD prognosis of other aetiologies than AKI induced DGF. Surprisingly however, no correlation between proliferative (Ki67) or regenerative (CD133) parameters and renal outcome was seen. Of note is that a failure to complete a full cell cycle potentially leads to G2/M phase transition arrest. Additionally, G2/M arrest is a correlate to increased fibrosis in the kidney (5). Whether Ki67 or CD133+ cells are truly proliferative or a subset cells represent failed regeneration will have to be studied further. Possibly the balance of true proliferative cells and failed regeneration underlie the lack of correlation found in chapter 2.

The relationship between plasma CTGF and the risk of cardiovascular events shown in chapter 3 corresponds nicely to the bulk of data that already exists with regards to CTGF and organ

fibrosis. Atherosclerosis as seen during cardiovascular disease is a form of fibrosis that manifests in arteries (11). Since CTGF is increased in almost every variant of fibrosis, it is thus not surprising that we find increased plasma CTGF levels in atherosclerosis.

CKD predisposes to atherosclerosis (12). Given the high co-occurrence of hypertension, cardiovascular and renal disease (13), and relation between cardiovascular disease and CKD progression (14), it not surprising that pCTGF corresponds to severity of CKD. For instance, pCTGF levels are independent predictors of mortality in patients suffering from type 1 diabetic nephropathy (7). This makes the observation that, despite cardiovascular risk being strongly correlated to CKD, pCTGF levels being an independent predictor of eGFR even more striking.

Since we live in a time and age where huge steps are made both technologically and with regards to bioinformatics, it is not surprising that mathematical models to predict the progression of CKD are currently being developed (15). However, computer models need input and input is delivered by biometric information. Plasma CTGF levels and, once validated in a larger cohort, our histological damage score might prove to be important contributors to such computerized prediction models.

Most of the therapeutics used in trials is administered systemically. Systemic treatment is prone to small therapeutic windows and thus efficacy due to side effects or toxicity. Since CKD can be regarded as a non-lethal slowly progressing disease, threshold levels for the acceptance of systemic side effects lie even higher. Targeted delivery systems are rapidly developed to bypass these effects and ample options are currently available in the kidney (16). We evaluated the feasibility of targeted subcapsular sustained Rapamycin release by injecting microspheres under the renal capsule during obstructive nephropathy in Chapter 5. Although suppressing myofibroblast proliferation and fibrosis, the effects were too restricted to the immediate vicinity of the deposit to be of any clinical use in current form with regards to human renal disease. However, the proof of principle that a local therapy using a sustained release device is feasible *in vivo* has been delivered, and as such further optimization of targeted therapies (potentially with other, more potent, anti-fibrotic agents; e.g. Tamoxifen as discussed in Chapter 6, or rhBMP7 as discussed in Chapter 7) would seem worthwhile. Of note is that Tamoxifen might have an even more profound fibrosis suppressing effect in females, a notion that emphasises that gender differences might need to be taken into account when treating patients suffering from CKD.

The work presented in Chapter 10 shows a clear association between later stages of obstructive nephropathy and lymphangiogenesis. An interesting notion is that Rapamycin, next to being anti-inflammatory and pro-autophagy, is also capable of reducing lymphangiogenesis (17). Whether lymphangiogenesis occurs during CKD in humans is largely unknown and warrants further investigation, especially given the availability of therapeutics targeting lymphangiogenesis such as Rapamycin. However, administration of Rapamycin during AKI has been shown to delay recovery (18), suggesting that care needs to be taken whom to treat and during what stage of disease. Alternatively, anti-CTGF therapy or anti-VEGF-C therapy might prove useful in combating both lymphangiogenesis and fibrosis, and anti-CTGF therapy may also be used to combat CKD progression. FG-3019, a human monoclonal antibody directed against CTGF, is the only anti-CTGF therapy in clinical trials, but currently, none of these address kidney disease.

In experimental fibrosis research, the reversibility of fibrosis upon anti-CTGF treatment has been shown in models for diabetic cardiomyopathy and idiopathic pulmonary fibrosis (19). In human trials, long-term open label administration of anti-CTGF is well tolerated in patients suffering from IPF and shows that some patients have a reduction of fibrosis and a better FEV1 (20). A randomized placebo controlled trial is underway but preliminary results provide evidence that inhibition of CTGF bioavailability can halt or even reverse pulmonary fibrosis and improve pulmonary function (clinicaltrial.gov number NCT01890265). In a phase 1 trial conducted in patients suffering from diabetic nephropathy, anti-CTGF was well tolerated and reduced albuminuria (21). Trials using mesenchymal stem cells (MSCs) to treat AKI and CKD are currently being conducted but show varying results (22), and MSCs have been shown to incorporate as myofibroblasts in the kidney during disease. In light of this, much effort is being put into careful dissection of pathways determining MSC fate. CTGF has



been shown to drive MSC differentiation towards a myofibroblast phenotype, and as such MSC therapy might benefit from simultaneous anti-CTGF therapy (23).

In rats, contrary to what has been thought previously, it was shown that CTGF is produced at a continuous high rate but is rapidly cleared in the kidney. Furthermore, FG-3019 is rapidly cleared from the circulation by target mediated excretion (24). As such, high doses of continuous FG-3019 might be required clinically to assure continuous CTGF inhibition. In Chapter 7, Chapter 9 and Chapter 10 respectively, we show that in the same model of renal disease (UUO), a 50% reduction of CTGF is sufficient to reduce renal damage and fibrosis for 7 days of obstruction, but not for 14 days. However, a near total reduction of CTGF (>90%) does sufficiently reduce fibrosis. Of note is that in the CTGF<sup>+/-</sup> mice, CTGF expression is still increased upon UUO compared to WT CLKs. In the CTGF full KO mice, CTGF expression levels upon UUO are still greatly reduced compared to WT CLKs. This provides precedent to suggest that there is a threshold level of CTGF reduction that needs to be reached depending upon the severity of disease. Clinically, it would thus seem attractive to initiate anti-CTGF therapy early. This could mean that anti-CTGF therapy needs to be initiated during early or mild manifestation of renal disease, and that a profound reduction of CTGF availability to near- or below normal levels is needed in advanced or severe disease. Furthermore, rapid clearing of anti-CTGF therapeutics might even further limit clinical efficacy.

Since CKD is usually progressive, treatment would need to be given continuously. However, to what extent long-term inhibition of CTGF bioavailability might lead to off target effects remains unknown. Sparse evidence shows an inverse correlation between CTGF and CKD development (25). Additionally, observations in Chapter 11 suggest that an age-associated loss of CTGF underlies the altered renal phenotype upon UUO in older mice. Since these older mice showed more morphological damage and less fibrosis, one might reason that CTGF associated fibrosis during renal injury is not detrimental per se. Furthermore, in experimental cardiac disease, CTGF has been shown to protect against hypertrophy (26). This suggests that, although a recent study we conducted showed that CTGF KO neither protects nor worsens cardiac hypertrophy and fibrosis upon chronic pressure overload (27), care needs to be taken to assure that anti-CTGF therapy is absolutely safe. Reports showing that CTGF is pro-fibrotic and pro-hypertrophic during cardiac disease make definitive interpretation difficult (28, 29). Possibly, FG-3019 can be used in combination with available targeting strategies to assure a higher half-life and therapeutic efficacy, thereby circumventing potential adverse effects on cardiac co-morbidity often seen in patients suffering from CKD. Whether long term CTGF reduction leads to loss of extracellular matrix integrity needed for parenchymal stability remains to be investigated.

#### *Concluding remark*

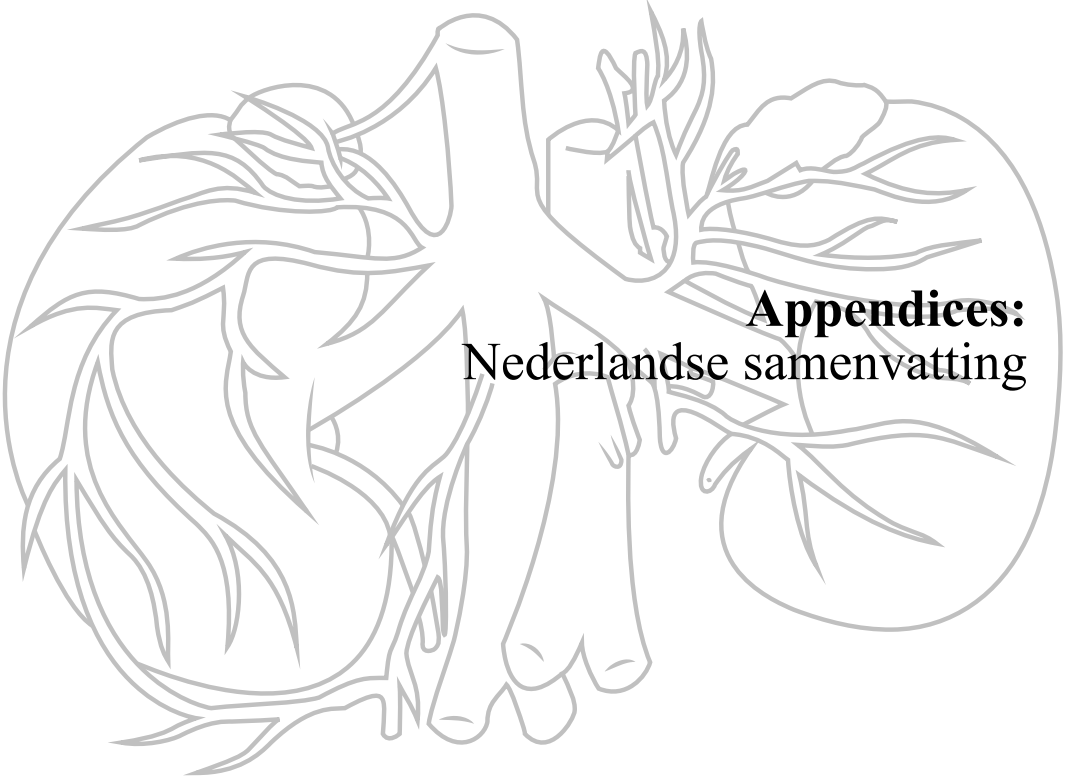
From the literature reviewed and work presented in this thesis, it becomes clear that the possible therapeutic arsenal to combat CKD is rapidly expanding. With the development of numerous biologicals, specific therapeutic antibodies and improved genetic, epigenetic and proteomic analytical methods, current practice in clinical oncology is shifting towards personalized cancer treatment (30). Cancer and fibrotic renal disease, although very different in aetiology, show many overlapping biological phenomena, especially with regards to stromal metabolism (e.g. altered cell-cell signaling, extracellular matrix metabolism and myofibroblast activation (31)). As such it is not surprising that many therapeutics developed for use in oncology might also be effective in renal pathology (32), and personalized renal therapy might be closer than we think.

**References**

1. Bydash JR, Ishani A. Acute kidney injury and chronic kidney disease: a work in progress. *Clin J Am Soc Nephrol.* 2011;6(11):2555-7.
2. Chawla LS, Eggers PW, Star RA, Kimmel PL. Acute kidney injury and chronic kidney disease as interconnected syndromes. *N Engl J Med.* 2014;371(1):58-66.
3. Eddy AA, Neilson EG. Chronic kidney disease progression. *J Am Soc Nephrol.* 2006;17(11):2964-6.
4. Mehta R, Bihorac A, Selby NM, Quan H, Goldstein SL, Kellum JA, et al. Establishing a continuum of acute kidney injury - tracing AKI using data source linkage and long-term follow-up: Workgroup Statements from the 15th ADQI Consensus Conference. *Can J Kidney Health Dis.* 2016;3:13.
5. Yang L, Besschetnova TY, Brooks CR, Shah JV, Bonventre JV. Epithelial cell cycle arrest in G2/M mediates kidney fibrosis after injury. *Nat Med.* 2010;16(5):535-43, 1p following 143.
6. Falke LL, Goldschmeding R, Nguyen TQ. A perspective on anti-CCN2 therapy for chronic kidney disease. *Nephrol Dial Transplant.* 2014;29 Suppl 1:i30-i7.
7. Nguyen TQ, Tarnow L, Jorsal A, Öliver N, Roestenberg P, Ito Y, et al. Plasma connective tissue growth factor is an independent predictor of end-stage renal disease and mortality in type 1 diabetic nephropathy. *Diabetes Care.* 2008;31(6):1177-82.
8. Guha M, Xu ZG, Tung D, Lanting L, Natarajan R. Specific down-regulation of connective tissue growth factor attenuates progression of nephropathy in mouse models of type 1 and type 2 diabetes. *FASEB J.* 2007;21(12):3355-68.
9. Yokoi H, Mukoyama M, Nagae T, Mori K, Suganami T, Sawai K, et al. Reduction in connective tissue growth factor by antisense treatment ameliorates renal tubulointerstitial fibrosis. *J Am Soc Nephrol.* 2004;15(6):1430-40.
10. Rucci P, Mandreoli M, Gibertoni D, Zuccala A, Fantini MP, Lenzi J, et al. A clinical stratification tool for chronic kidney disease progression rate based on classification tree analysis. *Nephrol Dial Transplant.* 2014;29(3):603-10.
11. Mackey RH, Venkitachalam L, Sutton-Tyrrell K. Calcifications, arterial stiffness and atherosclerosis. *Adv Cardiol.* 2007;44:234-44.
12. Parikh NI, Hwang SJ, Larson MG, Levy D, Fox CS. Chronic kidney disease as a predictor of cardiovascular disease (from the Framingham Heart Study). *Am J Cardiol.* 2008;102(1):47-53.
13. Braam B, Joles JA, Danishwar AH, Gaillard CA. Cardiorenal syndrome--current understanding and future perspectives. *Nat Rev Nephrol.* 2014;10(1):48-55.
14. Aguilar EA, Ashraf H, Frontini M, Ruiz M, Reske TM, Cefalu C. An analysis of chronic kidney disease risk factors in a Louisiana nursing home population: a cross-sectional study. *J La State Med Soc.* 2013;165(5):260-3, 5-7.
15. Norouzi J, Yadollahpour A, Mirbagheri SA, Mazdeh MM, Hosseini SA. Predicting Renal Failure Progression in Chronic Kidney Disease Using Integrated Intelligent Fuzzy Expert System. *Comput Math Methods Med.* 2016;2016:6080814.
16. Zhou P, Sun X, Zhang Z. Kidney-targeted drug delivery systems. *Acta Pharm Sin B.* 2014;4(1):37-42.
17. Huber S, Bruns CJ, Schmid G, Hermann PC, Conrad C, Niess H, et al. Inhibition of the mammalian target of rapamycin impedes lymphangiogenesis. *Kidney Int.* 2007;71(8):771-7.
18. Lieberthal W, Levine JS. Mammalian target of rapamycin and the kidney. II. Pathophysiology and therapeutic implications. *Am J Physiol Renal Physiol.* 2012;303(2):F180-91.
19. Lipson KE, Wong C, Teng Y, Spong S. CTGF is a central mediator of tissue remodeling and fibrosis and its inhibition can reverse the process of fibrosis. *Fibrogenesis Tissue Repair.* 2012;5(Suppl 1):S24.
20. Raghu G, Scholand MB, de Andrade J, Lancaster L, Mageto Y, Goldin J, et al. FG-3019 anti-connective tissue growth factor monoclonal antibody: results of an open-label clinical trial in idiopathic pulmonary fibrosis. *Eur Respir J.* 2016;47(5):1481-91.
21. Adler SG, Schwartz S, Williams ME, Arauz-Pacheco C, Bolton WK, Lee T, et al. Phase 1 study of anti-CTGF monoclonal antibody in patients with diabetes and microalbuminuria. *Clin J Am Soc Nephrol.* 2010;5(8):1420-8.
22. Kuppe C, Kramann R. Role of mesenchymal stem cells in kidney injury and fibrosis. *Curr Opin Nephrol Hypertens.* 2016.
23. Lee CH, Shah B, Muioli EK, Mao JJ. CTGF directs fibroblast differentiation from human mesenchymal stem/stromal cells and defines connective tissue healing in a rodent injury model. *J Clin Invest.* 2010;120(9):3340-9.
24. Brenner MC, Krzyzanski W, Chou JZ, Signore PE, Fung CK, Guzman D, et al. FG-3019, a Human Monoclonal Antibody Recognizing Connective Tissue Growth Factor, is Subject to Target-Mediated Drug Disposition. *Pharm Res.* 2016.
25. O'Seaghdha CM, Hwang SJ, Bhavsar NA, Kottgen A, Coresh J, Astor BC, et al. Lower urinary connective tissue growth factor levels and incident CKD stage 3 in the general population. *Am J Kidney Dis.* 2011;57(6):841-9.
26. Gravning J, Orn S, Kaasboll OJ, Martinov VN, Manhenke C, Dickstein K, et al. Myocardial connective tissue growth factor (CCN2/CTGF) attenuates left ventricular remodeling after myocardial infarction. *PLoS One.* 2012;7(12):e52120.
27. Fontes MS, Kessler EL, van Stuijvenberg L, Brans MA, Falke LL, Kok B, et al. CTGF knockout does not affect cardiac hypertrophy and fibrosis formation upon chronic pressure overload. *J Mol Cell Cardiol.* 2015;88:82-90.
28. Yoon PO, Lee MA, Cha H, Jeong MH, Kim J, Jang SP, et al. The opposing effects of CCN2 and CCN5 on the development of cardiac hypertrophy and fibrosis. *J Mol Cell Cardiol.* 2010;49(2):294-303.

29. Chatzifrangkeskou M, Le Dour C, Wu W, Morrow JP, Joseph LC, Beuvin M, et al. ERK1/2 directly acts on CTGF/CN2 expression to mediate myocardial fibrosis in cardiomyopathy caused by mutations in the lamin A/C gene. *Hum Mol Genet.* 2016.
30. Mandal R, Chan TA. Personalized Oncology Meets Immunology: The Path toward Precision Immunotherapy. *Cancer Discov.* 2016.
31. Vancheri C, Failla M, Crimi N, Raghu G. Idiopathic pulmonary fibrosis: a disease with similarities and links to cancer biology. *Eur Respir J.* 2010;35(3):496-504.
32. Bundela S, Sharma A, Bisen PS. Potential therapeutic targets for oral cancer: ADM, TP53, EGFR, LYN, CTLA4, SKIL, CTGF, CD70. *PLoS One.* 2014;9(7):e102610.





**Appendices:  
Nederlandse samenvatting**



**Nederlandse samenvatting**

(ook voor niet-ingewijden)

**Introductie**

Ouderdom komt met gebreken, helaas ook voor de nieren. Naarmate men ouder wordt ontstaat chronische nierschade. De combinatie van westerse levensstijl en een ouder wordende bevolking leidt er toe dat het aantal mensen met chronische nierschade sterk aan het toenemen is. In Nederland heeft ongeveer 7% van de bevolking chronische nierschade. Bij mensen met een leeftijd boven de 60 jaar ligt dit percentage zelfs rond de 30%. Hiermee is chronische nierschade een groot en groeiend gezondheidsprobleem.

Naast ouderdom zijn er vele andere oorzaken van chronische nierschade. Een aantal voorbeelden zijn suikerziekte (diabetes mellitus), langdurige hoge bloeddruk (hypertensie), maar ook andere complexe ziekten waarbij bijvoorbeeld het eigen afweersysteem schade in de nier veroorzaakt (soms na een infectie, soms zonder aanwijsbare oorzaak).

Acute nierschade wordt gekenmerkt door een plotselinge en snelle verslechtering van de nierfunctie. Deze ontstaat bijvoorbeeld ten gevolge van het wegvallen van de doorbloeding van de nier (zoals bij niertransplantatie) of een urinewegobstructie. Ook wordt gebruik van voor de nier giftige stoffen zoals bepaalde medicijnen of voedingssupplementen vaak gezien als oorzaak van acute nierschade. Na acute nierschade herstelt de nier over het algemeen, waarop de nierfunctie weer normaliseert. Vroeger dacht men dat dit geen consequenties had voor de toekomst, maar de afgelopen jaren is duidelijk geworden dat het doormaken van acute nierschade een verhoogde kans geeft op het uiteindelijk krijgen van chronische nierschade. Samengevat krijgt iedereen, als je maar oud genoeg wordt, chronische nierschade maar er zijn situaties die er toe kunnen leiden dat dit al eerder gebeurt. Het is dus van groot belang dat patiënten met een verhoogd risico op het ontwikkelen van chronische nierschade op tijd worden opgespoord.

Chronische nierschade wordt in de nier op weefselniveau vaak gekenmerkt door het ontstaan van littekenweefsel. Verlittekening in een orgaan wordt ook wel fibrose genoemd. Deze verlittekening kan in de nier op verschillende plaatsen ontstaan. Wanneer de verlittekening in het nierfiltrertje, de glomerulus, ontstaat noemt men dit glomerulosclerose. Als de verlittekening tussen het netwerk van buisjes waaruit de nier is opgebouwd ontstaat, noemt men dit interstitiële fibrose. Ten gevolge van deze verlittekening kan de nier niet goed meer functioneren waardoor afvalstoffen minder goed uit het lichaam worden gezuiverd. In gevorderde stadia kan ook de balans van belangrijke lichaamszouten als natrium, kalium, calcium of fosfaat verstoord raken. Ten gevolge van deze verstoorde zoutbalans (met name door calcium en fosfaat) verkalken de bloedvaten in de rest van het lichaam en ontstaat een sterk verhoogd risico op hart en vaatziekten. Hieraan komen mensen met chronische nierziekte dan ook vaak te overlijden.

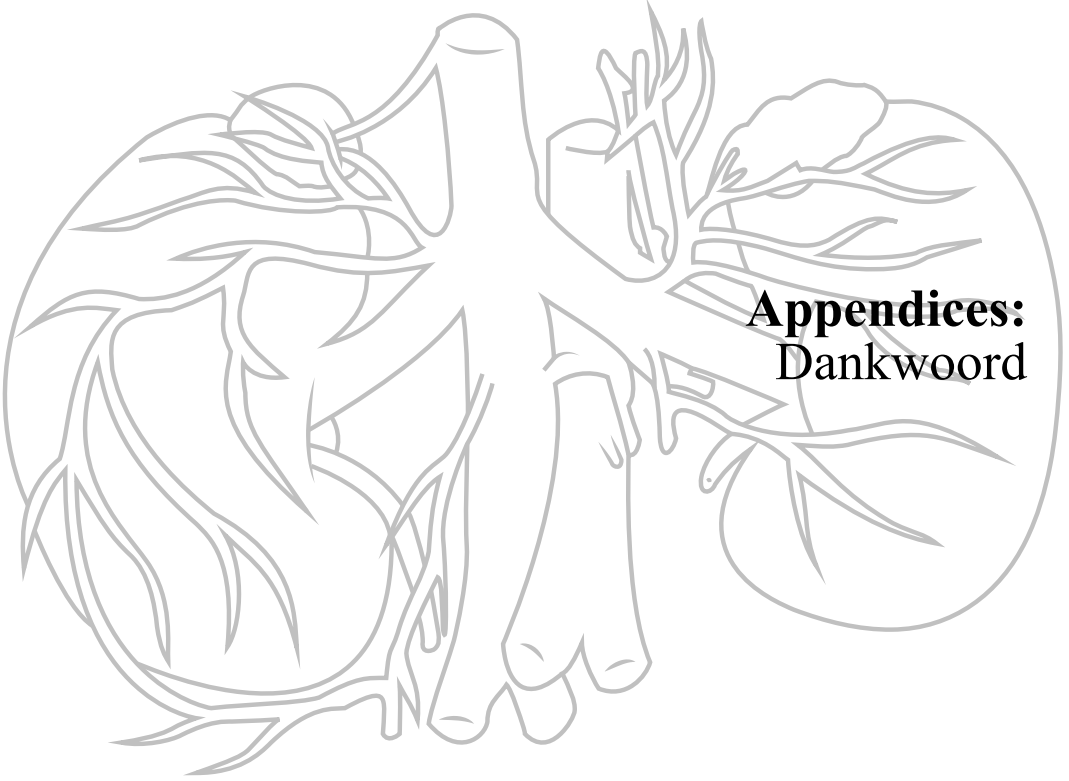
Het proces van deze verlittekening is complex en er zijn vele factoren bij betrokken. Over het algemeen begint de verlittekening na schade omdat er onder anderen signalerende eiwitten zoals groeifactoren en cytokinen aangemaakt worden. Deze eiwitten leiden tot infiltratie van ontstekingscellen (macrofagen en granulocyten) en later tot het ontstaan van zogenoemde myofibroblasten. Dit zijn gespecialiseerde cellen die grote hoeveelheden littekenweefsel aanmaken. De groeifactoren Transforming Growth Factor  $\beta$  (TGF $\beta$ ; transformerende groei factor bèta) en Connective Tissue Growth Factor (CTGF; bindweefsel groei factor) zijn factoren die uiterst potent zijn met betrekking tot bovenstaande. Factoren zoals Bone Morphogenetic Protein 6 en 7 (BMP6 en BMP7; bot morfogenetisch eiwit) zijn juist factoren die nierverlittekening remmen en herstel van de nier kunnen stimuleren.

**Dit proefschrift**

In dit proefschrift wordt in ingegaan op een aantal aspecten van acute en chronische nierschade. Zo wordt bestudeert of voorspellen van nierschade mogelijk is en welke factoren hierop van invloed zijn, waarbij een sterke focus op CTGF ligt. Om de omvang van het nierschade probleem (zowel chronisch als acuut) te accentueren én om belangrijke spelers hierbij te introduceren werd **hoofdstuk 1** geschreven. Het werk in **hoofdstuk 2** beschrijft een methode om in nierbiopten (kleine stukjes nier die onder de microscoop bekeken kunnen worden) van patiënten met acute nierschade direct na niertransplantatie te voorspellen wie wel en wie geen chronische nierschade ontwikkelen. De mate van schade in deze biopten is hiervoor een goede maatstaaf. Met speciale kleurtechniek is ook gekeken naar de regeneratie (de hoeveelheid regeneratieve cellen en de totale celdeling). Deze parameters bleken echter geen goede voorspellende waarde te leveren. In **hoofdstuk 3** is de studievraag of in het bloed van patiënten die bekend zijn met hart en vaatziekten de aanwezigheid van CTGF voorspellend is voor het uiteindelijk ontwikkelen van complicaties van de aanwezige vaatschade. Zoals al eerder genoemd is de kans op hart en vaatziekten bij patiënten met chronische nierschade aanzienlijk vergroot. Interessant genoeg bleek CTGF in het bloed onafhankelijk van de nierfunctie een voorspellende waarde te hebben voor het krijgen van complicaties. **Hoofdstuk 4** is een review dat exploreert wat tot dusver bekend is over myofibroblasten, waar zij vandaan komen tijdens nierfibrose en hoe zij in de toekomst mogelijk doelgericht aangepakt zouden kunnen worden. **Hoofdstuk 5** beschrijft een methode om dit te doen. In dit hoofdstuk worden met Rapamycine (een ontsteking onderdrukkend medicijn) geladen synthetische bolletjes onder het nierkapsel geplaatst bij ratten die een chirurgische urinewegobstructie hebben gekregen (Unilateral Ureter Obstruction, UUU). Deze bolletjes laten op een langzame en gecontroleerde manier de rapamycine los en zorgen op die manier voor onderdrukking van fibrose door middel van een lokale hoge dosis en minder bijwerkingen. In **hoofdstuk 6** wordt gebruik gemaakt van tamoxifen, een medicijn dat de oestrogeen receptor blokkeert. Tamoxifen wordt in wetenschappelijk onderzoek vaak gebruikt als handig hulpmiddel om dieren genetisch te kunnen manipuleren waarbij blokkade van de oestrogeen receptor geen direct doel is. Bekend is echter dat blokkeren of manipuleren van oestrogeen signalering ook effecten op het vormen van fibrose kan hebben. In dit hoofdstuk wordt getoond dat injectie van tamoxifen los van de genetische manipulatie ook al een reducerend effect op de fibrose heeft. In **hoofdstuk 7** wordt getoond dat BMP7 in staat is chronische nierschade en bijbehorende nierfibrose te remmen. Tevens wordt bewijs geleverd dat verlaging van CTGF hier mogelijk ten grondslag aan ligt. **Hoofdstuk 8** is een dieptereview over betrokkenheid van de eiwitten CTGF, Epithelial Growth Factor (EGF; epitheliale groei factor) en Platelet Derived Growth Factor (PDGF; groei factor uit bloedplaatjes) bij chronische nierschade. **Hoofdstuk 9** toont dat een halvering van CTGF in genetisch gemodificeerde muizen niet voldoende is om de vorming van schade en fibrose te verminderen in ernstige muismodellen van chronische nierschade. Aanvullend toont **hoofdstuk 10** dat een verlies van meer dan 90% van de oorspronkelijke CTGF productie wel voldoende is om nierfibrose te verminderen. Interessant hierbij is dat ook minder vorming van lymfevaten gezien wordt. Aanvullend celkweek en eiwit onderzoek laat vervolgens zien dat CTGF stimulatie leidt tot productie van lymfevat stimulerende eiwitten (Vascular Endothelial Growth Factor C; VEGF-C). Verder wordt getoond dat CTGF in staat is te binden aan VEGF-C en zo de signalering en vorming van lymfevaten weer beïnvloedt. Hiermee lijkt een nieuwe functie van CTGF te zijn ontdekt. In **hoofdstuk 11** wordt getoond dat oudere muizen anders reageren op nierschade dan jonge muizen. Zij hebben meer schade maar minder fibrose. In wetenschappelijk nieronderzoek wordt veelal gebruik gemaakt van juist jonge muizen (sneller te gebruiken en dus goedkoper). De bevindingen uit dit hoofdstuk suggereren nu dat dit zou kunnen leiden tot misinterpretatie van data aangezien de meeste patiënten met chronische nierziekten juist ouderen zijn. Een tweede gerelateerde bevinding is dat dit verschil in schade en fibrose mogelijk veroorzaakt wordt door een veranderde productie van CTGF (minder) en BMP6 (meer), twee eiwitten die aan elkaar kunnen binden. Hierbij remt CTGF de beschermende werking van BMP6. **Hoofdstuk 12** tot slot is een samenvattende discussie.







**Appendices:  
Dankwoord**



## Dankwoord

**B**este lezer, welkom op de voor u hoogstwaarschijnlijk eerste pagina van dit proefschrift. Terecht! De afgelopen jaren heb ik een hoop moeten leren en doen. Hier heb ik veel hulp bij nodig gehad. Dit is alleen mogelijk geweest doordat een forse achterban bereid was tijd en energie in mij te steken. Zowel in het lab als er buiten zijn er vele mensen die ik wil bedanken voor hun hulp, samenwerking, steun en vriendschap. In het bijzonder gaat mijn dank uit naar:

**Prof. Goldschmeding**, hartelijk dank voor zowel de mogelijkheid als de vrijheid die je mij geboden hebt de afgelopen jaren. Dit heeft mij enorm gesterkt in mijn wetenschappelijke vorming. De deur stond altijd open en alles was mogelijk (met de juiste argumenten). Je enorme enthousiasme en interesse in niet alleen het werk, maar ook op het persoonlijk vlak heb ik erg gewaardeerd.

**Dr. Nguyen**, gelukkig was jij er om al deze vrijheid te bundelen en te focussen. De momenten waarop jij vaak in eerste instantie niet zoveel zei, om vervolgens met een overweldigend argument of een fantastisch idee te komen zijn veelvuldig. Ook kan ik me (bijna) geen dag herinneren waarop jij niet vrolijk was, een effect dat je over lijkt te dragen op anderen. Wel baal ik een beetje dat ik nog nooit in je Infinity heb mogen zitten.

Beste **Roel** en **Tri**, met werkelijk veel plezier heb ik de afgelopen jaren in de niergroep onderzoek bij jullie gedaan. Hierbij kreeg ik al vrij snel het gevoel niet direct voor, maar eerder samen met jullie te werken. Hopelijk zullen wij in de ( nabije) toekomst verder gaan met onze onderzoeken of nieuwe projecten starten.

Geachte commissieleden, Beste **Prof. Knoers, Prof. van Goor, Prof. Kranenburg, Prof. Pasterkamp, Prof. van Osch**, en **Dr. Joles**, hartelijk dank voor uw bereidheid om mijn proefschrift te beoordelen.

Beste **Jaap**, jouw scherpe en kritische blik op de experimentele nefrologie heb ik erg bewonderd de afgelopen jaren. Ik zal niet ontkennen dat jouw zitting in de commissie mij hierdoor aan de ene kant enigszins zenuwachtig maakt; aan de andere kant had ik me een commissie zonder jou niet kunnen voorstellen. Ik kijk uit naar eventuele toekomstige samenwerking.

**Roel Broekhuizen**, ik kan niet anders dan jou na bovenstaanden als eerste enorm te bedanken en een eigen alinea te geven. Naarmate het aantal experimenten vermeerderde en deadlines naderden heb ik me vaak schuldig gevoeld wanneer ik jou weer een enorme berg werk kwam brengen. Weken lang snijden aan een enkele muizen embryo zonder blikken of blozen. Bovendien maken je fantastische droge gevoel voor humor en je creatieve geest het ook nog eens een plezier om met je samen te werken.

**Prof. van Diest, Prof. Offerhaus**, hartelijk dank voor de wijsheid, gastvrijheid en mogelijkheden die jullie mij geboden hebben op de afdeling. **Dr. de Weger** en **Dr. Derksen**, bedankt voor jullie waardevolle en opbouwende kritiek tijdens de aio/post-doc en monday morning meetings.

De **niergroep** (plus een stukje **granzyme**), de vaste groep mensen in de onderzoeksgroep met wie ik elke vrijdag (nouja elke... ) de hele ochtend aan de koekjes en koffie zat. Beste **Jan Willem** en **Amelie**, toen ik net begon waren jullie aan het afronden. Mede dankzij jullie onmiddellijke acceptatie en bereidheid overal bij te helpen heb ik me direct welkom gevoeld in de onderzoeksgroep. Onze samenwerking ging verder dan wetenschappelijk, waar de UMC estafettes mooi bewijs van leveren. Beste **Dionne**, met name tijdens de eerste jaren heb je mij enorm geholpen met het managen en behandelen van een forse hoeveelheid muizen. Ondanks je vertrek kom ik bijna dagelijks sporen tegen van jouw inzet bij mijn onderzoek. Hartelijk dank hiervoor. Beste **Krista**, je hebt het stokje moeiteloos overgenomen. Hopelijk heb ik je niet teveel in de war gebracht met mijn vele en soms onduidelijke wensen. Bedankt! Beste **Stefan**, wij zijn nagenoeg tegelijk begonnen met ons onderzoek en toch ben ben jij vele malen

sneller klaar; ik vraag me wel eens af wat ik fout heb gedaan. Ik heb een gezellige tijd met je gehad, met Philadelphia als hoogtepunt. Hopelijk heb je nu je plek gevonden. Beste **Ellen**, ook al was je mijn meest directe collega, ik zal je blijven onthouden als meest enthousiaste danseres, dat begrijp je. Snel weer eens een spelletje doen? Succes met het afronden van je nier- en granzymegroep onderzoek!

**Dr. Bovenschen**, beste **Niels**, jouw scherpe inzicht in de moleculaire biologie maakt telkens weer indruk op me. Het allerbeste en veel succes bij het managen van het PRL (en het onderzoek natuurlijk). Beste **Irma**, ik wil je graag bedanken voor het werk dat je achter de schermen hebt uitgevoerd. Dear **Hiroshi**, it was really nice working with you (and between you and me: the lymphangiogenesis work is one of my favourite chapters). Best of luck!

Beste collega pathologie onderzoekers: Beste **Geert, Danielle, Iordanka, Pan, Stefanie, Cigdem, Robert, Jeroen, Cathy, Annette, Petra, Manon, KaWai** en **Jolien**, toen ik startte was voor velen van jullie het onderzoek al in volle gang en ondertussen zijn de meesten van jullie (sommigen letterlijk) gevlogen. Ik wens jullie allemaal veel succes en bedank jullie voor de gezellige tijd op het PRL (P.s. de karaoke avond is helaas een stille dood gestorven). P.s. **Laurien**, jij hoort natuurlijk ook in dit rijtje maar ik bedank je pas als ik eens mag winnen met squashen....

**Wendy**, ik wilde jou nogmaals in het bijzonder bedanken voor de inzet en manier waarop jij (soms tegen grote weerstand in) het PRL tot een efficiënte werkomgeving hebt weten te vormen. **Jan** en **Folkert**, beiden coryfee in het lab. Dankzij jullie veelvuldige hulp en management heb ik het lab intact gelaten. **Miranda**, bedankt voor je hulp bij de administratie/registratie.

Als ik volgens oorspronkelijke planning klaar was geweest dan was dit het einde van de PRL bedankjes geweest. Gelukkig is mijn onderzoek uitgelopen. Hierdoor heb ik een volledig tweede cohort aan PRL onderzoekers mogen ontmoeten. Beste **Pauline, Rob, Yvonne, Justin, Koos, Marise, Joost, Huiying, Liling, Quirine** en **Emma**, heel veel succes met jullie verdere onderzoek en opleiding, hopelijk heb ik jullie niet teveel lastig gevallen met mijn intermitterende bezoeken. **Pauline!** IK BEN ZO BLIJ DAT JIJ OP HET PRL BENT GEKOMEN! Ik blijf me verbazen over hoe zo'n partiële alcoholiste met dubieuze morele standaard (zie documentaire van 1 april jl.) toch zo competent kan zijn. Al het goeds aan jou en Matthys. **Rob**, bedankt voor je bereidheid ons wekelijks op het bieruur te attenderen. Ik zie je op het hockeyveld (als teamgenoot en als tegenstander). Succes met (de start van) je opleiding! **Justin**, ik wens jou en je kersverse vrouw het allerbeste. Ook jij uiteraard succes met het vervolg van je opleiding (en het afronden van je proefschrift). **Koos**, GheGheGheGheGhe! **Aernout**, stop je nu met vragen of ik niet eens moet gaan promoveren....? **Marise**, veel plezier in je Indische nieuwe huisje! ik kom je vast nog wel tegen in onze (mogelijk dezelfde) vervolgopleiding.

Beste **Willy, Marjon** en **Ellen**, heel erg bedankt voor jullie behulpzaamheid de afgelopen jaren. Ook de rest van de pathologie wil ik bedanken voor hun betrokkenheid en inzet. Specifiek wil ik de (oud) medewerkers van het secretariaat, de weefselfaciliteit (met in het bijzonder **Jan Beekhuizen** en **Natalie**, ook als "nieuwe" PRL member), de histologie, de immunopathologie (met in het bijzonder **Domenico** en **Kevin**) en de moleculaire pathologie (met in het bijzonder **Marja**) bedanken.

Geachte **Prof. Verhaar, Dr. Fledderus, Dr. Giles, Dr. Rookmaker, Dr. Gerritsen, Dr. Mokry, Dr. Abrahams** en **Dr. Stoop**, hartelijk dank voor de samenwerking de afgelopen jaren.

Beste **Karin**, bedankt voor de kans die je mij gegeven hebt samen aan de SMART studie mee te werken. Beste **Gisela**, bedankt voor de fijne samenwerking. Ik heb het heel leuk gevonden om aan CEP164 te sleutelen, mijn meest fundamentele paper. **Hendrik**, ik heb jouw nieuwsgierigheid naar meer kennis en "vrije" geest binnen het onderzoek als zeer inspirerend beschouwd. Helaas krijg ik het beeld van jou als platinablonde Tinder date niet meer uit m'n hoofd. Beste **Tobias**, wat begon met een vraag over een kleuring is uitgegroeid tot een mooi hoofdstuk (en hopelijk publicatie). We komen elkaar vast nog tegen, alleen al omdat ik nog een etentje van je tegoed heb! ;)

Beste **Maarten (Wester)**, maar liefst twee maal zijn wij samen naar de States geweest. Twee mooie

trips die ik niet snel zal vergeten. Beste **Diana** en **Kirsten**, de tweede trip was ook met jullie. Nooit gedacht met collega onderzoekers op de plank te staan.

Beste **Nynke**, bedankt voor de gezellige samenwerking binnen en buiten het GDL. Beste **Olivier** en **Tim**, ook jullie bedankt voor een gezellige tijd! **Adele**, **Nel** en **Petra** heel erg bedankt voor de vriendelijke wijze waarop jullie mij technische hebben ondersteund tijdens de sporadische bezoeken aan het nefrologie lab.

Beste (oud) medewerkers van het GDL met in het bijzonder **Romy**, **Helma**, **Anja**, **Paul**, **Sabine**, **Willeke**, **Debby**, **Tamara**, **Kiki** en **Herma**: Heel erg bedankt voor jullie ondersteuning de afgelopen jaren. Ik ben blij dat jullie mij, ondanks de vele kleine tikjes op de vingers, nog steeds bij jullie op de werkvloer toelaten. Geachte **Dr. Poelma** en **Dr. Blom**, beste **Fred** en **Harry**, hartelijk dank voor de vriendelijke, snelle en zeer bruikbare ondersteuning bij de (toch wel) ingewikkelde proefdieradministratie. Tijdens de proefdiercursus drukken jullie ons op het hart dat jullie er zijn om de onderzoeker te helpen. Zo heb ik dit ook altijd ervaren.

Beste **Aletta**, **Chalana**, **Roy**, **Zeineb**, **Cindy** en **Yik**, hartelijk dank de inzet tijdens jullie respectievelijke onderzoeksstages.

De vele anderen die mij de afgelopen onderzoeksjaren geholpen hebben wil ik ook graag hartelijk danken.

Voor mijn beide paranimfen is een enorme dubbelrol toebedeeld. Wij hebben ons onderzoek in volledige overlap uitgevoerd en hierdoor samen vele uren in het UMC doorgebracht, maar hiervoor behoorden jullie al tot mijn beste vrienden. **Dimitri**, held, mijn eerste en daarmee oudste studiemaatje! We hebben zo gruwelijk veel leuks meegemaakt. Hopelijk zet deze trend zich door. Door dik en dun, jij het hart en ik de nieren. **Han**, ik vind het zo onwijs leuk dat je er bij kan zijn als mijn paranimf ondanks je drukke leven in de VS. Ik mis je enthousiasme en de lange discussies die we vaak hadden, dat... en je bourgondische kookkunst.

**JC Dekhengst/Baksteen/Fuore/Blauwe Kabouter**... 2005!! Wat bijzonder dat we nog steeds elke dinsdag (proberen) samen (te) eten. Helaas zijn de maaltijden ondanks mijn hevig verzet toch volledig vegan geworden. **De Chillers**, het groepje dat zijn naam eer aan doet. Altijd gezellig om impromptu aan te schuiven bij een random spelletjesavond. Hopelijk lukt het er weer wat vaker bij te zijn!

(Oud)huisgenoten van huize **Chaud Lapin**, **House of Justus** en het **Thijspaleis/the Hansion/the Lucastle/the Lion's Den/Casa Carien/Eric's Etablissement**, bedankt voor de leuke tijd en het geduld met mijn soms wat onhygiënische huishoudetiquette.

(Oud)medespelers en bestuursleden van **Mise-en-Scène, LTD.** en **Bureau Klein Leed**, ons samenspel en samenwerken heeft mijn afgelopen decade kleur gegeven!

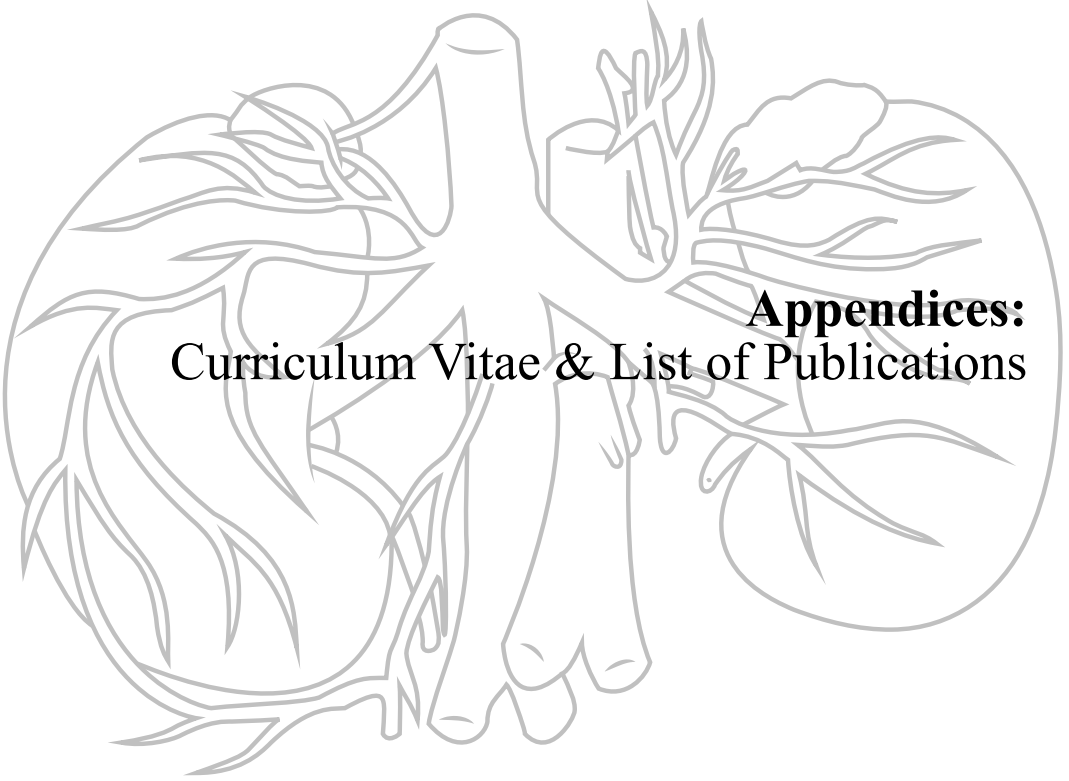
**Alexander**, **Barthold**, **Dimitri**, **Han**, **Heiko**, **Jasper**, **Joep**, **Laura**, **Lionel**, **Pim**, **Renée**, **Rinske**, **Thijs** en **Tristan**, ik wil jullie in het bijzonder bedanken voor de hechte vriendschap.

Mijn oude schoolvrienden: **Willem**, **Paul**, **Olivier** en **Fabienne**, ondanks onze lage ontmoetingsfrequentie is onze vriendschap me dierbaar.

Lieve **papa** en **mama**, wat moet ik nou tegen jullie zeggen... onvoorwaardelijke steun en liefde. Dat zijn twee dingen die ik altijd van jullie gekregen heb. Ik ben onbeschrijflijk dankbaar voor alles dat jullie mij hebben gegeven. Lieve **Jeroen** en **Steyn**, ik ben trots op jullie. Ik voel me minder en minder een oudere broer en steeds meer een super goede vriend (lees partner in crime). Feestje? Lieve **Dratar**, Woef Woef Waf Woef. Lieve familie, ik houd van jullie en de overweldigende hoeveelheid humor waarmee ons gezin in het leven staat.

Tot slot **Willemijne**, mijn moefie moefie, mijn liefje... als mijn geheime onderzoeksproject verdient je een eigen pagina. Ik vind het heel knap en inspirerend hoe jij jezelf staande weet te houden ondanks de enorme werkdruk die je tijdens dit schrijven ondervindt. En dan ook nog je fiets in beslag genomen! Bij jou ben ik helemaal mezelf en voel ik me goed. Jij bent mijn lievelingsmuisje Mijntje....





**Appendices:  
Curriculum Vitae & List of Publications**





Lucas Lodewijk Falke was born in Nashville, Tennessee on October 28 in 1985, but moved to the Netherlands at a young age. He completed grammar school (Stedelijk Gymnasium Leiden) in 2004 after which he enrolled into the Bachelor of Biomedical Science at the University of Utrecht for a year. In 2005 he enrolled via de-central selection (entrance exams) into Medicine at the Erasmus MC, Rotterdam. In 2007 he started the Molecular Medicine Research Master program in addition to his Medicine studies. After two internships at the department of Neuroscience and Orthopedics respectively, he obtained his Masters degree for Molecular Medicine in 2010. The same year he completed his pre-clinical Masters program in Medicine and started as a PhD student in the Kidney Group of Prof. Goldschmeding at the department of Pathology in the UMC Utrecht. For 3.5 years he worked as full time PhD student but in 2014 he started his clinical rotations as Medical Master student in the UMC Utrecht in parallel to his research. Currently Lucas is in the final stage of his second Master year and is projected to start his final rotation at the end of 2016. He is expected to receive his Medical licence in the beginning of 2017.



**List of Publications** (\* indicates equal contribution):

**Falke LL**, Kinashi H, Dendooven A, Broekhuizen R, Stoop R, Jaap JA, Nguyen TQ, Goldschmeding R. *Age dependent shifts in renal response to injury relate to altered BMP6/CTGF expression and signaling*. Am J Physiol Renal Physiol 2016 Aug 18 (in press)

Gerritsen KG, **Falke LL**, van Vuuren SH, Leeuwis JW, Broekhuizen R, Nguyen TQ, de Borst GJ, Nathoe HM, Verhaar MC, Kok RJ, Goldschmeding R, Visseren FL, for the SMART Study Group. *Plasma CTGF is independently related to an increased risk of cardiovascular events and mortality in patients with atherosclerotic disease: the SMART study*. Growth Factors. 2016 Aug 10. DOI: 10.1080/08977194.2016.1210142

Samarakoon R, Rehffuss A, Khakoo NS, **Falke LL**, Dobberfuhr AD, Helo S, Overstreet JM, Goldschmeding R, Higgins PJ. *Loss of expression of protein phosphatase magnesium-dependent 1A during kidney injury promotes fibrotic maladaptive repair*. FASEB J. 2016 Jun 21. DOI: 10.1096/fj.201500105R

Frydlová J, Příkryl P, Truska J, **Falke LL**, Dux X, Gurieva I, Vokurka M, Krijt J. *Effect of Erythropoietin, Iron Deficiency and Iron Overload on Liver Matriptase-2 (TMPRSS6) Protein Content in Mice and Rats*. PLoS One. 2016 Feb 4. DOI: 10.1371/journal.pone.0148540.

Fontes MS, Kessler EL, van Stuijvenberg L, Brans MA, **Falke LL**, Kok B, et al. *CTGF knockout does not affect cardiac hypertrophy and fibrosis formation upon chronic pressure overload*. J Mol Cell Cardiol. 2015 Sep 26. DOI:10.1016/j.yjmcc.2015.09.015.

Samarakoon R, Helo S, Dobberfuhr AD, Khakoo NS, **Falke LL**, Overstreet JM, et al. *Loss of Tumour Suppressor PTEN Expression in Renal Injury Initiates SMAD3 and p53 Dependent Fibrotic Responses*. J Pathol. 2015 Mar 25. DOI: 10.1002/path.4538.

**Falke LL\***, van Vuuren SH\*, Kazazi-Hyseni F, Ramazani F, Nguyen TQ, Veldhuis GJ, et al. *Local therapeutic efficacy with reduced systemic side effects by rapamycin-loaded subcapsular microspheres*. Biomaterials. 2015 Feb. DOI: 10.1016/j.biomaterials.2014.11.042

**Falke LL\***, Gholizadeh S\*, Goldschmeding R, Kok RJ, Nguyen TQ. *Diverse origins of the myofibroblast- implications for kidney fibrosis*. Nature reviews Nephrology. 2015 April 11. DOI: 10.1038/nrneph.2014.246

Slaats GG, Ghosh AK\*, **Falke LL\***, Le Corre S, Shaltiel IA, van de Hoek G, et al. *Nephronophthisis-associated CEP164 regulates cell cycle progression, apoptosis and epithelial-to-mesenchymal transition*. PLoS genetics. 2014 Oct 23. DOI: 10.1371/journal.pgen.1004594

**Falke LL\***, Kok HM\*, Goldschmeding R, Nguyen TQ. *Targeting CTGF, EGF and PDGF pathways to prevent progression of kidney disease*. Nat. Rev. Nephrol. 2014 Dec. DOI: 10.1038/nrneph.2014.184

**Falke LL**, Goldschmeding R, Nguyen TQ. *A perspective on anti-CCN2 therapy for chronic kidney disease*. Nephrology, dialysis, transplantation. 2014 Feb. DOI: 10.1093/ndt/gft430

**Falke LL\***, Dendooven A\*, Leeuwis JW, Nguyen TQ, van Geest RJ, van der Giezen DM, et al. *Hemizygous deletion of CTGF/CCN2 does not suffice to prevent fibrosis of the severely injured kidney*. Matrix biology. 2012 Aug-Sept. DOI: 10.1016/j.matbio.2012.06.002

Duraku LS, Hossaini M, Hoendervangers S, **Falke LL**, Kambiz S, Mudera VC, et al. *Spatiotemporal dynamics of re-innervation and hyperinnervation patterns by uninjured CGRP fibers in the rat foot sole epidermis after nerve injury*. Molecular pain. 2012 Aug 30. DOI: 10.1186/1744-8069-8-61

